Challenging Controlled Drug Delivery:

Matrix Systems for Oral and Parenteral Application

Dissertation zur Erlangung des akademischen Grades des

Doktors der Naturwissenschaften (Dr. rer. nat.)

eingereicht im Fachbereich Biologie, Chemie, Pharmazie

der Freien Universität Berlin

vorgelegt von

Stefanie Krenzlin

aus Brandenburg an der Havel

Berlin 2012

Die vorliegende Arbeit wurde von Mai 2007 bis Oktober 2011 am Institut für Pharmazeutische Technologie, Freie Universität Berlin und an der Faculté de Pharmacie, Laboratoire du Pharmacotechnie Industrielle, Université de Lille Nord de France unter der Betreuung von Prof. Dr. Roland Bodmeier und Prof. Dr. Jürgen Siepmann angefertigt.

1. Gutachter: Univ.-Prof. Dr. J. Siepmann

2. Gutachter: Univ.-Prof. Dr. R. Bodmeier

Tag der mündlichen Prüfung: 16.12.2011

Meiner Familie gewidmet.

Acknowledgements

First of all I want to express my sincere gratitude to all who contributed to the success of this work during the past four years.

Professor Bodmeier, who accepted me as a doctoral candidate in his research team, for his valuable and constructive co-supervision and for being an expert for my PhD thesis.

Professor Siepmann, who provided me with an interesting topic and gave me the opportunity to do my PhD thesis in a cooperative, international and motivated team. I am grateful for his scientific support and useful suggestions. He also generously gave me the opportunity to attend scientific meetings and international conferences, which always provided valuable input to my research.

Daniel Wils and Laëtitia Guerin-Deremaux from Roquette Frères for financial and material support. My sincere thanks go to David Veran, Dan Gnansia, Régis Roberton, Jean-Marc Valcin and his lab team from Neurelec for financial and material support and their kind hospitality in Vallauris in June 2010.

Professors Hédoux and Guinet, Laurent Paccou and Adrian Lerbret from the Université Lille 1 for helping with the Raman measurements and providing a deeper insight into Raman spectroscopy. Dr. Christel Neut, for useful advice on biological analysis. Professor Vincent from CHRU Lille for valuable suggestions and fruitful discussions on the cochlear implants.

A warm thanks goes to the team at the "Laboratoire du Pharmacotechnie Industrielle", - Dr. Florence Siepmann, who always kindly and patiently answered my questions, Dr Marie-Pierre Flament, for helpful suggestions, Professor Gayot, Hugues and Muriel and the secretaries Sandra, Jennifer andMonique.

This work would also not have been possible without the help and encouragement of former and actual members of our workgroup. Thanks to you all!

Among them I am tremendously obliged to:

Table of Contents

List of Abbreviations

5-ASA	5-Aminosalicylic acid
CD	Crohn's disease
DDS	drug delivery systems
DES	drug eluting stents
GIT	gastrointestinal tract
HAP	hydroxyapathite
HCl	hydrochloric acid
HEPES	2-[4-(2-hydroxyethyl)piperazin-1-yl]ethanesulfonic acid
IBD	inflammatory bowel diseases
IR	immediate release
LDH	L-lactic dehydrogenase
MCC	microcrystalline cellulose
PEG	polyethylenglycol
PHA	polyhydroxyalkanoates
PLA	poly(L-lactic acid)
PLG	poly(glycolic acid)
PLGA	poly(lactic-co-glycolic acid)
PMMA	polymethylmethacrylates
PVP	polyvinylpyrrolidone
RWM	round window membrane
SR	sustained release
T_c	collapse temperature
T_g	glass transition temperature
UC	ulcerative colitis

1   Introduction

1.1   General

The administration of pharmaceutical compounds intends to provide and maintain therapeutic drug concentrations at the site of action. With regard to safety, efficacy and reliability, the development of adequate drug delivery systems (DDS) for this purpose is highly challenging. Moreover, the specific physiological conditions, the physico-chemical or therapeutic properties of the drug as well as modifications of formulation parameters might strongly impact on the concentration-time profiles and thus, affect the efficacy and/or safety of the device (Banker and Rhodes, 2002).

Pharmaceutical compounds can be of chemical or biological origin; either inducing a simple physical interaction upon administration or exhibiting a complex mechanism of action. However, in both cases it is highly desirable to meet a maximum of preconditions to enable the drug to fulfill its therapeutic purpose. The drug should be (i) transported to a specific site of action, (ii) released in a desired amount (iii) over a controlled period of time. The achievement of these conditions is generally termed 'drug delivery'. Directing the transport of the drug to an explicit site is called 'site-specific' or 'targeted drug delivery'. Further, regulating the period of drug administration and delivery from the device leads to 'controlled drug delivery'. These conditions not only require knowledge on how to formulate a pharmaceutical compound but also how to influence the type of administration and drug release from the device.

Numerous controlled drug delivery systems have been developed so far. In general, the systems described in literature are based on three principles (Banker and Rhodes, 2002; Heller, 1987; Leong and Langer, 1988):

- Reservoir systems, consisting of a drug core surrounded by a release rate controlling membrane (e.g., coated pellets or tablets, microcapsules)
- Matrix systems, where the drug is dissolved or dispersed in a carrier matrix (e.g., pellets or tablets, microspheres)
- Hybrid systems, combining membrane and matrix systems (e.g., coated pellets in tablet matrix, pellets in a coated capsule)
  (Wen and Park, 2010).

An effective method is to formulate a drug reservoir consisting of a drug core and a polymeric coating in order to obtain broad spectra of drug release kinetics. Numerous studies have been shown the efficacy of coated dosage forms obtained by coating cores with synthetic and natural polymers, blends and grafts thereof (Lecomte et al., 2003 and 2004; Muschert et al., 2009). However, according to the type of technique, e.g., aqueous or organic based coatings, several problems may arise: aqueous coating techniques may result in incomplete film formation, due to immiscibility or incompatibility of the excipients or simply by employing inappropriate process parameters (Bodmeier et al., 1997; Mehta, 1997; Rowe, 1997). Organic coating techniques may overcome these problems, but harbor at the same time, the risk of residual organic solvents in the film. Additionally, the manufacturing procedure is associated with elevated personal and environmental risks. Addition of appropriate plasticizers might solve inconveniences arising with aqueous coating techniques. However, miscibility with the film-forming polymer, determined by the specific solubility parameters, limits the addition of large amounts of plasticizers (Wheatley and Steuernagel, 1997). In addition, hydrophilic plasticizers quickly leach out of the film coatings upon contact with the aqueous bulk fluid (Dyer et al., 1995; Frohoff-Hülsmann et al., 1999; Okarter and Singla, 2000), whereas lipophilic species might be volatile upon storage, which might impact the reproducibility of the resulting drug release kinetics. Moreover, polymeric film coatings are often exposed to mechanical stresses during processing, drug release or storage which can alter their mechanical properties and affect their function as release rate controlling membrane. Hence, the desired drug release kinetics might be poorly predictable.

An alternative approach is the formulation of matrix drug delivery systems. Here, the release rate is controlled by an interconnected network formed by the polymer and the embedded drug. Drug release is governed by diffusion through liquid filled pores, through the matrix itself, by erosion or by a combination of these mechanisms. Matrix drug delivery systems can be advantageous over coated systems exhibiting homogeneous character, a simple manufacture and the absence of problems which might arise during the coating procedure.

Matrix systems are widely used to deliver drugs either via oral or parenteral administration. However, controlling the drug release kinetics remains challenging and the underlying drug release mechanisms are yet not fully understood. The release conditions generated by the surrounding bulk fluid and its composition can also enormously impact the resulting drug release and the pharmacokinetics. In the case of oral administration, effects of pH, food

intake, gastric emptying and motility, fluid volumes, enzyme concentration and disease state are only some of the factors that might have an influence. In addition, intra- and inter-individual variability should not be neglected. Similar statements can be made for parenteral administration; here the volume of the surrounding bulk fluid, the pH, the plasma velocity and the composition of the surrounding tissue are crucial factors. At the same time, the properties and pharmacokinetic behavior of the incorporated drugs are of outmost importance to develop effective drug delivery systems (Davis, 1985). In recent years, complex drug molecules have gained growing importance over conventional small molecular drugs with a rapidly growing market for protein-derived drugs. The latter, in particular, require specific drug delivery systems, adapted to their physicochemical and biological properties (e.g., light, air and moisture sensitivity, susceptibility to chemical and physical denaturation). Consequently, enhanced research activity is required to further improve and optimize matrix drug delivery systems for oral and parenteral application.

1.2   **Oral Drug Delivery**

The most popular way to administer pharmaceutical compounds to the human body in order to achieve a systemic effect is the oral route. The lack of a complex application procedure and the self administration by the patient are only two of the numerous advantages associated with oral administration. Thus the patients' independence can be guaranteed during therapeutic treatment. In general, oral dosage forms can be classified in reservoir, matrix and hybrid systems. They can further be divided into two subgroups: single unit systems, where the drug is uniformly distributed in the homogenous matrix (e.g., tablets and soft capsules), and the multiple unit systems, characterized by drug containing subunits with identical or variable properties distributed in a carrier material (e.g., pellets filled in hard capsules). These smaller drug containing subunits can spread more easily in the gastro-intestinal tract (GIT), ensuring a uniform drug release within the GIT. At the same time, their sensitivity to alterations in environmental conditions is reduced (see *section 1.1 General*).

Single unit systems, containing the total amount of drug in one entity, either as a matrix or a coated dosage form, hold the risk of the all-or-othing effect, that is the undesired spontaneous release of the total amount of drug due to e.g., insufficient mechanical properties of the matrix or the coating layer. Multiple unit systems can overcome this problem: the distribution of the total amount of drug on numerous subunits minimizes the risk of possible severe side effects. Even if some of these subunits fail to control the drug release, only a small quantity of the drug is immediately released (Follonier and Doelker, 1992). Additionally, the resulting plasma drug levels are less variable. Thus, high local drug concentrations and possible saturation phenomena occurring during drug absorption can be avoided.

Maintaining therapeutic blood levels over an extended period of time requires certain considerations when choosing adequate drug candidates: important limitations are the therapeutic range and the ratio of absorption and elimination rate, the so-called half-life of the drug. Very short half-lifes, below 2 hours, require large amounts of drug and are thus not recommended for controlled drug delivery since the upper mass of a single dose is limited by the size of the dosage form. Exceeding these limits will render the dosage form too large to administer and disagreeable for the patient (Davies, 2009). Oral dosage forms can be classified in immediate release (IR) and sustained release (SR) systems. IR systems are designed to disintegrate and release the drug rapidly after administration to ensure instant drug action. Usually, the drug effect is maintained only for a short period of time. In contrast, SR systems aim at a prolonged or delayed drug release which intends to maintain therapeutic

blood levels over an extended period of time. Furthermore, optimization of drug concentrations at the site of action, namely site-specific or targeted release, is highly desirable. Consequently, uniform and local drug delivery can be achieved, reducing high systemic plasma levels (temporary peaks above or near the toxic concentrations), and allowing for the reduction of the administered drug dose. This in turn minimizes the risk of severe side-effects and the administration frequency, which offers an important benefit with regard to the patients' compliance.

The first steps in the development of drug delivery systems were made by Smith, Klein, and French in 1952 with the introduction of a dexedrine extended release capsule (Pillai et al., 2001). The so called Spansule® system consisted of a drug coated with a release rate controlling polymer in a capsule shell. Initially, the development of controlled release formulations focused on these reservoir systems (Sequels® by Lederle, Repetabs® by Schering). However, the development of controlled release formulations aiming at incorporating drugs in a matrix have soon gained increasing interest. Pioneers in the development of matrix drug delivery systems were Robins or Schering with the launch of the Extentabs® or the Chronotab® formulation respectively. Matrix formulations were either composed of insoluble natural or synthetic polymers, which remained intact and released the drug by diffusion, or consisted of soluble or erodable excipients, which disintegrated during dissolution. The resulting drug release mechanisms combine diffusion and dissolution of the matrix material, being hence far more complex. A more detailed description of the underlying drug release mechanisms is given in *section 1.3 Drug Release Mechanisms*.

1.2.1 Targeted Drug Delivery

In *section 1.1 General* the advantages of targeted drug delivery were depicted. In general, targeted delivery is based on two assumptions: (i) to circumvent arising problems, either because of small drug absorption windows in specific segments of the GIT, unfavorable conditions for drug dissolution and absorption, (ii) to prevent sensitive drugs from degradation and loss of efficacy due to varying physiological conditions in the GIT or (iii) to obtain a therapeutic effect at a particular site in the GIT. Conventional oral administration of drugs with a small absorption window in the proximal regions of the GIT might lead to limited bioavailability. Thus, the aim is to increase their concentration at or above these specific regions by mucoadhesive or floating drug delivery devices. These possibilities were

extensively reviewed in literature (Andrews et al., 2009; Bernkop-Schnürich, 2005; Davis, 2005; Pawar et al., 2011). In order to prevent drugs from degradation or to enhance their solubility the delivery systems can be provided with a protective coating that inhibits their contact with the gastric fluid but dissolves in the lower GIT regions. Alterations in pH can as well be used as varying osmotic, surfactant, proteolytic or microbiological conditions (Charman et al., 1997; Karrout et al., 2009b, Malaterre et al., 2009; McConnell et al., 2008; Siepmann, F. et al., 2008a; Sinha and Kumria, 2003). The second approach implies increasing local drug concentrations in order to maximize therapeutic and to minimize adverse effects.

1.2.2 Colon Targeting

Special interest has been drawn on site-specific drug delivery to the distal regions of the small intestine and the colon. This is of particular importance for the treatment of inflammatory bowel diseases (IBD), where high local concentrations of anti-inflammatory drugs are required. Inflammatory bowel diseases like Crohn's Disease (CD) and ulcerative colitis (UC) are characterized by local mucosal inflammations in the distal intestine and the colon. The inflammations accumulate at specific sites: in CD inflammatory reactions are predominantly localized in the distal ileum and the colon, whereas in UC the affected sites are mainly located in the proximal regions of the colon (Friend, 2004). However, the inflammation is generally limited to mucus or transmural locations and does not affect the systemic circulation.

Conventional dosage forms rapidly release the drug in the upper GIT with subsequent absorption into the systemic circulation. The drug is distributed within the human body and might engender potential severe side-effects. Additionally, the drug concentration at the site of action – the inflamed colon - is low, leading to low therapeutic efficacies. Consequently, therapeutic success enormously depends on the ability to develop site-specific drug delivery with maximized local drug concentrations, minimized undesired systemic side-effects resulting in an optimal benefit for the patient.

The principal conditions for colon-targeted delivery are the inhibition of drug release in the upper regions of the GIT, the stability of the dosage form during the intestinal transit and the complete and controlled drug release at the site of action. In general, four principles are employed to target drugs to the distal regions of the GIT: (i) time, (ii) pH, (iii) bacterial status, and (iv) pressure. In order to optimize the drug delivery devices, these approaches might as well be combined.

Table 1.2.1: Luminal pH in the GIT of healthy subjects and IBD patients (from König, 2004).

		Small bowel		Colon	
Study	**Patients**	**Jejunum**	**Ilium**	**Proximal**	**Distal**
Healthy					
Evans et al. (1988)	66	6.6	7.5	6.4	7.0
Press et al. (1998)	12	6.7	7.5	6.1	6.1
Fallingborg et al. (1989)	39	6.4	7.3	5.7	6.6
Ewe et al. (1999)	13	6.5	7.6	6.2	7.0
Ulcerative colitis					
Press et al. (1998)	11	6.6 - 6.8	7.9 - 8.2	6.5 - 7.2	6.5 - 6.8
Fallingborg et al. (1993)	6	6.4	7.4	6.8	-
Ewe et al. (1999)	4	6.5	6.8	5.5	7.5
Nugent et al. (2001)	6	7.3	8.3	5.8 - 7.3	4.8 - 7.3
Crohn's disease					
Press et al. (1998)	12	6.5 - 6.8	7.9 - 8.2	6.5 - 7.2	6.5 - 7.8
Ewe et al. (1999)	12	6.5	7.5	6.2	6.5
Fallingborg et al. (1998)	9	6.3	7.3	6.7	-
Schwartz (1997)	15	6.5	7.5	6.2	6.4

Particular conditions in the GIT have to be considered when developing site-specific drug delivery systems. Remarkable variations may arise between healthy subjects and IBD patients with regard to luminal pH, intestinal transit times, and bacterial status (Evans et al., 1988; Ewe et al., 1998; Fallingborg, 1989, 1993 and 1998; Ibekwe et al., 2008; McConnell et al., 2008a, 2008b; Nugent et al., 2001; Press et al., 1998; Schwartz, 1997).

Table 1.2.1 gives an overview of different pH measured in the GIT of patients suffering from CD or UC and healthy subjects. Clearly, great care has to be taken when the site-specific release is governed by a pH sensitive coating. Even if the system has proven to be effective in healthy subjects, it might fail in IBD patients. Furthermore, the transit time of pharmaceutical dosage forms in the GIT has also to be taken into consideration. It can be influenced by a large number of parameters. As stated by Olssen and Holmgren (2001) "almost everything seems to affect gastric emptying", for example, the caloric content of simultaneously ingested

food, dosage form diversity (single or multiple units), the type of excipients, or the timing of drug administration (Abrahamsson et al., 1996; Coupe et al., 1992a and1992b; Davis et al., 1984a and 1984b; Newton, 2010; Varum et al., 2010; Waterman et al., 2007; Yuen, 2010). Gastric emptying is followed by the intestinal transit, in general quoted at 3-4 hours (Davies et al. 1986; McConnell et al., 2008b). However, these values arise from pooled data based on different experimental setups. Davies et al., for example, reported that there are no differences between the intestinal transit times of liquids, tablets and pellets in contrast to the studies of McConnell et al. (2008a), Fadda et al. (2008), and Coupe et al. (1991). Here, clear variations between single unit (e.g. tablets) and multiple unit dosage forms (e.g. pellets) were shown. Further parameters with potential influence on the intestinal transit time are the state of food ingestion (Digenis et al., 1990), intestinal motility and flow (Kellow, 1986; Kerlin and Philips, 1982). The transit of dosage forms through the colon claims a major part of the total transit time in the GIT, at least it is one of the most variable processes: 6-48 hours with extreme intervals of 70 hours have been reported in literature (Coupe et al., 1991; Rao et al., 2004). The above mentioned influences of dosage form diversity, motility, pressure, and water content are also of high importance in the colon (Wilson, 2010). As a consequence from inflammations or ileocaecal resections, IBD patients often have accelerated intestinal transit times (Hebden et al., 2000; Munkholm et al., 1993; Vassallo et al., 1992).

Besides pH and intestinal transit the third important factor to consider is the gastrointestinal microflora. Figure 1.2.1 shows a summary of the quantitative bacterial
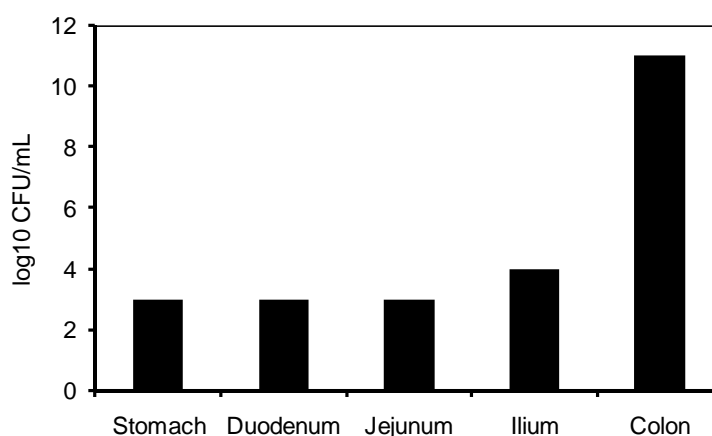
Figure 1.2.1: Quantitative distribution of bacteria in the GIT (from Sinha and Kumria, 2003).

Table 1.2.2: Microbacterial flora in human GIT (modified from Simon and Gorbach, 1984; Hill, 1995).

	Stomach	Jejunum	Ilium	Faeces
Total number of bacteria	$0 - 0^3$	$0 - 10^5$	$10^3 - 10^7$	$10^{10} - 10^{12}$
Aerobic and facultative anaerobic bacteria				
Enterobacterium spp.	$0 - 10^2$	$0 - 10^3$	$10^2 - 10^6$	$10^4 - 10^{10}$
Streptococcus spp.	$0 - 10^3$	$0 - 10^4$	$10^2 - 10^6$	$10^5 - 10^{10}$
Staphylococcus spp.	$0 - 10^2$	$0 - 10^3$	$10^2 - 10^5$	$10^4 - 10^7$
Lactobacillus spp.	$0 - 10^3$	$0 - 10^4$	$10^2 - 10^5$	$10^6 - 10^{10}$
Propionibacterium spp.	-	-	-	$10^9 - 10^{11}$
Escherichia spp.	-	-	-	$10^7 - 10^9$
Fungi	$0 - 10^2$	$0 - 10^2$	$10^2 - 10^3$	$10^2 - 10^6$
Anaerobic bacteria				
Bacteroides	rare	$0 - 10^2$	$10^3 - 10^7$	$10^{10} - 10^{12}$
Bifidobacterium spp.	rare	$0 - 10^3$	$10^3 - 10^5$	$10^8 - 10^{12}$
Bacillus spp.	-	-	-	$10^3 - 10^7$
Coccus (gram-positive)	rare	$0 - 10^3$	$10^2 - 10^5$	$10^8 - 10^{11}$
Clostridium spp.	rare	rare	$10^2 - 10^4$	$10^6 - 10^{11}$
Eubacterium spp.	rare	rare	rare	$10^9 - 10^{12}$

colonization in the GIT of healthy subjects. While the stomach and the small intestine are modestly colonized, bacterial concentrations are 4-fold higher in the colon.

Hence, a promising approach to develop colon targeting drug delivery systems is to make use of excipients which are susceptible to enzymatic degradation by colon-specific bacteria. The total amount of bacteria is estimated to 100 billion in the GIT covering 400 identified species (Eckburg et al., 2006). Table 1.2.2 gives an overview on the qualitative and quantitative occurrence of predominant bacteria in the gastrointestinal microflora. However, the bacterial state also undergoes inter- and intra-individual variability and is highly dependent on the disease status. Alterations in the intestinal transit time might also influence the quality and quantity of the microflora (Linskens et al., 2001; Mills et al., 2008). These basic information are of utmost importance for the development of colon targeting drug

delivery systems. The approaches mentioned earlier in *section 1.2.2 Colon Targeting* will now be described in detail.

1.2.2.1 Time-controlled Drug Delivery

The first attempt to develop a time-controlled drug delivery system for colon targeting was made by Wilding et al. (1992) with the Pulsincap[®] system, a drug containing insoluble capsule that was closed with a hydrogel plug. The plug swells upon contact with the gastrointestinal fluids and acts as a release rate controlling barrier. A similar approach, benefiting from the swelling properties of a hydrogel polymer network was employed by Gazzaniga et al. (1994) in order to control the drug release kinetics from a multi unit system. Pozzi et al. (1994) followed with the development of the TimeClock[®] system which consists of tablets with hydrophobic and hydrophilic coatings to achieve a predetermined lag time. In another case, the technology marketed as Pentasa[®], consisting of 5-ASA pellets with an insoluble but water permeable ethylcellulose coating, the dissolved drug is continuously released from the pellets. However, despite the proven efficacy the system releases significant drug amounts in the upper regions of the GIT. With regard to the required daily doses of up to 4.8 g (Frieri et al., 2005; Qasim et al., 2001; Travis et al., 2008), this formulation is not optimal. Another interesting approach was the use of rupturable polymeric coatings which explode and release the drug immediately after a preprogrammed interval (TES, Ueda et al., 1994a and 1994b). The Alza Cooperation presented an example for osmotic controlled release: the OROS[®] push and pull system. The basic principle of all these systems is to obtain a specific lag-time, long enough to avoid drug release in the upper regions of the GIT. However, a profound knowledge and adequate control of the swelling kinetics of the release rate controlling hydrogels are required. Additionally, variations in the environmental conditions in the GIT might lead to altered drug release profiles. Consequently, time-and pH-controlled approaches are often combined.

1.2.2.2 pH-controlled Drug Delivery

The most popular method to target the colon is to make use of the pH gradient along the GIT. In general, the dosage forms are coated with a polymeric film being insoluble in the stomach but soluble upon contact with media exhibiting a higher pH (enteric coating). Dependent on the chemical composition, the enteric polymers dissolve at pH values ranging

from 5 to 7, targeting specific sites in the GIT according to the increase in pH within the small intestine. Single and multiple unit dosage forms are available containing the drug either in a matrix core or layered on inert starter cores (Fukui et al., 2001; Khan et al., 1999; Nykänen, 2003). Dew et al. (1982) first introduced such a system, by coating sulphapyridine loaded capsules with an acrylic acid resin (Eudragit® S). Since then, numerous 5-ASA containing reservoir systems were marketed, in general based on acrylic acid or cellulose derivate based coatings, e.g., Asacol®, Salofalk®, Claversal® and the very recent MMX® system. Here, the drug is embedded in a lipid matrix which is itself dispersed in a hydrogel. The entire system is provided with an enteric coating. Even if this approach has proven to be effective, inter- and intra-individual variations, as mentioned in *section 1.1 General* and *section 1.2.2 Colon Targeting*, have to be taken into consideration. Furthermore, a steep increase in pH in the proximal colon and the slight decrease in the distal parts might result in a failure of drug release from the administered dosage forms, due to the incomplete or lacking dissolution of the protective coating (Ashford et al., 1993a and 1993b; Ibekwe et al., 2006a and 2006b).

1.2.2.3 Microbially-triggered Drug Delivery

The knowledge for specific enzymatic activities along the GI tract (see also Figure 1.2.1 and Table 1.2.2) allows for the development of colon targeting drug delivery systems employing this principle. By secreting specific enzymes (e.g., azoreductases, β-glucuronidase, dextranases, nitroreductases, esterases) colon-specific bacteria ferment indigested substrates arriving in the colon from the upper regions of the GIT. In general, two drug delivery approaches can be distinguished: the development of enzymatically degradable prodrugs or the formulation with excipients which are susceptible to enzymatic degradation. For instance, sulphasalazine, olsalazine, balsalazide, bensalazine are prodrugs based on the most frequently used drug for the treatment of IBD: 5-aminosalicylic acid. The latter is linked via an azo-bond with a second compound, which is responsible for the inhibition of premature drug release and absorption into the bloodstream. The idea is to increase the molecular weight of the resulting molecule or to render it more hydrophobic, thus less available for absorption until the dosage form reaches the targeted site. Once arriving in the intestine the azo-bond is cleaved by colon-specific azoreductase-secreting bacteria, resulting in the release of the active compound at the site of action. These systems have long been introduced to the market. Polysaccharides, including cyclodextrins, dextrans (Zou et al., 2005), dendrimers (Wiwattanapatapee, 2003) and low molecular weight compounds like amino acids (Jung et al.,

Table 1.2.3: Polysaccharide based materials used to deliver drugs to the lower intestine (adapted from Friend, 2005).

Polysaccharide	Dosage form/Method	Study
Pectin		
Calcium salt	Matrices, compression coated tablets, enteric coated matrix tablets	Adkin et al. (1997), Rubinstein et al. (1993), Rubinstein and Radai (1995)
Methoxylated derivatives	Compression coating	Ashford et al. (1994)
Amidated derivatives	Matrix tablets, coated beads	Munjeri et al. (1997), Wakerly et al. (1997)
Mixed films of pectin	Film coating for tablets and beads	Fernandez-Hervaz and Fell (1998), Semdé et al. (1998, 2000a/b), MacLeod et al. (1999a/b), Wakerly et al. (1996)
Chitosan		
Chitosan	Coated capsules and microspheres	Lorenzo-Lamosa et al. (1998), Tozaki et al. (1997, 1999)
Chitosan derivatives	Matrices	Aiedeh and Taha (1999)
Guar gum		
Guar gum	Matrix tablets, compression coated tablets	Kenyon et al. (1997), Krishnaiah et al. (1998, 1999, 2002, 2003a/b), Rama Prasad et al. (1998), Wong et al. (1997)
Guar gum derivatives	Coatings or matrix tablets	Gliko-Kabir et al. (2000), Rubinstein and Gliko-Kabir (1995)
Amylose		
Mixed films	Coated pellets, tablets, capsules	Cummings et al. (1996), Milojevic et al. (1996a/b), Siew et al. (2000a/b), Vilivalam et al. (2000), Watts and Illum (1997)

Table 1.2.3: Polysaccharide based materials used to deliver drugs to the lower intestine, continued

Polysaccharide	Dosage form/Method	Study
Chondroitin sulfate		
Cross-linked chondroitin	Matrix tablets	Rubinstein et al. (1992a/b)
Alginates		
Calcium salt	Swellable beads	Shun and Ayres (1992)
Inulin		
Mixed films	Tablet and bead coatings	Vervoort and Kinget (1996)
Methacrylate derivative	Cross-linked hydrogels	Vervoort et al. (1998)
Dextran		
Diisocyanate cross-linked dextran	Hydrogels	Brøndsted et al. (1995, 1998), Chiu et al. (1999), Salyers et al. (1977)

2000; Kim et al., 2008), glucuronide and glycoside prodrugs (Friend et al., 1985; Nolen III et al., 1995) were chosen as coupling agents. However, the major drawback of this approach is the high 5-ASA dose of up to 4.8 g per day required to treat IBD (Travis et al., 2008; Friend, 2005). Thus, by linking 5-ASA to a high molecular moiety the total mass of the dosage form increases and requires frequent dosing. An alternative to target the colon is the use of polysaccharides as excipients in anti-inflammatory drug devices. Table 1.2.3 illustrates a selection of polysaccharides susceptible to degradation by colon-specific bacteria and the correspondent conducted studies. Most of them are water-soluble so they have to be blended with insoluble polymers (Cummings et al., 1996; Karrout et al., 2009b/c; Milojevic et al., 1996a/b; Siew et al., 2000a/b) or derivatized to avoid premature drug release. This led to the development of small intestine-indigestible polymers or polysaccharides, respectively (Ashford et al., 1994; Brøndsted et al., 1995; Rubinstein et al., 1992a/b; Vervoort et al., 1998).

The efficacy of matrix systems highly depends on the capacity to retain the dosage form integrity, namely to control the degree of swelling and erosion. Mundargi et al. (2007)

characterized metronidazole matrix tablets containing several natural or grafted polymers as excipients. The *in vitro* drug release studies showed a premature release of at least 20 % of the drug in 0.1 N HCl after 2 h when the formulations contained no protective enteric coating. Another attempt is the preparation of matrix tablets with incorporated guar gum in order to obtain a swollen hydrogel barrier (Krishnaiah et al. 2003a). Drug release of 16 % after 5 h of dissolution was observed. Both studies resulted in considerable premature drug release with regard to the median transit time of 5-6 h before the dosage form reaches the colon. Only an additionally compression coating was able to effectively suppress premature drug release in the simulated gastric and intestinal conditions (Krishnaiah, 2003b). Consequently, to date, the development of colon-targeting matrix systems, susceptible to enzymatic degradation by colon-specific bacteria remains a challenging objective.

1.2.2.4 Pressure-controlled Drug Delivery

Taking advantage of the increasing pressure along the gastrointestinal tract, accurately adjusted pressure-controlled drug delivery to the colon can be an interesting approach. Reabsorption of water during the GI transit leads to an increase in viscosity of the gastrointestinal contents. Additionally, periodically occurring peristaltic movements (Kellow et al., 1986) induce a significant increase in the applied pressure on the device. When a specific pressure value is exceeded, the drug delivery system ruptures, releasing the active substance at the site of action. Takaya et al. (1995) proposed an ethylcellulose capsule containing a polyethylene glycol (PEG)/drug blend. PEGs are known to melt at physiological conditions. During transit through the upper parts of the GIT the capsule remains intact but contains the molten PEG/drug blend. By accurately adjusting the capsule wall thickness, the system can be programmed to burst when the surrounding pressure increases above a specific value. Hence, the drug can be released at a specific site in the colon (Yang et al., 2002). *In vivo* studies proved the feasibility of this concept, with the capsule wall thickness controlling the lag-time, the site of drug release, and the amount of absorbed drug (Takaya et al., 1997; Muraoka et al., 1998). However, the peristaltic movements follow a circadian rhythm (Rao et al., 2001), and the viscosity of the GIT contents might differ in healthy subjects and IDB patients. This might have an important impact on the efficacy and the reproducibility of the systems performance.

1.2.2.5 Combined Approaches

A system which combines three of the above mentioned approaches, namely pH, time-controlled and microbially triggered release is one of the most complex devices developed to date: the CODES® system. A drug/lactulose core is coated with two consecutive layers, an acid soluble polymer and an enteric coating. The latter avoids the premature drug release in the stomach and is quickly dissolved with increasing pH in the upper regions of the intestine. The acid soluble coating assures the integrity of the dosage form during the intestinal transit. Once the colon is reached, water and bacteria are able to cross the semi-permeable membrane leading to degradation of the lactulose core in low molecular weight acids. In consequence the acid soluble coating dissolves and releases the drug at the site of action. Recently, MMX® was commercialized as Lialda® in the US and Mesavant® in Europe. Advantages and drawbacks of this system were described in more detail in *section 1.2.2.2 pH-controlled Drug Delivery*.

Despite the efficacy of the systems mentioned above most of them are single unit dosage forms possibly suffering from the all-or-nothing effect and an eventual inhomogeneous distribution in the GIT (Follonier and Doelker, 1992). In addition they often require a coating step to avoid premature drug release in the upper parts of the GIT. Only few attempts were made to develop pure matrix drug delivery systems to target the colon. This is surely due to the difficulty to control all parameters which account for the fate of an orally administered dosage form during its GI transit. In addition the burst release, namely the immediate release of drug particles located at the matrix surface, is an undesired feature for colon-specific delivery. However, matrix dosage forms offer various considerable advantages (see *section 1.1 General*), thus, intensified research activity is required in order to promote the progress in the field of colon-targeting.

1.3 Drug Release Mechanisms

Drug release from matrix drug delivery systems is controlled by (i) diffusion, (ii) swelling and erosion, (iii) geometrylarea changes, (iv) non-uniform drug distribution, or a combination of these phenomena (Wen and Park, 2010).

1.3.1 Diffusion

Diffusion processes account for non-erodible matrix drug delivery devices (e.g., non-disintegrating tablets). Firstly, the device is hydrated by the imbibing of the surrounding bulk fluid. Subsequently, a stable dissolution layer forms, its velocity towards the center of the device depends on the properties of the polymer. Within this layer a dissolution front can be found, its position is a function of the drug solubility. In general, the resulting release profile shows first order kinetics as a function of the square root of time and decreasing release rates towards the end of release. This is due to the decreasing surface area available at the dissolution front in combination with the increasing distances the dissolved drug molecule has to overcome. In practice, the dissolved molecular drug often diffuses through (initially existent) water filled pores rather than through the matrix former, or at least through both. Pure diffusion controlled drug delivery devices are rare (e.g., Fero-Gradumet®, Abbott). Diffusion-controlled release from matrix drug delivery systems often occurs in combination with swelling and erosion processes (Wen and Park, 2010).

1.3.2 Swelling and Erosion

Swelling and erosion phenomena are the main processes controlling drug release in disintegrating matrix drug delivery devices. Assuming a swellable matrix, a stable gel layer is formed, its formation rate and thickness depending on the polymer-liquid interaction. This gel layer acts as a barrier, externally limited by the matrix-liquid interface and internally limited by the swelling front, that separates resistant polymer with highly entangled chains (glassy state; T_g of the polymer higher than the surrounding temperature) from hydrated polymer with disentangled chains (rubbery state; T_g below surrounding temperature). Within this gel layer a second, the diffusion layer can be found, separating dissolved and solid drug. The position of this front within the gel layer is highly dependent on the drug solubility and the drug loading of the device. High drug solubility leads to a diffusion front close to the swelling front, whereas high drug loadings result in a high drug concentration gradient within the gel layer.

In general, drug release kinetics from swellable matrices is Fickian in the beginning, exhibiting liquid penetration, formation of a gel layer, drug dissolution and diffusion. With progressing time, they convert to anomalous kinetics with a constant gel layer thickness due to the similar rate of liquid penetration and swelling processes and therefore exhibit a constant drug dissolution rate or concentration gradient respectively, and thus constant drug diffusion. Finally, drug release kinetics become first order with a decreasing gel layer thickness due to erosion or dissolution of the polymeric matrix and a decreasing drug concentration gradient within the gel layer (Colombo et al., 2000). In conclusion, drug release patterns from swellable erodible matrix drug delivery devices are a result of the specific contributions of drug diffusion, polymer relaxation and matrix erosion.

1.3.3 Geometrylarea Changes

In order to overcome the restrictions of decreasing drug concentration gradients within the gel layer and thus, a continuous diminishing diffusional release rate, attempts were made to coat the matrix devices in order to decrease the surface initially available for swelling (Geomatrix®). With time and increasing liquid penetration, the polymer swells, mostly to compensate the rapid decreasing drug concentration gradients and therefore the release rate remains constant.

1.3.4 Nonuniform Drug Distribution

In order to obtain uniform zero-order drug release profiles, this approach of controlled drug delivery, is based on decreasing drug concentration from the device core to the surface. The device is loaded with increasing amounts of drug from the core to the surface (e.g., multi-layered or press-coated tablets) resulting in a constant drug concentration gradient within the device during release.

1.4   **Parenteral Drug Delivery**

Parenteral drug delivery covers all routes of administration excluding the GIT. The European Pharmacopoeia defines parenteral preparations as "sterile preparations for administration by injection, infusion or implantation into the human or animal body". While the oral route remains the most popular, parenteral application of drugs is favorable when high blood plasma levels are immediately required (e.g., anesthesia, first aid medication in stroke or heart attack) or when oral administration is not indicated (e.g., unconscious patient, nausea, high first-pass metabolism). Furthermore, the implantation of specific devices is the only technique to obtain controlled drug delivery aiming at maintaining therapeutic concentrations over an extended period or at a specific site.

The simplest form of parenteral application is the injection (1-20 mL) or infusion (>100 mL) of liquid preparations. The European Pharmacopoeia distinguishes between concentrates, powders and gels for injection or infusion, respectively. Different parenteral preparations result from the stability, storage issues and the therapeutic purpose. Marketed preparations comprise, for example, injectable drug solutions, drug suspensions (zinc or NPH insulins), infusible emulsions (parenteral nutrition), infusions to substitute plasma fluids (plasma expanders), electrolytes, infusions for osmotherapy or peritoneal dialysis, and radiopharmaceutics.

Implantable devices for parenteral drug administration are far more complex. Implants are solid, drug containing controlled-release dosage forms for subcutaneous insertion. Administration usually happens via surgery into body tissue, blood vessels, hollow organs or fluid filled cavities. They are intended to control the release rate of the incorporated drug for an extended interval in order to locally maintain effective therapeutic concentrations at the application site, to reduce the administration frequency and to protect the drug from degradation in the human body (Kreye et al., 2008). In general, the dosage forms appear as implantable tablets made of different excipients with various dimensions. Recent research also focuses on the development of *in situ* forming implants which might avoid surgery (Hatefi et al., 2002; Packhaeuser et al., 2004). The idea is to inject a liquid drug formulation containing excipients which, upon contact with body fluids, undergo chemical or physical transformation into a solid or semi-solid implant. The principles of solidification include thermogelling, *in situ* polymerization and crosslinking, as well as self assembling, as a consequence to the contact with body fluids, altered polymer solubility or ionic conditions (Kretlow et al., 2007).

20

Readily implantable solid systems can be divided into two groups: inert non-biodegradable and biodegradable systems. The first group comprises medical grade silicone elastomers, polyvinyl- and polyethylene acetates and their copolymers, polypropylenes or dendrimers and polyethylenimine (Folkman and Long, 1964; Hoffman, 2008; Vorhies and Nemunaitis, 2008; Zaffaroni, 1971) and are already commercialized in form of ophthalmic inserts, intrauterine or subcutaneous devices (e.g., Ocusert®, Progestasert® from ALZA Corp. or Norplant® from the Population Council). The implants provide a controlled zero-order release which allows for maintaining therapeutic drug concentrations over an extended period of time. Despite their great contribution to controlled and sustained drug delivery in the past and present, systems like Norplant® have one inconvenience in terms of long-term biocompatibility: once the drug is completely released, the system has to be removed from the human body. This requires revision surgery. Even if it is only a matter of minimal invasive surgery, with regard to optimized patient acceptance and compliance future research should predominantly focus on biodegradable materials. Lloyd (2002) summarized the most important properties of biodegradable biomaterials as follows:

- The material should not evoke a sustained inflammatory or toxic response upon implantation in the body.
- The material should have acceptable shelf-life.
- The degradation time of the material should match the healing or regeneration process.
- The material should have appropriate mechanical properties for the indicated application and the variation in mechanical properties with degradation should be compatible with the healing or regeneration process.
- The degradation products should be non-toxic, and able to get metabolized and cleared from the body.
- The material should have appropriate permeability and processability for the intended application.

  (adapted from Nair and Laurencin, 2007)

Biodegradation takes place either by hydrolysis or enzymatic cleavage of the polymer bonds and subsequent polymer erosion. To date, a large range of synthetic and natural polymers are used for this purpose and they will surely gain growing importance in the upcoming years (Nair and Laurencin, 2007). Hydrolysis is the process of degradation for e.g.,

polyanhydrides, polyurethanes or the large group of poly(α-esters) like polylactides (PLA), polyglycolides (PLG) and their copolymers (PLGA), respectively. The latter are extensively studied in the form of resorbable sutures, orthopaedic fixation devices, in tissue engineering and regeneration, and for drug delivery (Biondi et al., 2007; Firestone and Lauder, 2010; Gentzkow et al., 1996; Schwartz et al., 1999). Existing dosage forms range from microparticles over nanostructures to electrospun fibers (Hans and Lowman, 2002; Sill and von Recum, 2008; Singh and Lillard, 2008; Tran et al., 2011). In recent years, PLGA became the most often investigated polymer for parenteral controlled drug delivery (Dong and Bodmeier, 2006; Elkharraz et al., 2001; Klose et al, 2006 and 2009; Lagarce et al., 2005; Moebus et al., 2009). In general, microparticles, containing the drug dissolved or dispersed in the PLGA matrix, are prepared. The resulting drug release kinetics is based on diffusion of the dissolved drug through water filled pores and to a lower extent through the polymer matrix, as well as by polymer erosion. Unfortunately, the PLGA degradation products create an acidic microclimate within the dosage form which promotes an autocatalytic acceleration of the ester bond cleavage and thus increased polymer erosion (Klose et al, 2006). The solubility of the incorporated drugs might alter and, more important, chemical interactions between drug and polymer are highly likely. This is especially problematic if the incorporated drug is a protein or a peptide (Estey et al, 2006; Lucke et al., 2002). As a result, the drug release patterns might significantly alter; become less controllable and predictable (Dunne et al., 2000; Giteau et al., 2002; Siepmann and Göpferich, 2001).

Lipid based implantable devices can overcome these restrictions and have gained growing interest in the past two decades (Kreye et al., 2008; Mohl et al., 2004; Koennings et al., 2006). Beneath collagen, albumin, poly(amino acids) and polysaccharides, lipids belong to the group of enzymatically degradable polymers (Nair and Laurencin, 2007). They offer several advantages, like biocompatibility (Guse et al., 2006b) and less expensive manufacture. Similar to hydrolytic biodegradable materials, the choice of the excipient properties is a means of tailoring the resulting dosage forms. Lipid implants appear in the shape of pellets, tablet-shaped discs of small diameter or as micro- and nanoparticles. The manufacturing strategies comprise compression, extrusion, melting and casting, solvent evaporation and coazervation techniques as well as high pressure homogenization (Kreye et al., 2011a/b; Maschke et al., 2007; Müller and Lucks, 1993; Pongjanyakul et al., 2004; Reithmeier et al., 2001; Schulze et al., 2008, Windbergs et al., 2009). Initially, research focused on the formulation with conventional drugs of chemical nature, which permitted to study release

behavior of a large range of lipid excipients as well as the underlying drug release mechanisms (Siepmann F. et al., 2008b). However, since then the scientific interest switched to biomolecules of therapeutic interest, predominantly with polypeptide and protein structure. Unfortunately, in terms of stability this group of therapeutic molecules is less easy to handle.

1.4.1 The Challenge: Protein Therapeutics

Protein drugs are a specific group of pharmaceuticals, with a high molecular weight and a particular structure required to provide a therapeutic effect. The defined and specific interplay between molecular composition and macromolecular conformation, a prerequisite for biological activity, renders them extremely sensitive to alterations of internal and external conditions (Wang, 2005). In general, proteins consist of four hierarchically classified structures: (i) the primary structure, the amino acid chain sequence, (ii) the secondary structure, the local organization of the primary structure by forming α-helix, β-sheet, random coil or turn structures (iii) the tertiary structure, the three-dimensional organization of the secondary structure, and the (iv) quaternary structure which is formed by several polypeptide chains (subunits) in order to create protein complexes. The mechanisms constituting the different structures include covalent bonds (primary structure), hydrogen bonds, salt bridges, hydrophobic and dipole interactions (secondary to quaternary structure). The preservation of these conformations is of utmost importance for the biological activity of a protein. Protein denaturation can affect each level and is often resulting in the formation of aggregates and subsequent loss of protein activity (Fersht, 2001). Protein aggregation can be reversible and follows specific pathways, as shown in Figure 1.4.1. Native proteins tend either to self-aggregate directly or to form intermediate species. In general, this step is rate limiting, due to the thermodynamically unfavorable state of the intermediates. Subsequently, they might form denatured species of the protein, which is usually a reversible process, or they aggregate. Aggregation itself might be reversible, but to a minor extent. If the aggregated state of the protein is kept for an extended interval it will result in irreversible precipitation. Factors responsible for protein denaturation will be discussed in more detail in *section 1.4.2 Freeze Drying*.

Liquid protein formulations hold the risk of potential protein aggregation, a diminished or absent biological activity, an increased immunogenic potential or the apparition of other side effects (Wang, 2010). Moreover, a protein solution which exhibits visible signs of precipitated proteins is barely accepted in commercial products (Wang, 2005). Therefore, protein
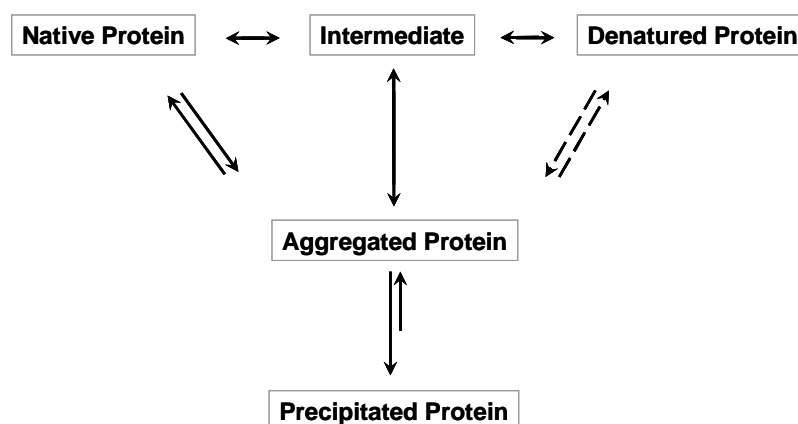
Figure 1.4.1: Major protein aggregation pathways (adapted from Wang, 2010).

therapeutics are often commercialized as dried products. Due to the sensitivity of those biomolecules to environmental stresses such as light, oxygen and in particular the temperature (see *section 1.4.2.4 Protection against Environmental Stresses/Storage*) freeze drying is the method of choice to obtain a solid protein product.

1.4.2 Freeze Drying

The freeze drying process consists of two distinct phases: the freezing of the protein solution, and the drying of the frozen protein solid under vacuum. The drying phase is divided in primary drying, characterized by the sublimation of ice; and the secondary drying, the desorption of water from the powder surface (Figure 1.4.2). Even if the freeze drying process is considered as a gentle method to prepare solid protein therapeutics, it generates stresses which destabilize proteins to various degrees (Kasper and Friess, 2011). An overview of the potential stresses for each freeze drying phase will be given in the next section.

1.4.2.1 Freeze Drying Stresses: Freezing

The most significant parameter in the first phase of a freeze drying process is the cooling rate and its influence on the ice crystal growth in the protein solution. Rapid cooling leads to formation of small ice crystals, being responsible for a large specific surface and small pores, whereas slow cooling rates create large ice crystals, large pores and small specific surfaces
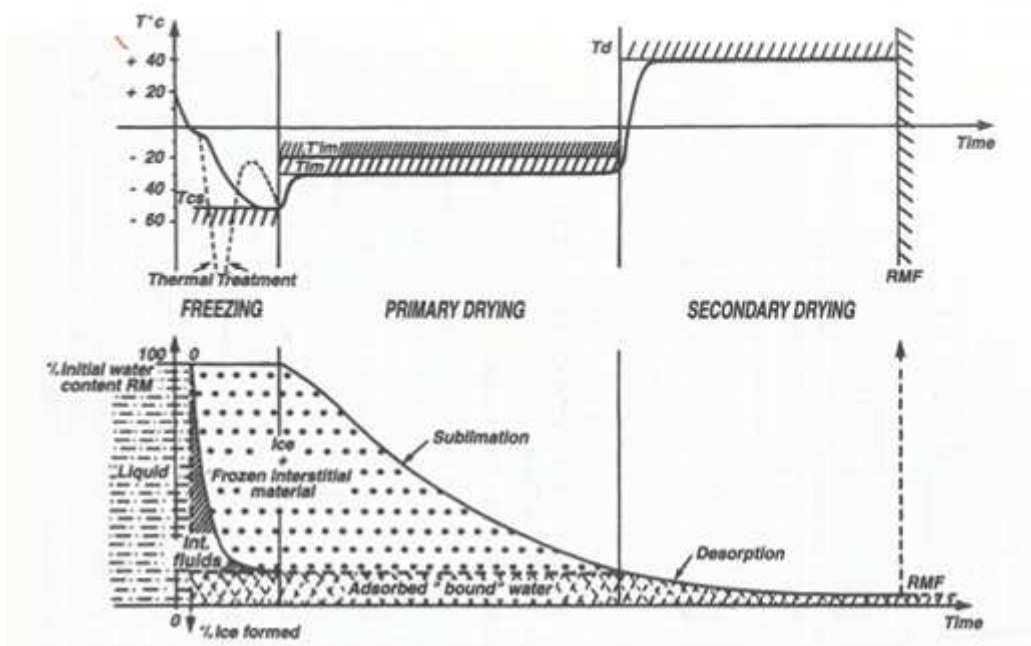
Figure 1.4.2: Schematic evolution of the freeze drying process. Temperatures (upper curve) and water content (bottom curve) are plotted versus time. In the temperature diagram T_{cs} = maximum temperature of complete solidification; T_{im} = minimum temperature of incipient melting; T_{lm} = absolute limit for fast process; T_d = maximum allowed temperature for the dry product; RMF, final requested residual moisture (from Rey, 2007).

(Bhatnagar et al., 2008; Kasper and Friess, 2011). This might significantly influence the drying behavior of the frozen solution (see *section 1.4.2.2 Freeze Drying Stresses: Drying*). Furthermore the ice crystal shape determines the properties of the ice-water interface, being responsible for potential surface-induced protein denaturation. Similarly, proteins can denature at liquid-liquid interfaces, created by phase separation of incompatible polymeric components in the protein solution or the altered solubility of a polymeric excipient upon freezing, forming liquid-solid interfaces (Heller et al, 1997, Kasper and Friess, 2011; Mathes and Friess, 2011). Moreover, protein stability largely depends on pH and ionic strength, which are limited to a narrow range. The choice of the cooling rate has an important impact on the freeze concentration of the buffered protein solution. Slow cooling results in more concentrated solutions and might lead to the crystallization of buffer components (Chang and Randall, 1992). This in turn might alter the pH of the remaining protein solution and increases the risk of protein denaturation (Anchordoquy and Carpenter, 1996, Pikal-Cleland et al., 2001). Also the buffer composition itself might impact the extent of protein aggregation

25

(Sarciaux et al., 1999). Another principal parameter is the specific cold denaturation temperature of a protein. Although its origins and principles are yet not fully understood, it was shown, that quantitative differences in protein denaturation might be linked to specific temperature intervals (Jaenicke, 1990). A possible explanation is the increasing solubility of proteins with decreasing temperatures due to extended hydrophilic intramolecular interactions and thus, enhanced external exposure of hydrophobic residues. Consequently, the hydrophobic intramolecular interactions, being responsible for the stabilization of the protein secondary and tertiary structure, decrease; and lead to protein cold denaturation. Other research groups showed similarities between cold and hot denaturation (Djikaev and Ruckenstein, 2008; Hatley and Franks, 1989; Scharnagl et al., 2005).

1.4.2.2 Freeze Drying Stresses: Drying

The principal stress affecting protein formulations during drying is based on the loss of the stabilizing hydration shell of the protein (Wang, 2000). In general, the hydration shell covers 30 to 35 % weight gain of the protein, whereas residual moisture after freeze drying is less or equal to 10 %. In order to compensate the loss of stabilizing water molecules the protein tends to eliminate charges (Rupley and Careri, 1991). This favors hydrophobic interactions, denaturation and aggregation of the protein. Additionally, the sublimation rate in the drying phase might significantly affect protein integrity. The latter is a function of several parameters: the surface area of the frozen solid, resulting from the creation of small or large ice crystals and a more or less porous network; the difference between the product and condenser temperature; the pressure conditions and the formulation composition (Bindschaedler, 1999; Willemer, 1992). Importantly, the drying phase should be well adapted to the protein formulation and be as short as possible, to avoid excessive exposition of the protein to unfavorable conditions. Therefore, temperature should be selected below but close to the collapse temperature of the protein to ensure a frozen cake with an optimized porous network, minimal resistance against water evaporation at the sublimation front and an optimal product/chamber pressure ratio. The endpoint of the drying phase is determined by the desired residual moisture of the system. However, care has to be taken in order to prevent overdrying of the formulation and potential inhomogeneous distribution of the residual moisture (Pikal and Shah, 1997).

1.4.2.3 Mechanisms of Protein Stabilization during Freeze Drying

According to the above mentioned factors potentially affecting protein biological activity during freeze drying, certain procedures have to be adopted to stabilize those formulations. In addition to the adjustment of the ionic strength and the pH by choosing an appropriate buffer composition, the protein solutions can be blended with stabilizing excipients. Depending on their mechanism of action during freezing and/or during drying, these excipients are classified as cryo- and lyoprotectants. Table 1.4.1 gives an overview on commonly used stabilizers and the corresponding mechanisms of action.

Several mechanisms of protein protection during freezing and drying processes are proposed in literature, being more or less confirmed by experimental data. Initially, a protein formulation intended for freeze drying is liquid. Consequently, mechanisms, valid for the stabilization of protein solutions, are also applicable to the freezing process. In order to effectively preserve the native state and their activity, proteins need to maintain their specific conformation. This is ensured by intra- and inter-molecular interactions, a certain molecular flexibility and the hydration shell that stabilizes the proteins via hydrogen bonds. The first, and also the most widely accepted stabilizing mechanism is **preferential interaction**. In solution, proteins prefer either to interact with water or an excipient. If the solution contains a stabilizing excipient, the latter is preferentially excluded from the proteins surface. The preferential surface hydration is based upon the formation of more stable hydrogen bonds between proteins and water (Arakawa et al., 1991; Lin and Timasheff, 1996; Timasheff, 1993). Nema and Avis (1992) demonstrated the validity of this theory for a broad range of stabilizers. However, the concentration of the stabilizer in solution, the stabilizer:protein molar ratio and their maximum concentrations should also be considered (Arakawa et al., 1993; Carpenter and Crowe, 1989; Tanaka et al., 1991). Additionally, the size of the formed ice crystals might have a stabilizing effect due to its influence on the created **ice-water interface** and thus, the surface denaturation of proteins (Cochran and Nail, 2009).

Other proposed stabilizing mechanisms during freezing include the inhibition of **pH alterations** or an increased **viscosity**. Freeze concentration of all solution components may initially increase denaturing interactions, but a steep increase in viscosity occurring at the same time hinders the diffusion of reactive species in the solution and hence, the chemical denaturation of the protein (Pikal, 1999). In addition, an elevated viscosity immobilizes the protein molecules and avoids intermolecular interactions.

Table 1.4.1: Commonly used cryo- and lyoprotectants in freeze drying.

Stabilizer	Type of stabilization	Study
Sugars/Polyols	Cryo- and Lyoprotectants	
Monosaccharides		Nema and Avis (1992)
Di- and Polysaccharides		Carpenter et al. (1987), Moreira et al. (1998)
Polyols		Tanaka et al. (1991), Kadoya et al. (2010)
Polymers	Cryo- and Lyoprotectant	Allison, et al. (1998), Anchordoquy and Carpenter (1996)
Proteins	Cryo- and Lyoprotectant	Anchordoquy and Carpenter (1996), Ruddon and Bedows (1997)
Nonaqueous solvents	Cryoprotectant	Arakawa et al. (1991), Greiff et al. (1976), Yong et al. (2009)
Salts	Cryo- and Lyoprotectant	Carpenter et al. (1987), Izutsu et al. (2009), Yoshioka et al. (1993)
Metal ions	Cryo- and Lyoprotectant	Carpenter et al. (1987 and 1988)
Amphiphilic excipients	Cryoprotectant	Anchordoquy et al. (2001), Izutsu et al. (1993a), Yong et al. (2009)
Amino acids	Cryo- and Lyoprotectant	Carpenter et al. (1990), Pikal-Cleland et al. (2002)

In general, the stabilizing capacity of certain excipients during the drying phase can only be explained by their combinatory effect. Some authors, among them Franks (1994), mentioned **glass formation** of the excipient which immobilizes the protein structure and prevents the relaxation of its conformation, a major reason for protein denaturation. This is consistent with the theory of increased viscosity as discussed above. Carpenter et al. (2007) doubted this theory, at least when glass formation is considered as exclusive mechanism: a protein solution without excipients already forms glasses but turned out to be instable. A theory which is related to the preferential interaction in solution is the **replacement of water**.

In order to stabilize the protein conformation, a hydration shell (of approximately one third of the protein molecular weight) on the surface is necessary to interact via hydrogen bonds. As mentioned above, during the dehydration phase less than 10 % of residual moisture remains in the freeze dried product. In order to stabilize the protein structure, water molecules might be replaced by excipients with hydrogen bond forming capacities (e.g., sugars, polyols and polymers) on the protein surface (Arakawa et al., 1991; Carpenter et al. 1990; Carpenter and Crowe, 1989).

This theory can be accepted within the limits of a contradictory sterical hindrance as it can be observed for high molecular weight protectants like polymers. However, they have been proved to be effective stabilizers. The polymer molecular weight can also be of advantage in preventing protein interaction through **sterical hindrance** by intercalating polymer chains. Another advantageous property of polymers and also other stablizers is the ability to increase the **glass transition temperature** (T'_g) of protein formulations (Costantino et al., 1998; Crowe et al., 1993a and 1993b). The higher the T'_g the less likely is the loss of α-helices and the increase of β-sheet, random and turn structures, which are predominantly responsible for protein aggregation, at least due to their lower dipole moment (Querol et al., 1996).

Furthermore, **electrostatic interactions** can stabilize proteins by the inhibition of charge elimination resulting from the dehydration step (Gibson, 1996; Izutsu et al., 2009, Rupley and Careri, 1991). In conclusion, a combinatory effect of several stabilizing mechanism during freeze drying of protein formulations seem to be more likely than a single one.

1.4.2.4 Protection against Environmental Stresses/Storage

Optimal stabilization of a protein formulation during preparation is not necessarily a guarantee for its stability during storage. Knowing for the sensitivity of proteins against temperature, light, moisture, pH and oxidative stresses, destabilization of solid protein formulations by numerous mechanisms might occur. In general, instabilities can be of physical and chemical nature. A major reason for instability is protein aggregation due to either non-covalent or covalent interaction (Wang, 2000). Non-covalent interactions often imply a change in intra- and inter-molecular hydrogen bonds, hydrophobic interactions and thus, altered protein conformation. Covalent interactions are mainly due to chemical degradation processes like deamidation, oxidation, hydrolysis, browning reactions and the formation of disulfide bonds. However, it has to be pointed out that aggregation can be reversible and does not automatically lead to protein precipitation and subsequent activity loss

(Figure 1.4.1). In order to preserve the native protein structure during storage several preliminary measures should be considered. Solid protein formulations are stabilized somewhat similarly to liquid formulations (see *section 1.4.2.3 Mechanisms of Protein Stabilization during Freeze Drying*) by immobilization in a glassy matrix, water replacement and hydrogen bonding. Therefore, the appropriate choice of the pH, ionic strength, buffer components, bulking agents, type and concentration of stabilizers as well as the protein concentrations are of utmost importance for the resulting dried product.

Additionally, factors that affect protein stability, like storage temperature, formulation T_g, residual moisture and crystallinity of amorphous excipients should be considered. Importantly, protein stability is a function of the combinatory effect of all those parameters. Freeze dried proteins always contain a certain residual moisture which creates a solid state microenvironmental pH (Strickley and Anderson, 1997), determines the crystallized amount of amorphous components, the decrease in T_g, an increase in protein molecular mobility and an increase in chemical degradation reactions. Water also plays an important role: upon reconstitution of a freeze dried protein formulation: the resulting pH might differ due to volatilization of buffer components during drying. Accurate adjustment of the reconstitution medium is therefore required. Further, the temperature is an important parameter to consider. Firstly, because of its influence on the protein rehydration and refolding upon reconstitution, secondly by its capacity to accelerate chemical and physical degradation of the proteins and finally by its influence on the T_g of the formulation. In general, the T_g of a freeze dried formulation should be as high as possible to ensure the preservation of the glassy state. The latter is associated with an elevated stability due to a reduced molecular mobility of the protein within the glassy matrix (Duddu and Dal Monte, 1997). Consequently, the resulting T_g of a protein formulation is recommended to be at least 20 °C above the storage temperature (Franks, 1994). Furthermore, the T_g is also affected by excipients added to the formulation. Cryo- and lyoprotectants like sugars, polyols and polymers in particular, are known to increase the T_g and might even multiply their efficiency in combination (Arakawa et al., 2001; Carpenter et al., 1993; Espinosa et al., 2006; Izutsu et al., 1993b and 1995; Liu et al., 2005; Prestrelski et al., 1993a). However, the high molecular weight of polymers might limit their stabilizing effect due to an insufficient capacity to form hydrogen bonds with the protein (Kreilgaard et al., 1998; Schebor et al., 1996).

Consequently, the advantageous and detrimental effects of all influencing factors have to be well balanced to obtain a stable freeze dried protein product. Despite the progress in

research on protein stabilization, stabilizing and destabilizing parameters and their mechanisms are yet not fully understood. Thus, giving general recommendations for the formulation of stable protein products remains highly challenging. In order to avoid the often excessive trial-and-error based studies for the development of new protein formulations (Nail et al., 2002) extensive effort in protein (formulation) research is needed.

1.4.3 Protein Delivery Systems Based on Lipids

As already mentioned in the preceding section, extended and controlled delivery of protein therapeutics requires maintaining protein bioactivity during processing, storage and release, together with the compatibility of the protein with the excipient and adjusted release profiles. Attempts to combine protein therapeutics with polymeric devices might engender protein instabilities or require additional excipients to stabilize the protein from denaturation due to potential interactions with polymer degradation products (Estey et al., 2006; Kang and Schwendemann, 2002; Kang et al., 2008; Schwendemann, 2002). Therefore, lipid carriers for controlled delivery of proteins were proposed as alternatives by several authors. With regard to simplicity, a desired form of application is the injectability of lipid protein carriers. Therefore, special requirements for the size of these dosage forms are necessary. Cui and Mumper (2002), for example, introduced antigen coated wax nanoparticles to enhance the immunogenic response in mice.

Furthermore, protein loaded microparticles were proposed by different research groups (Del Curto et al., 2003; Maschke et al., 2007; Reithmeier et al., 2001; Ribeiro Dos Santos et al., 2002). The peptides and proteins GnRH, BSA, or insulin were processed either by coating, melting, solvent evaporation or spray congealing on or with lipid excipients resulting in *in vitro* release profiles from 30 min up to 1 month. The type of lipid used, especially the fatty acid chain length, the degree of esterification as well as the preparation technique have shown to be of great importance. Lipid implants of larger size, either in disc shape, as an implantable cylinder or in pellet or tablet form are also discussed in literature (Kaewvichit et al., 1994; Pongjanyakul et al., 2004; Killen and Corrigan, 2006; Mohl and Winter, 2004; Koennings et al., 2006 and 2007a; Appel et al., 2006). Similar to the microparticle formulations, the formulation parameters impacted the resulting drug release profiles. Diffusion through water filled pores and erosion of the lipid matrix material were identified as predominantly underlying drug release mechanisms (Guse et al., 2006a; Zaky et al., 2010). Thus, to ensure complete protein release a consistent porous network with adequate pore sizes

needs to be created (Mohl and Winter, 2004). Incorporation of hydrophilic fillers might affect the porosity and thus the performance of the device (Herrmann et al., 2007a/b; Killen and Corrigan, 2006; Vogelhuber et al., 2003). In contrast, this might also be impedimental with regard to the protein release. Incorporation of hydrophilic excipients might lead to an undesired increase in the initial burst. However, a double effect on the release of IFN-α was shown upon the incorporation of polyethylene glycol 6000 (PEG) as a release rate modifier in compressed and extruded implants (Mohl and Winter, 2004; Herrmann et al., 2007a/b; Schulze et al., 2009). Firstly, the burst effect decreased with increasing PEG content due to a more compact packing density of the matrix forming particles. Upon contact with water the PEG slowly dissolves, creating a barrier for the IFN-α diffusion through the water filled porous network of the matrix. Subsequently, with progressing PEG dissolution the porosity of the implants gradually increased, resulting in faster drug release rates which ensured the complete recovery of the protein. In general, the drug release kinetics from lipid implants mainly depends on following parameters: the type and amount of the lipid, the drug and additional excipients, the drug distribution within the implant, the type of preparation method and the mechanical stability of the system.

1.4.3.1 Drawbacks

The major challenge in the development of protein loaded lipid implantable devices is to ensure the release of an active biomolecule. Protein stability might be affected by numerous parameters. Firstly, the process parameters, namely the choice of solvents, excipients and environmental conditions should carefully be chosen to avoid possible sources for protein denaturation. Koennings et al. (2006 and 2007a/b) conducted studies on lipid implants and reported that the protein denatured at the oil-water-interface during preparation via an emulsion technique. Pongjanyakul et al. (2004) prepared lysozyme loaded lipid pellets by two distinct techniques: compression and melting of a lipid/lysozyme powder blend. Additionally, they investigated the effect of hydrophilic excipients, PEG 4000 and Gelucire 50/13 on the resulting drug release kinetics. While for both preparation methods the lysozyme activity was almost completely recovered, the incorporation of Gelucire 50/13 led to decreasing enzymatic activities. This was attributed to lysozyme adsorption on the surface of dispersed lipid material, resulting in surface-induced protein denaturation (see *section 1.4.2.1 Freeze Drying Stresses: Freezing*). Furthermore, the conditions during *in vitro* drug release studies might engender a loss of biological activity as reported by Maschke et al. (2007). Here, the insulin

activity considerably decreased due to dimer formation and a generally increased degradation rate at higher humidity levels.

1.4.3.2 How to Preserve Protein Activity?

Mechanisms and techniques relevant for the protection of proteins during freeze drying and storage can also be applied for the stabilization of sensitive biomaterials in lipid implants (see *section 1.4.2.4 Protection against Environmental Stresses/Storage*). Mohl and Winter (2006) proposed trehalose and hydroxypropyl-β-cyclodextrin (HP-β-CD) as stabilizing excipients for the lyophilized IFN-α loaded tristearin implants. They reported that HP-β-CD was more effective in protein stabilization than trehalose, probably due to the particular properties of the cyclodextrin to form drug-cyclodextrin inclusion complexes. Hence, protein aggregation could be prevented by reducing hydrophobic interactions with the lipid matrix during drug release. Furthermore, an interesting approach, namely to embed the sensitive protein in a protective hydrophilic coating, was proposed by Lee et al. (2005). In contrast to the enormous research activity to protect biomolecules from denaturation during freeze drying performed in the last decades, the protection of protein structures in lipid implants have attracted minor attention. Even though biological activity of proteins is often preserved to an acceptable extent during release from lipid implants, optimization of these systems is highly desirable, especially with regard to administration frequencies and thus patients' compliance. Therefore, further studies investigating the effects of protectants on protein stability during preparation and release are of utmost importance.

1.5   Hybrid Drug Delivery Systems

Parenteral drug delivery also comprises the combination of implantable medical devices and an active pharmaceutical ingredient. As it was already discussed in *section 1.1 General*, two different strategies can be distinguished: blending of the drug with the device or at least parts of the device (matrix systems) or drug deposition on the device surface (coated systems) (Simchi et al., 2011). These approaches are implemented in practice by the development of drug loaded bone cement, drug-eluting stents, impregnated pace makers or cochlear implants for the delivery of anti-inflammatory drugs or growth hormones. Drug loaded bone cements, originally used as medical device to promote bone neogenesis and tissue replacement (Wu and Grainger, 2006) are now utilized for nearly two decades as drug delivery systems. They contain antibiotics, antimicrobial peptides or growth factors. The conventionally used non-biodegradable drug loaded polymethylmethacrylates (PMMA), commercialized as Simplex®, Palacos® or Septopal® recently are often replaced by alternative materials, for example synthetic hydroxyapathite (HAP) or polyesters [poly(L-lactic acid), PLA; poly(glycolic acid), PGA; poly(lactic-*co*-glycolic acid), PLGA] or polyhydroxyalkanoates (PHA) due to their improved biocompatibility or biodegradability (Ginebra et al., 2006; Habraken et al., 2007; Lee and Shin, 2007; Luginbuehl et al., 2004).

A further important field of research are drug eluting stents (DES) aiming at the delivery of antibiotics, anti-inflammatory or immune-suppressive drugs to blood vessels and hollow organs concomitantly to cancer therapy or in the aftermath of cardiovascular diseases. Inert or biodegradable materials like stainless steel and metal alloys or poly(L-lactic acid) and polycarbonate are combined with a controlled release drug formulation: either by direct absorption of the drug on the surface, incorporation in a matrix or on-stent coating (Ormiston, 2009; Wu, 2006).

Polymeric drug coating on medical devices is a common technique not only for DES but can also be found for urinary and central venous catheters, tissue engineering for pacemakers, and other implantable devices as for example cochlear implants. The latter will be discussed in more detail in the next section.

1.6   Cochlear Implants

The origins of hearing loss are diversified: they can be of physical or chemical origin, caused by certain diseases or autoimmune reactions (Swan et al., 2008). Physical factors affecting the hearing capacity are chronic or acute noise exposition, head and neck radiation in line with cancer therapy or intracochlear surgical trauma. Ototoxic antibiotics as well as chemotherapeutics for cancer treatment are held responsible for chemical-induced hearing loss. Furthermore, viral infections or vascular events are considered to be responsible for sudden sensoneurinal hearing loss, whereas a deficiency in autoimmune regulation might also decrease the hearing capacity. Hair cell loss, degeneration of the stria vascularis, loss of spiral ganglion cells are only some examples for the possible damage in the complex hearing apparatus (Jereczek-Fossa et al., 2003). The extent and reversibility of the hearing loss highly depends on its nature.
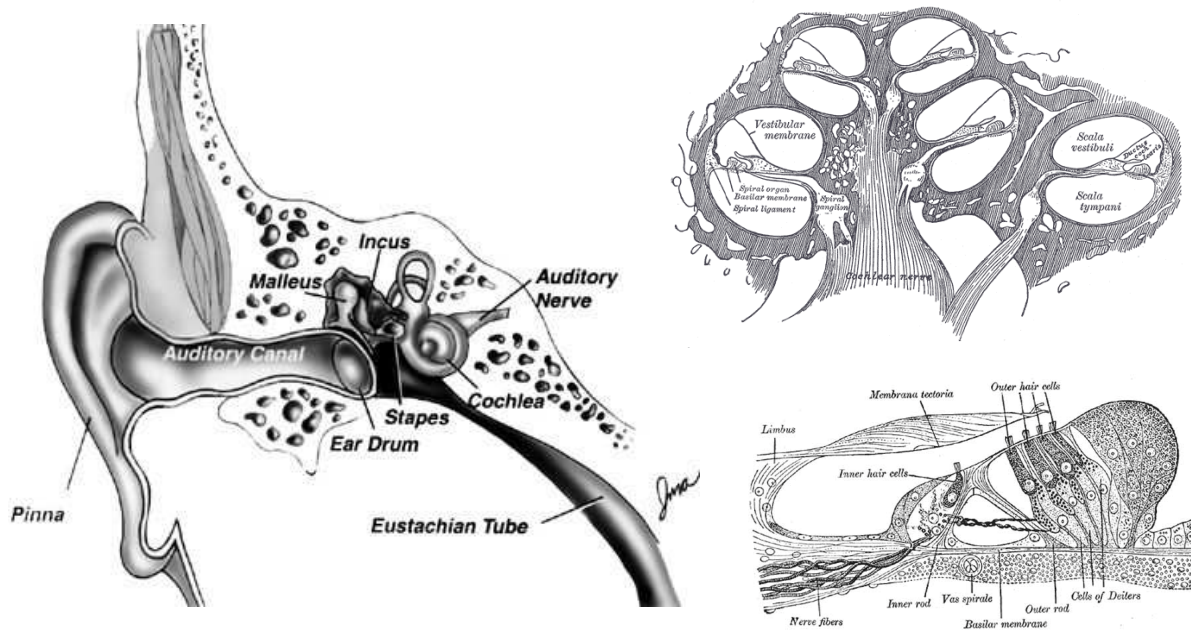

Figure 1.6.1: Schematic drawing of the auditory apparatus (left), a cross section of the cochlea (upper right) and the organ of corti (bottom right). (Images from NIDCD; Gray's Anatomy).

The cochlea is an intermediate part in the hearing apparatus, connecting the receiving (the acoustic organ) to the processing unit (auditory regions of the brain). Sound waves are received, transformed in mechanical signals and transmitted to the cochlea. Figure 1.6.1 gives an overview on the anatomy of the auditory apparatus. In the cochlear, exactly, in the scala

tympani, filled with perilymph (the main fluid in the cochlea with a composition similar to plasma), the transformed mechanical signals are received by hair cells, which move to different extents according to the frequency and the amplitude of the initial acoustic signal. This movement induces an electric impulse which is subsequently emitted to the auditory regions of the brain. This elaborated process results in the perception of sound. If this system is perturbed or the hair cells exhibit defects - for reasons mentioned above - cochlear implantation can be a useful tool to restore hearing capacity. The idea is to insert an electrode array embedded in a silicone elastomer body into the scala tympani of the cochlea. The electrodes are connected to an amplifier, subcutaneously inserted behind the patients' ear. Acoustic signals are received, transformed and transmitted to the electrodes, replacing the physiologic system (Figure 1.6.1). Subsequently, an electric stimulus, according to the initial signal, is emitted to the hair cells and transmitted to the responsible cerebral regions. Consequently, the patient is able to regain hearing capacity.

1.6.1 Drug Delivery to the Cochlea

In general, therapeutic approaches focus on steroid treatment, antioxidants, if the damage is caused by free radical species, growth factors and methotrexate in the case of autoimmune diseases. However, successful treatment and prevention of hearing loss is a function of the amount and interval of therapeutic drug levels that can locally be achieved in the cochlea. Systemic administration often requires elevated drug doses due to the relatively low passage of drugs between plasma and the intracochlear cavity. The blood-cochlear barrier, which is anatomically and functionally similar to the blood-brain barrier effectively hinders drug transport from the systemic circulation via tight junctions. Hence, the increased risk of possible severe side-effects might require a premature abandoning of the therapy. Attempts to overcome these restrictions are local administration of drug solutions or placing drug delivery systems at or in proximity of the site of action (e.g., round window membrane).

Intratympanic drug delivery is extensively reviewed in literature (Doyle et al., 2004; Salt and Plontke, 2005; Staecker et al., 2010; Swan et al., 2008) including intratympanic injection, hydrogel-based and polymeric controlled release devices, nanoparticles, microcatheters, mini osmotic pumps and microwicks. In general, the drug is placed in the middle ear, precisely in the intratympanic cavity, where it is left to diffuse through the round window membrane (RWM) to access the scala tympani. This approach can cause several disadvantages due to the barrier function of the RWM: diffusion of the drug often results in a steep concentration

gradient from the cochlear base to the apex (Plontke et al., 2007 and 2008); in the worst case apical concentrations remain below the effective therapeutic concentrations. In addition, RW membrane properties, like thickness, hydration, pore size, disease state and charge extremely depend on the intra- and inter-individual variability and the nature of the applied drug delivery system (Goycoolea and Lundman, 1997; Mikulec et al., 2008; Nordang et al., 2003). Thus, a system which has proven to be effective in some patients might fail in others.

Alternatively, drugs can be delivered directly to the cochlear cavity. The simplest method is the injection of a drug bolus through the RWM into the scala tympani (Borkholder, 2008; De Ceulaer et al., 2003; Paasche et al., 2009). Salt et al. (2007) first demonstrated the pharmacokinetics of the model substance trimethylphenylammonium (TMPA) after injection in the basal turn of the scala tympani. Drug distribution occurs mainly by diffusion, however the flow in the cochlea is extremely slow (Ohyama et al., 1988; Plontke et al., 2007). Consequently, when the injection ends, the drug concentration at the injection site decreased with time. This is further promoted by drug loss to other compartments, like cerebrospinal fluid or blood. Importantly, the injection procedure might lead to visibly undetectable leaks, resulting in low drug concentrations in the scala tympani. Hence, controlling the injection procedure is essential. However, this technique requires frequent injections and harbors the risks of infections. Drug release over an extended interval can also be obtained by implantable drug delivery systems in the form of osmotic pumps (Brown et al., 1993, Paasche et al., 2003) or reciprocating perfusion systems (Chen et al., 2005). The idea is to connect a catheter, implanted in the cochlear cavity, to a pump containing or being connected to a drug reservoir. The drug can hence be released in a controlled manner at predetermined time points or over an extended interval. However, an inconvenience is the necessity of a surgery to remove the device after successful treatment. Therefore, recent research activities focus on the development of drug delivery systems which are able overcome these restrictions.

1.6.2 Drug Delivery from Cochlear Implants

A straightforward approach is to profit from the cochlear implant for drug delivery purposes. The cochlear implant can, for example, be provided with a polymeric coating (Richardson et al., 2009; Simchi et al, 2010). However, this approach might alter the implant and electrode properties. Moreover, the coating polymer might have possible toxic effects (Staecker et al., 2010). Hochmair et al. (2006) reviewed a port and septum cochlear implant allowing for multiple injections with minimal risk of bacterial contamination. What appears to

be the simplest approach is the incorporation of a drug in the silicone part of the cochlear implant. However, several obstacles have to be overcome, as for example the homogeneous distribution of the drug in the hydrophobic silicone, possible alterations of the mechanical properties of the implant and, importantly, tailoring of the drug release kinetics. Fahramand et al. (2010) first presented a drug eluting cochlear implant containing dexamethasone in the silicone elastomer part of the electrode. Dexamethasone, an anti-inflammatory drug commonly used for the prevention and treatment of postsurgical inflammations of cochlea tissue and apoptosis of hair cells was investigated for its ability to control and sustain the drug release. The presented hybrid systems exhibited a burst release, possibly due to drug particles on or near the device surface. Micronized dexamethasone was successfully dispersed in the silicone elastomer forming a monolithic device which exhibits diffusion controlled drug release. The resulting drug release profiles range from approximately 30 to 60 % after 90 weeks, being adaptable to the disease state. However, the provided data might be completed by detailed information about the mechanical properties of the system and the behavior of the latter in conditions mimicking those within the cochlea on a larger scale. With regard to the targeted extended release periods the optimization of such devices is time- and cost-consuming and often based on trial and error series. Hence, identification of a suitable simplified mathematical theory allowing for the quantitative prediction of the effects of key formulation parameters of these miniaturized implants (including system dimensions and device composition) on the resulting drug release kinetics can provide a straightforward and inexpensive method to achieve this objective.

1.7   Research Objectives

According to the information provided in the preceding sections the purposes of this work were defined as follows:

- To develop a colon targeting matrix formulation comprising an anti-inflammatory drug for oral administration and a polysaccharide which is susceptible to enzymatic degradation by colon-specific bacteria. Furthermore, to characterize and optimize a selected system with regard to process parameters, pharmacokinetics and patient compliance.

- To gain further insight on the mechanisms of cold denaturation of protein therapeutics during the freeze drying process by using model proteins with various properties and sensitivities to environmental stress. Additionally, to identify and characterize selected protein formulations containing stabilizing excipients using biochemical and physical analytical methods. Based on these results, to develop and characterize protein loaded matrix formulations for parenteral administration containing stabilizing excipients.

- To develop and characterize a hybrid drug delivery device for cochlear implantation containing an anti-inflammatory drug in the matrix forming part aiming at the prevention and prevention and treatment of implant insertion-induced inflammatory reactions and apoptosis of hair cells. Furthermore, to develop a simplified mathematic model by applying an analytical solution of Fick's second law of diffusion on the results of *in vitro* drug release measurements from model devices allowing for the quantitative prediction of key formulation parameters on the drug release kinetics from miniaturized implants of various dimensions.

2 Experimental

2.1 Materials

Drugs: 5-Aminosalicylic acid (5-ASA; Falk Pharma, Freiburg, Germany); α-chymotrypsine, dexamethasone base (Discovery Fine Chemicals, Dorset, United Kingdom); L-lactic dehydrogenase (LDH) from rabbit muscle Type II (ammonium sulfate suspension) and lysozyme from chicken egg white (lyophilized powder) (Sigma Aldrich; Lyon, France).

Matrix formers: glyceryl behenate (Compritol® 888 ATO) and glyceryl palmitostearate (Precirol® ATO 5) (Gattefossé, St. Priest, France); glyceryl trimyristate, glyceryl tripalmitate, glyceryl tristearate, hardened soybean oil (Dynasan® 114/116/118/120) and synthetic hard paraffines (Sasolwax® Spray 30 and Synthetic Wax) (Sasol, Witten, Germany); hydrogenated soybean oil (Sterotex® HM) and hydrogenated cottonseed oil (Sterotex® NF) (Abitec, Janesville, Wisconsin, USA); Microwax® HG and Microwax® HW (Paramelt, Heerhugowaard, The Netherlands); kit for the preparation of a silicone elastomer (MED-4735; consisting of two parts: Part A = amorphous silica, Part B = amorphous silica, dimethyl-methylhydrogen siloxane copolymer and a platinum based curing system; NuSil Technology, Carpinteria, CA, USA).

Fillers: chitosan (Protasan® CL 213, 75-90 % degree of deacetylation; Novamatrix, FMC BioPolymer, Drammen, Norway); microcristalline cellulose (MCC, Avicel® PH 101; FMC BioPolymer, Brussels, Belgium); Nutriose® FB 06 (Nutriose, a water-soluble, branched dextrin with high fiber contents obtained from wheat starch; Roquette Freres, Lestrem, France); poly(vinylpyrrolidone) (PVP, Povidone® K 30, Cooperation Pharmaceutique Francaise, Melun, France).

Stabilizers: glucose, sucrose, maltose, maltitol, sorbitol, poly(vinylpyrrolidone) (Povidone® K 25 and K 90, ISP Technologie; Roissy, France); glycerol, polyethylene glycol 400, D-(+) trehalose dehydrate (Sigma Aldrich, Lyon, France); polyethylene glycol (PEG 6000 and PEG 10000) (Clariant; Gendorf, Germany).

Reagents: albumine from bovine serum (Cohn V fraction), bicinchoninic acid solution, copper (II) sulfate pentahydrate, guanidine hydrochloride, micrococcus lysodeikticus (lyophilized cells), β-nicotinamide adenine dinucleotide (reduced disodium salt, NADH), sodium azide, sodium pyruvate, urea (Sigma Aldrich, Lyon, France); pancreatin (from mammalian pancreas = mixture of amylase, protease and lipase) and pepsin (Fisher Bioblock, Illkirch, France); calcium chloride dihydrate, magnesium sulfate tetrahydrate, potassium

40

chloride, sodium chloride, 4 (2 hydroxyethyl)piperazine-1-ethanesulfonic acid (HEPES Pufferan) (Carl Roth, Lauterbourg, France).

Emulsifiers: Brij®78 (ICI Surfactants, Wilton, UK).

Solvents: acetonitrile, dichloromethane, tetrahydrofuran (HPLC grade, Fisher Scientific, Illkirch, France).

Medical device: a cochlear implant prototype, consisting of an array of electrodes embedded in a silicone matrix (Neurelec, Vallauris, France);

2.2   Methods

Colon Targeted Drug Delivery

2.2.1   Preparation of Matrix Pellets

Matrix pellets containing 60 % 5-ASA were prepared by extrusion-spheronisation. The drug, Nutriose and the respective lipid(s) were blended and granulated manually with demineralized water in a mortar with a pestle. The obtained wet mass was extruded using a cylinder extruder with two counter-rotating rollers (1 mm orifice, 3 mm thickness, extrusion speed = 32 rpm, GA 65 extruder; Alexanderwerk, Remscheid, Germany). The extrudates were subsequently spheronized (Caleva model 15; Caleva, Dorset, UK) for 180 s at 364 rpm. The obtained pellets were dried for 24 h in an oven at 40 °C and sieved (fraction: 0.71-1.00 mm). If indicated, the pellets were cured for specific time periods at defined temperatures in an oven. The homogeneity of the drug content of the pellets was within specifications (data not shown).

2.2.2   Preparation of Mini Tablets

5-ASA, Nutriose and the respective lipid(s) were blended manually in a mortar with a pestle. Mini tablets (50 % drug loading) were prepared by:

(i) direct compression on a Frank 81802 (Karl Frank, Birkenau, Germany), equipped with a 2 mm diameter punch set (Korsch, Berlin, Germany), or

(ii) compression of granules obtained via melt granulation. If not otherwise stated, the respective compounds were heated and mixed on a water bath at 85 °C. After cooling to room temperature, the obtained mass was ball milled, sieved (fraction 50-100 µm) and compressed using the same equipment as in (i).

The tablet height was 2 mm. Optionally, the tablets were cured in an oven for different time periods at various temperatures, as indicated.

2.2.3   Drug Release Measurements

Drug release from matrix pellets was measured in 120 mL cylindrical plastic flasks (diameter: 5.5 cm, height: 6.5 cm) containing 100 mL release medium: 0.1 N HCl [optionally containing 0.32 % (w/V) pepsin] for 2 h and phosphate buffer pH 6.8 (USP 34) [optionally containing 1.0 % (w/V) pancreatin] for 8 h (complete medium change after 2 h). The flasks were agitated in a horizontal shaker (37 °C, 80 rpm, n = 3)

(GFL 3033; Gesellschaft fuer Labortechnik, Burgwedel, Germany). At pre-determined time points, 3 mL samples were withdrawn (replaced with fresh medium), filtered and analyzed UV-spectrophotometrically at $\lambda = 302.4$ nm (0.1 N HCl), or $\lambda = 331.2$ nm (phosphate buffer pH 6.8) (UV-1650PC; Shimadzu, Champs-sur-Marne, France). In the presence of enzymes, the samples were centrifuged at 13000 rpm for 10 min (Universal 320 centrifuge; Hettich, Tuttlingen, Germany) and filtered (0.2 μm, PTFE) prior to UV measurements.

Drug release from mini tablets was measured using the USP 34 apparatus 3 (Bio Dis; Varian, Les Ulis, France) (37 °C, 5 dpm, n = 3) in 200 mL release medium: 0.1 N HCl for 2 h and phosphate buffer pH 6.8 (USP 34) for 8 h (complete medium change after 2 h). At pre-determined time points, 3 mL samples were withdrawn (replaced with fresh medium), filtered and analyzed UV-spectrophotometrically as described above.

2.2.4 Determination of Drug Solubility

Excess amounts of 5-ASA were placed in contact with 0.1 N HCl and phosphate buffer pH 6.8 at 37 °C in a horizontal shaker (80 rpm, GFL 3033). Samples were withdrawn every 12 h, filtered and analyzed for their drug content as described in *section 2.2.3 Drug release Measurements* until equilibrium was reached.

2.2.5 Thermal Analysis

Thermograms of different types of pellets and raw materials (for reasons of comparison) were measured by differential scanning calorimetry (DSC1; STARe Software; Mettler Toledo SAS, Viroflay, France). Pellets were gently crushed in a mortar with a pestle and approximately 7 mg samples were heated in sealed aluminum pans (investigated temperature range: 20 to 90 °C, heating rate: 10 °C/min).

Protein Drug Delivery

LDH

2.2.6 Preparation of Freeze Dried Protein Samples

LDH (suspension as received) was dialyzed against phosphate buffer (10 mM, pH 7.5) at 4 °C for 20 h prior to use. The protein concentration of the dialyzed solution was measured spectrophotometrically at $\lambda = 280$ nm (UV-1650PC, Shimadzu, Champs-sur-Marne, France). Aliquots of dialyzed LDH, phosphate buffer and optionally stabilizer solutions (in phosphate buffer at different concentrations) were blended in a 7 mL glass vial so as to give 1 mL samples with final concentration of 5-100 µg/mL. The solutions were placed in a freeze dryer (Epsilon 2-4 LSC; Martin Christ Gefriertrocknungsanlagen; Osterode, Germany), frozen to -45 °C and equilibrated for 1 h. Primary drying was conducted at -9 °C and a pressure of 0.014 mbar for 10 h, followed by secondary drying (T = 20 °C, P = 0.0014 mbar) for another 10 h. The samples were stoppered under vacuum.

2.2.7 Determination of Protein Activity

The activity of LDH samples was measured by monitoring the decrease in absorbance of NADH at $\lambda = 340$ nm due to the oxidation to NAD^+ at 37 °C (as a consequence of the enzymatic conversion of pyruvate to lactate, catalyzed by LDH). The sample activity is expressed as percentage of the initial activity determined before freeze drying and optional storage. Freeze dried samples were reconstituted with 1 mL distilled water. Care was taken to ensure the complete dissolution of the freeze dried powder prior to the determination of the protein activity. If indicated, the samples were stored at 4, 25 or 40 °C and a relative humidity of 11.4 % for 1, 3 or 6 months prior to the activity measurement. Each experiment was conducted in triplicate.

2.2.8 Raman Microspectroscopy

LDH solutions: samples were analyzed using a Renishaw microspectrometer (inVia, Renishaw; Marne la Vallee, France) with a 514.5 nm Ar laser and 30 mW of incident power. Spectra were recorded in the 1000-1900 cm^{-1} range (amide I band region) by measuring in backscattering geometry. The freeze dried powders were analyzed in hermetically sealed Hellma quartz-Suprasil cells by focusing the laser beam through the X50 long-working

distance objective of a Leica microscope. The analyzed volume was about $1800\,\mu m^3$. A fluorescence contribution to the spectra appeared systematically in the background signal. Its magnitude was approximated by a second-order polynomial using a fitting procedure, and then subtracted from the spectra.

Freeze drying of LDH solutions: Sample solutions were prepared by dissolving LDH powder in distilled water at a concentration of 2.5 % (w/V). The solutions were placed in a freeze drying cryo stage (FDCS196, Linkam Scientific Instruments, Guildford, UK) and freeze dried following the same procedure as described in *section 2.2.6 Preparation of Freeze Dried Protein Samples.* Raman spectra were recorded at predetermined time points during the freeze drying process with the same setup as described above. Hot denaturation was monitored by increasing the temperature in increments of 5 °C up to 95 °C and simultaneous recording of Raman spectra.

Lysozyme

2.2.9 Preparation of Protein Solutions

50 mg of lysozyme powder and 239 mg of demineralized water were accurately weighed into 7 mL glass vials and vortexed until a clear solution was obtained. Different amounts of the denaturants urea or guanidine hydrochloride were added (as indicated). The enzymatic activity of the lysozyme solutions right after preparation was determined as described in the following section. The same protein solutions were used for Raman measurements.

2.2.10 Preparation of Lipid Implants

Two gram batches of protein loaded lipid implants were prepared using an emulsion method. The lipid powder was heated to 70-72 °C on a water bath until a clear liquid was obtained. Lysozyme powder was dissolved in 600 µL distilled water and heated to 70 °C shortly before addition to the molten lipid. The blends were either emulsified under magnetic stirring for 2 min at 250 rpm (RET basic, IKA Werke, Staufen, Germany) or by application of ultrasound (intensity 30, Sonopuls HD 2070, MS 72; Bandelin Electronics, Berlin, Germany) for 1 min.

The obtained emulsion was cast in cylindrical moulds with a diameter of 3 mm using preheated glass pipettes and subsequently cooled to room temperature. Upon solidification, excess of lipid on the top of the implants was removed using a heated blade. The implants

were stored at -80 °C until further use. In order to remove water, the implants were freeze dried in an Epsilon 2-4 (Martin Christ Gefriertrocknungsanlagen, Osterode, Germany). The freeze drying procedure consisted of freezing to -45 °C for 2 h, primary drying (-9 °C, 0.014 mbar) for 10 h and secondary drying (20 °C, 0.0014 mbar) for 10 h. The implants were stored at 4 °C and 11.4 % relative humidity.

2.2.11 Determination of the Total Protein Content

The total protein content of the implants was measured by dissolving the latter in 1.5 mL dichloromethane. An equal volume of phosphate buffer containing 1 mol/L guanidine hydrochloride was added and the blend vortexed for 1 min. Upon centrifugation at 2500 rpm for 2 min (Universal 320; Hettich), the two phases were separated and the supernatant was sampled. The organic solvent was evaporated under vacuum; the residual was again dispersed in 1.5 mL phosphate buffer pH 7.4, vortexed for 1 min and centrifuged at 2500 rpm for 2 min (Universal 320, Hettich). The two aqueous phases were combined and stored at -20 °C until further analysis.

2.2.12 Protein Release Measurements

Implants were placed in Eppendorf tubes containing 1.5 mL of phosphate buffer (USP 34) with addition of 0.01 % sodium azide. The tubes were placed in a horizontal shaker (37 °C, 80 rpm; GFL 3033; Gesellschaft für Labortechnik, Burgwedel, Germany). At predetermined time points 1.5 mL samples were withdrawn and replaced with fresh medium. The samples were stored at -20 °C. Each experiment was conducted 6 times.

2.2.13 Determination of the Protein Concentration

Concentration measurements were conducted according to the bicinchoninic acid assay (BCA). Briefly, standards were prepared by dissolving 10 mg lysozyme powder in phosphate buffer pH 7.4 (USP 34) (containing 0.01 % sodium azide). Separately, 200 µL of a solution of copper (II) sulfate pentahydrate in distilled water (40 mg/mL) was added to 9.8 mL of a 0.001 % bicinchoninic acid solution. On a 96 well microtiter plate, 100 µL samples and 100 µL standards were blended with 100 µL of the copper (II) sulfate pentahydrate/bicinchoninic acid solution. The plate was placed in an oven at 60 °C for 1 h. Upon 15 min cooling to room temperature, the absorptions were measured

spectrophotometrically at $\lambda = 562$ nm (EL 405 microtiter plate reader, Bio-Tek; Cysoing, France).

2.2.14 Determination of Protein Activity

Lysozyme activity was determined according to the following enzymatic assay provided by Sigma: Samples were diluted so as to give final concentrations of 200 - 400 units/mL. One hundred µL aliquots of the lysozyme samples were added to 2.5 mL of a 0.015 % (w/w) suspension of Micrococcus lysodeikticus in phosphate buffer pH 6.24. The protein activity was measured by monitoring the decrease in the absorbance at $\lambda = 450$ nm (UV-1650PC, Shimadzu, Champs-sur-Marne, France) at 25 °C due the lysis of Micrococcus lysodeikticus cells. The recovered activity is proportional to the slope of the obtained absorbance-time curve (considering the absorption of pure phosphate buffer pH 6.24).

2.2.15 Microcalorimetry

Differential Scanning Calorimetry (DSC) experiments were also carried out on a very sensitive microcalorimeter (microDSC III, Setaram, Caluire, France). Hermetically closed aluminum pans were used. A mass of 600 mg of lysozyme aqueous solution was placed in a furnace, and a similar mass of water was placed in the second furnace. The sample is heated up to 100 °C with a scanning rate of 1 °C/min.

2.2.16 Raman Microspectroscopy

Lysozyme solutions

Raman spectroscopy of lysozyme solutions was performed using a XY Dilor spectrometer (Dilor, Les Ulis, France) with a 514.5 nm Ar-Kr laser and 20 mW of incident power. Spectra were recorded in the $10\ \text{cm}^{-1}$ - $350\ \text{cm}^{-1}$ range and in the $1500\ \text{cm}^{-1}$ - $1800\ \text{cm}^{-1}$ range (amide I region) by measuring in back-scattering geometry. The spectrometer is composed of a double monochromator comprising four mirrors characterized by a focal length of 800 mm, and a spectrograph. The entrance and exit slits are opened and kept at 300 µm, determining the incident radiation and a resolution of nearly $2\ \text{cm}^{-1}$ in the low-frequency range. The mixtures were loaded in spherical glass cells and hermetically sealed. Raman investigations were either performed at room temperature for each concentration of urea and guanidine HCl or - for selected concentrations - between 20 °C and 100 °C using an Oxford nitrogen-flux

device that keeps temperature fluctuations within 0.1 °C.

Lysozyme loaded lipid implants

Lysozyme powder and lysozyme loaded implants were analyzed using a Renishaw microspectrometer (inVia, Renishaw; Marne la Vallee, France) with a 514.5 nm Ar laser and 30 mW of incident power. Spectra were recorded in the 1000-1900 cm^{-1} range (amide I band region) by measuring in backscattering geometry. Implants were placed on glass slides in order to analyze surface and radial cross sections by focusing the laser beam through a X50 or X100 long working distance objective of a Leica microscope. Furthermore, selected implant surfaces and cross sections were subjected to a mapping analysis with the laser beam collecting spectra along a preliminarily drawn grid. The obtained spectra were compared to those of lysozyme and lipid alone to analyze the distribution and status of each component. A fluorescence contribution to the spectra appeared systematically in the background signal. Its magnitude was approximated by a second-order polynomial using a fitting procedure, and then subtracted from the spectra. Photomicrographs of selected samples were taken with the incorporated light microscope. Magnifications are indicated in the figures.

Cochlear Implants

2.2.17 Preparation of Drug Loaded Films

Dexamethasone-loaded, silicone-based films (20 g) were prepared as follows: Equal amounts of MED-4735 Part A and B were softened separately by passing them 10 times through a two roll mill (Chef Premier KMC 560/AT970A, Kenwood, Havant, UK). Subsequently, both parts were manually blended and passed another 10 times through the mill. This mixing initiated polymer crosslinking. Dexamethasone (fine powder, as received) was added and the resulting mixture was passed 40 times through the mill so that a homogenous film was obtained. The latter was cured at 60 °C for 24 h in an oven in order to assure the desired degree of crosslinking. For reasons of comparison drug free films were prepared accordingly (without adding dexamethasone). Film thicknesses were determined with a thickness gauge (Minitest 600; Erichsen, Hemer, Germany).

2.2.18 Preparation of Drug Loaded Extrudates

Blends of MED-4735 Part A + B and dexamethasone were prepared as described in *section 2.2.17 Preparation of drug loaded films*. The obtained mass was transferred into a 20 mL polypropylene luer lock syringe and extruded with a pressure of 2 bars (custom made piston extruder, equipped with a syringe fixation device, connected to a hydraulic press). The obtained extrudates (2 mm in diameter) were cured at 60 °C for 24 h in an oven to assure the desired degree of crosslinking.

2.2.19 Preparation of Drug loaded Cochlear Implants

Blends of MED-4735 Part A + B and dexamethasone were prepared as described in *section 2.2.17 Preparation of drug loaded films*. The obtained mass was injected into a stainless steel mould, containing glued stainless steel electrodes with wires. The mould was placed under a hydraulic press at 4.5 bars and heated to 116 °C for 10 min. Ethanol (96 % V/V) was injected into the mould in order to dissolve the glue and allow for implant removal.

2.2.20 Drug Release Measurements

<u>From thin, free films</u>: Film pieces of 3.5 x 3.5 cm were placed into 10 or 500 mL artificial perilymph (an aqueous solution of 1.2 mmol calcium chloride dihydrate, 2 mmol magnesium sulfate tetrahydrate, 2.7 mmol potassium chloride, 145 mmol sodium chloride and 5 mmol HEPES Pufferan) in glass flasks and protected from light. The flasks were kept constant at 37 °C and either horizontally shaken at 80 rpm (GFL 3033, Gesellschaft fuer Labortechnik, Burgwedel, Germany) or "non-agitated" (as indicated). At predetermined time points, samples were withdrawn (1 and 3 mL in the case of 10 and 500 mL release medium, replaced with fresh artificial perilymph). "Non-agitated" flasks were manually shaken prior to each sampling to assure homogenous drug content in the bulk fluid. The drug concentration was measured by HPLC analysis (Prostar 230, equipped with an autosampler: Prostar 410 and UV-Vis detector: Prostar 325; Varian, Les Ulis, France). One hundred µL samples were injected into a C18 RP column (Gemini 5u C18 110A, 150 mm x 4.6 mm; Phenomenex, Le Pecq, France) (mobile phase = acetonitrile:water 33:67 V:V, flow rate = 1.5 mL/min, 25 °C). Dexamethasone was detected UV-spectrophotometrically at $\lambda = 254$ nm. If required, the samples were diluted with artificial perilymph prior to injection into the HPLC column. Each experiment was conducted in triplicate.

From cylindrical extrudates: Extrudates (2 mm in diameter, 3 cm in length) were treated as thin films described above, using 1 and 500 mL release medium. Each experiment was conducted in triplicate.

From cochlear implants: Implants were placed into 2 mL HPLC glass vials containing 70 µL artificial perilymph and protected from light. Drug release was measured at 37 °C "without agitation". At predetermined time points, the release medium was completely renewed. The drug content in the samples was determined as described above, using a lower injection volume (30 µL). Each experiment was conducted in triplicate.

2.2.21 Determination of the Initial Drug Content of the Devices

Accurately weighed amounts of films, extrudates or implants were placed in defined volumes of tetrahydrofuran (THF) and shaken for 2 h (Vortex, IKA-Werke, Staufen, Germany) until the polymer matrices became fully translucent and colorless as described by Lee et al. (1997). The drug content of the supernatants was determined by HPLC analysis as described in *section 2.2.20 Drug release measurements*, using a lower injection volume (10 µL) and higher flow rate (2.5 mL/min) (samples were appropriately diluted with THF, if required).

2.2.22 Determination of Drug Solubility and Stability in Artificial Perilymph

Excess amounts of dexamethasone were added to 20 mL artificial perilymph (37 °C, 80 rpm, protected from light). Every 24 h, samples were withdrawn, filtered and analyzed for their drug content (as described in *section 2.2.20 Drug release measurements*) until equilibrium was reached (= drug solubility). To monitor dexamethasone stability when dissolved in artificial perilymph, samples ($c = 20$ µg/mL) were stored at 37 °C. At predetermined time points, their drug content was measured as described in *section 2.2.20 Drug release measurements*.

2.2.23 Measurement of the Mechanical Properties of Thin Films

The mechanical properties of thin, free films in the dry and wet state were determined using the puncture test and a texture analyzer (TAXT plus, Stable Micro Systems, Surrey, UK) (n = 6). Dry films were measured at room temperature, wet films at 37 °C upon exposure to artificial perilymph for predetermined time periods. Film specimens were mounted on a

film holder. The puncture probe (spherical end: 5 mm diameter) was fixed on the load cell (50 kg) and driven downward with a cross-head speed of 0.1 mm/s to the center of the film holder's hole (diameter: 10 mm). Load versus displacement curves were recorded until rupture of the film and used to determine the mechanical properties as follows:

(Equation 2.2.1) $\qquad$ puncture strength $= \dfrac{F}{A_{cs}}$

where F is the load required to puncture the film; A_{cs} represents the cross-sectional area of the edge of the film located in the path.

(Equation 2.2.2) $\qquad elongation\ at\ break = \dfrac{\sqrt{R_f^2 + d^2} - R_f}{R_f} \cdot 100\ \%$

Here, R_f denotes the radius of the film exposed in the cylindrical hole of the holder and d the displacement to puncture.

(Equation 2.2.3) $\qquad$ energy at break $= \dfrac{AUC}{V_c}$

where AUC is the area under the load versus displacement curve and V_c the volume of the film located in the die cavity of the film holder (the energy at break is normalized to the film's volume).

2.2.24 Thermal Analysis

The glass transition temperature (T_g) of thin silicone films was determined by differential scanning calorimetry (DSC Q10, TA Instruments, Guyancourt, France). Approximately 10 mg of drug loaded and, for reasons of comparison, drug free films were heated in sealed aluminum pans (investigated temperature range: -160 to 25 °C, heating rate: 10 °C/min). The samples were flushed with nitrogen. Temperature and enthalpy readings were calibrated using indium.

2.2.25 Scanning Electron Microscopy

Scanning electron microscopy (SEM) was used to characterize the internal morphology of the thin films and cylindrical extrudates (S-4700 FEG, Hitachi High-Technologies Europe,

Krefeld, Germany). Samples were covered under vacuum atmosphere with a fine chrome layer (Xenosput XE200, Edwards, Gennevilliers, France). Cross sections were obtained by freezing the samples in liquid nitrogen and subsequent manual breaking.

3 Results and Discussion

3.1 Matrix Systems for Colon Targeting

The local treatment of Inflammatory Bowel Diseases is highly challenging, because conventional dosage forms rapidly release the drug in the upper gastro intestinal tract (GIT). Upon absorption into the blood stream the drug is distributed throughout the human body, resulting in potentially severe side effects. In addition, the drug concentration at the site of action – the inflamed colon – is low, leading to low therapeutic efficacies. To overcome these restrictions, drug release from the dosage form should ideally be suppressed in the stomach and small intestine, but set on as soon as the target site is reached (Ashford et al., 1993c; Watts and Illum, 1997; Friend, 2005).

The objective was to prepare and characterize novel, non-coated, multiparticulate dosage forms (matrix pellets and mini tablets) containing the colon targeting compound Nutriose and high doses of the most frequently used drug for the local treatment of IBD, 5-aminosalicylic acid (5-ASA). The high drug content is of major practical importance, because up to 4.8 g 5-ASA is administered per day (Quasim et al., 2001; Frieri et al. 2005; Travis et al., 2008). Recently, Nutriose containing film coatings have been proposed for colon targeting in IBD patients (Karrout et al., 2009a-c). Nutriose is a water-soluble, branched dextrin with high fiber contents obtained from wheat starch (Van den Heuvel et al., 2004, 2005; Pasman et al., 2006) Importantly, it serves as a substrate for enzymes secreted from colonic bacteria present in the feces of patients suffering from Crohn's Disease and Ulcerative Colitis (Karrout et al., 2009c). However, so far only Nutriose-based film coatings have been described. The potential of matrix systems containing this colon targeting compound is unknown. The latter offer the advantage of not necessitating a coating step during production. In these cases, the drug is embedded within the release rate controlling material (Krishnaiah et al., 2001; Amrutkar and Gattani, 2009). Since Nutriose as well as 5-ASA are water soluble at 37 °C, an additional, water-insoluble excipient is needed, for instance a lipid (Brabander et al., 2000; Hamdani et al., 2002; Zambito et al., 2005). Different types of lipids were added to minimize premature drug release in the upper GIT and the effects of various formulation and processing parameters were studied.

3.1.1 Nutriose-containing Matrix Pellets

Extrusion-spheronisation allowed for obtaining spherical pellets in all cases. The systems contained 60 % 5-ASA, 15 % Nutriose and 25 % lipid(s) (optionally partially replaced by MCC or PVP). The high drug loading is of great practical importance, because 5-ASA is highly dosed (up to 4.8 g per day). The presence of Nutriose in the pellets aims at providing colon-specific drug delivery: This polymer has been reported to be degraded by enzymes present in feces of IBD patients (Karrout et al., 2009b). The lipids, MCC and PVP aim at avoiding immediate drug release upon contact with aqueous body fluids (note that the drug and Nutriose are both water soluble at 37 °C).

Figure 3.1.1 shows the release of 5-ASA from pellets containing 25 % (w/w) of the following lipids: (a) hardened soybean oil, (b) glyceryl tristearate, (c) Sasolwax or Synthetic Wax, or (d) Microwax HG or Microwax HW. The systems were cured at different temperatures for 1, 2 or 3 min (as indicated) in order to allow for a more homogeneous lipid distribution, more efficient embedding of the drug particles and eventually the (partial) transformation of a lipid into a more stable modification. The melting points of the investigated lipids (glyceryl tristearate: 70-73 °C, hardened soybean oil: 67-72 °C, Sasolwax: 96-100 °C, Synthetic Wax: 94-97 °C, Microwax HG: 80-86 °C, Microwax HW: 75-80 °C) were close to or well below the investigated curing temperatures. As it can be seen in Figure 3.1.1, immediate drug release is avoided and the release rate generally decreased with increasing curing temperature and time, irrespective of the type of lipid. Thus, in principle the applied strategy is successful.

However, in all cases drug release was too rapid and most of the drug was released during the observation period (corresponding to the simulated transit period through the upper GIT; note that long residence times have been assumed, simulating unfavorable conditions for the drug delivery system). Hence, premature drug release *in vivo* is highly likely. The fact that after complete medium change (at $t = 2$ h), the release rate decreased in most cases can probably (at least partially) be attributed to the lower aqueous solubility of 5-ASA in phosphate buffer pH 6.8 compared to 0.1 N HCl at 37 °C: 4.4 mg/mL versus 10 mg/mL. In order to reduce the undesired premature drug release in 0.1 N HCl and phosphate buffer pH 6.8, parts of the lipid were substituted by MCC or PVP. Figure 3.1.2 shows 5-ASA release from pellets containing 60 % drug, 15 % Nutriose, 15 % hardened soybean oil and 10 % MCC or PVP. For reasons of comparison, also drug release from MCC/PVP-free systems (containing 25 % hardened soybean oil) is shown.
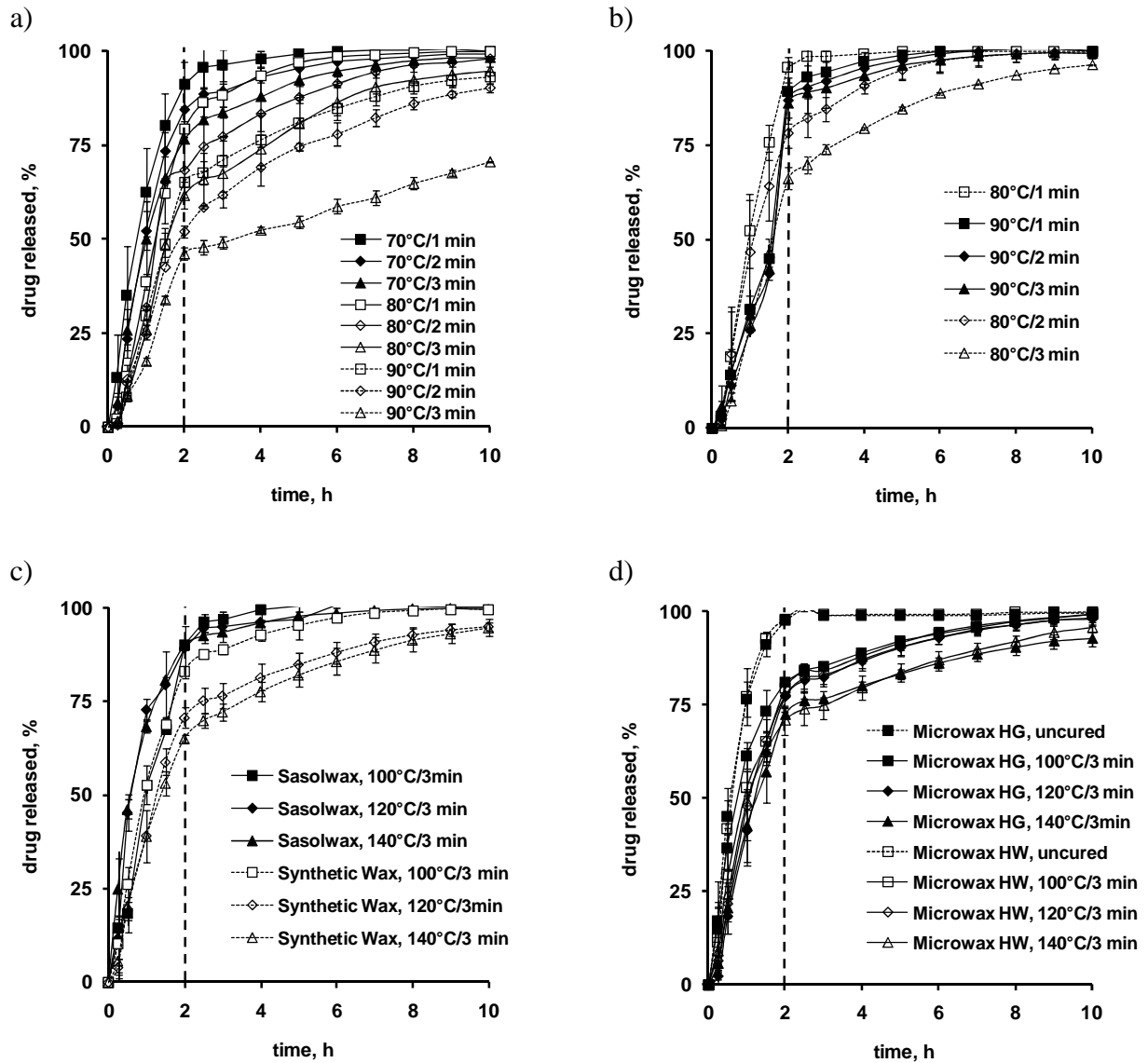
Figure 3.1.1: 5-ASA release from pellets consisting of 60 % drug, 15 % Nutriose and 25 % lipid: (a) hardened soybean oil, (b) glyceryl tristearate, (c) Sasolwax or Synthetic Wax, or (d) Microwax HG or Microwax HW. The release medium was 0.1 N HCl (for the first 2 h) and phosphate buffer pH 6.8 (for the subsequent 8 h). The curing conditions are indicated in the diagrams.

All pellets were cured for 3 min at 70, 80 or 90 °C (as indicated). Interestingly, the replacement of 10 % (w/w, referred to the total system mass) lipid by MCC resulted in accelerated drug release, irrespective of the curing conditions. Thus, the lipid is more efficient in hindering drug release from these pellets than MCC. In contrast, the partial replacement of hardened soybean oil by PVP led to slightly/moderately decreased drug release rates, if the systems were cured at 70 and 80 °C. However, upon curing at 90 °C, also in this case drug release was accelerated upon lipid substitution. Thus, these approaches are not suitable to effectively minimize premature drug release in the upper GIT.
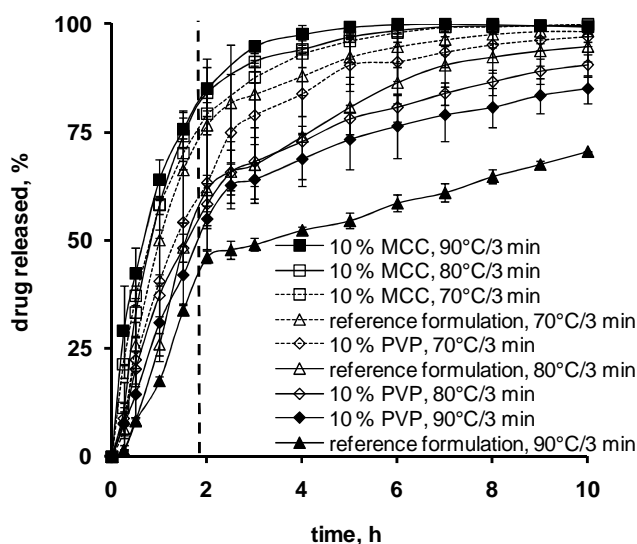
Figure 3.1.2: Effects of the replacement of 10 % hardened soybean oil by MCC or PVP (as indicated) on 5-ASA release from pellets containing 60 % drug and 15 % Nutriose. The reference formulations contained 25 % hardened soybean oil. The curing conditions are indicated in the diagram, the release medium was 0.1 N HCl for 2 h, followed by phosphate buffer pH 6.8 for 8 h.

In a further attempt to avoid the observed undesired drug release in 0.1 N HCl and phosphate buffer pH 6.8, a short term curing for 3 min at 90 °C was followed by a long term curing at 40 °C for 7 d. Figure 3.1.3 shows 5-ASA release from pellets containing 25 % glyceryl trimyristate, hardened soybean oil, glyceryl behenate, glyceryl palmitostearate, glyceryl tripalmitate, hydrogenated cottonseed oil, or glyceryl tristearate upon exposure to 0.1 N HCl for 2 h, followed by phosphate buffer pH 6.8 for 8 h (dotted curves). For reasons of

comparison, also drug release from pellets, which were only cured for 3 min at 90 °C are shown (solid curves). Clearly, the release rate significantly decreased in most cases upon long term curing.
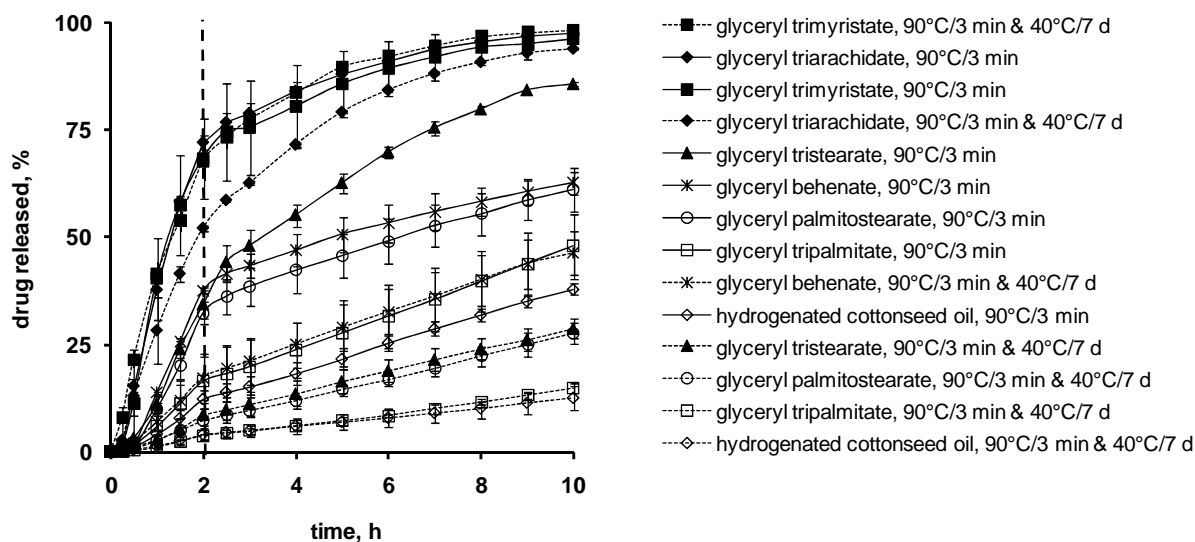

Figure 3.1.3: Effects of an additional long term curing on drug release from pellets consisting of 60 % 5-ASA, 15 % Nutriose and 25 % lipid (the type is indicated in the diagram) upon exposure to 0.1 N HCl (for 2 h) and phosphate buffer pH 6.8 (for 8 h). The solid curves indicate drug release from pellets, which were only cured for 3 min at 90 °C. The dotted curves show drug release from pellets, which were additionally cured for 7 d at 40 °C.

This can at least partially be attributed to changes in the modifications of the lipids: Figure 3.1.4 shows exemplarily DSC thermograms of pellets consisting of 60 % 5-ASA, 15 % Nutriose and 25 % glyceryl palmitostearate or tripalmitate (as indicated). The pellets were cured for 3 min at 90 °C and optionally subsequently for 7 d at 40 °C. For reasons of comparison, also thermograms of 5-ASA, Nutriose and of the lipid powders as received are shown in Figure 3.1.4. The melting peaks of the powders as received correspond to the melting peaks of the stable β-modifications of these lipids (Kellens et al., 1991; Hamdani et. al, 2003). In contrast, pellets which were only cured for 3 min at 90 °C also showed the melting/transformation of a less stable modification, irrespective of the type of lipid. Importantly, pellets cured for 7 d at 40 °C again only showed the melting of the stable lipid modification (in both cases). It has to be pointed out that the curing temperature during long term curing was well below the melting point of the respective lipids. Hence, the observed
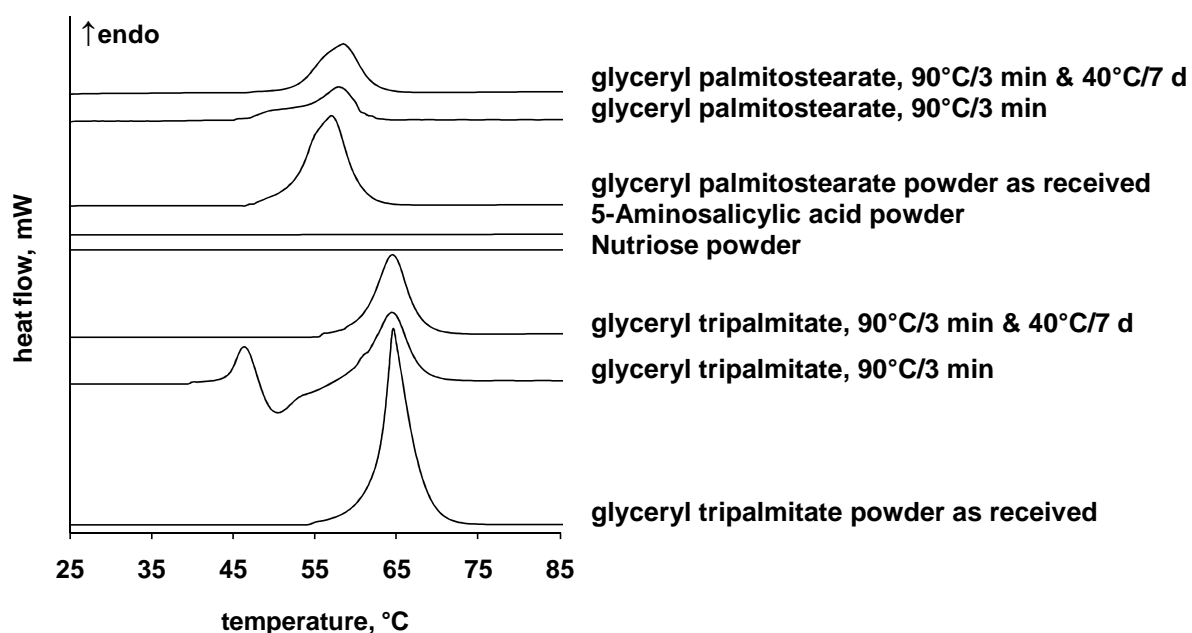
Figure 3.1.4: DSC thermograms of pellets consisting of 60 % 5-ASA, 15 % Nutriose and 25 % glyceryl palmitostearate or tripalmitate. The curing conditions are indicated in the diagram. For reasons of comparison, also thermograms of 5-ASA, Nutriose and the lipid powders as received are shown.

changes in the resulting drug release rates during long term curing are probably not caused by potential local redistributions of the lipids.

As lipids were used to slow down drug release within the upper part of the GIT, it was important to measure the effects of the presence of enzymes in the bulk fluids on drug release. Figure 3.1.5 shows 5-ASA release from pellets consisting of 60 % drug, 15 % Nutriose and 25 % hydrogenated cottonseed oil, glyceryl tripalmitate or glyceryl palmitostearate (as indicated). The release medium was either 0.1 N HCl for the first 2 h, followed by phosphate buffer pH 6.8 for the subsequent 8 h (solid curves), or 0.1 N HCl containing 0.32 % (w/V) pepsin for the first 2 h, followed by phosphate buffer pH 6.8 containing 1 % (w/V) pancreatin for the subsequent 8 h (dotted curves). All pellets were cured for 3 min at 90 °C, followed by 7 d at 40 °C. Clearly, drug release significantly increased in the presence of enzymes in the case of hydrogenated cottonseed oil and glyceryl tripalmitate, due to the (at least partial) degradation of these lipids.
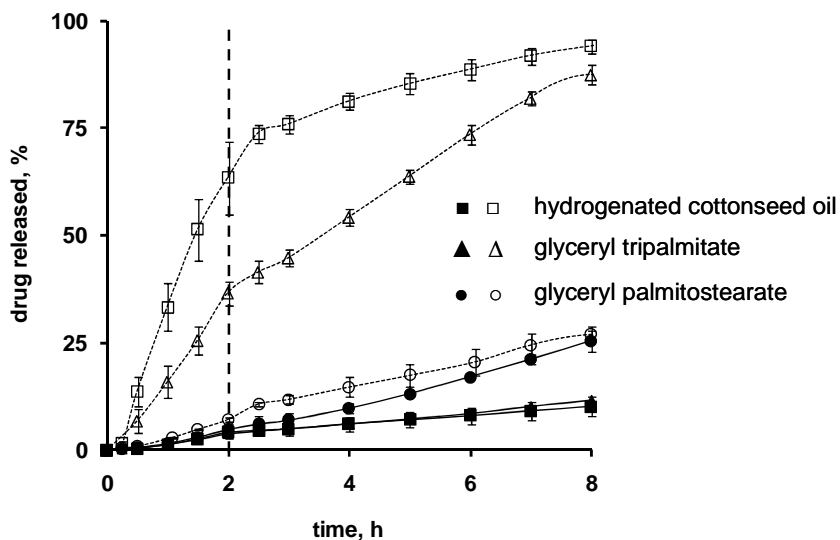
Figure 3.1.5: Impact of the presence of enzymes in the bulk fluid [0.32 % (w/V) pepsin in 0.1 N HCl (for 2 h), and 1 % (w/V) pancreatin in phosphate buffer pH 6.8 (for 8 h)] on 5-ASA release from pellets consisting of 60 % drug, 15 % Nutriose and 25 % lipid (the type is indicated in the diagram). All pellets were cured at 90°C for 3 min, followed by 7 d at 40 °C. Dotted curves: with enzymes, solid curves: without enzymes.

In contrast, the release rate only slightly increased in the case of glyceryl palmitostearate. Thus, this lipid seems to be much less affected by the added enzymes under these conditions. For this reason, glyceryl palmitostearate was used as standard lipid in all further experiments (if not otherwise stated).

When developing controlled drug delivery systems, special care needs to be taken with respect to potential changes in the systems' properties during long term storage. Modifications in the molecular structures might alter the resulting matrix permeability for the drug and, thus, the release rate. For these reasons, it is of great practical importance to measure drug release before and after long term storage from such dosage forms. Storage under stress conditions (e.g., elevated temperature) can allow obtaining results more rapidly than under ambient conditions. Figure 3.1.6 shows the release of 5-ASA from pellets consisting of 60 % drug, 15 % Nutriose and 25 % glyceryl palmitostearate. The pellets were cured for 3 min at 90 °C, followed by 7 d at 37, 40 and 45 °C (as indicated) (the melting range of glyceryl palmitostearate is 53-57 °C). For reasons of comparison, also drug release from pellets, which were only cured for 3 min at 90 °C and from pellets, which were cured for 3 min at 90 °C,
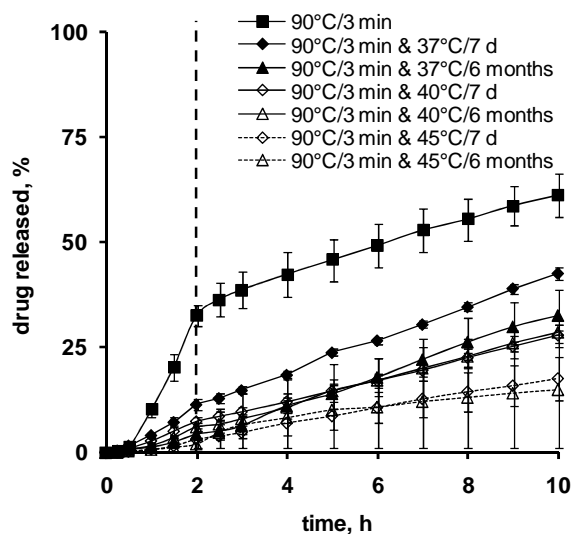
Figure 3.1.6: Long term stability (under stress conditions) of pellets containing 60 % 5-ASA, 15 % Nutriose and 25 % glyceryl palmitostearate: Drug release in 0.1 N HCl (for 2 h) and phosphate buffer pH 6.8 (for 8 h) from systems, which were cured for 3 min at 90 °C, optionally followed by 7 d or 6 month at 37, 40 or 45 °C (as indicated).

followed by 6 months at 37, 40 and 45 °C is illustrated.

Clearly, a 7 d curing is required to slow down drug release, irrespective of the curing temperature. Interestingly, the resulting release profiles do not overlap, indicating possible differences in the lipid distribution within the system. Importantly, drug release further slowed down when increasing the curing period to 6 month in the case of curing at 37 °C, but not in the case of curing at 40 or 45 °C. Thus, the latter pellets are likely to be stable during long term storage at room temperature.

### 3.1.2 Nutriose-containing Mini Tablets

As an alternative to matrix pellets, also mini tablets (diameter: 2 mm; height: 2 mm) consisting of 50 % 5-ASA, 15 % Nutriose and 35 % lipid were prepared. Again, the high drug loading was important because of the high daily doses of 5-ASA. Nutriose was the colon targeting compound and the lipid was intended to minimize drug release in the upper GIT. To evaluate the suitability of different types of lipids in these dosage forms, hardened soybean oil, glyceryl tristearate, glyceryl tripalmitate, glyceryl behenate, glyceryl palmitostearate, hydrogenated cottonseed oil as well as hydrogenated soybean oil were studied (Figure 3.1.7). The mini tablets were prepared by direct compression, followed by a curing for 24 or 48 h at 60, 65, 70 or 75 °C (as indicated), according to the melting points of the lipids: hardened soybean oil 67-72 °C, glyceryl tristearate 70-73 °C, glyceryl tripalmitate 61-63 °C, glyceryl behenate 69-74 °C, glyceryl palmitostearate 53-57 °C, hydrogenated cottonseed oil 60-62.5 °C hydrogenated soybean oil 66.5-69.5 °C. As it can be seen in Figure 3.1.7, drug release upon 2 h exposure to 0.1 N HCl, followed by 8 h exposure to phosphate buffer pH 6.8 is considerable in all cases. Generally, the release rate decreased with increasing curing time and temperature, due to altered lipid modifications and/or lipid distribution within the system. As for the case of matrix pellets, glyceryl palmitostearate showed the most promising potential as release rate controlling lipid. For this reason it was studied in more detail.

In order to minimize the undesired, premature drug release in the upper GIT, the curing time and temperature were further increased. Figure 3.1.8 shows 5-ASA release from mini tablets consisting of 50 % drug, 15 % Nutriose and 35 % glyceryl palmitostearate. The systems were cured for 3 min at 90 °C, followed by 7 d, 14 d or 1 month at 40°C, or by 12, 24 or 48 h at 60 °C. For reasons of comparison, also 5-ASA release from mini tablets cured for 24 h at 60 °C is shown. Clearly, the release rate was not very much affected by the curing conditions, except for the 1 month curing. As the latter is difficult to realize at an industrial scale and as the release rate still remains considerable, this approach was not further investigated.

Since the distribution of the lipid within the mini tablets can be expected to significantly alter its ability to hinder drug release, four different preparation techniques were studied, which are likely to result in a more or less intense embedding of the drug within the glyceryl palmitostearate: (i) direct compression, (ii) partial melt granulation & compression, (iii) separate melt granulation & compression, and (iv) melt granulation & compression. In the case of "partial melt granulation & compression", 5-ASA, Nutriose and 60 % of the glycerol
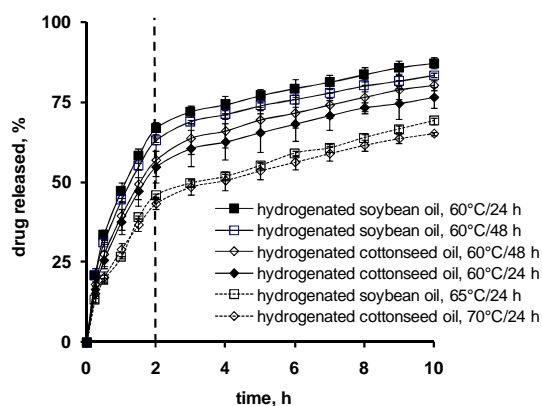
a)
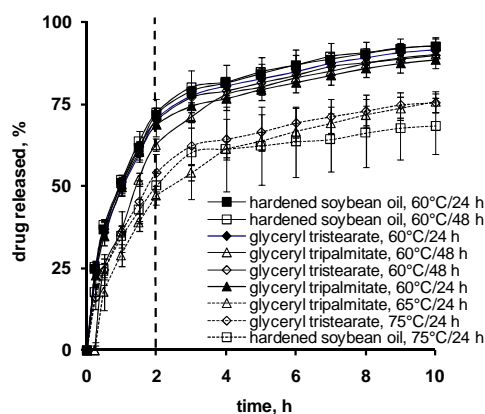
b)
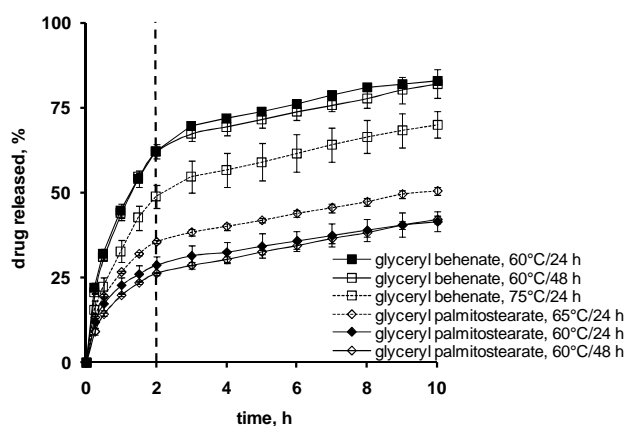
c)

Figure 3.1.7: 5-ASA release from mini tablets consisting of 50 % drug, 15 % Nutriose and 35 % lipid: (a) glyceryl tripalmitate, glyceryl tristearate, or hardened soybean oil, (b) glyceryl behenate or glyceryl palmitostearate, (c) hydrogenated cottonseed or hydrogenated soybean oil. Drug release was measured in 0.1 N HCl for 2 h and phosphate buffer pH 6.8 for 8 h. The curing conditions are indicated in the diagrams. All tablets were prepared by direct compression.
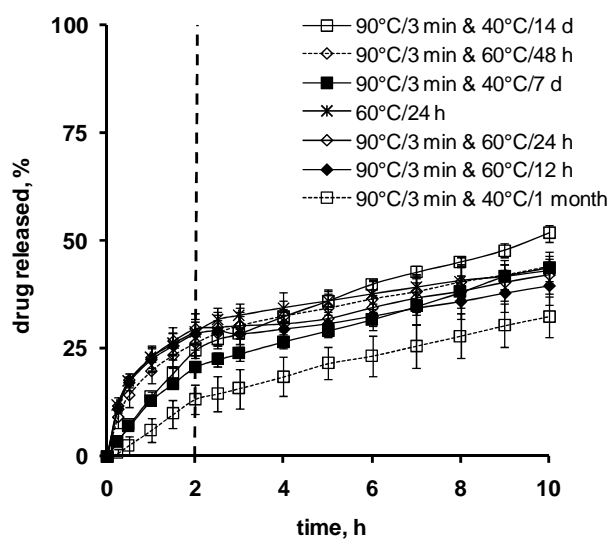
Figure 3.1.8: Effects of the curing conditions on 5-ASA release from mini tablets consisting of 50 % drug, 15 % Nutriose and 35 % glyceryl palmitostearate in 0.1 N HCl (for 2 h) and phosphate buffer pH 6.8 (for 8 h). All tablets were prepared by direct compression.

palmitostearate were molten at 85 °C on a water bath, cooled down to room temperature, ball milled and sieved (fraction 50 – 100 µm).

The obtained powder was blended with the remaining glyceryl palmitostearate and compressed. In the case of "separate melt granulation & compression", glyceryl palmitostearate and Nutriose were blended in equal parts and molten at 85 °C on a water bath. The remaining glyceryl palmitostearate was blended with the drug and also this blend was molten at 85 °C on a water bath. Both melts were cooled down to room temperature, ball milled, sieved (fraction 50 – 100 µm), blended and compressed. In the case of "melt granulation & compression", all compounds were molten together at 85 °C on a water bath, cooled down to room temperature, ball milled, sieved (fraction 50 – 100 µm) and compressed. The mini tablets were optionally cured for 24 h at 60 °C. As it can be seen in Figure 3.1.9, the drug release rate decreased in the following ranking order: direct compression > partial melt granulation & compression > separate melt granulation & compression > melt granulation & compression. This was true for uncured as well as for cured mini tablets and can probably be attributed to a more and more intense embedding of the drug within the lipid.

As also chitosan has been reported to allow for site specific drug delivery to the colon (Tozaki, 1997, 2002; Lorenzo-Lamosa et al., 1998), the partial substitution of glyceryl palmitostearate by chitosan was studied.
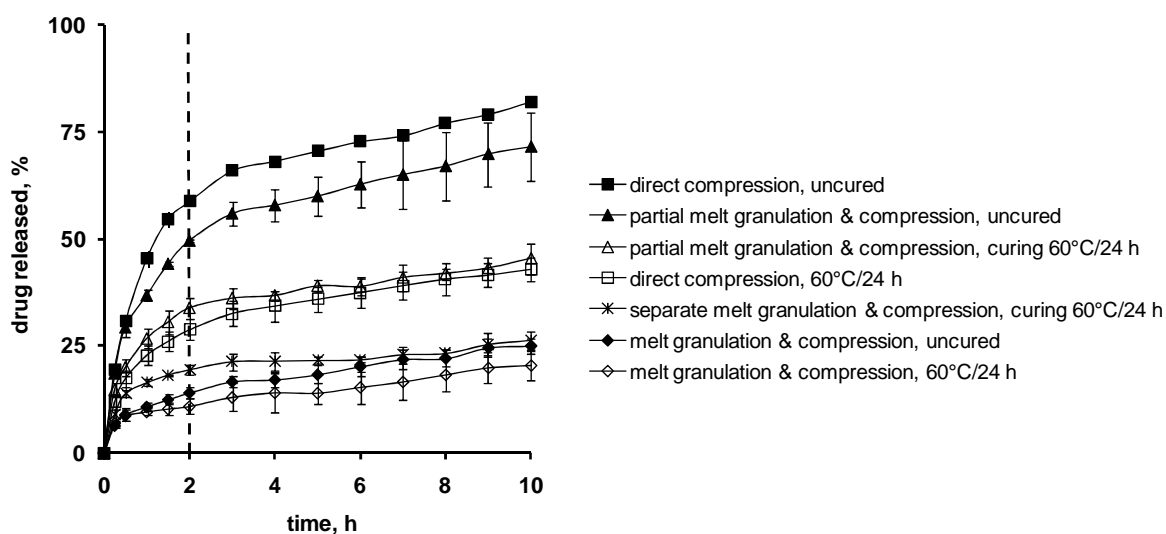
Figure 3.1.9: Effects of the type of preparation method: direct compression versus partial melt granulation & compression versus separate melt granulation & compression versus melt granulation & compression. Details on the different preparation methods are given in the text. The mini tablets consisted of 50 % 5-ASA, 15 % Nutriose and 35 % glyceryl palmitostearate. The release medium was 0.1 N HCl during the first 2 h, followed by phosphate buffer pH 6.8 during the subsequent 8 h.

Figure 3.1.10 shows drug release from mini tablets consisting of 50 % 5-ASA, 15 % Nutriose, 30 % glyceryl palmitostearate and 5 % chitosan. For reasons of comparison, also drug release from mini tablets free of chitosan (containing 35 % glyceryl palmitostearate) is shown. All systems were prepared by melt granulation & compression. The tablets were either uncured or cured for 24 h at 60 °C (as indicated). Clearly, the presence of only 5 % chitosan significantly increased the resulting drug release rate, leading to undesired, premature drug release. This was true for uncured as well as for cured tablets and can be attributed to the higher permeability of the hydrogel chitosan for the low molecular weight drug 5-ASA and/or rapid leaching of this compound into the surrounding bulk fluid at low pH. It has to be pointed out that an enteric coating can avoid an undesired dissolution of chitosan at low pH. However, as the objective of this work was to optimize non-coated multiparticulates, only Nutriose was maintained as "colon targeting compound" in this work.
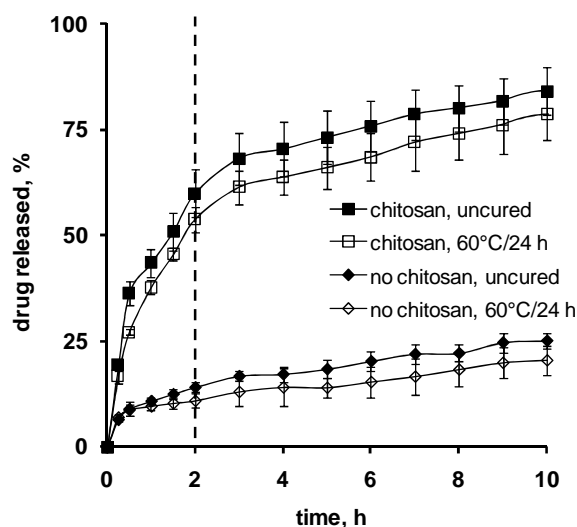
Figure 3.1.10: Effects of the replacement of 5 % glyceryl palmitostearate by chitosan on 5-ASA release from mini tablets (prepared by melt granulation & compression). The systems consisted of 50 % drug, 15 % Nutriose and 35 % glyceryl palmitostearate [5 % of which was replaced by chitosan, if indicated]. The release medium was 0.1 N HCl during the first 2 h, followed by phosphate buffer pH 6.8 during the subsequent 8 h.
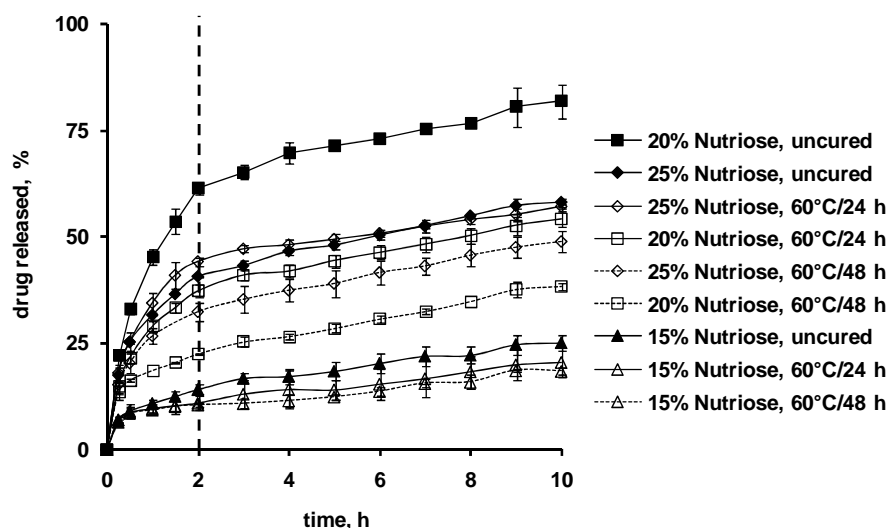

Figure 3.1.11 Impact of the Nutriose content and curing conditions on 5-ASA release from mini tablets containing 50 % drug and 50 % "Nutriose + glyceryl palmitostearate" in 0.1 N HCl (for 2 h) and phosphate buffer pH 6.8 (for 8 h). The curing conditions are indicated in the diagram. All tablets were prepared by melt granulation & compression.

Figure 3.1.11 shows the effects of the Nutriose content (while keeping the "Nutriose + glyceryl palmitostearate content" constant at 50 %) and of the curing conditions on the resulting drug release kinetics from mini tablets prepared by melt granulation & compression upon exposure to 0.1 N HCl for 2 h and subsequent exposure to phosphate buffer pH 6.8 for 8 h. The Nutriose content was increased from 15 to 25 % (while the glyceryl palmitostearate content was decreased from 35 to 25 %), the tablets were optionally cured for 24 or 48 h at 60 °C (as indicated). As it can be seen, the release rate increased with increasing Nutriose content, because glyceryl palmitostearate is more effectively hindering drug release than Nutriose. Note that Nutriose is more effectively hindering drug release than chitosan in this type of dosage forms: When comparing 5-ASA release from mini tablets cured for 24 h at 60 °C, containing 50 % drug, 30 % glyceryl palmitostaerate and 20 % Nutriose (open squares and solid curves in Figure 3.1.11) versus 15 % Nutriose + 5 % chitosan (open squares in Figure 3.1.10), it can be seen that drug release was slower in the case of 20 % Nutriose. Furthermore, the release rate decreased with increasing curing temperature and time, irrespective of the Nutriose content (Figure 3.1.11). Importantly, at a Nutriose level of 15 %, 5-ASA release from mini tablets cured at 60 °C for 24 and 48 h is virtually overlapping (open triangles: dotted and solid curves), indicating that a stable system is likely to be achieved. Thus, mini tablets consisting of 50 % 5-ASA, 15 % Nutriose and 35 % glyceryl palmitostearate prepared by melt granulation & compression and subsequent curing for 24 h at 60 °C show an interesting potential for colon-specific drug delivery.

The previous section dealt with several approaches to formulate matrix systems for oral controlled drug delivery, in this case specifically intended for colon targeting. Another field of application where matrix systems gain importance is the parenteral route. In general, drugs are dissolved or dispersed in a matrix forming excipient or modified to serve themselves as matrix forming agent and drug at the same time. Beside conventional drugs, therapeutics of biological origin are often administered by the parenteral route due to enzymatic degradation of e.g., protein therapeutics occurring during the gastrointestinal transport.

The next sections will provide further insight into the mechanisms which might destabilize proteins for therapeutic purpose during preparation and storage. Furthermore, the feasibility of formulating the latter in parenteral controlled drug delivery devices by using stabilizing agents was investigated.

3.2   Drug Delivery of Protein Therapeutics

Proteins undergo denaturation at both increasing and decreasing temperatures. The spontaneous protein unfolding at low temperature, known as cold denaturation, is recognized as a general phenomenon (Franks et al., 1988; Privalov, 1990) and one of the major origins of protein degradation during the freeze drying process (Tang and Pikal, 2005a and 2005b). Cold denaturation usually occurs at temperatures from -20 to -50 °C, e. g. below the temperature range where ice formation is detected (Franks et al., 1988, Tang and Pikal, 2005b). Denaturants [e.g., urea, guanidine hydrochloride (guanidine HCl)] increase the cold denaturation temperature and thus, render the analysis of the unfolding process possible (Tang and Pikal, 2005b). However the use of denaturants generates modifications in the structural organization of the solvent at the protein-solvent interface, and partial denaturation. Moreover, the mechanism behind the denaturing power of urea and guanidine hydrochloride is still not well understood. Chemical denaturants may exert their effect directly, by binding to the protein, or indirectly by changing the structure of the solvent (Courtenay et al., 2001; Makhatadze and Privalov, 1992; Tanford, 1970; Timasheff, 2002). In this context, the determination of the protein structure in the presence of chemical denaturants and a better understanding of chemical denaturation are required to describe the mechanisms of protein cold denaturation in the presence of denaturants.

Recently, Raman spectroscopy investigations carried out in the low-frequency range (10 - 300 cm^{-1}) and in the amide°I°band region (1500 - 1800 cm^{-1}), have shown to be a very well adapted method to analyze simultaneously the structural organization of the solvent, the coupling between the dynamics of the protein and the solvent, and to monitor the unfolding process of the secondary structure (Hédoux et al., 2006a). The analysis of lysozyme thermal denaturation processes, using D_2O as solvent, pointed out the transformation of the tertiary structure in a more flexible structure without alterations of secondary structure. This was attributed to the penetration of the solvent into the protein interior detected by the enhancement of isotopic exchanges (Hédoux et al., 2006a). Low-frequency investigations showed a simultaneous transformation of the hydrogen bond (H-bond) network, considered as the origin of denaturation process. This method is used to analyze the effects of both denaturants on the secondary structure in relation with the transformation of the H-bond network of the solvent, the dynamics of lysozyme and the coupling between protein and solvent dynamics.

Raman spectroscopy of protein secondary structure requires general knowledge of the band shapes that constitute their spectrum. General statements were made for the frequencies where characteristic bands for α-helix, β-sheet, random coil and turn (the major structures constituting the proteins secondary structure) can be found. However, the specific band maxima vary as a function of the quantity, the type of folding and their composition within the proteins secondary structure. This is particularly the case for the amide I band which will be focused in the following sections. The amide I band arises mainly from the $C = O$ stretching vibration with minor contributions of the $C - N$ stretching vibration, and the $N - H$ in-plane bend of the peptide bond (Surewicz et al., 1993). The band shape of the amide I mode can be considered as overlapping bands representing α-helices, β-sheets, turns and random structures. Figure 3.2.1 shows typical Raman spectra recorded at frequencies between 1500 and 1800 cm^{-1} (amide I band region) for four proteins in dry state containing different amounts of the mentioned folding structures.
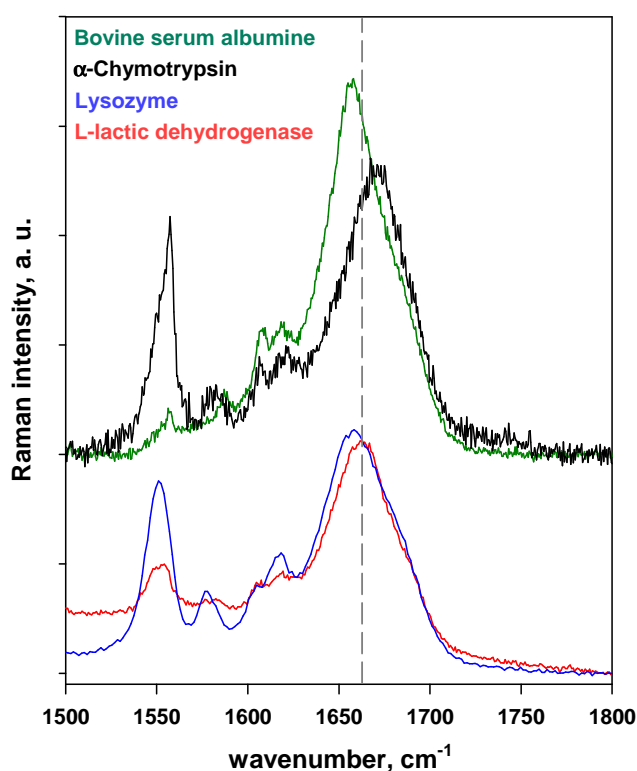

Figure 3.2.1: Comparison of Raman spectra of dry powders of bovine serum albumin (green), α-chymotrypsine (black), lysozyme (blue) and L-lactic dehydrogenase (red) recorded in the amide I band region (1500 - 1800 cm^{-1}). The grey dotted line serves as orientation.

Clearly, the maxima and the shape of the amide I mode differ for the anlayzed proteins. Bovine serum albumin and lysozyme are globular proteins mainly composed of α-helices (Hedoux et al., 2009; Williams and Duncker, 1981; Williams et al., 1980), with lysozyme containing some β-sheet structures. This is expressed in the similarity of the band maxima shown in Figure 3.2.1. The spectrum also gives information about the β–sheet of lysozyme content represented by a slight shoulder at around 1690 cm^{-1}. In contrast, the maxima of the amide I band of α-chymotrypsin completely differed due to its high content of β-sheet (Williams et al., 1980) accompagnied by few helices. The spectrum of L-lactic dehydrogenase, a tetrameric protein, exhibits similar maxima to those obtained for lysozyme. Thus, the amount and composition of helices and sheets in the secondary structure is likely to be comparable. However, to date little is known on the secondary structure and the attribution of folding types to the amide I band of this protein.

Protein Denaturation and Stabilization

3.2.1   Effects of Denaturants: Analysis of the Amide I Mode

Lysozyme was analyzed by Raman spectroscopy in the amide I region and compared with measurements of the enzymatic activity and microcalorimetric analysis in order to correlate the structural changes to the loss of protein activity.

Enzymatic activities of aqueous lysozyme solutions in the presence of denaturants are reported in the Figures 3.2.2a and 3.2.2b for urea and for guanidine HCl, respectively. Importantly, guanidine HCl is a stronger denaturant than urea. However, a weak loss of activity (~ 40 %) in the most denatured state in the presence of 10 mol/L guanidine HCl was observed. Microcalorimetric data obtained by heating lysozyme aqueous solutions in the presence of urea and guanidine HCl for concentrations ranging from 0 up to 8 mol/L are reported in Figures 3.2.3a and 3.2.3b. The endotherms significantly broadened with increasing denaturant concentration, for both denaturants. Furthermore, the great ability of guanidine HCl to destabilize lysozyme was confirmed, since the endotherms of denaturation are shifted toward lower temperatures and the areas of endotherms were weaker for guanidine HCl than for urea. For 8 mol/L guanidine HCl, the endotherm of denaturation was quasi undetectable while activity measurements indicated only 40 % of activity loss.

Table 3.2.1: Thermodynamical parameters of the thermal denaturation of lysozyme in aqueous solutions in the presence of various denaturant concentrations, determined from microcalorimetry experiments. Empty cells correspond to non measurable values.

Denaturant concentration, mol/L	T_m, °C		ΔH, J/g	
	Urea	guanidine HCl	Urea	guanidine HCl
n = 0	74.5 ± 0.1		4.5 ± 0.2	
n = 2	69.1 ± 0.1	60.2 ± 0.1	4.1 ± 0.2	3.1 ± 0.2
n = 4	66.5 ± 0.1	48.8 ± 0.1	3.3 ± 0.2	1.7 ± 0.2
n = 6	63.2 ± 0.1	42.3 ± 0.1	3.2 ± 0.2	0.9 ± 0.3
n = 8	59.5 ± 0.1	-	3.1 ± 0.2	-
n = 10	56.8 ± 0.1	-	2.0 ± 0.2	-

Raman spectra of lysozyme dissolved in H_2O and D_2O in the presence of up to 10 mol/L denaturants were recorded in the amide I region (1500-1800 cm^{-1}). Additionally, Raman spectra of the solvents were recorded at the same conditions as for the lysozyme solutions. The N - H in plane bend is responsible for the sensitivity of the amide I band to NH/ND exchanges in the protein backbone. There is no vibrational contribution of D_2O to the spectrum of the protein in the amide I region, while the Raman spectrum of H_2O is characterized by a broad band around 1630 cm^{-1} corresponding to the bending vibration of the molecule. Sytematically, the Raman spectrum of the solvent was subtracted from those of lysozyme aqueous solutions in the presence of denaturants, after normalization of the spectra over the 1500-1800 cm^{-1} range.

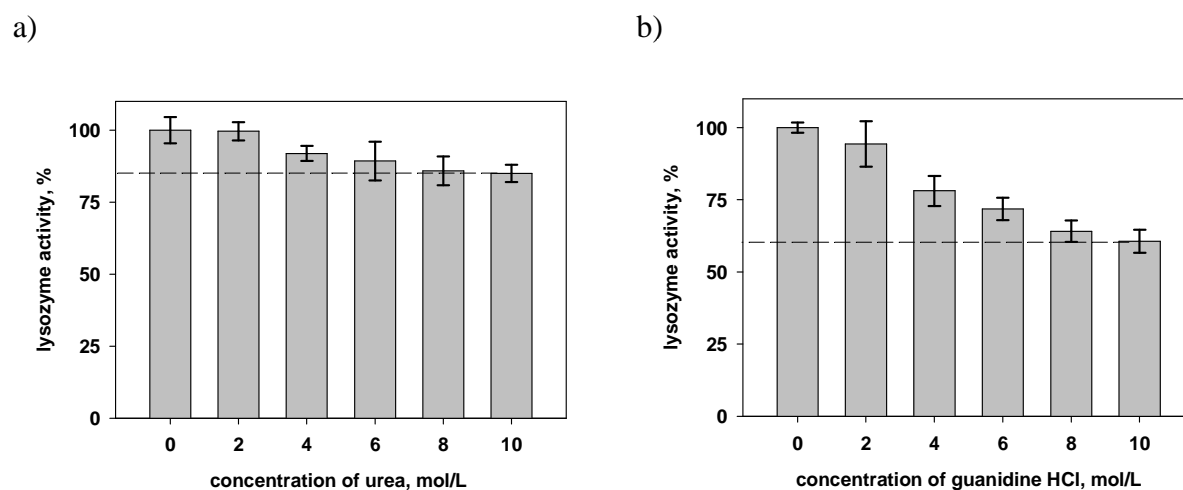a)   b)

Figure 3.2.2: Impact of the presence of different concentrations of (a) urea and (b) guanidine HCl on the enzymatic activity of lysozyme in aqueous solutions.

The resulting spectra are plotted in Figure 3.2.4a and 3.2.4b, giving information on the secondary structure of lysozyme in the presence of urea and guanidine HCl, by the band shape and the frequency of the amide I mode. Figure 3.2.4a reveals that the band shape of the amide I mode did not significantly change with the addition of urea, except for a slight enhancement of the Raman intensity near 1600 cm^{-1}. This feature suggests that no significant change of secondary structure was detected in the presence of urea, despite a significant loss of activity as reported in Figure 3.2.2a (~15 % for 8 mol/L urea). In contrast to urea, guanidine HCl induced a broadening and a frequency shift of the amide I band, clearly observed in Figure 3.2.4b in agreement with Figure 3.2.2b.

3.2.1 Effects of Denaturants: Analysis of the Amide I Mode

Table 3.2.2: Temperature parameters of unfolding curves of lysozyme in aqueous solutions in the presence of various denaturant concentrations, obtained from the fitting procedure of the amide I mode frequency described in the text. Non investigated solutions correspond to empty cells.

Denaturant concentration, mol/L	T_m, °C		ΔT, °C	
	Urea	guanidine HCl	Urea	guanidine HCl
n = 0	77.9 ± 0.2		2.5 ± 0.2	
n = 2	75.6 ± 0.5	63.6 ± 0.2	3.6 ± 0.5	3.0 ± 0.2
n = 4	-	42.5 ± 0.2	-	2.7 ± 0.3
n = 5	70.7 ± 0.6	-	3.7 ± 0.5	-
n = 6	-	35.0 ± 0.4	-	2.7 ± 0.4
n = 8	62.3 ± 0.6	28.6 ± 1	4.3 ± 0.6	2.5 ± 0.4

The Tables 3.2.1 and 3.2.2 show that urea slightly destabilized lysozyme since the midpoint temperature (T_m) slightly decreased with increasing urea concentration. The difference detected in the T_m-values determined from calorimetric data (Table 3.2.1) and Raman investigations (Table 3.2.2) can be explained by the consideration that the frequency of the amide I band only reflects the unfolding of the secondary structure, while the endotherms of denaturation correspond to the whole denaturation process including the transformation of the tertiary structure and the unfolding process, as shown in a previous study by Hédoux et al. (2006a). The broadening of the endotherms, observed in Figure 3.2.3a and the slightly increasing ΔT-values (Table 3.2.2) with increasing urea concentration indicate that both transformations (tertiary and secondary structures) occur over a wider temperature range than in the absence of urea.

It was previously shown that the frequency of the amide I band is closely connected to the nature of the secondary structure (Williams and Dunker, 1981), and can be used for monitoring the protein unfolding (Hédoux et al. 2006a and 2009). The frequency of the amide I band was determined for lysozyme in urea and guanidine HCl aqueous solutions, from a fitting procedure using a Gaussian to describe the band shape of the amide I mode. These frequencies are reported in Figure 3.2.5 and compared with the temperature dependence of the amide I band for lysozyme dissolved in H_2O in the absence of denaturant.

Interestingly, the amide I frequency for lysozyme in the 10 mol/L guanidine HCl solution was significantly lower (27 %) than that determined in the thermal denatured state in the absence of denaturant indicating that the denatured state of lysozyme in a concentrated solution of guanidine HCl is different from the thermal denatured state in absence of denaturant, as previously observed (Tanford and Aune, 1970). The temperature dependence of the amide I band was analyzed for lysozyme aqueous solutions in the presence and absence of denaturants and compared with microcalorimetric data. Figures 3.2.6a and 3.2.6b show the temperature dependences of the frequency of the amide I band for urea and guanidine HCl respectively. The thermal denatured states of lysozyme in the presence of both denaturants were different from those of lysozyme dissolved in H_2O in the absence of denaturant. Moreover, guanidine HCl induced a stronger temperature shift of the denaturation curves toward low temperatures than urea. The temperature dependences of the amide I band frequencies were fitted using the equation:

(Equation 3.2.1) $$\nu = \left[(\nu_N - \nu_D)/(1 + \exp((T - T_m)/\Delta T)) \right] + \nu_D$$

where T_m is the transition midpoint temperature, $2 \times \Delta T$ corresponds to the temperature domain of the transition, and ν_N, ν_D are the frequencies of the amide I band in the native (for $n = 0$) and denatured states. The (T_m, ΔT) values, determined by the fitting procedures, are reported in Table 3.2.2. Calorimetry and Raman data respectively reported in Tables 3.2.1 and 3.2.2 are converging into the main conclusion that guanidine HCl has stronger denaturing and destabilizing effects on lysozyme than urea. However some discrepancies were detected between midpoint temperatures of thermal denaturation determined from Raman and calorimetric investigations. T_m-values determined by Raman spectroscopy were higher than those determined by microcalorimetry, for aqueous lysozyme solutions with the addition of urea. Furthermore, the ΔT-values did not reflect the significant broadening of the endotherms observed in Figures 3.2.3a and 3.2.3b with increasing concentration of both denaturants. Additionally, T_m-values of lysozyme thermal denaturation in guanidine HCl solutions determined by Raman measurements were lower than those obtained from calorimetric investigations with increasing denaturant concentration. From the analysis of the amide I band, no change in the secondary structure of lysozyme was detected in the presence of urea. However, the temperature dependence of the amide I band and the microcalorimetric data clearly revealed that urea destabilized lysozyme. As a consequence, the data obtained

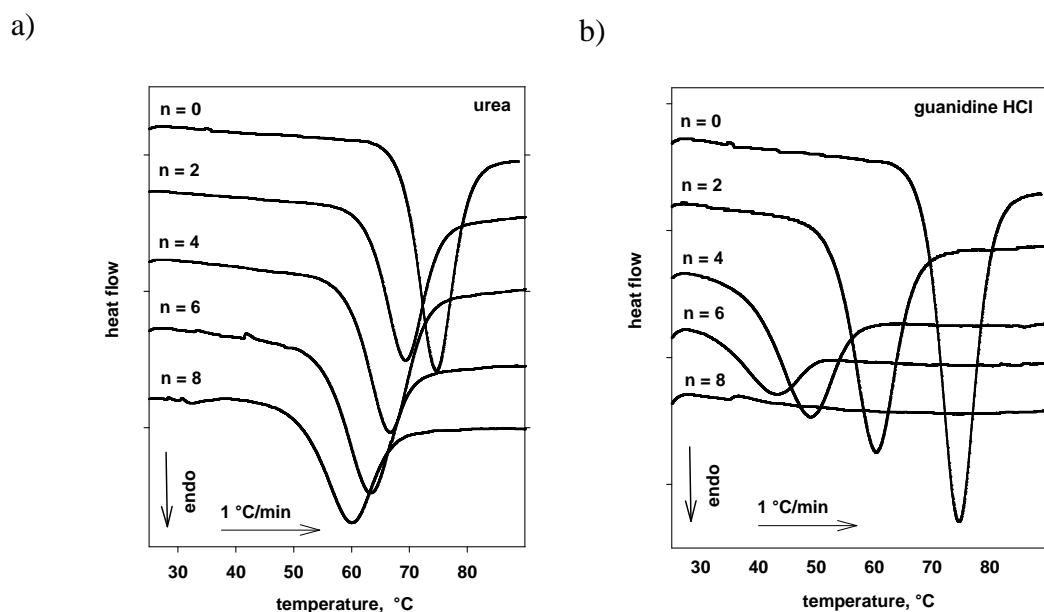a)   b)

Figure 3.2.3: Heat-flow curves during heating runs of aqueous lysozyme solutions in the presence of various concentrations (mol/L) of (a) urea and (b) guanidine HCl.

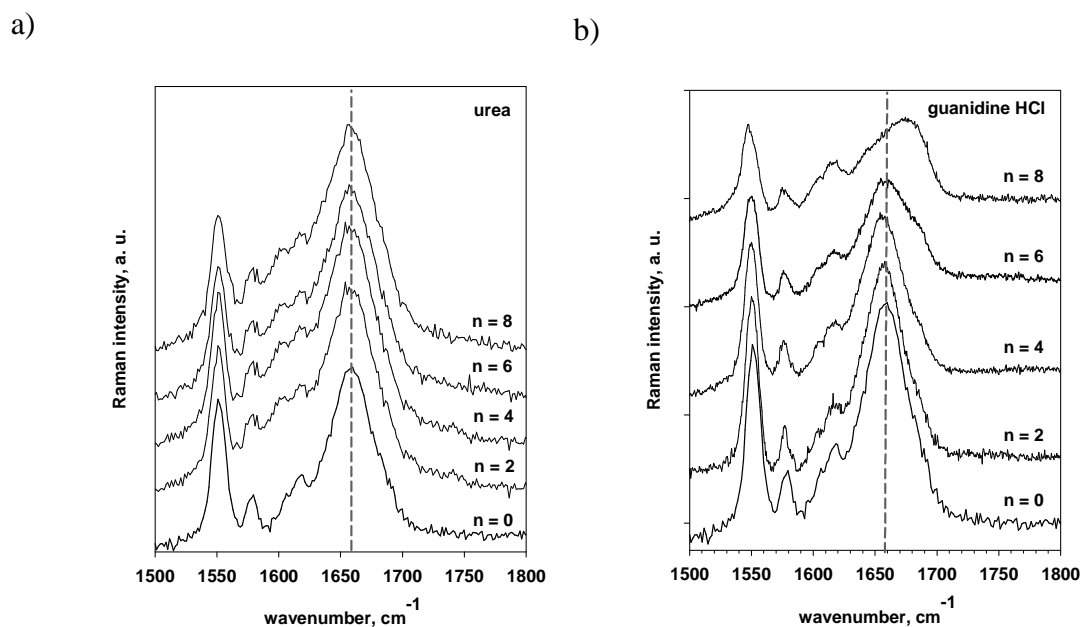a)   b)

Figure 3.2.4: Influence of the denaturants at various concentrations (mol/L) on the amide I band shape of lysozyme in aqueous solution for (a) urea and (b) guanidine HCl.
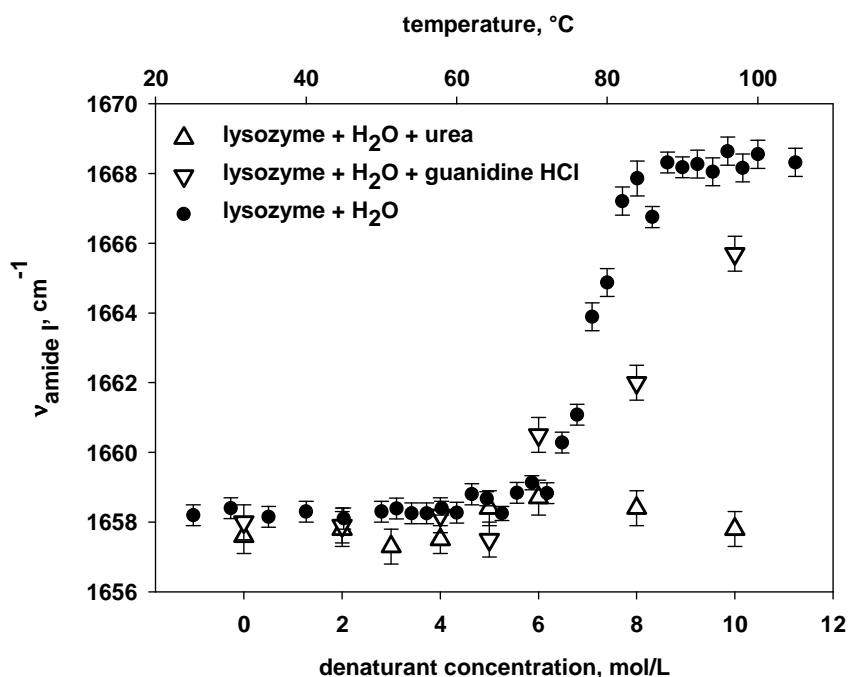
Figure 3.2.5: Influence of the denaturants on the amide I frequency of lysozyme in aqueous solution, compared to its temperature dependence in the absence of denaturants.

from DSC measurements can not be considered as representative for the degree of denaturation of lysozyme in the presence of urea.

In order to get better insight into the effects of denaturants on the native state of lysozyme, Raman investigations in the amide I region were carried out on lysozyme dissolved in D_2O in the presence and absence of denaturants. The influence of denaturants on the frequency of the amide I band was compared to the temperature dependence of the same band of lysozyme dissolved in D_2O (Figure 3.2.7a). It was clearly observed that the addition of urea in lysozyme solutions prepared with D_2O induced a down-shift of the amide I mode frequency for concentrations higher than 2 mol/L, while guanidine HCl induced an opposite frequency shift. From the analysis of aqueous lysozyme solutions in the presence of denaturants reported in Figure 3.2.5, the down shift of the amide I band in the presence of urea can be assigned to isotopic exchanges.

It is probably the experimental evidence for direct interaction between urea and buried hydrophilic residues, not normally accessible in the native tertiary structure, as observed in Figure 3.2.7a by heating lysozyme dissolved in D_2O in the absence of urea. For high urea
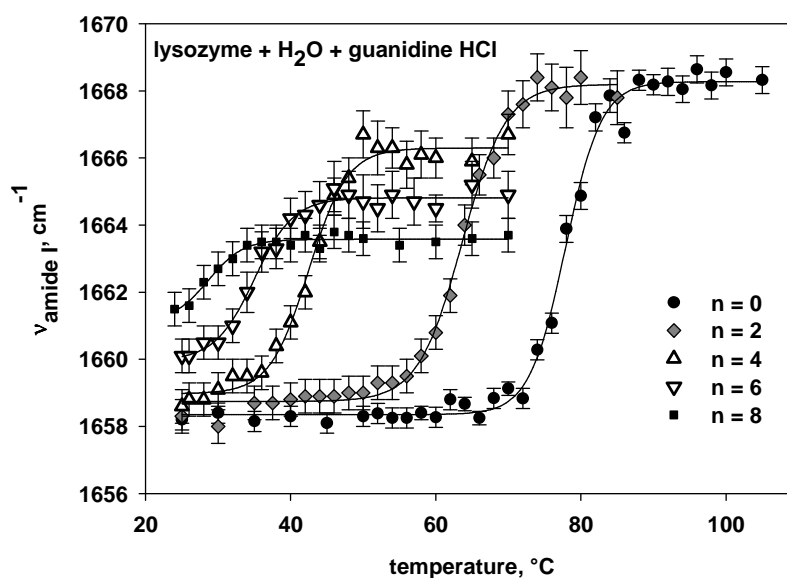
a)
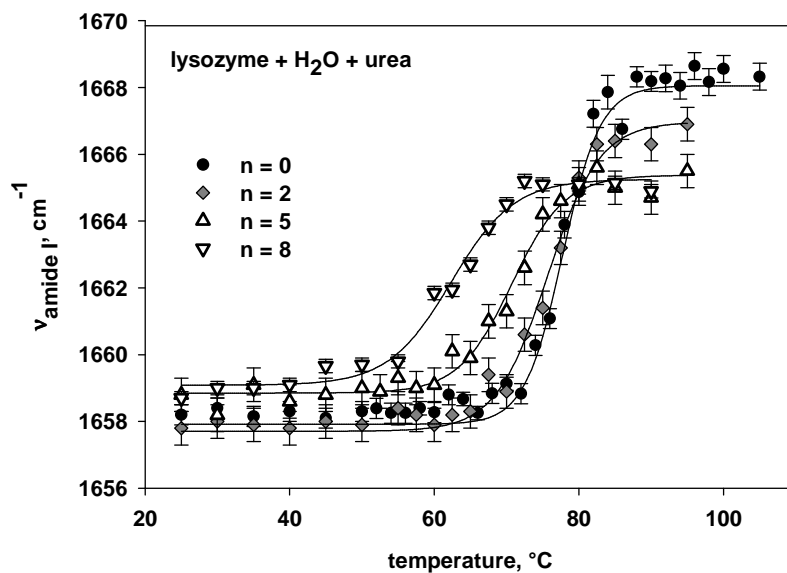
b)

Figure 3.2.6: Influence of denaturants on unfolding curves of lysozyme, obtained by heating for (a) urea and (b) guanidine hydrochloride. Symbols correspond to experimental data, and lines to the fitting procedure described in the text; T_m and ΔT parameters obtained from the fitting procedure are reported in Table 3.3.2.

contents (> 4 mol/L) the frequency of the amide I band reflected the molten globule state of lysozyme, corresponding to a soft tertiary structure with intact secondary structure (Hédoux et al., 2006a). For lower urea concentrations, hydrogen bonding between urea and polar groups might be assumed. However, they are limited to surface residues, since Figure 3.2.6a and Table 3.2.2 indicated lower T_m-values than that determined in the absence of urea, and Figure 3.2.7a indicated no enhancement of isotopic exchanges for concentrations lower than 4 mol/L. Direct interactions between urea and exposed polar groups have been predicted from molecular dynamics simulations (Bennion and Daggett, 2003; Caflisch and Karplus, 1999).

In order to investigate the nature of the isotopic exchanges observed in Figure 3.2.5 in the presence of high urea concentrations, the temperature dependence of the amide I band in a lysozyme solution prepared with D_2O and by the addition of 5 mol/L urea was analyzed by heating and reported in Figure 3.2.7b. Heating induced a strong downshift of the amide I band due to enhanced isotopic exchanges corresponding to the solvent penetration into the protein interior as observed without denaturant (Hédoux et al, 2006a), a process preceding the unfolding of the secondary structure. Importantly, the down-shift of the amide I mode frequency was observed over a wide temperature range in line with the observation of the endotherm broadening with increasing urea concentration. Furthermore, the down-shift observed by heating, was stronger in the presence of 5 mol/L urea than in the absence of urea. This indicates preferential hydrogen bond formation between urea and the backbone amides, as suggested by previous studies (Courtenay et al., 2001; Pike and Acharya, 1994). The present investigations revealed that the secondary structure mainly composed of helices did not undergo significant changes in agreement with structural investigations (Pike and Acharya, 1994). The strong enhancement of isotopic exchanges in the presence of high content of urea (> 4 mol/L) detected in the amide I region, can be considered as the signature of direct interaction of urea with polar residues and the lysozyme backbone, in agreement with molecular dynamics simulations (Bennion and Daggett, 2003). This type of binding due to the formation of additional hydrogen bonds, probably affects the protein flexibility and thus limits the degree of thermal denaturation as observed in Figure 3.2.6a with increasing urea concentration.

In order to determine the mechanisms by which guanidine HCl destabilizes lysozyme the temperature dependence of the amide I frequency of a lysozyme solution prepared with D_2O in the presence of 4 mol/L guanidine HCl was also plotted in Figure 3.2.7b. In contrast to urea, guanidine HCl induced significant modifications in the shape of the amide I band
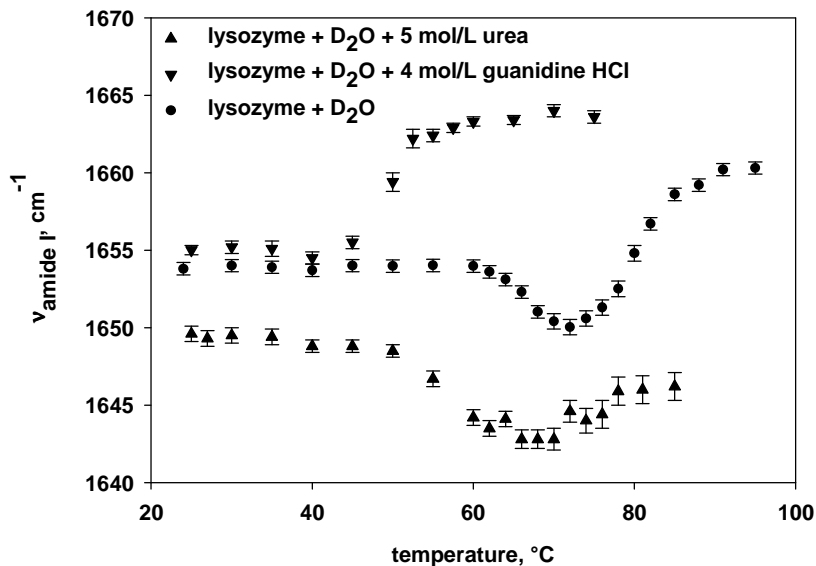
a)
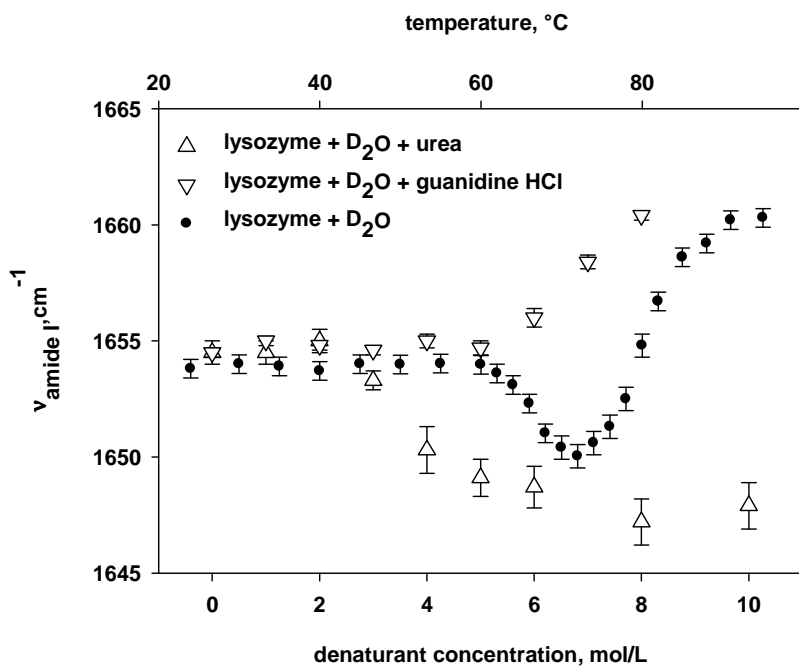
b)

Figure 3.2.7: Influence of denaturants on the amide I mode frequency and unfolding curves obtained by heating for lysozyme dissolved in D₂O.

(Figure 3.2.4b). The shift toward high frequencies reported in Figure 3.2.5 reflected the signature of the unfolding of α-helix structures (Hédoux et al., 2006a and 2009). Moreover, the dependency of the amide I mode frequency shift on the temperature and the concentration of guanidine HCl in aqueous lysozyme solutions (Figures 3.2.7) induced no down-shift of the frequency. Hence, no enhancement of isotopic exchanges at room temperature and during the thermal denaturation process was observed. Consequently, guanidine HCl probably binds to hydrophobic residues of the protein, as suggested in previous studies (Mason et al., 2004 and 2007).

As observed for urea solutions, Figure 3.2.6b shows that the thermal denatured state of lysozyme in the presence of guanidine HCl is different from that analyzed in the absence of denaturant, since decreasing amide I mode frequencies in the thermal denatured state were systematically observed with increasing guanidine HCl concentration. The low degree of denaturation determined by Raman spectroscopy in the 8 mol/L guanidine HCl solution explains the quasi undetectable endotherm in Figure 3.2.3b, while Figure 3.2.2b indicates a relatively weak decrease of activity of about 35 % in the same solution. The direct binding of both urea and guanidine HCl molecules might lead to a restriction of the conformational freedom within the polypeptide chain of lysozyme. In this context, the polypeptide chain of lysozyme in concentrated solutions of denaturants might not be representative of a standard random coil conformation, as previously suggested by calorimetric investigations (Makhatadze and Privalov, 1992). This can explain that the degree of unfolding at room temperature in the presence of 10 mol/L guanidine HCl, determined from the frequency of the amide I mode, was 73 % compared to the thermal denatured state of lysozyme in absence of denaturant. Moreover, this might be responsible for the difference between the thermal denatured states of lysozyme in the presence and absence of denaturants as demonstrated in Figures 3.2.6 and 3.2.7b.

3.2.2 Effects of Denaturants in the Low-Frequency Region

In order to determine characteristic Raman signatures for the effects of denaturants and bioprotectants on the dynamics of the lysozyme solution, data obtained by the analysis of lysozyme in aqueous denaturant solutions in the low-frequency region were put in relation to previous investigations (Hédoux et al., 2006b) on lysozyme dissolved in trehalose aqueous solution.

The scattered low-frequency intensity is composed of quasielastic intensity and harmonic vibrations which overlap in the $10 \text{ cm}^{-1} - 100 \text{ cm}^{-1}$ range. It was transformed into a reduced intensity plotted in Figure 3.2.8a, defined by

(Equation 3.2.2)
$$I_r(\nu) = I(\nu)/(\nu[n(\nu)+1])$$

where n(ν) is the Bose-factor. This transformation enhanced the observation of the quasielastic contribution. The two contributions to the Raman intensity were estimated from a fitting procedure of the reduced intensity described in Figure 3.2.8a, using a Lorentzian line shape for the first contribution (quasielastic) and a lognormal distribution function for the second (harmonic vibrations) (Caliskan et al., 2003; Hédoux et al., 2006a). After subtracting the quasielastic and the baseline contributions from the spectra, the Raman intensity was transformed into Raman susceptibility, according to the relation

(Equation 3.2.3)
$$\chi''(\nu) = \nu I_r(\nu)$$

and plotted in Figure 3.2.8b. This contribution is related to g(ν), the vibrational density of state (VDOS), by

(Equation 3.2.4)
$$\chi''(\nu) = C(\nu)g(\nu)/\nu$$

where C(ν) is the light-vibration coupling coefficient. Usually, it is observed that C(ν) has a linear ν-dependence in the Boson peak region (Hedoux et al., 2001; Novikov et al., 1995; Saviot et al., 1999), and the Raman susceptibility is then considered as representative of the VDOS. The Raman susceptibility χ''(ν) of lysozyme dissolved in H_2O in the $10 - 300 \text{ cm}^{-1}$ region is composed of two broad bands represented in Figure 3.2.8b from a fitting procedure
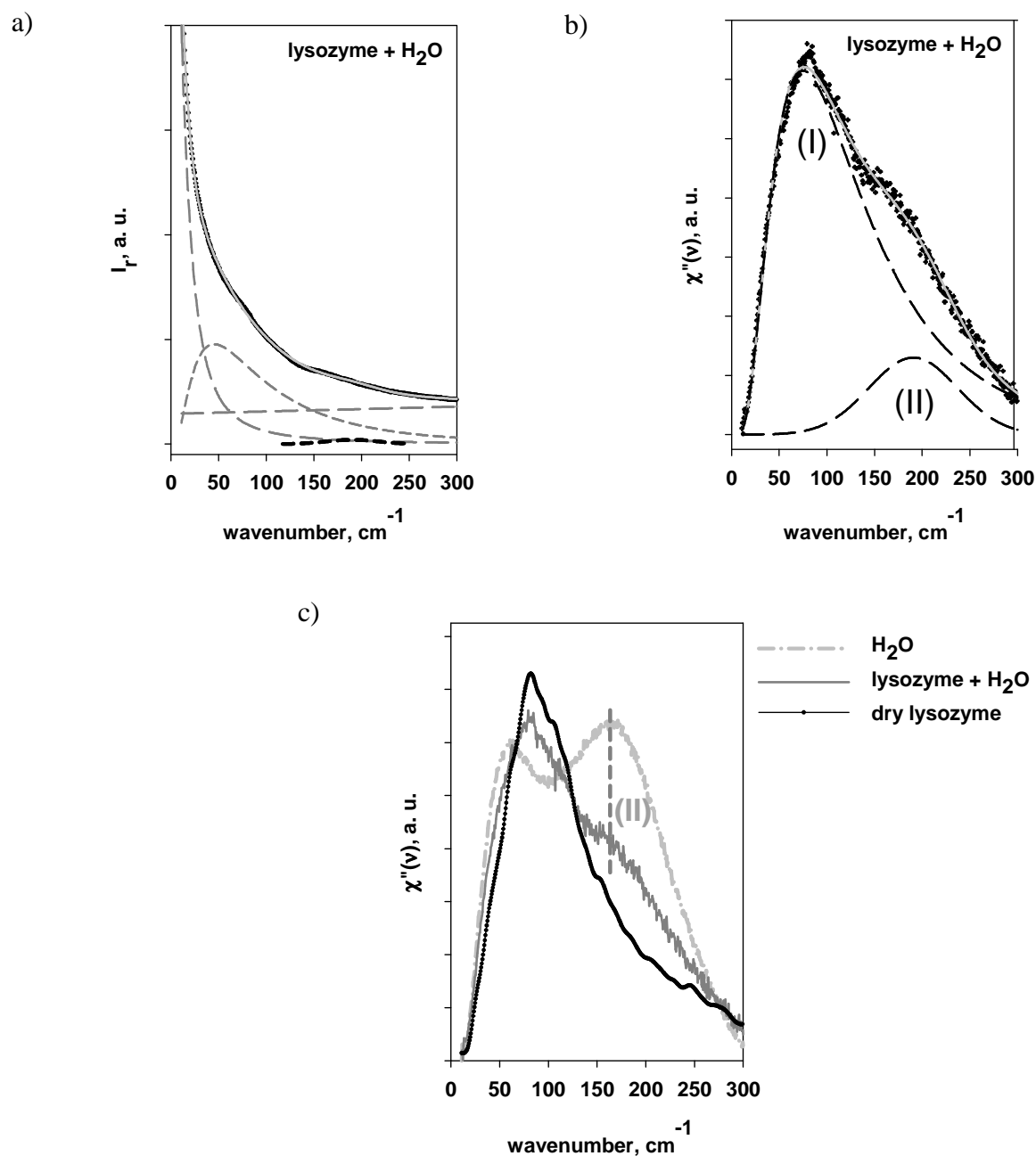
Figure 3.2.8: Representation of the low-frequency range of (a) the reduced Raman intensity of lysozyme aqueous solution; (b) the Raman susceptibility of lysozyme aqueous solution (crosshair symbols correspond to the conversion of the reduced Raman intensity, the full line to the result of the fitting procedure and the dashed lines to the components used in the fitting procedure); and (c) the Raman susceptibilities of lysozyme aqueous solution, dry lysozyme and H_2O.

using a lognormal function for the low-frequency band and a Gaussian for the high-frequency component to obtain the best description of the low-frequency $\chi''(\nu)$-shape. The two broad bands of the $\chi''(\nu)$-spectrum can be identified from the relevant comparison to the spectra of H_2O and dry lysozyme plotted in Figure 3.2.8c. The high-frequency band (II) observed around 185 cm^{-1} in both spectra of D_2O and lysozyme aqueous solutions is assigned to the intermolecular O - H stretching vibrations reflecting the tetrahedral order in water (Walrafen et al., 1996). Analysis of this band in lysozyme solutions can be used to probe the dynamics of the H-bond network of water. The low-frequency band (I) in lysozyme solutions can be primarily assigned to the protein dynamics widely influenced by the dynamics of water. The low-frequency band in the low-frequency Raman spectrum (LFRS) of water is assigned to the cage effect corresponding to the vibrations of a water molecule restricted by neighbouring molecules (Nakayama, 1998; Padro and Marti, 2003).
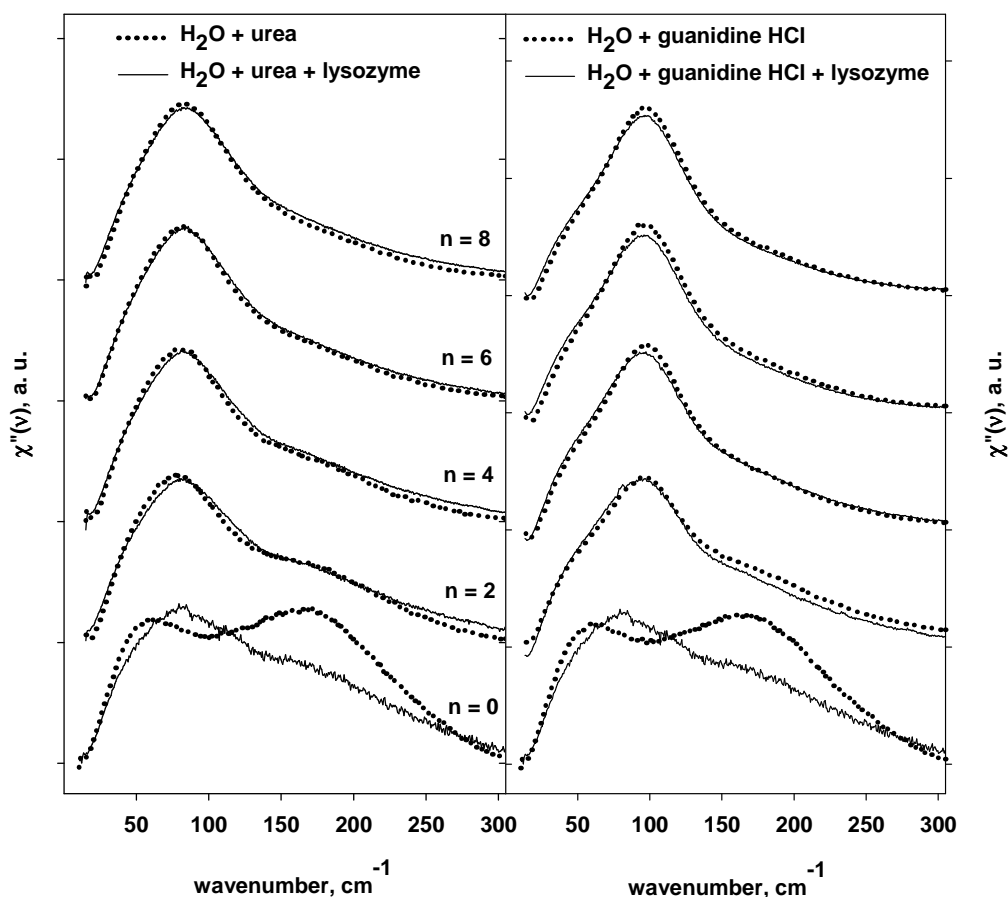

Figure 3.2.9: Influence of denaturants on the Raman susceptibility of H_2O and lysozyme aqueous solutions for (a) urea and (b) guanidine HCl.

The addition of lysozyme in water induced a shift of this band toward high frequencies, reflecting a more rigid cage in the presence of lysozyme, imposed by protein-solvent hydrogen bonding. Consequently, the analysis of this band gives information on the protein dynamics and on the coupling between the protein and solvent dynamics. An intensity decrease of the high-frequency band (II) was clearly observed in the presence of lysozyme, reflecting the breakdown of the tetrahedral H-bond network of water.

The $\chi''(\nu)$-spectra in the presence of denaturant for concentrations ranging from 0 to 8 mol/L were plotted in Figures 3.2.9a and 3.2.9b corresponding respectively to urea and guanidine HCl. These spectra were compared to $\chi''(\nu)$-spectra of both solvents. Figures 3.2.9a and 3.2.9b clearly reveal that both denaturants dissolved H-bonds in water since the intensity of the band (II) strongly decreased with the addition of denaturants.
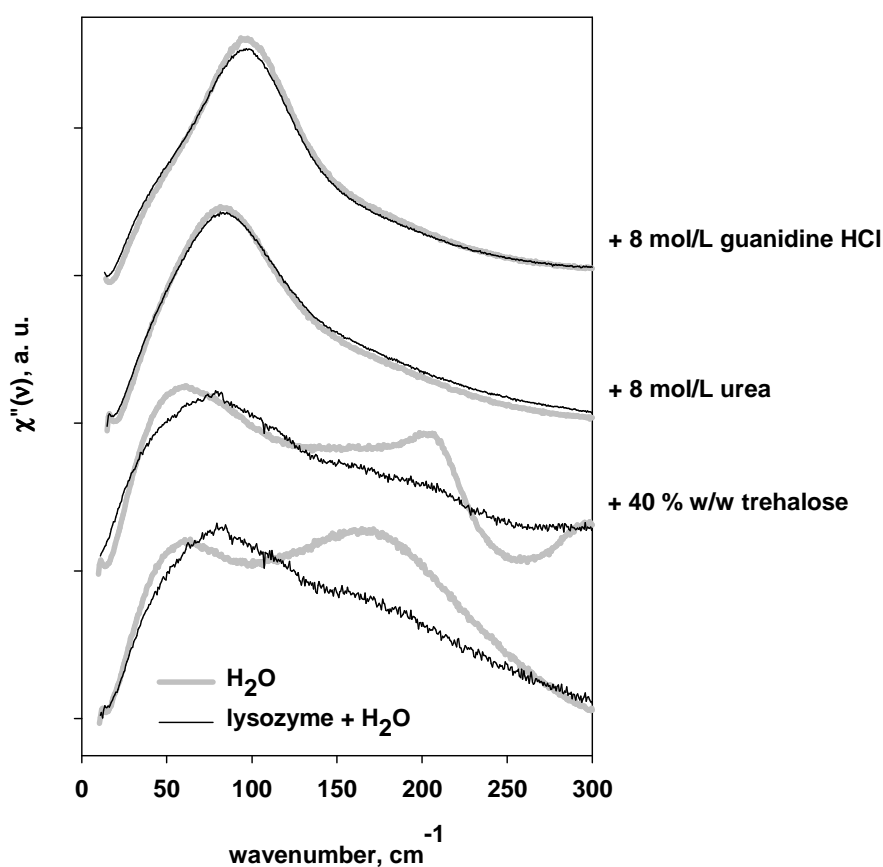

Figure 3.2.10: Comparison of the Raman susceptibility in the low-frequency range of lysozyme aqueous solutions in the presence and absence of cosolvents (8 mol/L urea, 8 mol/L guanidine HCl and 40 % w/W of trehalose).

The most striking feature resulting from the analysis of the low-frequency Raman spectrum, reported in Figures 3.2.9a and 3.2.9b is that the $\chi''(\nu)$-spectra of lysozyme aqueous solutions mimicked those of the solvents, while the spectra were significantly different in the absence of denaturants. This indicates that solvent dynamics closely control protein dynamics in the presence of denaturants. The difference between the spectra of lysozyme aqueous solution and H_2O, probably resulted from the existence of the hydration water which has not the same dynamics properties than bulk water. Consequently, the striking resemblance between spectra of lysozyme solutions and the solvents in the presence of both denaturants is probably the signature of direct binding between the protein and the solvent.

In this context, the low-frequency spectra of lysozyme solutions in the presence of denaturants or a high content of trehalose ($\sim$ 40 % w/w) were compared in Figure 3.2.10. It was shown that the low-frequency band shape of the lysozyme solution and the solvent was significantly different in the presence of 40 % w/w of trehalose, reflecting the preferential exclusion of sugar from the protein surface, in agreement with previous investigations (Lerbret et al., 2007; Xie and Timasheff, 1997). The analysis of the low-frequency spectra of solvents plotted in Figures 3.2.9 and 3.2.10, indicated that the intensity of the band (II) characteristic for the H-bond network of water strongly decreased in the presence of denaturants. Hence, both denaturants were establishing strong hydrogen bonds with the solvent. In contrast to denaturants, trehalose is considered as hydrogen bond "maker" (Lerbret et al., 2005a/b) inducing a change in the shape of the band (II) associated with a strengthening of intermolecular O‑H interactions in the tetrahedral organization of water molecules (Hédoux et al., 2006b and 2009). This destructuring effect of sugar on the H-bond network of water is considered to be principally responsible for the stabilizing effect on proteins (Branca et al, 1999 and 2005; Hédoux et al., 2006b and 2009; Magazu et al., 2005a/b and 2006)

The effect of cosolvents on the H-bond network of water mainly induced a change in the dynamics of H_2O detected by a frequency shift of the band (I). The frequencies of the band (I) for the lysozyme solutions and the solvents, obtained from the fitting procedure shown in Figure 3.2.8b, were plotted against the denaturant concentration in Figure 3.2.11. This figure confirmed that the frequency of the band (I) shifted toward the high frequencies in the presence of denaturants, for lysozyme solutions and the solvent. Addition of guanidine HCl induces a strong shift at very low denaturant concentration, compared with the addition of urea. Knowing that this band is assigned to the cage effect, e.g. molecular vibrations restricted by the neighboring molecules, it can be concluded that guanidine HCl molecules generated a
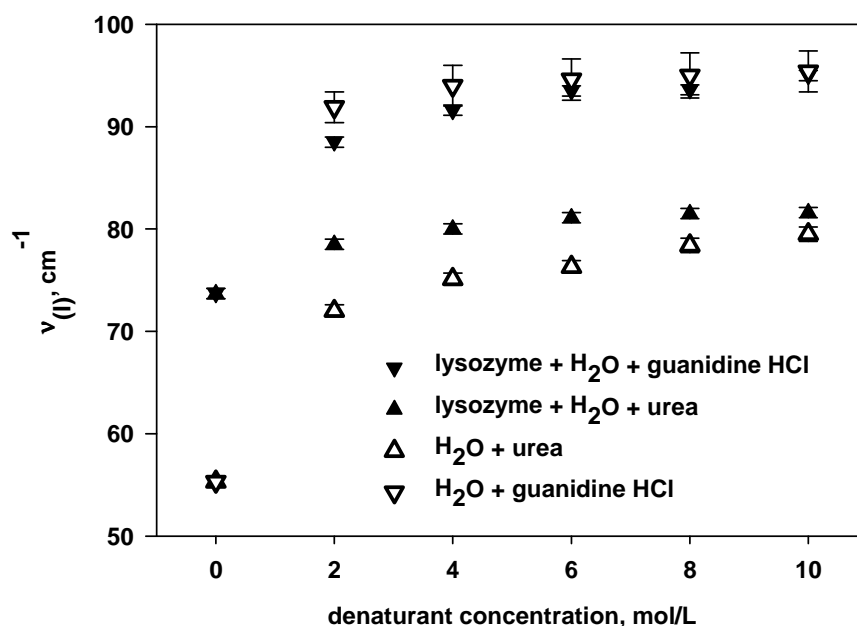
Figure 3.2.11: Influence of denaturants (urea and guanidine HCl) on the frequency of the band I for the solvent and the lysozyme aqueous solutions.

considerable stiffening of the cage, inherent to the dissolution of the H-bond network of water, and then imposed a significant hardening of the protein dynamics. Consequently, the properties of guanidine HCl solutions can be responsible for a strong binding between the denaturant and the protein, leading to a stronger denaturing power of guanidine HCl. This result is in line with previous investigations about the influence of different types of guanadinium salts on the protein stability (Arakawa and Timasheff, 1984).

Direct binding between lysozyme and both denaturants were observed. However, the binding sites were different from the analysis of isotopic exchanges in lysozyme solutions prepared with D_2O. Urea interacted with hydrophilic residues, while guanidine HCl molecules revealed direct interaction with hydrophobic groups. Urea induced a transformation of the tertiary structure into a softer structure, similar to the molten globule state observed during heating (Hédoux et al., 2006a) without unfolding of the secondary structure mainly composed of α-helices in agreement with a previous structural analysis (Pike and Acharya, 1994). Interestingly, such a transformation with quasi intact secondary structure is associated with a loss of activity of about 15 %. The strong denaturing power of guanidine HCl can be correlated to the strong hardening of the protein dynamics imposed by the solvent, leading to

a strong binding between guanidine HCl and lysozyme. Furthermore, the experimental evidence was given that the molecular basis for the denaturing effect of urea and guanidine HCl can be described by the consideration of both direct and indirect models, e.g. direct binding between denaturant and protein, and indirect changes of the solvent properties. The low-frequency Raman investigations revealed the signatures of the hydration water dynamics, as well as direct binding between the protein and the cosolvent. In this context, preferential hydration of water in the presence of trehalose (Xie and Timasheff, 1997) was clearly evidenced.

3.3 Conformational Stability of LDH during Freeze Drying and Storage

In order to complete gain more information on denaturation phenomena, especially on cold denaturation, a second model protein L-lactic dehydrogenase (LDH), was investigated for its enzymatic activity before and after freeze drying, subsequent storage and correlated with the corresponding Raman spectroscopic analysis. As already mentioned in *section 3.2 Drug Delivery of Protein Therapeutics*, LDH has amide I band shape and frequencies similar to that of lysozyme due to the comparable α-helix, β-sheet, random coil and turn content of the secondary structure. However, LDH is a protein composed of tetramers which significantly alters the characteristics of the protein with regard to the susceptibility to denaturation phenomena and loss of activity. When LDH is subjected to freeze drying, freezing and drying stresses might lead more easily to cold denaturation and thus a loss of protein activity than it is the case for lysozyme. This can among other reasons be due to its tetrameric structure and possible dissociation during freezing and drying. In order to determine the stabilizing effects of excipients of various chemical classes during freeze drying and storage, the latter were added to LDH solutions and tested for their capacities to protect the protein from denaturation and loss of activity.

3.3.1 Conformational Analysis of LDH: Cold Denaturation during Freeze Drying

L-lactic dehydrogenase, having a molecular weight of 140 kDa was analyzed by Raman microspectroscopy during freeze drying. Figure 3.3.1 shows Raman spectra of a 2.5 % (w/V) aqueous solution of LDH recorded in the 1000 to 1800 cm^{-1} frequency range and, for reasons of comparison, the spectrum of LDH powder as received. Interestingly, the spectra of LDH in solid state and dissolved in an aqueous solution significantly differ with regard to the amide I band. The solid state spectrum exhibits a maximum at 1162.48 cm^{-1} whereas for LDH in the dissolved state a maximum at 1657.06 cm^{-1} was determined. According to the observations of Costantino et al. (1998) they can be attributed to short and long α-helical structures. Having this in mind, the spectra resulting from the freeze drying process have to be carefully evaluated. Initially, the recorded amide I band is similar to that of LDH in solution as it is shown for the freezing phase to -45 °C and initial drying at 9 °C (red dotted line). With advancing drying time the amide I bands are shifting to higher frequencies exhibiting maxima similar to those shown for LDH powder (green dotted line). Thus, it might be assumed that the secondary structure of LDH during freezing and initial drying resembles the dissolved

state of the protein and that of the solid state at advanced drying. This might further imply that the loss of protein activity - in this particular experiment a total amount of 88.65 % of the initial LDH activity was recovered - might not be due to a loss of α-helices in the secondary structure of the protein. However, a shoulder at 1692 cm^{-1} in the spectra recorded at advanced primary drying and secondary drying phases might lead to the conclusion that the amount of β-sheet in the dried formulation increased since bands appearing at these frequencies are generally attributed to this type of secondary structure (Costantino et al., 1998). Two types of β-sheet were described: (i) the formation of the intermolecular type, simply resulting from the loss of solvent molecules leading to shorter distances between the protein molecules and (ii) the intramolecular type, resulting in an energetically more favorable protein conformation in this particular condition. Moreover, since the amide I band maxima remained at a frequency of 1660.97 cm^{-1} the increased amount of β-sheet structures was not imperatively linked to a loss in α-helices, which are mandatory for the native state of LDH. Hence, loss of LDH activity might assumed to be due to aggregation phenoma resulting from increased amounts of β-sheet structures (Dong et al., 1994). Furthermore, the particular quarternary structure of LDH, a tetramer which can dissolve in dimers and monomers as a consequence to freezing and sublimation stresses occuring during the initial phases of the freeze drying procedure, can also be held responsible as mechanism for the loss of protein activity. Anchordoquy et al. (1996) showed by freeze-thaw cycles and lyophilization of LDH solutions that freezing and alterations of the sample temperature respectively, induced the dissolution of tetramers. In particular, the disruption of the quarternary structure during freezing led to increased susceptibility of the protein to dehydration stresses during sublimation. Consequently, the recovered protein activities were decreased upon rehydration of the investigated samples.

### 3.3.2 Addition of Stabilizers: Effects on LDH Stability

Generally, proteins exhibit sensitivity proteins to thermal stresses. Attempts to preserve their conformation and hence their enzymatic activity include adjustment of the formulation and at this principally the addition of stabilizers (Carpenter et al., 2007). In order to identify the most effective single stabilizer and stabilizer blend, representative excipients from three distinct groups, saccharides, polyols and polymers, were investigated.

Figure 3.3.2 shows the analysis of enzymatic activities of aqueous LDH solutions (25 µg/mL) with addition of the above mentioned stabilizers after freeze drying. The percentage recovered activities are calculated based on the initial activity of the LDH solution before freeze drying. Freeze drying of all saccharide formulations resulted in visibly intact cake structures. Small differences were detected between LDH formulations mono- and disaccharides which are consistent with literature findings (Arakawa et al., 1993; Prestrelski et al., 1993b). While glucose yielded average activities of around 75 %, the disaccharide outcomes averaged 80 % (Figure 3.3.2a). In addition, the Raman microscopic spectrum of LDH freeze dried in the presence of 0.005 M trehalose exemplarily shown in Figure 3.3.3 exhibited no significant shift of the amide I band confirming the capacity of the disaccharide to virtual completely stabilize the native protein structure during freeze drying.

With the exception of sucrose containing lyophilisates, where the maximum recovered enzymatic activities are obtained at concentrations equal to or above 0.05 mol/L of stabilizer (as also observed by Anchordoquy et al., 2001; Luthra et al., 2007a; Suzuki et al., 1998), a clear relationship between the stabilizer concentration and the recovered enzymatic activity can not be stated. The particular behavior of glucose can be attributed to its structural properties together with the mechanisms of protection which are proposed in literature. Saccharides are considered as cryo- and lyoprotectants, developing their stabilizing potential during the freezing and the drying phase (Wang, 2000). Their efficiency is generally explained by three mechanisms: (i) preferential exclusion of the saccharide or more general the solute from the proteins surface, also known as preferential interaction; (ii) the formation of an amorphous matrix, which is able to immobilize the protein and thus to avoid intermolecular interaction a precursor for aggregation phenomena; and (iii) the replacement of hydrogen bonds upon water sublimation (Carpenter et al., 2007, Nail et al., 2002). Though glucose exhibits similar capacities to stabilize proteins by water replacement during the dehydration phase compared to that of disaccharides, it is less effective with regard to stabilization during the freezing phase (Allison et al., 1999; Carpenter et al., 1987). This can

a)
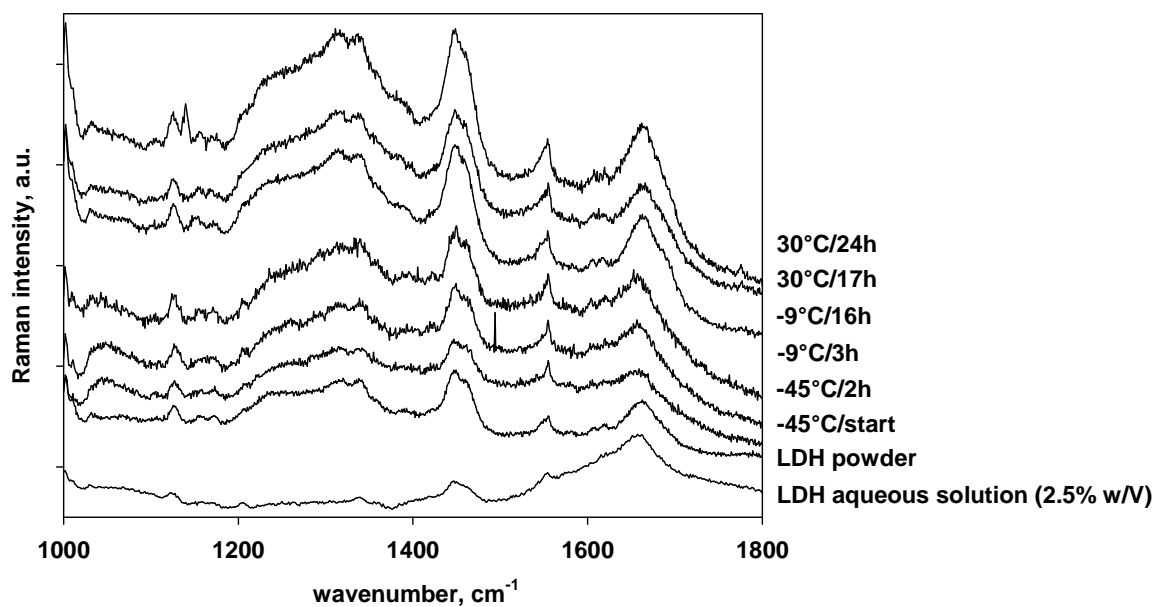
b)

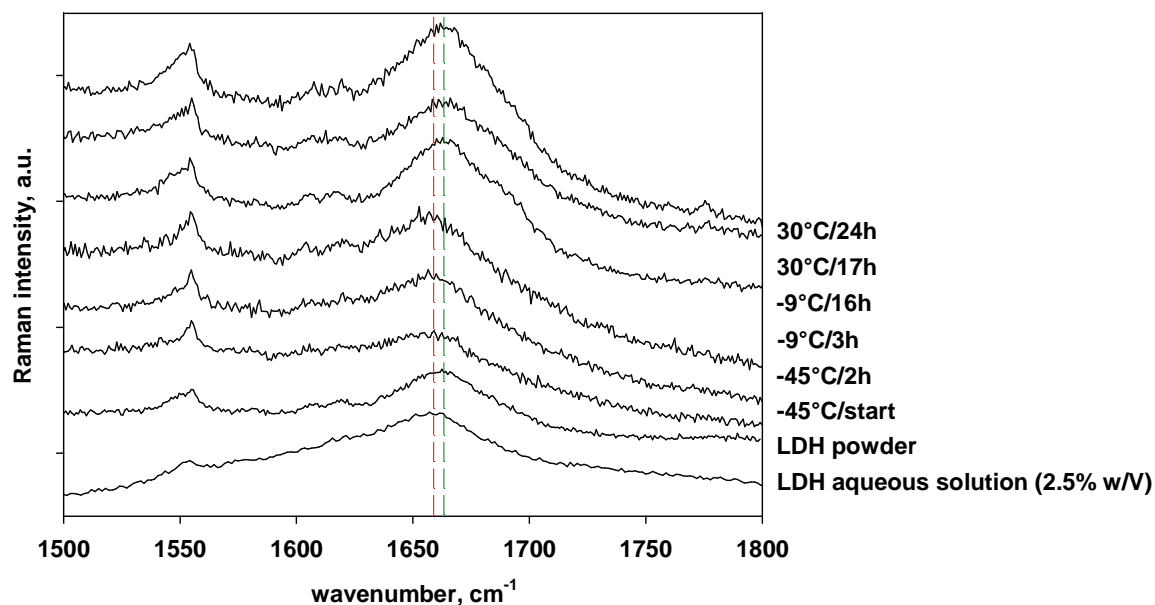*Figure 3.3.1: Raman spectra of an aqueous LDH solution (c = 2.5 mg/mL) freeze dried in a cryo stage. Spectra are shown for the (a) 1000-1800 cm^{-1}range and (b) a zoom to the 1500-1800 cm^{-1} amide I band region. Time points of the recorded spectra are indicated in the figure.*

at least partially be attributed to the low T'_g of the frozen glucose formulation at about -42 °C (Kadoya et al., 2010) with regard to the freezing temperature of -45 °C used in our study. The closer both temperatures the higher the probability to induce physical collapse of the freeze dried solids and thus potential protein denaturation.

Interestingly, the recovered enzymatic activity of LDH lyophilized during the Raman microscopic analysis and the LDH lyophilized as reference formulation without protectant differed. The Raman microscopy experiment was conducted with a different setup, comprising of different intervals and temperatures for the distinct freeze drying phases. Furthermore, they were carried out with larger sample volume and a container of different dimensions. All these parameters can contribute to the variation in the recovery of enzymatic activity as reported by several authors (Anchordoquy and Carpenter, 1996; Prestrelski et al., 1993a; Ramos et al., 1997). Literature values for freeze dried LDH in potassium phosphate buffer at various conditions ranged from 12 to 66 %

The second group of stabilizers investigated was polyols. Figure 3.3.2b shows recovered enzymatic activities of LDH freeze dried with 3 polyols, including mannitol and sorbitol as isomeric molecules. In general, the latter are less effective in preserving the LDH enzymatic activity during freeze drying than maltitol which is a complex polyol. Additionally, mannitol and sorbitol exhibited a concentration dependent stabilizing potential. This was also stated by Luthra et al. (2007b) for sorbitol. Furthermore, they reported saturation phenomena at sorbitol concentrations equal to or above 0.5 % (w/V) with recovered activity of about 80 %. Importantly, sorbitol has poor glass formation properties due to its low T_g and thus stabilizes simply by replacing hydrogen bonds between water and the protein. Mannitol, being a homologue of sorbitol exhibited similar behavior and thus yielded similar results (Izutsu et al., 2003). The higher potency of maltitol to stabilize LDH can be attributed to its improved glass-forming abilities, which reduce the molecular mobility of LDH and thus the destabilization of the native structure (Kadoya et al., 2010). Furthermore, the molar protein:stabilizer ratio in the maltitol formulations was higher, which is known to positively impact on the protein stabilization (Tanaka et al., 1991).

The third group of stabilizers investigated was of polymeric origin, based on various (poly)alcohols. Figure 3.3.2c compares the capacity of glycerol and PEG (M_w: 400, 6000 or 10000 Da) to stabilize LDH during freeze drying. Addition of glycerol and PEG 400 resulted in very low recoveries of LDH activity after freeze drying. This can partially be attributed to the poor outcome of the freeze drying process with collapsed cakes for almost all investigated
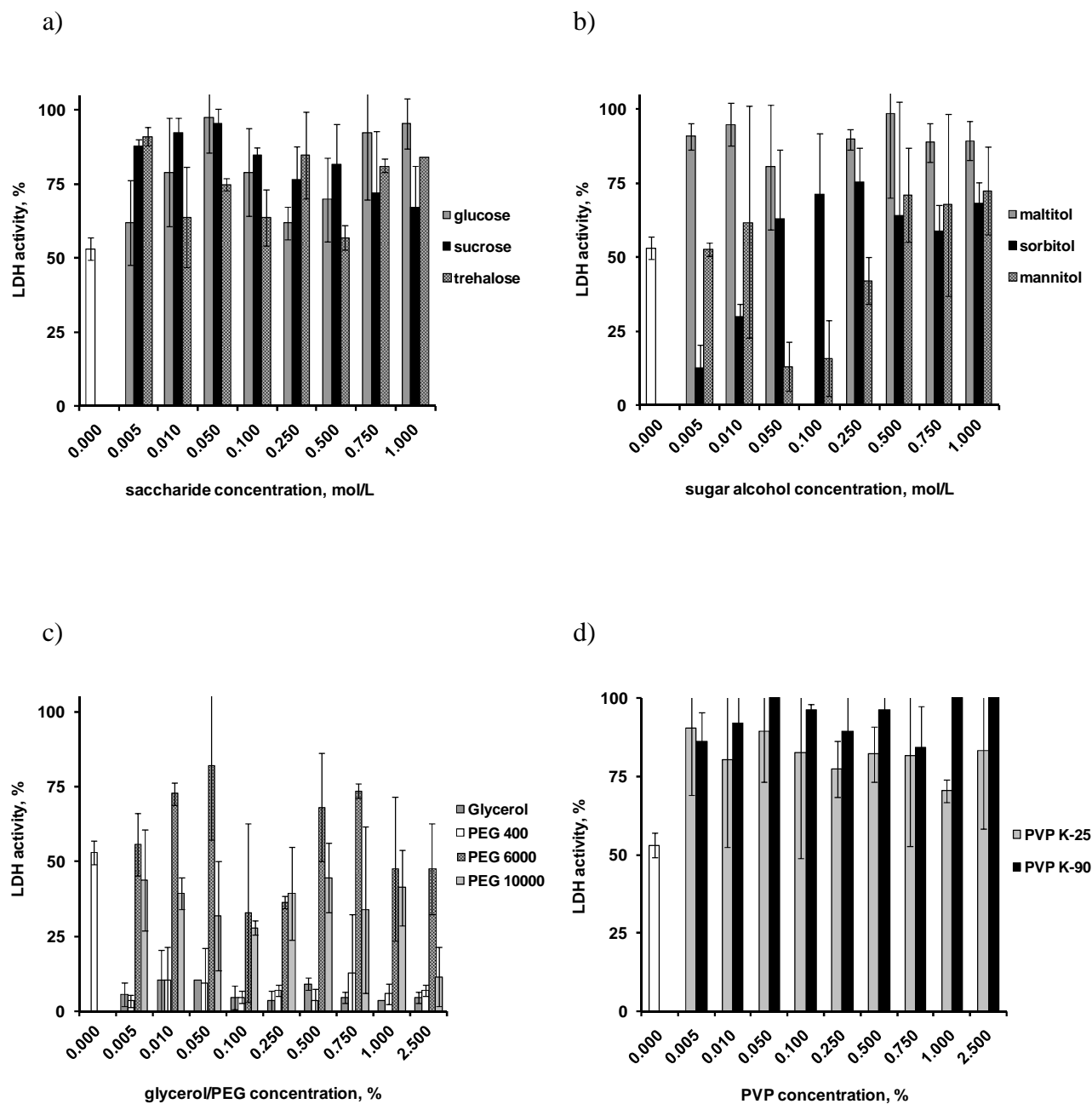
Figure 3.3.2: Activity of LDH freeze dried in the presence of: (a) saccharides, (b) sugar alcohols, (c) polyols or (d)°polymers. The freeze dried solutions contained 0.025 mg/mL LDH in 10 mmol potassium phosphate buffer pH 7.5 and different stabilizer concentrations (as indicated in the figures). The white bars indicate the LDH activity upon freeze drying without addition of a stabilizer.

concentrations. The Raman microspectroscopic analysis revealed a broadened peak with a shoulder at frequencies around 1688 cm^{-1} indicating protein aggregation (Figure 3.3.3). Higher molecular PEGs as additives improved the recovery of LDH activity. Importantly, the efficiency of PEG 6000 was superior to its homologue with higher molecular weight. Pikal (2007) reported variations in the protein stabilizing potential due to the molecular weight dependent increase of the proteins chemical potential. The latter is a factor for the free energy necessary to transfer the protein from the native to the denatured state. Generally, the principal mechanisms of cryoprotection of PEGs are the formation of an amorphous glassy matrix as well as the preferential exclusion from the proteins surface in the liquid phase and during freezing, which allows for preferential hydration (Bhat and Timasheff, 1992). Additionally, they have surface-active characteristics and can thus reduce protein denaturation induced at air-water, ice-water or vial-water interfaces (Winterhalter et al., 1995). However, they are poor lyoprotectants due to their tendency to crystallize during the dehydration phase (Carpenter et al., 2007). In addition the molecular weight and the chain length of the polymer can be disadvantageous causing sterical hindrance for hydrogen bond formation (Izutsu et al., 1995).
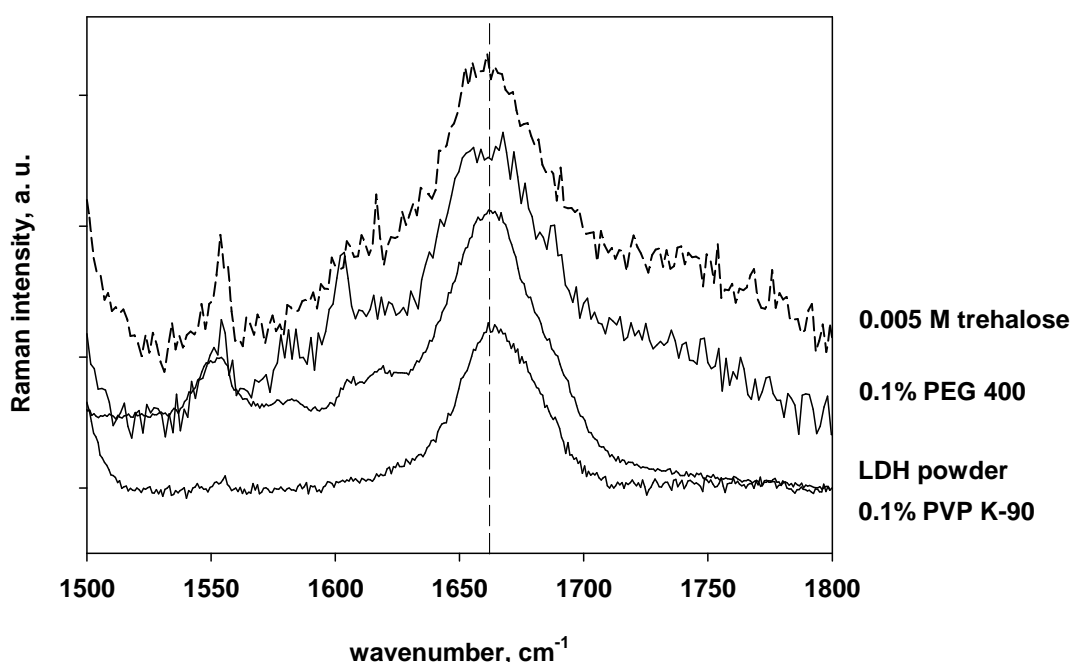

Figure 3.3.3: Raman spectra of freeze dried LDH solutions in 10 mmol potassium phosphate buffer pH 7.5 with addition of 0.005 M trehalose, 0.1 % (w/V) PEG 400 or 0.1 % (w/V) PVP K-90. The spectra were recorded in the amide I band region at 1500-1800 cm^{-1}.

By exceeding a specific chain length the stabilizing effect diminished, as demonstrated in Figure 3.3.2c.

Preferential exclusion of the polymer from the proteins surface and particularly the formation of amorphous glasses during drying are the main responsible mechanisms for the stabilization of LDH with polyvinylpyrrolidone (PVP) as stabilizer. Visible evaluation of the freeze dried cakes resulted in a homogeneous and uncollapsed structure. Figure 3.3.2d demonstrates the enzymatic activity of LDH after freeze drying with two PVP of different molecular weight. Importantly, the activities of LDH after freeze drying exceeded the value obtained for the protein without addition of a stabilizer and thus resulted in almost complete activity recovery. Water replacement by PVP during drying is unlikely as method of stabilization due to the high molecular weight of the polymers and thus the sterical hindrance for hydrogen bond formation. In contrast, the molecular weight of the polymer seems to influence the potential to stabilize during freezing and drying due to increased viscosities of the freeze concentrates and the amorphous glasses. This can effectively prevent the dissociation of the quarternary structure of the LDH, a process which may result in protein aggregation of multimeric proteins upon freeze drying and subsequent sample rehydration (Anchordoquy and Carpenter, 1996). Figure 3.3.3 shows the correspondent Raman spectrum of LDH with addition of 0.1 M PVP K-90. A slight deviation in the amide I band shape might be indicative for the formation of inter- and/or intramolecular β-sheet structures, possibly resulting in protein aggregation Hence, with regard to the recovered enzymatic activity of 96.06 %, a good correlation between Raman microspectroscopic and biochemical evaluation can be stated.

In order to benefit from the stabilizing capacities of trehalose and to investigate on the ability of an additional effect by a second excipient, stabilizers were blended in different ratios. Figure 3.3.4 shows the resultant enzymatic activities of LDH freeze dried in the presence of trehalose blended with (a) PVP K-90, (b) glycerol or (c) PEG 6000. The addition of PEG 6000 or PVP K-90 significantly increased the recovery of the enzymatic activity with virtually complete preservation. Interestingly, compared to trehalose as single stabilizer, the addition of glycerol did not impact on the recovery of native protein. This can be attributed to the dominating effect of trehalose in the stabilizer blend. In addition, glycerol, a stabilizer for proteins in solution might act, at least partially, in the same manner during the initial freezing when liquid and frozen parts are co-existing in the formulation. Thus, an additive effect to the lyoprotective properties of trehalose might be presumed for these initial phase.

a)

b)

c)
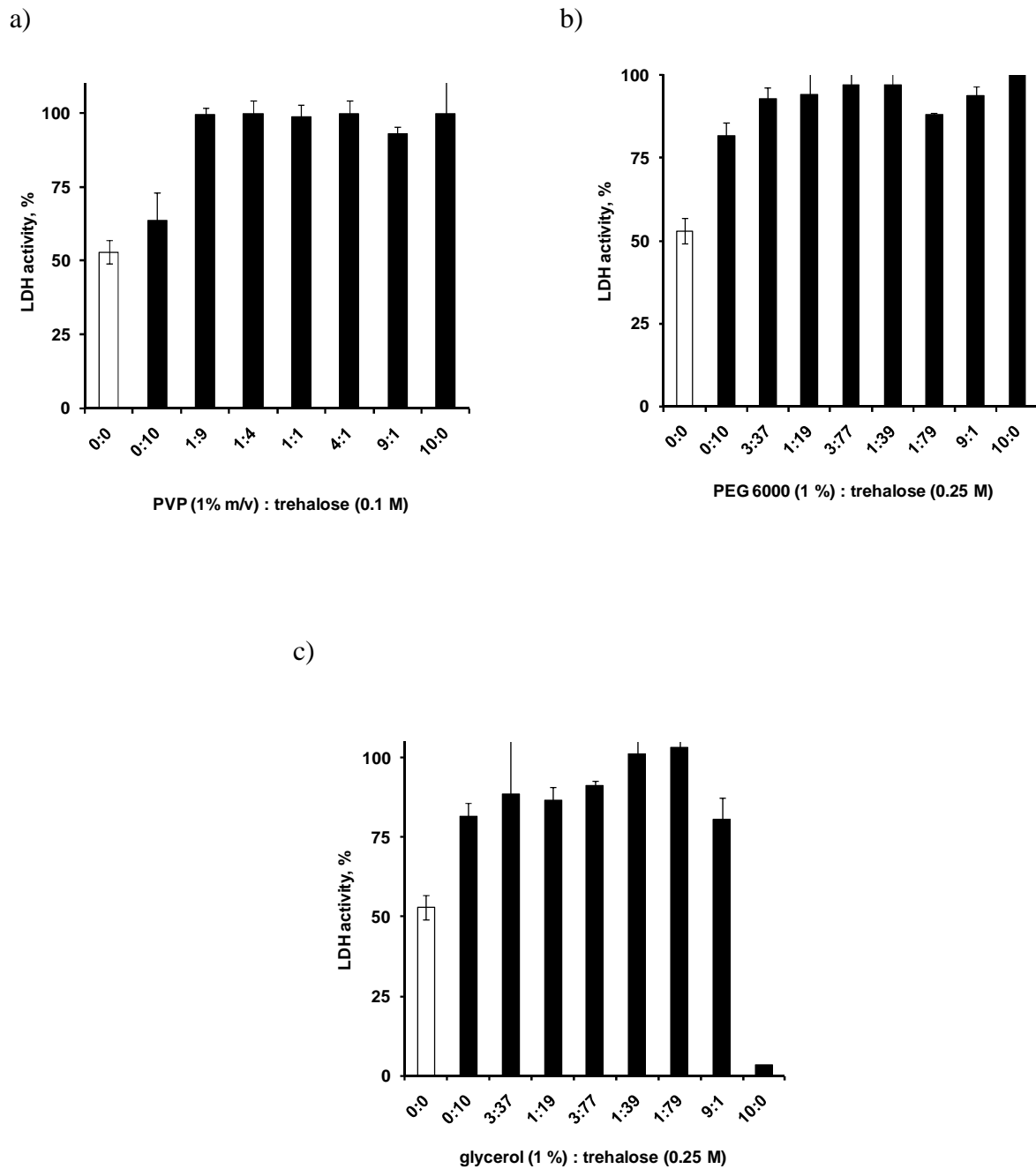
Figure 3.3.4   Efficacy of stabilizer blends upon freeze drying: (a) trehalose dihydrate and PVP K-90, (b) trehalose dihydrate and glycerol, and (c) trehalose dihydrate and PEG 6000. The freeze dried solutions contained 0.025 mg/mL LDH in 10 mmol potassium phosphate buffer pH 7.5 and different stabilizer ratios and concentrations (indicated in the figures). The white bars show the LDH activity upon freeze drying without addition of a stabilizer.

3.3.3 Stabilizer Blends: Effects on LDH Storage Stability

As a consequence from the promising results obtained with stabilizer blends in freeze dried protein solutions, further research intended on the investigation of the stabilizing potential of cryo- and lyoprotectant blends during storage at different conditions. In order to use adequate reference values for the specific experimental setups, LDH was first freeze dried in phosphate buffer pH 7.5 without the addition of a stabilizer. Figure 3.3.5 shows the resulting enzymatic activities of the formulations measured immediately after freeze drying or after storage. Storage was conducted at a relative humidity of 11.4 % at 4, 25 or 40 °C respectively. The preservation of the enzymatic activity strongly depended on the concentration of the initial protein solution which is consistent with literature data (Allison et al., 1996; Anchordoquy and Carpenter, 1996; Carpenter et al., 2007; Luthra et al., 2007b). Two mechanisms are so far reported to be responsible: firstly LDH, being a tetrameric protein was shown to be more stable in its assembled state in solution with increasing concentrations (Allison et al., 1996; Anchordoquy and Carpenter, 1996). Increasing protein concentration might decrease the tendency of LDH to dissociate during freezing due to sterical repulsion. Thus, the precursor state for possible subsequent aggregation, the formation of intermediate dimeric or monomeric structures is reduced (Wang, 2005). Furthermore, protein denaturation might also occur at the ice-water interface generated during the freezing phase. Its magnitude is closely related to the ice surface which is exposed to the protein. The latter, is a function of the cooling rate. Larger surfaces are created by rapid cooling which result in the formation of smaller ice crystals (Chang et al., 1996; Chen and Cui, 2006). Thus, assuming a finite amount of protein involved in denaturation at the ice-water interface, the higher the concentration the less is the activity loss on a per cent base.

Importantly, the enzymatic activity loss is considerably even at a storage temperature of 4 °C. At storage intervals above 3 months even the concentration dependence of the resulting activities became negligible. However, ambient storage conditions or an increase in temperature up to 40 °C resulted in complete loss of LDH activity after only 3 months. This observation is further proved by Raman microspectroscopic data shown in Figure 3.3.6. Freeze dried formulations of LDH were analyzed for eventual alterations of the amide I band shape or frequency. Spectra of LDH stored at 25 or 40 °C for 3 months with almost complete loss of the enzymatic activity exhibited a slight shift to higher frequencies and a broadening of the amide I band. While the shift might be associated to the loss of α-helices, the broadening

a)
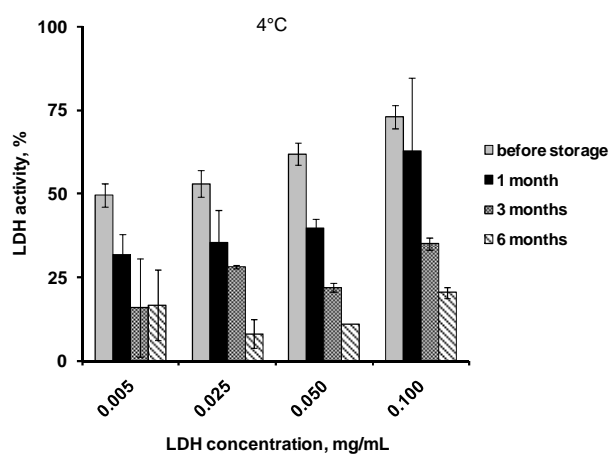
b)
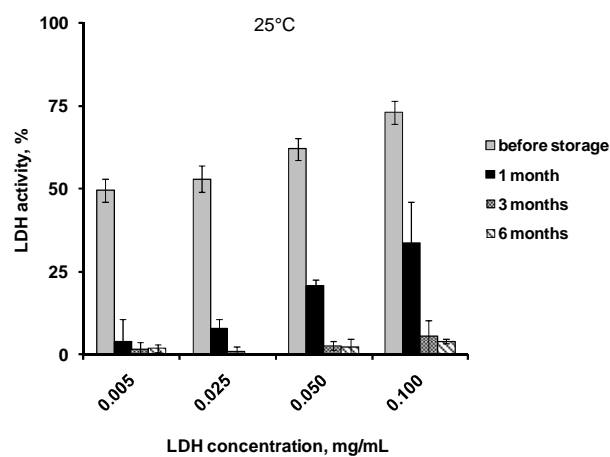
c)

Figure 3.3.5: Enzymatic activity of freeze dried LDH solutions before and after storage at: (a) 4 °C, (b) 25 °C or (c) 40 °C for 1, 3 and 6 months. The freeze dried solutions contained 5-100 μg/mL LDH (as indicated in the figures) and 10 mmol potassium phosphate buffer pH 7.5.
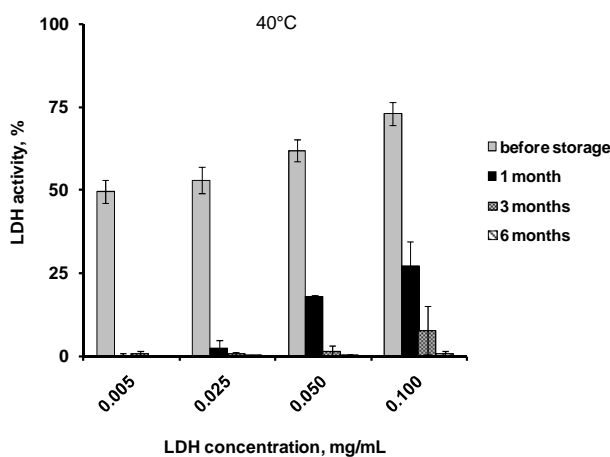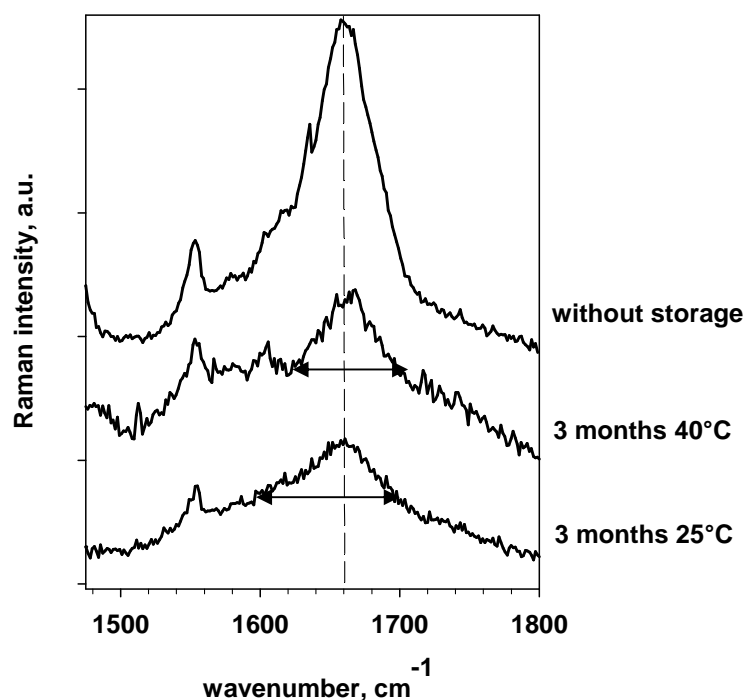
Figure 3.3.6: Raman spectra of LDH solutions after freeze drying and subsequent storage for 3 months at 25 °C or 40 °C. The freeze dried solutions contained 25 µg/mL LDH and 10 mmol potassium phosphate buffer pH 7.5.

of the peak in general indicates protein aggregation resulting from the formation of inter- and intramolecular β-sheet structures. Amide I bands shown for stored samples exhibit significantly decreased intensities at around 1660 cm^{-1} (α-helices) and increased intensities at frequencies corresponding to β-sheet structures (around 1625 cm^{-1} and 1690 cm^{-1}) as reported by Costantino et al., 1998 and Elkordy et al., 2008. It is worth noting, that to date little is known on band assignments of Raman vibrational modes for LDH. Thus, band assignments given in this work are based on the respective results from different proteins or results on LDH obtained by infrared spectroscopy. Increasing intensities at the above mentioned frequencies for samples stored at 25 °C and 40 °C for 3 months emanate from intra- or intermolecular formation of β-sheet. Intermolecular β-sheet enhances the proteins tendency to aggregate due to increased exposure of the hydrophobic residues to the solvent and weakened intramolecular interactions (Wang, 2005). Additionally, this process is also affected and enhanced by a minimal amount of residual moisture in the freeze dried product. Residual moisture analysis of the freeze dried solids after freeze drying (data not shown) demonstrated

a)

b)

c)
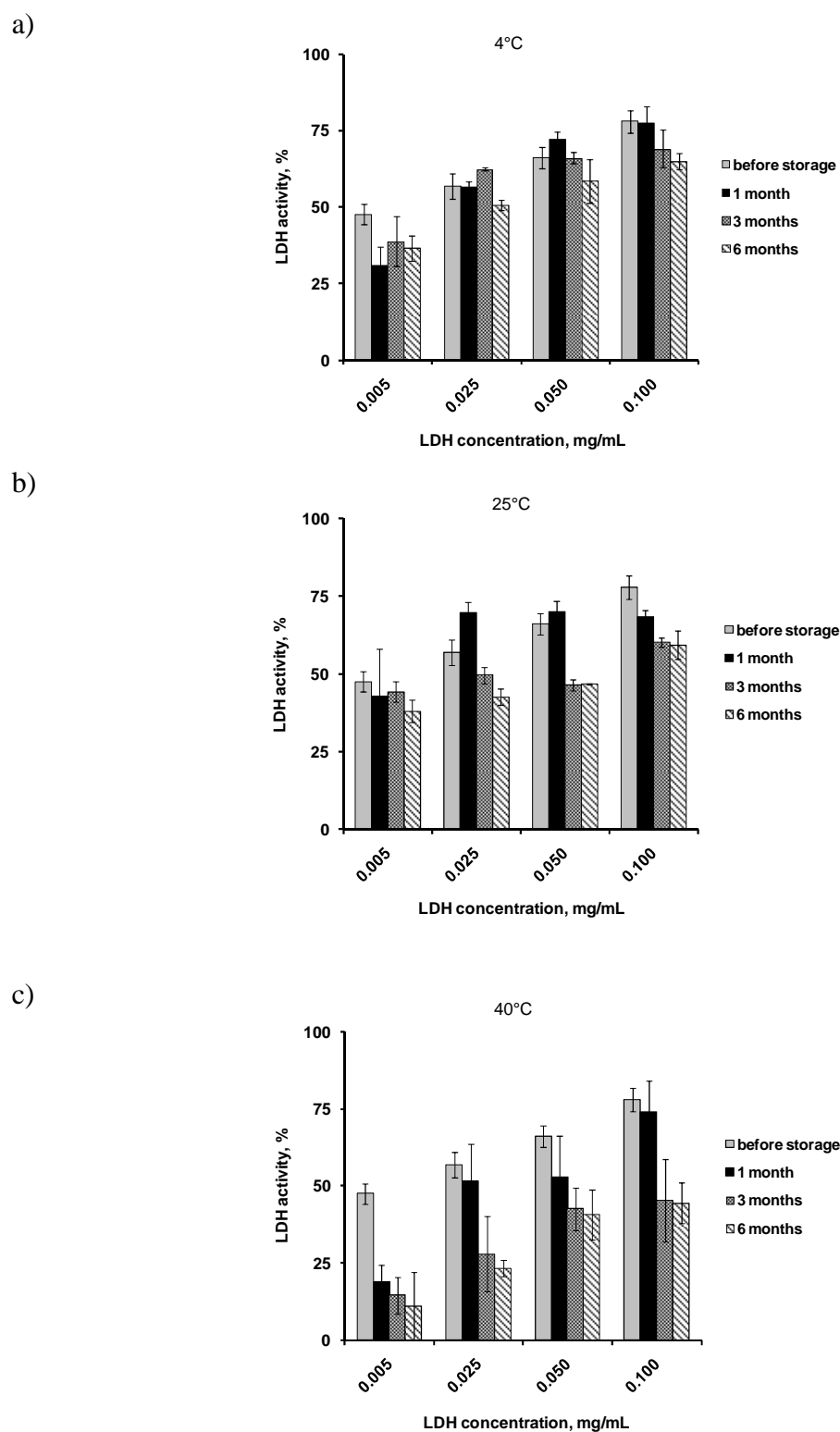
Figure 3.3.7: Storage stability of LDH solutions freeze dried in the presence of 0.5 M trehalose dihydrate at: (a) 4 °C, (b) 25 °C and (c) 40 °C. The freeze dried solutions contained 25 µg/ml LDH and 10 mmol potassium phosphate buffer pH 7.5.

a)
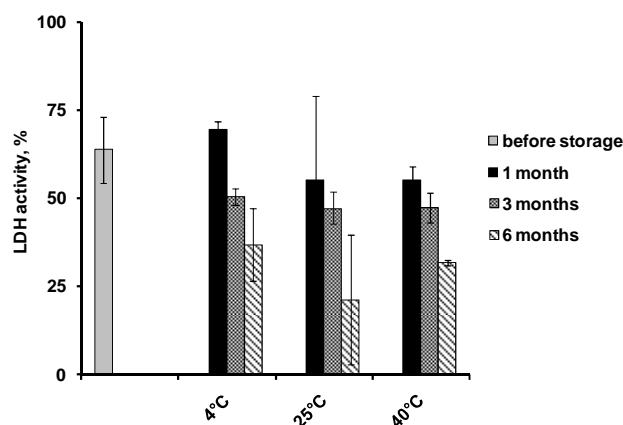
b)
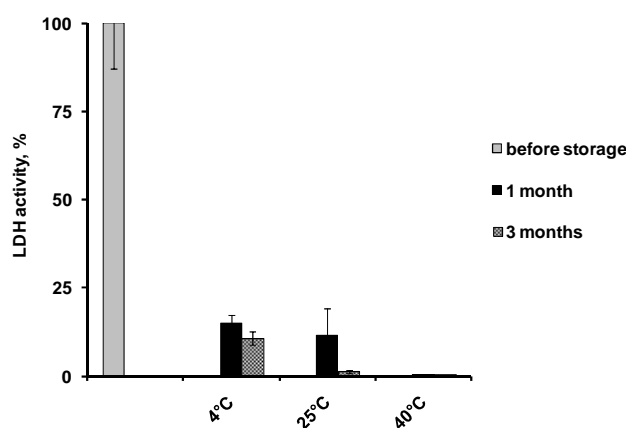
Figure 3.3.8   Storage stability of LDH solutions freeze dried in the presence of (a) 0.1 M trehalose dihydrate or (b) 1 % (w/V) PVP K-90 before and after storage at: 4 °C, 25 °C or 40 °C for 1, 3 and 6 months. The freeze dried solutions contained 25 µg/mL LDH and 10 mmol potassium phosphate buffer pH 7.5.

that even with moisture contents below 1 %, molecular interactions were considerable and led to gradual aggregation of the protein.

In order to overcome the restrictions resulting from the freezing, drying and storage induced activity loss of LDH, 0.5 M trehalose was added to the formulations. Trehalose is known to be an efficient stabilizer during both the freezing as well as the drying phase. In addition, its capacities to form amorphous glasses can be effective in preserving the native protein structure during storage. Literature suggests a minimum concentration of 0.3 M of a saccharide, which corresponds to a monomolecular layer of the stabilizer on the protein surface (Arakawa et al., 1993; Tanaka et al., 1991). Figure 3.3.7 shows the recovered

enzymatic activities of LDH after freeze drying and storage of the freeze dried solids at 4, 25 or 40 °C for 1, 3 or 6 months. Similar to the results obtained for LDH formulations without stabilizer the recovery of native protein was concentration dependent. Interestingly, the activity values of LDH freeze dried in the presence of trehalose did not significantly differ from those obtained for pure LDH systems subjected to freeze drying. However, similar observations were also made in literature where this behavior is principally attributed to specific freeze drying conditions, as for example cycle intervals, cooling and heating rates or container specifications (Wang, 2000). However, trehalose provided effective protection during storage: at 4 °C the initial enzymatic activity was virtually completely preserved.

Table 3.3.1: *Peak maxima of the amide I band of LDH in the presence of trehalose, PVP K-90 or blends thereof determined by Raman microspectroscopic analysis and their correspondent enzymatic activities. The blend ratios were PVP K-90:trehalose 9:1 stored for 3 months at 4, 25 or 40 °C.*

Sample	Peak$_{amide\ I\ band}$, cm^{-1}	Enzymatic activity, %
LDH powder	1662.54 ± 0.12	100
0.01 M trehalose	1664.87 ± 2.37	53.61 ± 3.45
0.1% PVP K-90	1663.60 ± 0.19	94.87 ± 2.59
PVP:trehalose (4 °C/3 months)	1660.62 ± 0.18	57.87 ± 4.25
PVP:trehalose (25 °C/3 months)	1667.55 ± 0.08	38.19 ± 17.16
PVP:trehalose (40 °C/3 months)	1667.31 ± 0.16	7.66 ± 0.72

Storage temperatures of 25 or 40 °C resulted in significant lower enzymatic activities after 3 months. Importantly, in formulations containing 0.1 mg/mL LDH stored at 25 °C the recovered enzymatic activity was comparable to similar samples stored at 4 °C. Preferential exclusion of trehalose during the freezing phase, the replacement of hydrogen bonds and the formation of an amorphous glassy matrix during the drying phase are the main responsible mechanisms for the stabilization of the LDH native structure during freeze drying. The latter is also considered to be the dominant mechanism during storage. Storage temperatures usually located below the T_g of the formulation. Hence, the relaxation intervals of the system are much longer as during drying, resulting in larger time scales for interactions within or

3.3.3 Stabilizer Blends: Effects on LDH Storage Stability

a)

b)

c)

Figure 3.3.9: Impact of the stabilizer blend ratio on the activity of LDH solutions freeze dried in the presence of 0.1 M trehalose and 1 % (w/V) PVP K-90 (ratios indicated in the figures) before and after storage at (a) 4 °C, (b) 25 °C and (c) 40 °C for 1, 3 and 6 months.

between the protein molecules. Consequently, time scales for protein denaturation are increased (Pikal, 2007).

In order to optimize the LDH formulation intended for freeze drying and to study the performance of trehalose:PVP K-90 blends during storage, formulations were tested at following conditions: Stability studies of freeze dried LDH were conducted in the presence of (a) 0.1 M trehalose or (b) 1 % PVP K-90 as shown in Figure 3.3.8. The potential of 0.1 M trehalose to preserve native LDH during freeze drying was superior to concentrations of 0.5 M. This can be attributed to the tendency of trehalose to crystallize during dehydration at elevated concentrations resulting in decreased hydrogen bonding to the dried protein (Carpenter and Crowe, 1989). Clearly, PVP was superior to trehalose in preserving the native protein structure after freeze drying with complete recovery of the enzymatic activity (Figure 3.3.8b). However, PVP exhibited a poor performance during storage even at favorable conditions of 4 °C with virtually complete loss of LDH activity. This can, at least partially, be attributed to a phase separation of the solutes from the protein and thus reduced stabilization (Izutsu and Kojima, 2000; Izutsu et al., 2005; Padilla et al., 2011). In contrast, by adding 0.1 M trehalose to the LDH solutions nearly 50 % of the initial protein activity after 6 months storage at 25 and 40 °C was preserved. All formulations containing 0.1 M trehalose were even more efficient at 40 °C storage temperature than the formulations containing 0.5 M of the protectant (Figure 3.3.7c). This is consistent with the findings for LDH samples analyzed directly after freeze drying in the presence of different concentrations of trehalose. Assuming similar denaturation mechanisms during dehydration and storage but within a larger time scale as reported by Pikal (2007), the same conclusions can be drawn, stating that the efficiency of the hydrogen bonding might be decreased at higher trehalose concentrations due to its increased crystallization tendency.

As a consequence from the recovered enzymatic activity of LDH in the presence of PVP K-90 or trehalose the idea was to blend the two stabilizers in different ratios to obtain an additive effect. Complete recovery of the initial LDH activity was possible irrespective of the stabilizer blend ratio (Figure 3.3.9). However, while the stabilizers yielded similar results during storage at 4 °C the blends containing equal amounts of stabilizers or an excess of trehalose showed increased preservation of LDH activity at 25 °C (Figure 3.3.9b). Similar results were obtained at 40 °C storage temperature up to a ratio of 1:4 (Figure 3.3.9c). Thus, blends of PVP and trehalose can fully preserve native LDH during freeze drying. However, the effect of trehalose during storage is dominant and is not amplified by the addition of PVP.
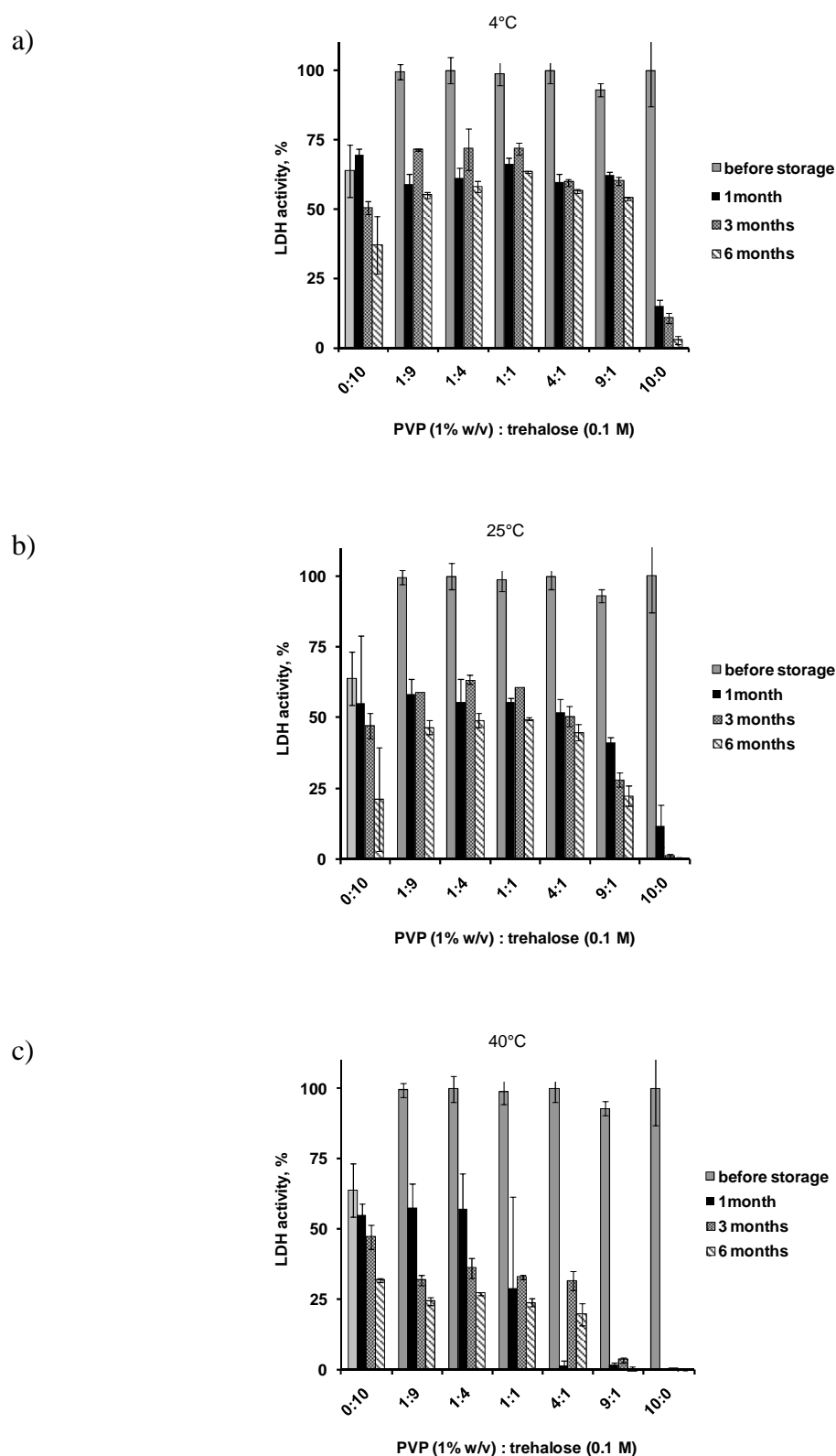
a)

b)

c)
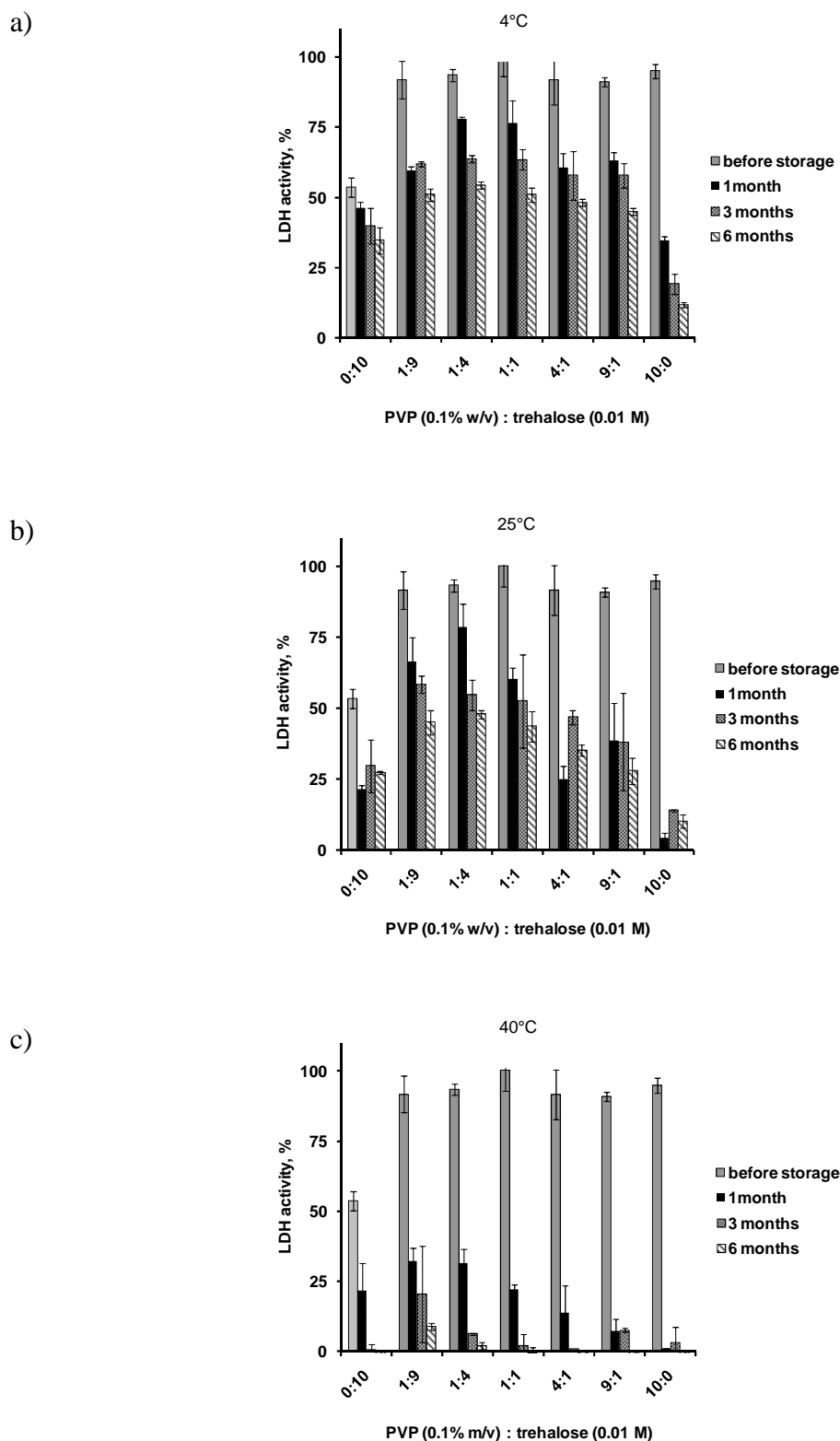
Figure 3.3.10: Impact of the stabilizer blend ratio on the activity of LDH solutions freeze dried in the presence of 0.01 M trehalose and 0.1 % (w/V) PVP K-90 (ratios indicated in the figures) before and after storage at (a) 4 °C, (b) 25 °C and (c) 40 °C for 1, 3 and 6 months.

a)

b)
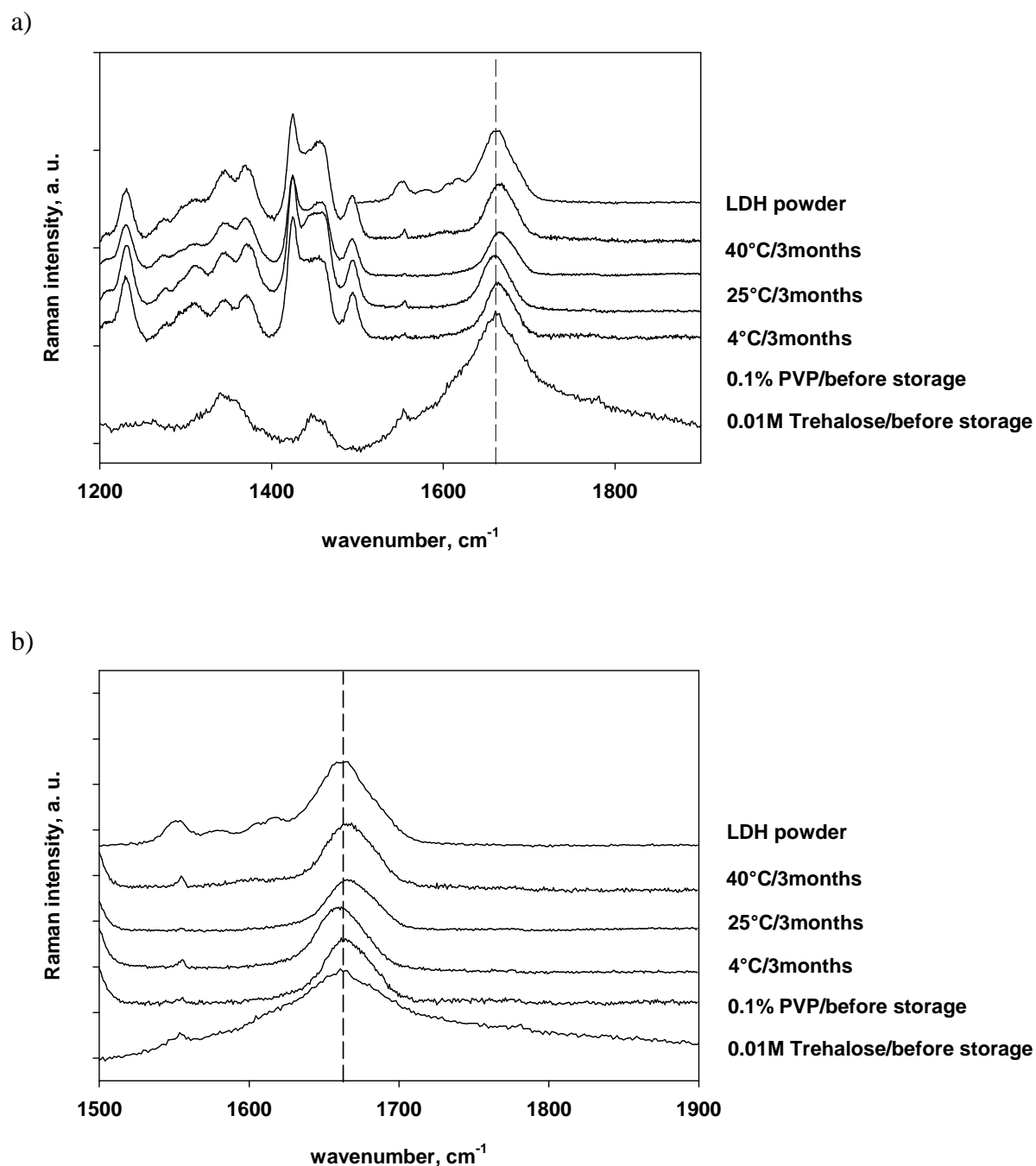
Figure 3.3.11: Raman spectra of freeze dried LDH solutions in the presence of 0.01 M trehalose, 0.1 % (w/V) PVP K-90 or 0.01 M trehalose and 0.1 % (w/V) PVP K-90 blends (ratio 9:1) after freeze drying and subsequent storage for 3 months at 4 °C, 25 °C or 40 °C. The freeze dried solutions contained 25 μg/mL LDH and 10 mmol potassium phosphate buffer pH 7.5. The bottom figure shows a zoom to the amide I band region between 1500-1900 cm^{-1}.

Because of the difficulties to determine the amide I band of LDH in the trehalose and the PVP matrix via Raman spectroscopy lower concentrations of the two stabilizers were used for the following experiments. PVP:trehalose stabilizer blends were added to LDH solutions containing 0.025 mg/mL protein (Figure 3.3.10). The initial concentration of the saccharide was 0.01 M and 0.1 % for PVP. The potential to preserve the native protein structure was slightly decreased compared to the elevated stabilizer concentrations at all investigated temperatures. Blend ratios of 1:4 and 1:1 exhibited a slight superiority to lower amounts of trehalose except for storage temperatures of 40 °C, were 1:9 and 1:4 were the most effective stabilizer blends. This strengthens the above made statement that trehalose provided the major contribution to protein stabilization. The PVP:trehalose ratio 9:1 was further investigated by Raman microspectroscopic experiments due to its decreasing enzymatic activity values during storage. Figure 3.3.11 shows Raman spectra of solid LDH and LDH solutions lyophilized with each of the single stabilizers as well as the mentioned blend ratio. The data was collected after 3 months of storage at 4, 25 and 40 °C at frequencies of (a) 1200-1900 cm^{-1} and (b) in the amide I band region. The dotted line indicates the characteristic peak at 1662.54 cm^{-1} corresponding to the C = O stretching vibration of amide groups coupled to the bending of the N - H bond and the stretching of the C - N bond. According to the state of LDH denaturation the spectra with a trehalose stabilizer concentration of 0.01 M exhibited a peak broadening but no shift to higher frequencies (Table 3.3.1). Consequently, aggregation phenomena probably due to dissocation of the LDH tetramers can be presumed but no substantial loss of the protein secondary structure was observed. PVP at a concentration of 0.1 % (w/V) exhibited the same peak as the native LDH powder which is consistent with the measured enzymatic activity after freeze drying and subsequent storage (Table 3.3.1). Samples stored at different temperatures showed both a shift to higher frequencies and/or peak broadening (25 and 40 °C). Compared to the correspondent activity values Raman spectra confirmed the obtained results. The underlying mechanisms of denaturation are predominantly aggregation at lower and both aggregation and alterations in the secondary structure of LDH at higher storage temperatures.

3.4 Lysozyme Loaded Lipid Implants

The addition of stabilizers to protein solutions intended for freeze drying was shown to be of utmost importance to preserve the native protein structure during freeze drying and subsequent storage. The stabilizing additive trehalose had shown potential either as a single stabilizer or as a part in a stabilizer blend. Consequently, this stabilizer was investigated for its capacities to preserve the native state of the model protein lysozyme acting as the active pharmaceutical ingredient (API) in an implantable drug delivery system. Small cylindrical implants of 3 mm diameter containing lysozyme, a triglyceride and optionally trehalose were manufactured and analyzed for their release profiles and the conformational stability of the released lysozyme and the remaining protein in the implant. As in the previous sections a combination of two analytical methods, determination of protein activity by a specific enzymatic assay and Raman microspectroscopy were employed.

3.4.1 Raman Microspectroscopy of Lipid/Lysozyme Blends

Preliminary studies aimed at obtaining Raman spectra of the investigated triglyceride/lysozyme blends in order to identify characteristic bands, which allow for the simultaneous observation of the molecular structure of the two components. Figure 3.4.1 shows Raman spectra of (a) powdered hardened soybean oil and (b) lysozyme powder as received. A zoom to the green and red highlighted areas in each spectrum is shown on the right hand side of the figure. The spectrum of hardened soybean oil exhibited two characteristic bands between 1050 and 1300 cm^{-1} and one band at 1740 cm^{-1}: The first two indicate the bending of C - O and C - H bonds, the latter the C = O stretching vibration of the ester group established between the glycerol and the fatty acids of the lipid. A large band at 1300 cm^{-1} is attributed to the molecular vibration of the carbohydrate chain. For lysozyme the amide I band can clearly be seen in the green highlighted area of the spectrum in Figure 3.4.1. Importantly, the spectra exhibited two distinct bands for the protein at 1660 cm^{-1} and the lipid at 1740 cm^{-1}. Thus, simultaneous analysis of both, protein and excipient, during manufacturing and release experiments is possible.

a)

b)

-1)

*Figure 3.4.1: Raman spectra of: (a) hardened soybean oil powder and (b) lysozyme powder.
On the right hand side a zoom to the high frequency area (amide I band region) is shown.*

3.4.2 Effect of the Preparation Method on Protein Release

In order to determine the release profile of lysozyme from lipid implants, *in vitro* drug
release experiments were conducted with 2, 6, and 10 % protein loaded lipid implants based
on hardened soybean oil. Figure 3.4.2 shows the release profiles of implants prepared by the
emulsion method with magnetic stirring. Lysozyme was rapidly released from the implants,
irrespective of the initial drug loading, with approximately 80 % of the total protein amount
released after only 3 days and complete release after 14 days (10 % drug loading) or 28 days
(2 and 6 % drug loading) respectively. This can be attributed to a rather inhomogeneous
protein distribution within the implants resulting in zones with high and low protein content.
Upon contact with the surrounding bulk fluid, the latter imbibed into the implant, the lyozyme
dissolved and diffused through the implant following the concentration gradient between the
implant and the surrounding bulk fluid. Consequently, void spaces or pores created which are

filled with bulk fluid. The dimension and the connectivity of these pores are important parameters for the rate of protein release from the lipid implants assuming that the predominant mass transport is protein diffusion (Guse et al., 2006a, Siepmann and Siepmann, 2011b). Low homogeneity and large protein agglomerates (Figure 3.4.3a) within the implants, which were additionally located close to the surface resulted in a less coherent porous network of the lipid (Figure 3.4.3).

a)
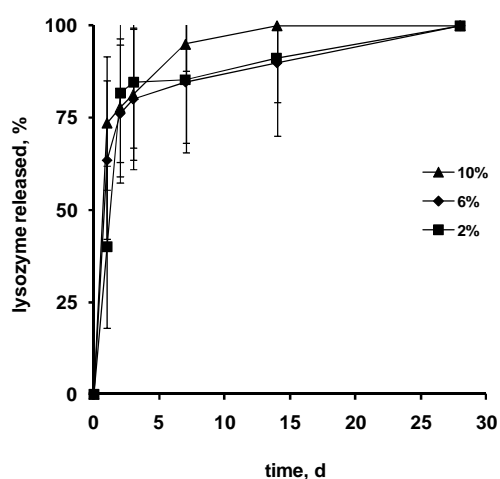
b)
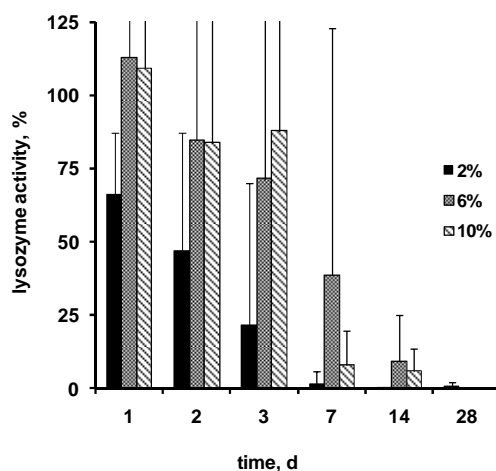
Figure 3.4.2: Protein release from implants based on hardened soybean oil loaded with 2, 6 or 10 % lysozyme (as indicated in the diagrams) into phosphate buffer pH 7.4 (containing of 0.01 % sodium azide) at 37 °C: (a) cumulative total protein release, (b) lysozyme activity in the withdrawn samples. The implants were prepared using the emulsion technique with magnetic stirring.

In general, this indicates slow drug release rates due to the poor water permeability of the lipid (Kreye et al., 2008; Siepmann and Siepmann, 2011a). However, the above mentioned inhomogeneous distribution and aggregates of lysozyme in the implants close to the surface resulted in a rapid dissolution and thus the initial release was high (Figure 3.4.2a).
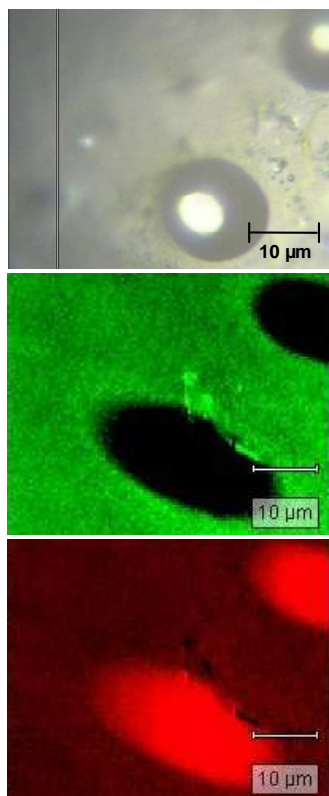
a)   b)
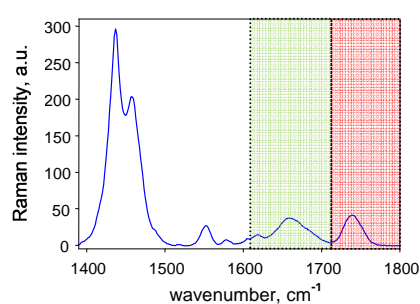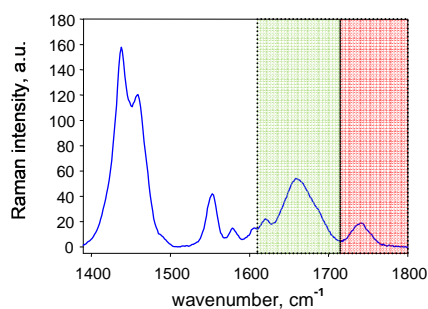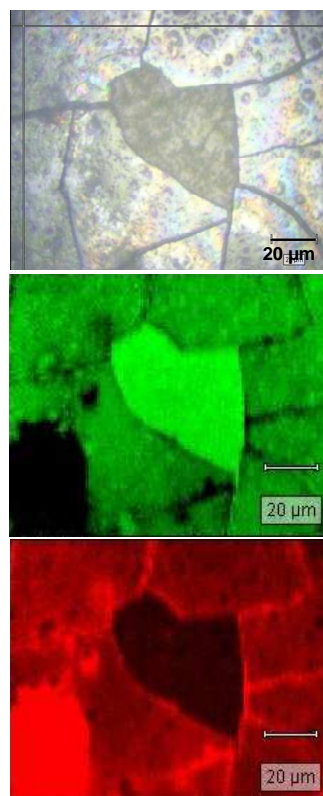
Figure 3.4.3: Optical and Raman images and corresponding Raman spectra of lysozyme loaded implants based on hardened soybean oil (protein loading 2 %) (a) before and (b) after freeze drying. Red and green highlighted areas display the lysozyme and triglyceride components.

While high enzymatic activities of the released lysozyme were observed for the first 3 days of release, they considerably decreased after 1 week due to lysozyme denaturation occurring during implant preparation or during the release experiment.

The above made assumption was further confirmed by optical and Raman microscopic images exemplarily shown in Figure 3.4.3 for a lysozyme loaded implant (2 % protein loading) based on hardened soybean oil prepared by magnetic stirring after (a) manufacturing and (b) subsequent freeze drying. The corresponding Raman spectra are displayed at the bottom of the figures. The impression of a rather inhomogeneous distribution of lysozyme within the lipid matrix, given by the optical image is further enhanced by the Raman microscopic images of the protein and the lipid. Green areas designate the lipid matrix, red areas the protein. Protein rich and lipid rich phases can be identified, both, before and after sublimation of the incorporated aqueous phase. Consequently, magnetic stirring as emulsification method for the molten lipid and the protein solution was considered inappropriate.

Importantly, the Raman spectra in Figure 3.4.3a and 3.4.3b show amide I bands similar to those of the native lysozyme, indicating that no protein denaturation occurs during manufacturing. However, the freeze drying process can be detrimental to protein stability, due to various occurring stresses (e.g., ice formation, freeze concentration of the protein in solution, denaturation at ice-water interfaces) (Wang, 2005). Furthermore, the release experiment itself might induce protein denaturation. After complete saturation of the implant with the surrounding bulk fluid, the protein remains in an aqueous environment until it is released by diffusion. Consequently, denaturation processes (e.g., deamidation, oxidation, hydrolysis or steric interaction) are highly likely (Brummer, 2008; Koennings et al., 2007a/b; Koppenol, 2008). Additionally, the increased molecular mobility of the lysozyme chains carried the risk of increased intermolecular interaction and subsequent aggregation phenomena. Nevertheless, increased protein concentration in the implant resulted in increased preservation of the biological activity. This can be attributed to the ability of proteins to self-stabilize their conformation and thus their native state with increasing concentration (Jiang et al., 1998; see also *section 3.3 Conformational Stability of LDH during Freeze Drying and Storage*).

Similar phenomena were observed for implants of the same composition but prepared by emulsification via ultrasound. Compared to the magnetic stirring method, the lysozyme release profiles altered only to a minor extent. The most significant change was the differentiation of the drug release rates with regard to the protein loadings. For implants

composed of hydrogenated soybean oil and lysozyme only, release from 10 % drug loaded implants was slower which might be explained by the experimental error (standard deviations are overlapping) or the fact that the protein solubility was slower than the diffusion of the dissolved lysozyme from the implants. In this case dissolved and non-dissolved lysozyme co-exist within the matrix. Only dissolved protein is available for diffusion and thus, by increasing the absolute amounts of protein in the matrix, the relative protein release rates decrease (Kreye et al., 2008). On the other hand, erosion phenomena of the lipid matrix
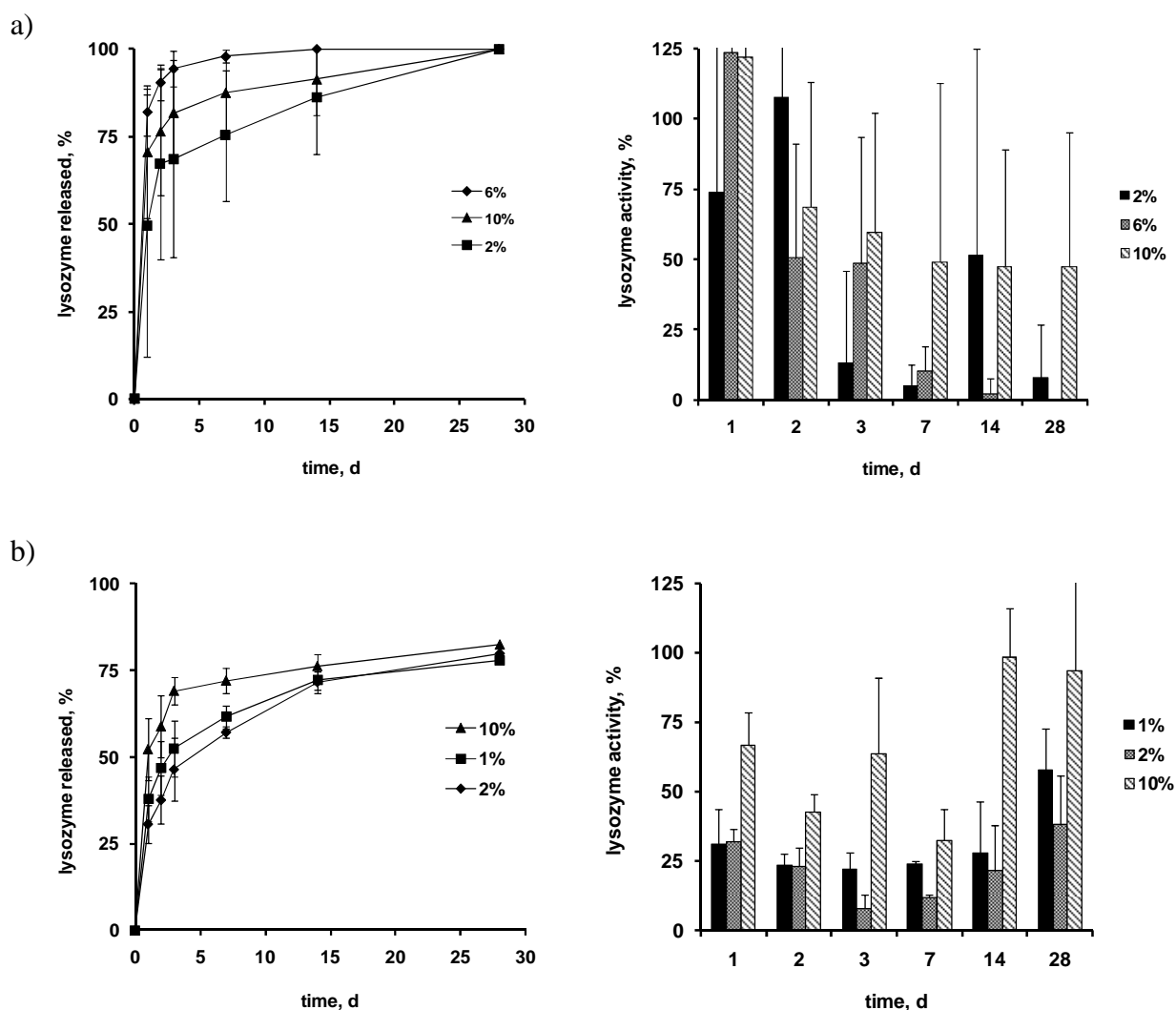
Figure 3.4.4: Protein release from implants based on hardened soybean oil loaded with 2, 6 or 10 % lysozyme (as indicated in the diagrams) and optionally 0.05 M trehalose in phosphate buffer pH 7.4 (containing 0.01 % sodium azide) at 37 °C: cumulative total protein release and lysozyme activity (a) without and (b) with addition of trehalose. The implants were prepared using the emulsion technique and ultrasound.
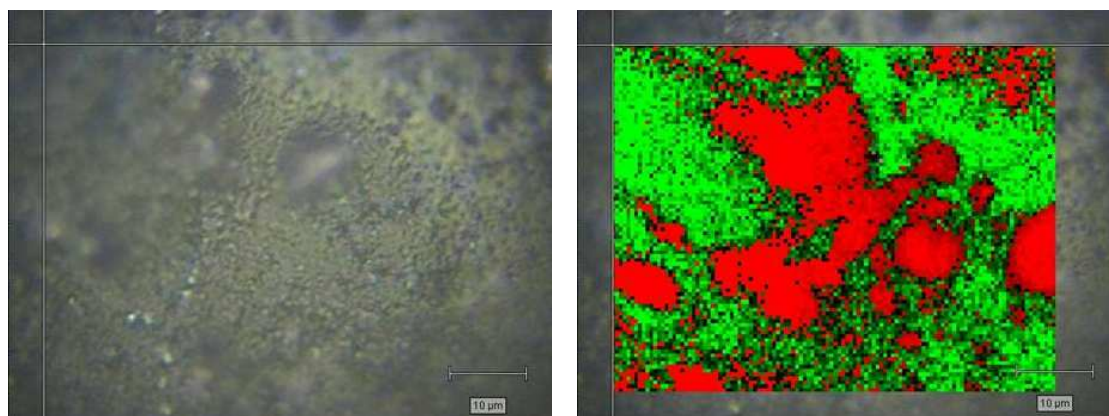
Figure 3.4.5: Optical and Raman images of lysozyme loaded implants based on hardened soybean oil and 0.05 M trehalose (protein loading 6 %) (a) before and (b) after freeze drying. Lysozyme and triglyceride contributions to the spectra correspond to the red and green highlighted areas.

should also be considered even if in the present study erosion was not observed. However, complete drug release was achieved after 28 days in all cases. Additionally, implants prepared by ultrasonic emulsification exhibited slightly higher recoveries of enzymatic activity at later stages of the drug release experiments, especially for the 10 % drug loading (Figure 3.4.4a). However, the trend of decreasing biological activities with progressing release remained.

   In order to investigate the effect of a stabilizer on the recovery of the enzymatic activity of lysozyme, trehalose was incorporated in the implant formulation at a concentration of 0.05 M. Figure 3.4.4b shows that the trend was inversed showing increased lysozyme activities at the end of the drug release experiment. This can be attributed to a stabilizing effect of trehalose during the freeze drying step as well as during the release experiment, resulting in the preservation of the native lysozyme within all parts of the implant. Assuming diffusion controlled release, protein located in the center of the implant is released at advanced stages of the release experiment. Hence, the interval the latter remains in an aqueous environment are prolonged due to the greater distance the protein has to cover to be released. Additionally they might lose activity as a consequence of denaturation at the lipid-water interface. Trehalose is able to protect lysozyme from this type of denaturation by assuring preferential interaction at the proteins surface. Interestingly, the drug release rates of the implants containing trehalose were slower even if the amount of the hydrophilic compounds in the

implant was increased. In general, the wettability and therefore the imbibing of the surrounding bulk fluid are facilitated with increasing hydrophilicity of the device. However, the amount of trehalose per implant on a percentage weight base was approximately 0.5 % which might be neglected with regard to the hydrophilicity. Emulsion via ultrasound in general led to a more homogeneous distribution of the protein in the implants which is exemplarily shown in Figure 3.4.5 for trehalose containing implants. However, randomly distributed lysozyme aggregates within the lipid matrix can as well be found for this type of implants. Thus, a continuous network of lysozyme within the implant might not be assumed.

The difference in the release kinetics can be explained by the particular manner the protein is distributed in the implants. The addition of trehalose might have influenced the coherence of the lysozyme network within the implants, which was formed during preparation resulting in a less homogeneous distribution of the protein. This again led to a decreased accessibility of the protein by the surrounding bulk fluid and thus a slower and incomplete release. Moreover, protein release leveled off at the end of the experiment which is consistent with the above made assumption.

This theory is substantiated by the photomicrographs of lysozyme loaded implants (Figure 3.4.7) which demonstrate a more porous structure for the implants without addition of trehalose. As proteins are polymers and might exhibit a certain surface activity the emulsification of the lysozyme solution and the molten lipid might have been more efficient without the addition of trehalose. Trehalose was reported to alter the binding structure between water and protein at elevated temperatures, resulting in a more rigid structure (Hedoux et al., 2006). Thus, relaxation of the protein tertiary structure and the externalization of hydrophobic residues might be decreased leading to a decreased surface activity of lysozyme and a less effective emulsification.

3.4.3 Raman Microspectroscopy: Lysozyme Conformation during Release

Investigation on lysozyme denaturation during freeze drying and release for implants based on hardened soybean oil containing 6 % protein and 0.05 M trehalose were continued by Raman microscopic analysis. The aim was to correlate the results obtained by biochemical analysis and *in vitro* drug release experiments with this technique. In Figure 3.4.6 Raman spectra of native and denatured lysozyme were plotted against spectra of the protein within the lipid implants (surface and cross section) at different time points during release. Clearly, a shift of the amide I band to higher frequencies was detected for the denatured lysozyme powder, indicating a loss of α-helical structures and an increase of β-sheet and random coil structures. In general, β-sheet structures are predominantly responsible for protein aggregation at least due to their lower dipole moment (Querol et al, 1996). Moreover, a partial loss of secondary protein structure is indicated by the slight peak broadening with higher unordered contents in the secondary structure due to the formation of irreversible aggregates (Sane et al., 2003; Seo et al., 2010; Wang, 2005). Implants analyzed by Raman spectroscopy immediately after freeze drying exhibited intact lysozyme structures on the surface as well as in the cross section as shown in the first columns of Figure 3.4.6a and 3.4.6b. Samples, analyzed after 7 and 28 days of the release experiment exhibited amide I band shifts to higher frequencies, irrespective of the position the measurement was made (surface or cross section), indicating a decrease in α-helix. However, the surface and cross sectional spectra of implants analyzed on day 7 of the release experiment as well as the cross section of implants analyzed on day 28 exhibited no visible amide I band shift. In contrast, the surface spectra of lysozyme in implants after 28 days of release exhibited both, a shift of the amide I band and peak broadening of. Correlation of the Raman results with the enzymatic activity data led to the conclusion that the protein secondary structure was preserved in the interior of the implants but might decrease due to surface induced denaturation and/or aggregation during release or upon contact with the surrounding bulk fluid which is consistent with observations made in literature (Koennings et al., 2006). Moreover, with the measured Raman spectra only limited statements with regard to the lysozyme structure could be made since the investigated areas are a function of the magnification of the microscope and the size of the laser beam. In contrast, the measured enzymatic activity reflected the state of the whole sample. Thus, correlation and interpretation of data obtained by both techniques should be done having this in mind.

Figure 3.4.6: Raman spectra of lysozyme loaded lipid implants based on hardened soybean oil (6 % drug loading) prepared by the emulsion technique and ultrasound. Horizontal: a) surface and b) cross sections. Vertical: before, after 7 and 28 days of release. A zoom to the amide I band region is shown in the inserted figures. Arrows in the scheme preceding the figures indicate the areas where samples were analyzed.

Figure 3.4.7 shows the surface and cross sectional microscopic images of the 6 % lysozyme loaded implants based on hardened soybean oil (a) containing optionally 0.05 M trehalose (b). The surface of the trehalose containing implants was visibly smoother than that of the implants without stabilizer, indicating that the faster release rate of the systems without stabilizer (Figure 3.4.4a) might be attributed to a higher porosity. This theory is further substantiated by the photomicrographs of the implants after 28 d of drug release. Clearly, the implants without addition of trehalose exhibit a more porous network of the lipid matrix. In contrast, a less porous structure of the lipid matrix in implants containing 0.05 M trehalose was observed. Castellanos et al. (2002) reported incomplete release of protein due to the formation of insoluble aggregates which remained entrapped in the implant matrix due to the larger size of the aggregates compared to the pore size in the surrounding matrix. The photomicrographs (Figure 3.4.7b) and the results of the protein release from trehalose containing lipid implants can be explained by this observation.
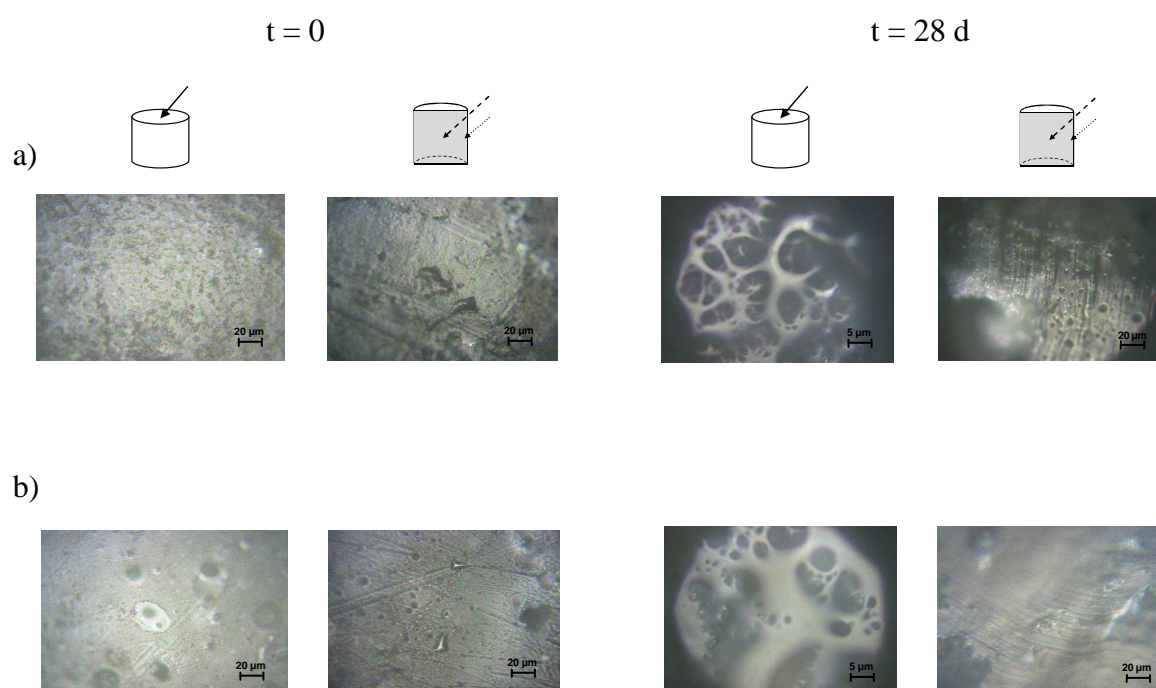
Figure 3.4.7: Microscopic images of surfaces and cross sections of lysozyme loaded lipid implants based on hardened soybean oil (protein loading 6 %) (a) without or (b) with the addition of 0.05 M trehalose before and after 28 d release.

3.4.4 Lysozyme Stability Using an Alternative Lipid Excipient

In order to investigate the capacities of a second triglyceride to obtain sustained release of the incorporated protein, implants based on glyceryl tristearate were prepared by the emulsification via ultrasound. The choice of the lipid was made according to Kreye et al. (2011a and b), stating that shorter fatty acid chain lengths result in slower drug release rates. The protein release profiles and the corresponding activities are shown in Figure 3.4.8.

a)
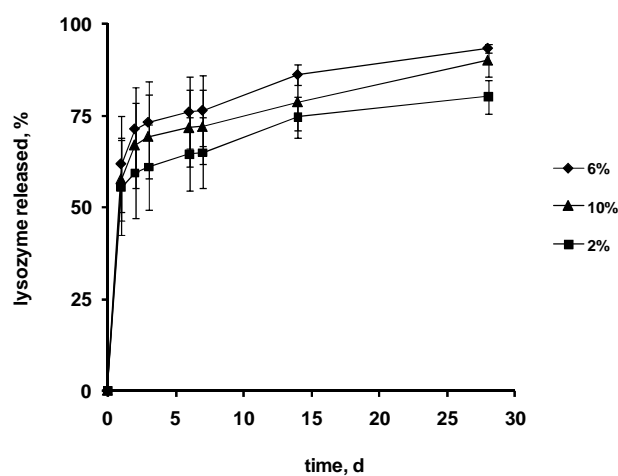
b)
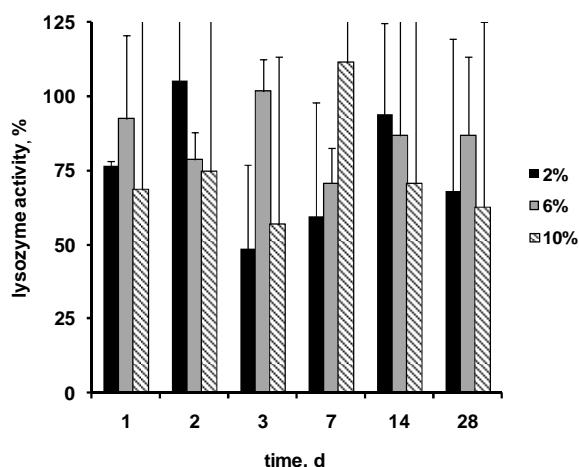
Figure 3.4.8: Protein release from implants based on glycerol tristearate loaded with 2, 6 or 10 % lysozyme (as indicated in the diagrams) in phosphate buffer pH 7.4 (containing 0.01 % sodium azide) at 37 °C: (a) cumulative total protein release, (b) lysozyme activity in the withdrawn samples. The implants were prepared using the emulsion technique and ultrasound.
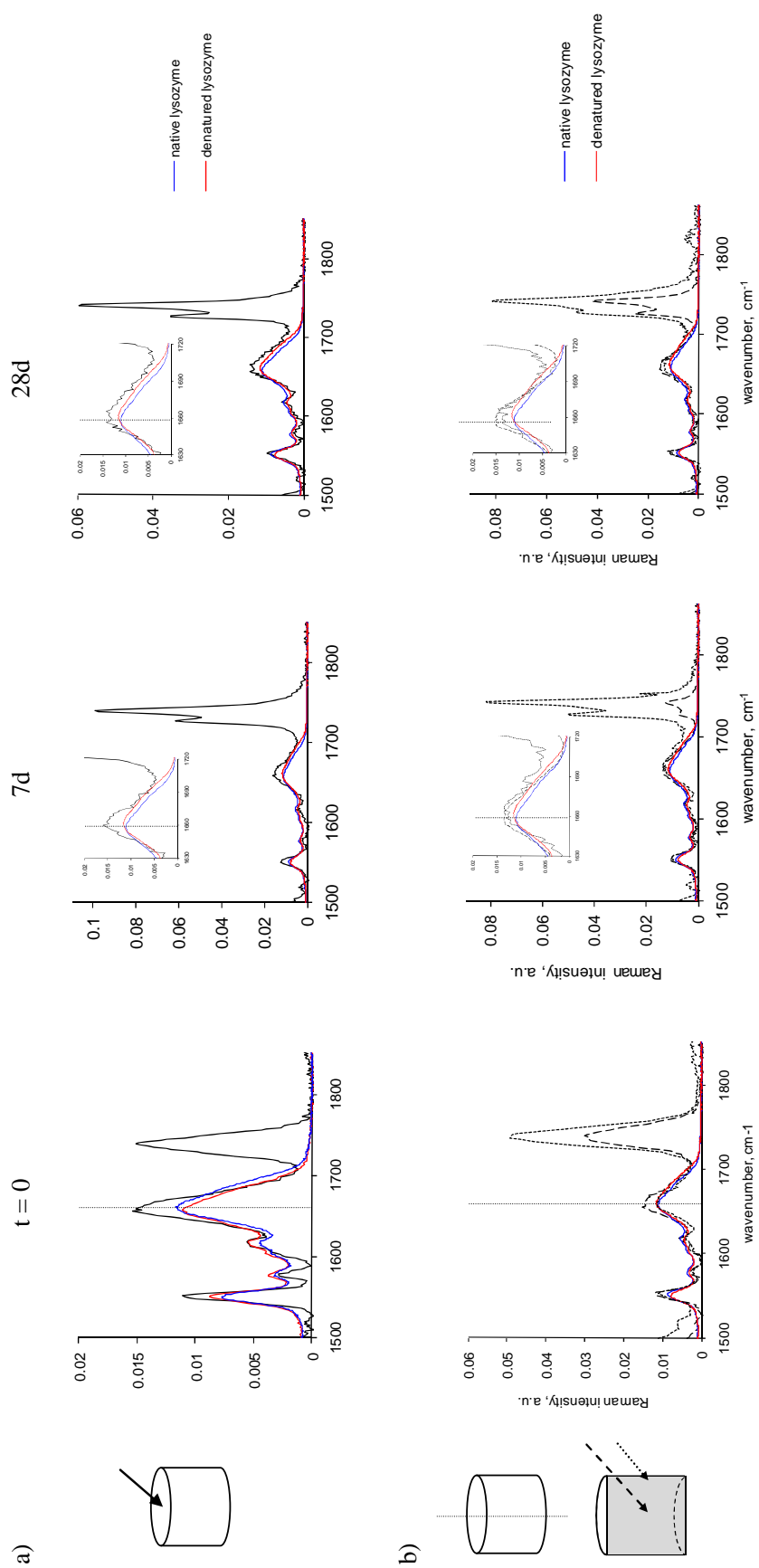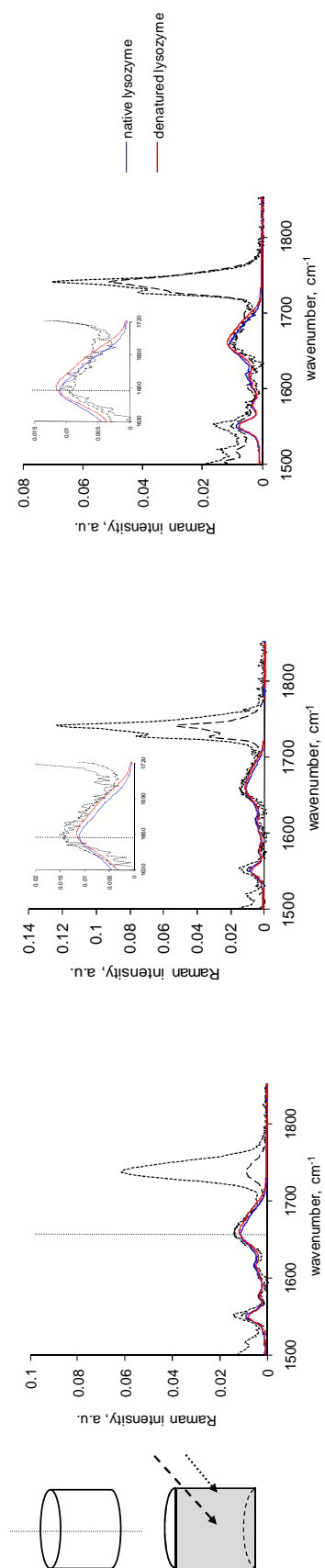
Figure 3.4.9: Raman spectra of lysozyme loaded lipid implants based on hardened soybean oil (6 % drug loading, 0.05 M trehalose) prepared by the emulsion technique and ultrasound. Horizontal: a) surface and b) cross sections. Vertical: before, after 7 and 28 days of release. A zoom to the amide I band region is shown in the inserted figures. Arrows in the scheme preceding the figures indicate the areas where samples were analyzed.

Interestingly, the drug release rates were faster compared to the implants of the same composition based on hardened soybean oil. This might be due to the type of preparation method and the composition of the implants which can greatly impact the resulting protein release kinetics. Mohl and Winter (2004) for example obtained similar results for the investigated lipids confirming the high variability for the above mentioned parameters.

Importantly, the recovered enzymatic activities of the incorporated lysozyme increased and never dropped below the 50 per cent level during the entire interval of the drug release study. Therefore a superiority of the glyceryl tristearate as excipient in the lipid implants can be assumed. A clear tendency with decreased enzymatic activities in the beginning of the drug release study and increasing values at the end as for the implants based on hardened soybean oil could not be identified. Raman spectra recorded for glyceryl tristearate were similar to those of hardened soybean oil and exhibited a characteristic peak at 1740 cm^{-1}. Lysozyme incorporated in the lipid implants and analyzed before the drug release study was in its native state as shown in the first column of Figure 3.4.9. From 7 days of drug release lysozyme could no longer be found on the implants surface. This might probably be attributed to the limited penetration depth of the laser into the implants and protein molecules residing in more profound regions. However, lysozyme situated in the center of the implant was detectable and remained native exhibiting no peak shift or broadening of the amide I band (Figure 3.4.9).

Similar to the implants based on hardened soybean oil with the addition of trehalose, the native protein in the implants center remained native even after contact with the bulk fluid present in the drug delivery devices. Spectra recorded of the cross section of implants analyzed on day 28 of the release experiment showed a clear shift of the amide I band to 1662.65 cm^{-1}. In comparison: native lysozyme exhibits a peak maximum at 1658.33 cm^{-1}, the denatured state at 1662.17 cm^{-1}. This is less consistent with the activity data shown in Figure 3.4.8b for the respective days. However, again it has to be mentioned that the Raman spectra investigating on the lysozyme activity shown in Figure 3.4.9 were based on a small number of measured points within the implants. Hence, conclusions with regard to the native or denatured state of lysozyme are only representative for these areas. In contrast, the activity data obtained by the enzymatic assay provided information on the conformational stability of the whole freeze dried solid. Consequently, care has to be taken in comparative interpretation of the data. Mapping analysis by Raman microspectroscopy with subsequent qualitative and quantitative analysis of the protein content could be a powerful tool for the optimization of key formulation parameters of this type of drug delivery devices.

3.5   Cochlear Implants as Drug Delivery Devices

Parenteral drug delivery is not only limited to implantable devices which undergo swelling, biodegradation and might release the incorporated drug by combined diffusion and erosion processes. A different approach is to deliver drugs from non degradable matrices, where the drug, either dissolved or dispersed, is released by simple diffusion. This is the case for miniaturized implants like medical devices, initially prepared to mend physical defects. The idea was to functionalize these implants in order to assure an often simultaneously required therapeutic treatment. The latter becomes necessary because adverse effects, e.g. inflammatory reactions or rejection of the implanted device often occur during or after implantation even if these devices are highly developed. In general, drugs are administered via the oral or parenteral route. Therapeutic plasma levels might be achieved, resulting in sufficient drug concentrations at the site of action. However, high initial doses are often required, engendering additional risks for the patient. Rarely, local drug concentrations remain above minimum therapeutic concentrations, due to a high clearance of the drug from body fluids, low drug solubility at the site of action, or a compartment with limited accessibility.

The above described points apply for cochlear implants, a medical device initially developed to improve the auditory function after sensoneurinal hearing loss. Implant insertion almost always leads to inflammatory reactions in the surrounding tissue, requiring an anti-inflammatory therapy. However, drug delivery to the inner ear is highly challenging due to the blood-cochlear barrier, which is anatomically and functionally similar to the blood-brain-barrier (Juhn, 1988; Juhn and Rybak, 1981). Upon drug administration via common routes (including oral, i.v., i.m. etc.) only minor amounts of the active agent reach the target site, because tight junctions effectively hinder the passage from the systemic circulation into the inner ear. To overcome these restrictions the drug might be directly administered into the inner ear. However, since the cochlea is a very small, closed space and sensitive to minor changes in fluid volume, such direct administrations are highly delicate. Furthermore, if a drug solution is injected, the active agent is likely to be rapidly eliminated from the inner ear (partially due to efflux through the injection channel). Thus, frequent injections might be required. This is not feasible due to the risk of infections and continued alterations in the volume of the perilymph (which is the major bulk fluid in the cochlea).

Implants with the geometry of long, very thin cylinders (like thin "spaghetti"), which are placed directly into the scala tympani of the cochlea, can offer an interesting potential to

overcome all these restrictions. A particularly attractive approach is to combine such a controlled drug delivery system with electrode arrays improving auditory functions. The miniaturized electrodes are embedded within a polymeric matrix (e.g. silicone-based). The latter can be loaded with a drug, such as dexamethasone, which is released in a time controlled manner along the scala tympani during prolonged periods of time. Dexamethasone could help to prevent post-surgical inflammation within the cochlear cavity and apoptosis of hair cells (Dinh et al., 2008; Eastwood et al., 2010; Eshraghi et al., 2007) Application of analytical solutions of Fick's law of diffusion allowed for determination of the apparent drug mobility in the systems and to quantitatively predict the resulting drug release kinetics as a function of key formulation parameters.

3.5.1   System Morphology and Thermal Properties

Figure 3.5.1a shows an optical macroscopic picture of the cochlear implant prototype investigated in this study. It consists of an array of miniaturized electrodes, which are embedded (except for the decisive surfaces) in a flexible and transparent silicone matrix (of medical grade). The same type of electrodes, but embedded within a silicone matrix loaded with 10 % dexamethasone, is illustrated in Figure 3.5.1b. As it can be seen, the polymer is no more transparent, but appears white. This is a first indication for the fact that the drug is not *dissolved* (molecularly distributed), but *dispersed* (in the form of small particles) within the polymeric matrix. Importantly, the drug particle distribution appears to be homogenous. Figures 3.5.1c shows a macroscopic picture of a free, dexamethasone containing film (5 % drug content) based on the same type of silicone (but not containing any electrode). Obviously, also in this case (and at this drug loading) the drug can be expected to be (at least partially) dispersed in the form of small particles (and not to be completely dissolved) in the silicone matrix. This was true for all the investigated initial drug contents (1-40 % w/w, data not shown). Furthermore, also in this case no signs for inhomogeneous drug distribution were visible. The experimentally measured dexamethasone content in 3 different film pieces (3.5 x 3.5 cm in size) confirmed the homogeneous drug distribution (data not shown) and the determined values agreed well with the theoretically expected drug loadings. Figure 3.5.1d shows a picture of a 10 % dexamethasone loaded, cylindrical extrudate (2 mm in diameter). Again, the drug is likely to be (at least partially) dispersed in the form of small particles (and not completely dissolved) in a homogeneous manner throughout the system. This information is decisive for the mathematical modeling of drug release from these systems.

Figures 3.5.2a-c show cross-sections of a polymeric film loaded with 10 % dexamethasone and of cylindrical extrudates loaded with 1 and 10 % drug, respectively. In all cases, drug particles are clearly visible. This is in good agreement with the above described micro- and macroscopic observations, indicating that the drug is indeed (at least partially) dispersed in the form of small particles (and not completely dissolved) in the silicone matrix. Again, this was true for all the investigated drug loadings (1-40 %, data not shown). Importantly, the SEM pictures also confirmed the homogenous distribution of the drug particles throughout the systems, irrespective of the device geometry and drug loading.

Furthermore, dexamethasone loaded silicone elastomer films were subjected to thermal analysis. Figure 3.5.3 shows heating curves recorded after cooling the samples to -160 °C and subsequent heating to 25 °C at 10 K/min. At -44.48 °C an endothermic event corresponding to the melting temperature of the silicone elastomer, said the loss of the crystalline structure, was detected for the pure silicone. Importantly, the melting temperatures (-43.62 °C to-44.37 °C) did not alter irrespective of the initial drug loading. Hence, chemical interaction between
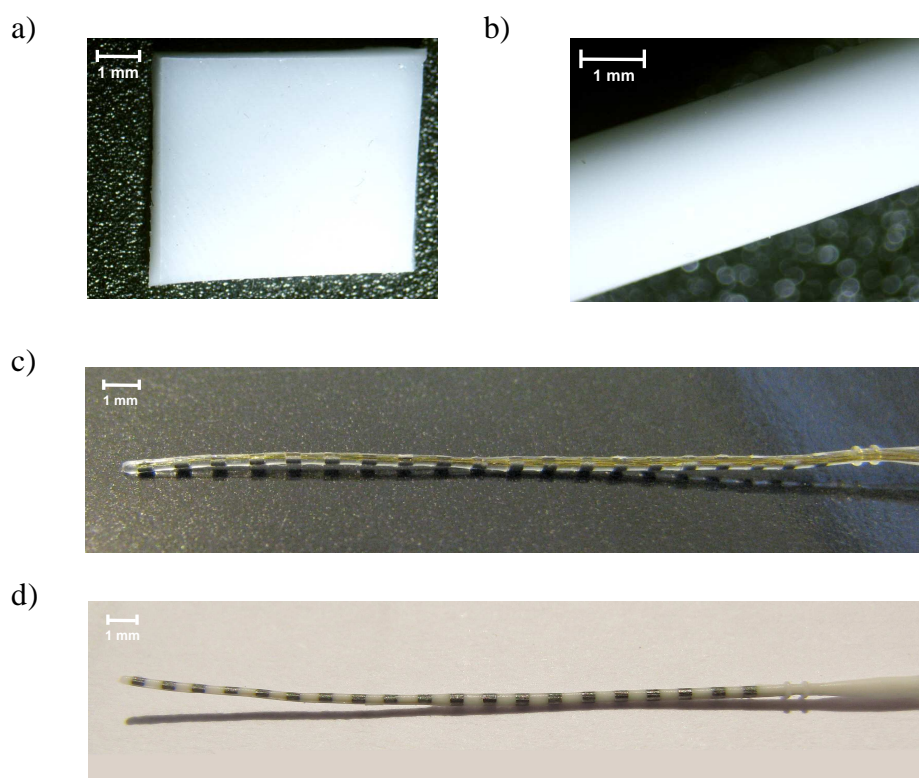
Figure 3.5.1: Macro/microscopic images of: (a) a polymeric film loaded with 5 % dexamethasone, (b) a cylindrical polymeric extrudate loaded with 10 % dexamethasone. (c) a drug-free cochlear implant, and (d) a 10 % dexamethasone-containing cochlear implant.

dexamethasone and the silicone elastomer was excluded.

To elucidate the effect of dexamethasone on the glass transition (T_g) of the silicone matrix, the change from glassy to rubbery state, a zoom to the temperature range between -140 °C and -90 °C is shown in Figure 3.5.3b. The characteristic T_g can be seen at -123.21 °C for pure silicone films. These results are in agreement with literature values (Aranguren, 1998; Lee and Johannsen, 1969). The glass transition temperatures for dexamethasone loaded silicone matrices as found to be at -122.59 °C to -125.76 °C. Consequently, the glass transition temperature of the silicone elastomer remains unaffected by dexamethasone even at high drug loadings. This is consistent with the beforehand made observations of dispersed drug particles within the silicone elastomer matrix.
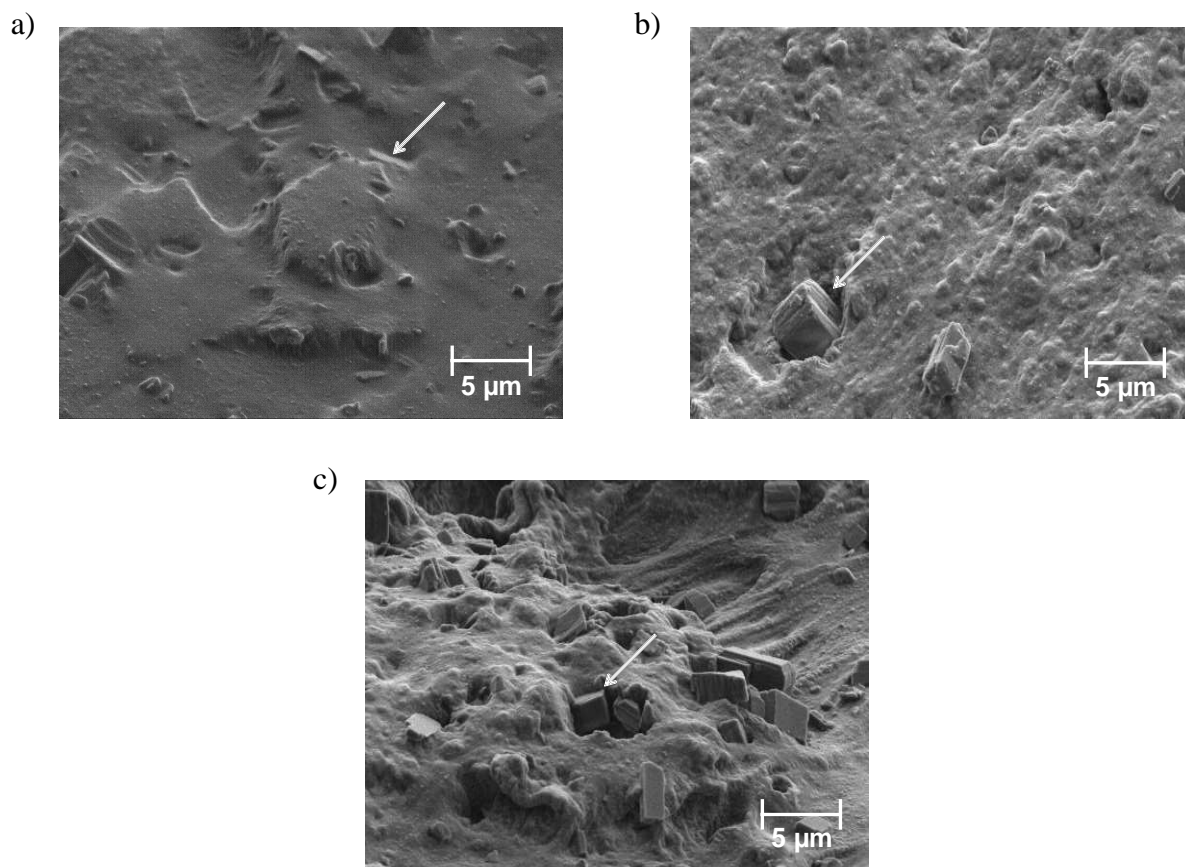
Figure 3.5.2: SEM pictures of the: (a) cross section of a polymeric film loaded with 10 % dexamethasone, (b) cross section of an extrudate loaded with 1 % dexamethasone, and loaded with 10 % dexamethasone (arrows indicate drug crystals).

3.5.2 Mechanical Properties of Thin, Free Films

The mechanical properties of cochlear implants are obviously of crucial importance. The devices must exhibit appropriate flexibility: They must neither be too flexible, nor too rigid to allow for easy insertion into the cochlea, without causing significant damage. Figure 3.5.4a shows the puncture strength, percent elongation and energy at break of thin, free silicone films at room temperature loaded with 1-40 % dexamethasone (as indicated). For reasons of comparison, also drug free systems were investigated. As it can be seen, all three parameters – the puncture strength, percent elongation and energy at break –decreased with increasing drug content. This can be explained by the decreasing relative silicone content in the system with increasing drug content (these are binary silicone:drug blends). Importantly, the observed changes are unlikely to significantly affect the easiness to administer the respective cochlear implants: Manual handling of the films (including folding) did not give the impression of major changes, being crucial for device handling. However, this aspect will be studied in more detail in the future using an appropriate experimental setup simulating implant insertion into the cochlea.

It has to be pointed out that the mechanical properties of a polymeric system can significantly change upon exposure to aqueous media, e.g. due to the leaching of film compounds into the surrounding bulk fluid or water penetration into the device (Siepmann and Siepmann, 2008). This can be of importance when the implant is removed from the cochlea of the patient. For this reason, the mechanical properties of thin silicone films containing 1 or 10 % dexamethasone were also measured upon exposure to artificial perilymph at 37 °C. As it can be seen in Figure 3.5.4b, there was no significant change in the systems' puncture strength, percent elongation and energy at break during the observation period, irrespective of the initial drug content. The same was true for drug free systems, studied for reasons of comparison. However, potential alterations after much longer time periods, especially at high initial drug loadings, cannot be excluded and should be addressed in the future.

3.5.3 *In vitro* Drug Release

The release of dexamethasone from thin, free silicone films into 500 mL artificial perilymph at 37 °C is illustrated on the left hand side of Figure 4. The upper diagram shows the relative drug release kinetics, the diagram in the middle the absolute amounts of drug released as a function of time and the lower diagram the ratio "drug concentration within the withdrawn

a)

b)
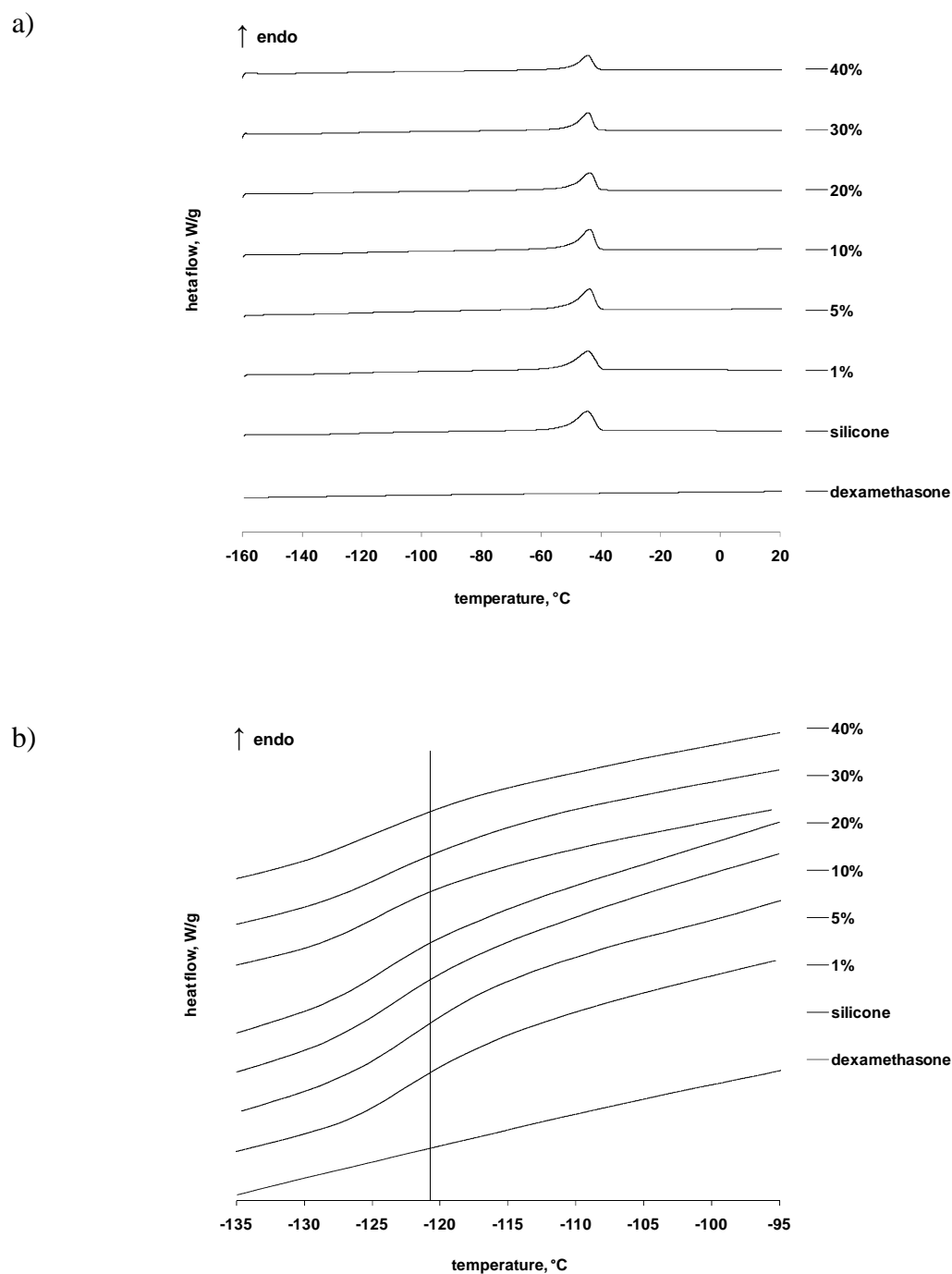
Figure 3.5.3:   Impact of the initial drug loading (indicated in the diagrams) of thin polymeric films on the thermal properties of the systems: (a) DSC thermograms of drug loaded films and - for reasons of comparison - of pure polymer and pure drug. (b) Zoom on the temperature range, in which glass transition is observed.

sample: drug solubility" (dexamethasone solubility in artificial perilymph at 37 °C was determined to be equal to 82.3 mg/L±1.7 mg/L, which is in good agreement with values reported in the literature (Fahramand et al., 2010). The symbols represent the experimentally determined drug release kinetics. The initial drug content of the films was varied from 1 to 40 %. As it can be seen, the relative dexamethasone release rate decreased with increasing drug loading of the films, whereas the absolute drug release rate increased. The latter effect can be explained by the increasing porosity of the system upon drug exhaust: The matrix becomes more and more porous, thus, the hindrance for water and drug diffusion through the matrix decreases. The higher the initial drug loading, the higher the resulting porosity and the faster is drug release. The fact that the relative drug release rate decreased with increasing drug loading can serve as a first indication for the fact that limited drug solubility within the system is likely to be of importance for the control of drug release: Probably not all of the drug is dissolved in the matrix upon exposure to the release medium. Thus, dissolved and non-dissolved drug co-exist. Importantly, only dissolved drug is available for diffusion. When increasing the initial drug loading, the concentration of dissolved drug does not further increase once the matrix is saturated with dexamethasone and the concentration gradient (the driving force for diffusion) remains unaltered. However, the 100 % reference value for the calculation of the relative drug release rate increases.

Another very important aspect when analyzing drug release kinetics *in vitro* is the degree of drug saturation of the withdrawn samples: If the bulk fluid is nearly saturated with drug, the frequency of sampling and volume of added fresh release medium can strongly impact the observed release kinetics. Thus, great caution must be paid to the experimental setup and sampling procedure. As it can be seen on the left hand side of Figure 3.5.5c, under the given conditions the degree of sample saturation is limited in all cases. Sink conditions are provided and already released drug is unlikely to significantly slow down further drug release. However, the "film volume:release medium volume ratio" in this case is not representative for the expected "implant volume:perilymph volume ratio" *in vivo*. Based on the average volume of the film samples and considering a volume of 76 µL perilymph in humans (Igarashi et al., 1986), a volume of 10 mL bulk fluid can be expected to be more representative in this case. The right hand side of Figure 3.5.5 shows the respective drug release profiles observed upon film exposure to 10 mL perilymph at 37 °C. As it can be seen, the relative and absolute drug release rates are lower than under sink conditions (right versus left hand side of Figure 3.5.5), especially at elevated initial drug loadings. This can be attributed to decreasing drug

a)

b)
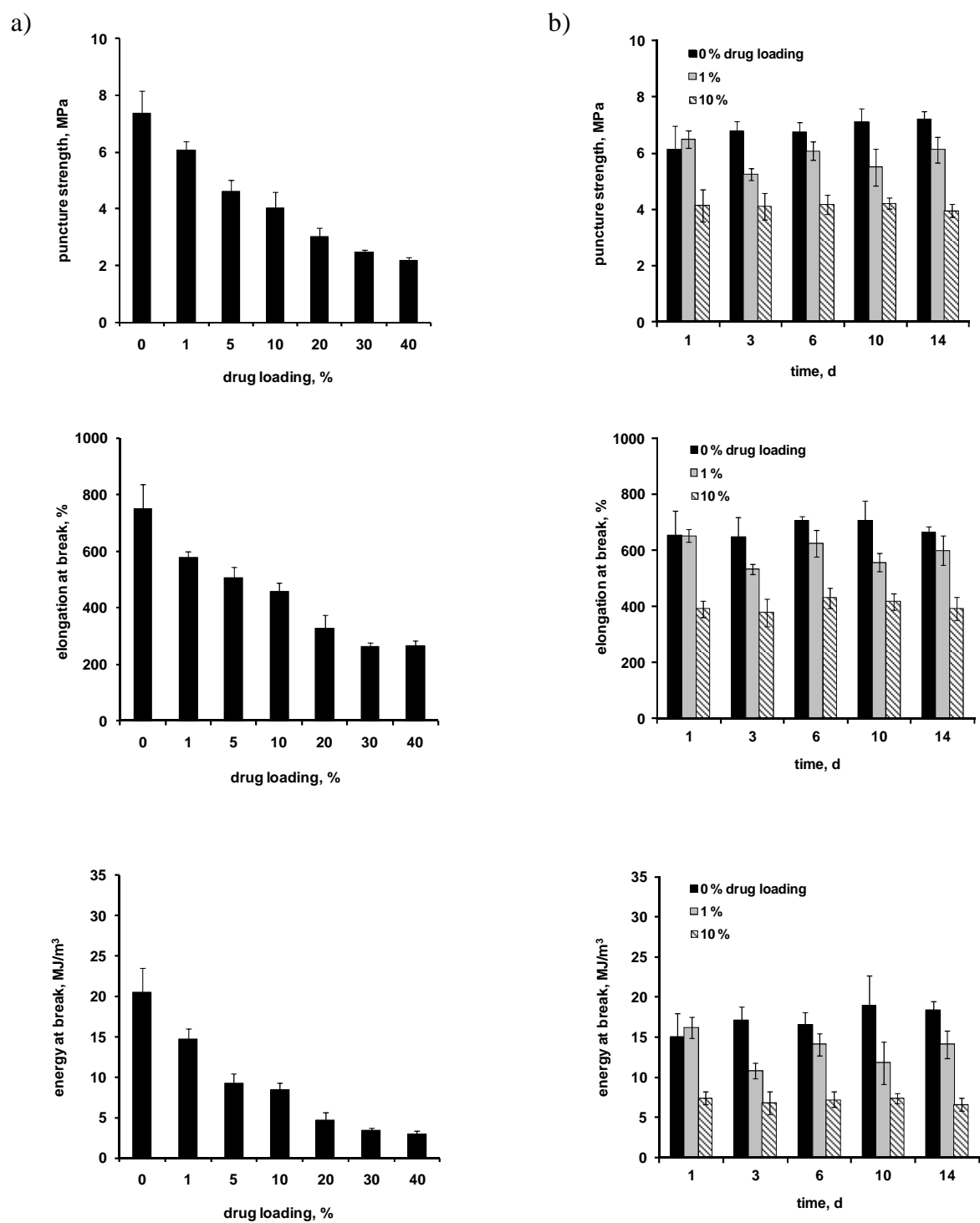
Figure 3.5.4: Impact of the initial drug loading of thin polymeric films on the mechanical properties of systems in the: (a) dry state, and (b) wet state (upon exposure to the artificial perilymph at 37 °C, the dexamethasone loading is indicated in the diagram).

concentration differences "inside versus outside" of the films: Already released dexamethasone molecules decrease the drug concentration gradients, which are the driving forces for diffusion (Siepmann and Siepmann, 2008). However, the general tendencies: increasing initial drug loadings lead to decreasing relative drug release rates and increasing absolute drug release rates, remain the same. On the right hand side of Figure 3.5.5c the experimentally measured degrees of drug saturation of the withdrawn samples are illustrated. Comparing the diagram on the left hand side (500 mL release medium) and the diagram on the right hand side (10 mL release medium), the difference in drug release hindrance under these two conditions becomes obvious. This illustrates the fundamental importance of the experimental conditions during drug release measurements. *In vivo* the elimination rate of dexamethasone from the inner ear will determine at which rate the drug leaves the surrounding bulk fluid. Salt and co-workers presented very interesting mathematical models to take this phenomenon quantitatively into account (Plontke and Salt, 2003; Plontke et al., 2004 and 2007; Salt and Plontke, 2009). In the future it will be decisive to combine these *in vivo* models with mechanistic realistic theories quantifying mass transport within the controlled drug delivery systems. Such an analysis should be ideally based on experimentally measured drug concentrations in the inner ear *in vivo*.

Since the flow of perilymph in the cochlea is extremely slow (Ohyama et al.,1988; Plontke et al., 2007), the flasks used for the *in vitro* release measurements shown in Figure 3.5.5 were not continuously agitated, but only (manually) shaken at each sampling time point to assure a homogenous drug concentration in the bulk fluid (and to be able to calculate the amount of drug released). Overall, dexamethasone release from the investigated films was very slow in all cases (Figure 3.5.5), which is desired in the case of local drug administration to the inner ear over prolonged time periods. This can mainly be attributed to the limited mobility of dexamethasone in the investigated silicone matrix and to the limited solubility of this drug in this matrix. Importantly, the drug was found to be stable during the observation period in artificial perilymph at 37 °C (data not shown).

3.5.4   Drug Release Mechanism and Mathematical Modeling

In order to better understand the mass transport phenomena, which control drug release out of the investigated silicone films, an analytical solution of Fick's second law of diffusion was used. The model is based on the following assumptions:

1) The surface of the films is large compared to their thickness (the films were 3.5 x 3.5 cm in size and 1000 µm in thickness).

2) Both sides of the films are exposed to the release medium (this was assured using film holders).

3) The films do not dissolve and do not significantly swell upon exposure to the release medium (this was confirmed by visual observation and film dimension measurements, data not shown).

4) Drug diffusion through the film matrix is the dominant mass transport step.

5) Perfect sink conditions are provided throughout the experiments. This assumption was not fulfilled in the case of 10 mL release medium at higher initial drug loadings (right hand side of Figure 3.5.5). This simplification is intentionally made in order to keep the mathematical analysis simple. *In vivo*, the ratio "elimination rate of dexamethasone out of the inner ear": "drug release rate out of the implant" is decisive. As long as the release rate is higher than the elimination rate, the drug concentration in the perilymph increases. In the future it will be very interesting to combine a mathematical model quantifying drug transport within the implant with a model describing the fate of the drug in the living organism. In any case, it should be kept in mind that the "apparent" diffusion coefficients determined with the presented, simplified model are not the "real" values.

6) The drug is initially homogenously and molecularly distributed within the system (monolithic solutions). Also this assumption is not fulfilled in reality, as discussed above. Also this simplification is made intentionally in order to avoid the need to know the drug solubility within the polymeric matrix upon exposure to the release medium at 37 °C. Unfortunately, it is not straightforward to measure this parameter experimentally. Some interesting attempts have been presented, but they require special equipment and/or do not allow drug solubility measurements under real release conditions, e.g. upon exposure to artificial perilymph at 37 °C (Malcolm et al., 2002 and 2003). Furthermore, potential changes in the composition/structure of the matrix during long term release might lead to time-dependent drug solubility in the system. Again, due to this simplification, the obtained "apparent" diffusion coefficients" cannot be regarded as the "real" values. The
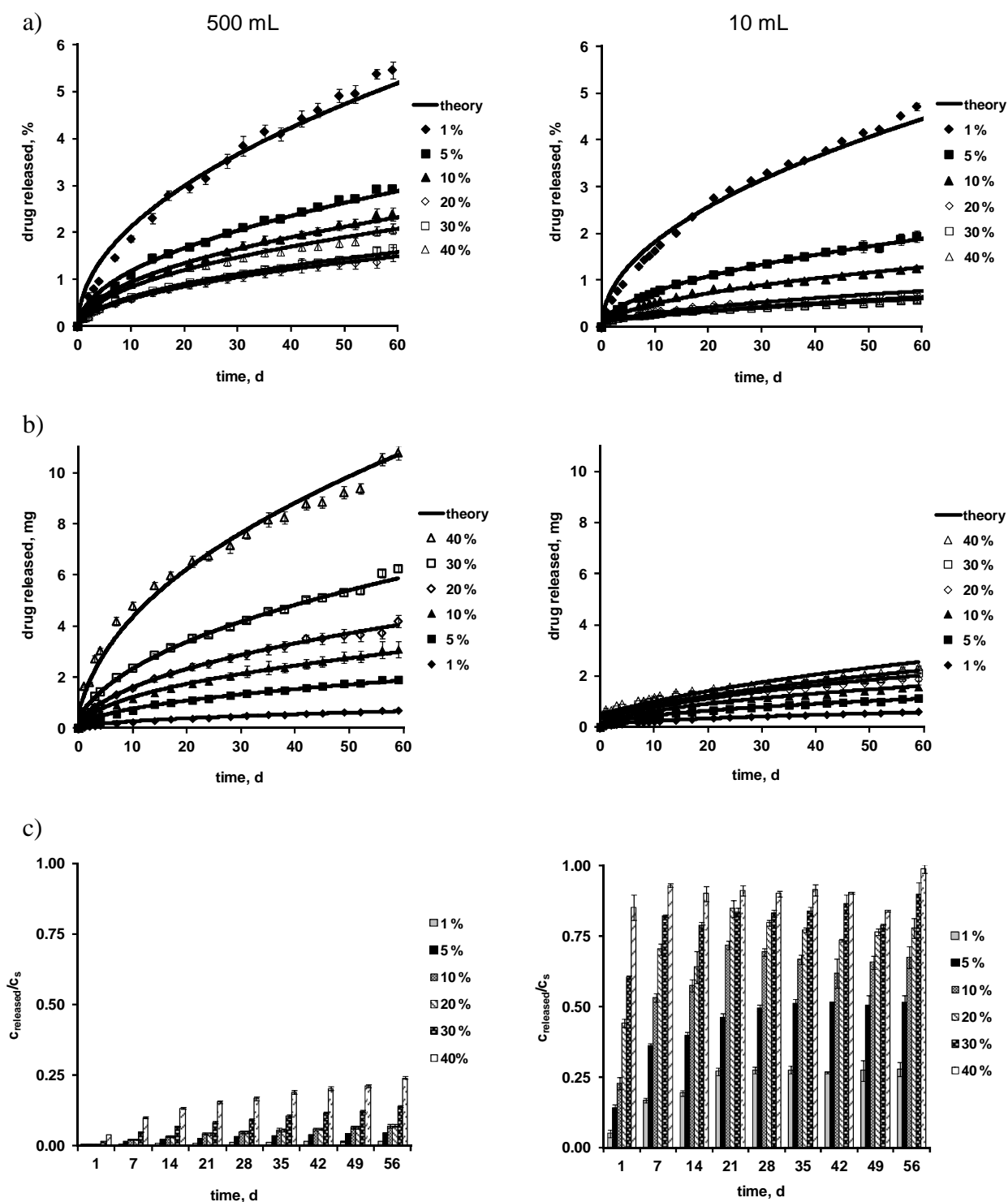
Figure 3.5.5: Effects of the initial drug loading on dexamethasone release from thin films into 500 mL artificial perilymph (left hand side), or 10 mL artificial perilymph (right hand side → physiologically realistic "film volume:perilymph volume" ratio) at 37 °C (no agitation): a) relative drug release rates, b) absolute drug release rates, c) degree of drug saturation of the withdrawn samples. The symbols represent the experimentally measured values, the solid curves the fitted theory (Equation 3.5.1).

latter can be expected to be higher, since in reality not the entire drug is available for diffusion. But it is not the aim of this mathematical analysis to determine the "real" diffusion coefficient of the drug in the given silicone matrix. Instead, these "biased" parameters are to be used to make quantitative predictions of the impact of the device geometry and dimensions on drug release (to facilitate device optimization). Since the same simplifications apply for the systems from which drug release is predicted, the introduced error might be limited.

Under these conditions, the following equation can be derived (Crank, 1975):

(Equation 3.5.1)
$$\frac{M_t}{M_\infty} = 1 - \frac{8}{\pi^2} \sum_{n=0}^{\infty} \frac{1}{(2n+1)^2} \exp\left(\frac{-D(2n+1)^2 \pi^2 t}{L^2}\right)$$

where M_t and M_∞ denote the absolute cumulative amounts of drug released at time t and infinity, respectively; n is a dummy variable, D the "apparent" diffusion coefficient of the drug within the polymeric system; L represents the thickness of the film.

Fitting Equation 3.5.1 to the experimentally determined dexamethasone release kinetics from thin films upon exposure to 500 and 10 mL perilymph at 37 °C resulted in good
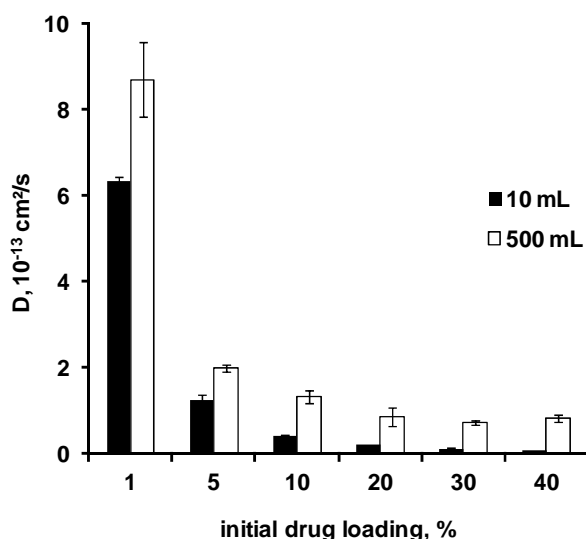
Figure 3.5.6: Dependence of the determined "apparent" diffusion coefficient of dexamethasone in the investigated silicone films on the initial drug loading and volume of artificial perilymph (indicated in the diagram). The values were obtained by fitting Equation 3.5.1 to the experimentally measured drug release kinetics shown in Figure 3.5.5.

agreement between theory (curves) and experiment (symbols) (Figure 3.5.5). This illustrates the fact that obtaining good agreement between a *fitted* theory and experimental results is not a proof for the validity of the theory. As discussed above, not all of the model assumptions were fulfilled in practice and the determined "apparent" diffusivities are biased. Figure 5 shows these values as a function of the drug loading and volume of release medium. Clearly, the "apparent" diffusion coefficient significantly decreased with increasing initial drug content. This is due to the intentional simplification of the model: the applied theory does not take into account limited drug solubility within the matrix: The higher the real drug excess in the system, the more pronounced is the introduced error. In reality, much higher diffusivities can be expected. Furthermore, the obtained D-values are higher upon exposure to 500 mL perilymph compared to 10 mL (Figure 3.5.6 white versus black bars). This is due to the intentional model simplification assuming perfect sink conditions in all cases. To evaluate the potential impact of continuous flask agitation on drug release from the thin films, dexamethasone release from samples exposed to 500 and 10 mL perilymph was also measured under continuous stirring at 37 °C (80 rpm). The symbols in Figure 3.5.7 show the
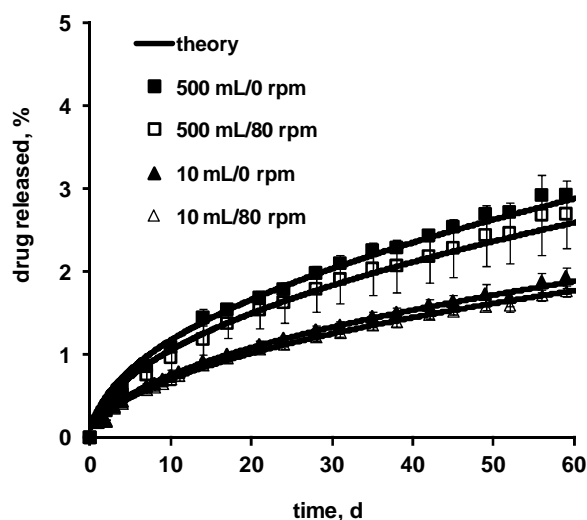
Figure 3.5.7: Impact of the degree of agitation and volume of the artificial perilymph (indicated in the diagram) on dexamethasone release from thin films (5 % initial drug loading). The symbols represent the experimentally measured values, the solid curves the fitted theory (Equation 3.5.1). Note that "0 rpm" indicates "no continuous stirring". However, the respective flasks were manually shaken at each sampling time point to assure homogeneous bulk fluid concentrations.

experimentally determined drug release rates under these conditions. For reasons of comparison, also drug release from films, which were not continuously agitated, are shown (note that they were manually shaken at each sampling time point). Clearly, the impact of continuous sample stirring is limited, irrespective of the bulk fluid volume. The observed release rates were even slightly lower in the case of agitation. This is likely to be attributable to the experimental error (standard deviations are overlapping). The curves in Figure 3.5.7 show the respective fittings of Equation 3.5.1 to the experimentally determined dexamethasone release kinetics. Again, good agreement between theory and experiment was observed in all cases. Based on these fittings the "apparent" (biased) diffusion coefficients were determined (Table 3.5.1).

Table 3.5.1 "Apparent" (biased) diffusion coefficient of thin free dexamethasone loaded films determined by fitting Equation 3.5.1 to the experimentally determined dexamethasone release kinetics shown in Figure 3.5.7.

agitation	D, 10^{-13} cm^2/s	
	10 mL	500 mL
0 rpm	1.23 ± 0.15	2.00 ± 0.09
80 rpm	1.22 ± 0.16	1.71 ± 0.39

3.5.5 Quantitative Predictions and Independent Experimental Verification

In order to evaluate the suitability of the determined "biased" diffusion coefficients (determined with the simplified mathematical model and thin free films), they were used to theoretically predict dexamethasone release from cylindrical extrudates. For this geometry, the following analytical solution of Fick's second law of diffusion can be derived (Vergnaud et al., 1983):

(Equation 3.5.2)

$$\frac{M_t}{M_\infty} = 1 - \frac{32}{\pi^2} \cdot \sum_{n=1}^{\infty} \frac{1}{q_n^2} \cdot \exp\left(-\frac{q_n^2}{R^2} \cdot D \cdot t\right) \cdot \sum_{p=0}^{\infty} \frac{1}{(2 \cdot p + 1)^2} \cdot \exp\left(-\frac{(2 \cdot p + 1)^2 \cdot \pi^2}{H^2} \cdot D \cdot t\right)$$

where M_t and M_∞ represent the absolute cumulative amounts of dexamethasone released at time t and infinite time, respectively; q_n are the roots of the Bessel function of the first kind of zero order $[J_0(q_n)=0]$; R and H denote the radius and height of the cylinder. This equation is based on the following assumptions:

1) The entire surface of the cylinder is exposed to the release medium.
2) Drug diffusion occurs in radial and axial direction.
3) The cylinder does not dissolve and does not significantly swell upon exposure to the release medium.
4) Drug diffusion through the silicone matrix is the dominant mass transport step.
5) Perfect sink conditions are provided throughout the experiment.
6) The drug is initially homogenously and molecularly distributed within the system (monolithic solution).

Analogous to the thin films, the last assumption is not fulfilled in this study at the investigated initial drug loadings, and perfect sink conditions are not always provided. The dotted curves in Figure 3.5.8 show the theoretically predicted dexamethasone release from cylinders with a diameter of 2 mm and a length of 24 mm in artificial perilymph at 37 °C. The initial drug loading was 1 or 10 %, as indicated. The volume of the release medium was either 500 or 1 mL (the latter condition provides a "physiologically expectable" "device volume:bulk fluid volume ratio"). As it can be seen, the theory predicts much higher relative drug release rates in the case of 1 % initial drug loading compared to 10 %, due to the above discussed "limited dexamethasone solubility effect". Furthermore, the theory predicts slightly
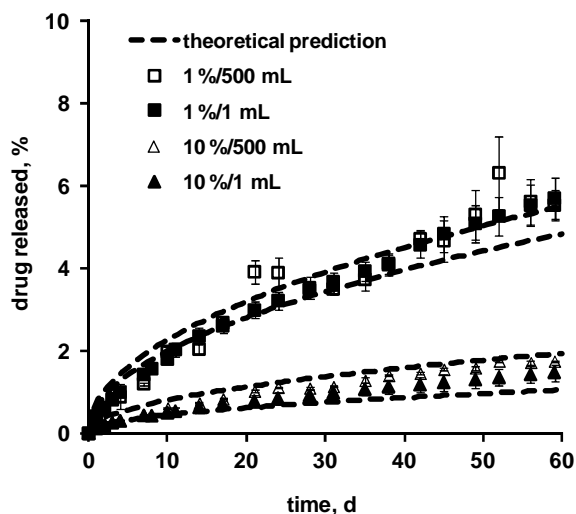
Figure 3.5.8: Theoretical predictions (dotted curves, Equation 5) and independent experiments (symbols): Dexamethasone release from silicone-based cylindrical extrudates (length = 24 mm, diameter = 2 mm) in 1 or 500 mL artificial perilymph (37 °C, no agitation) (initial drug loading = 1 or 10 %, as indicated).
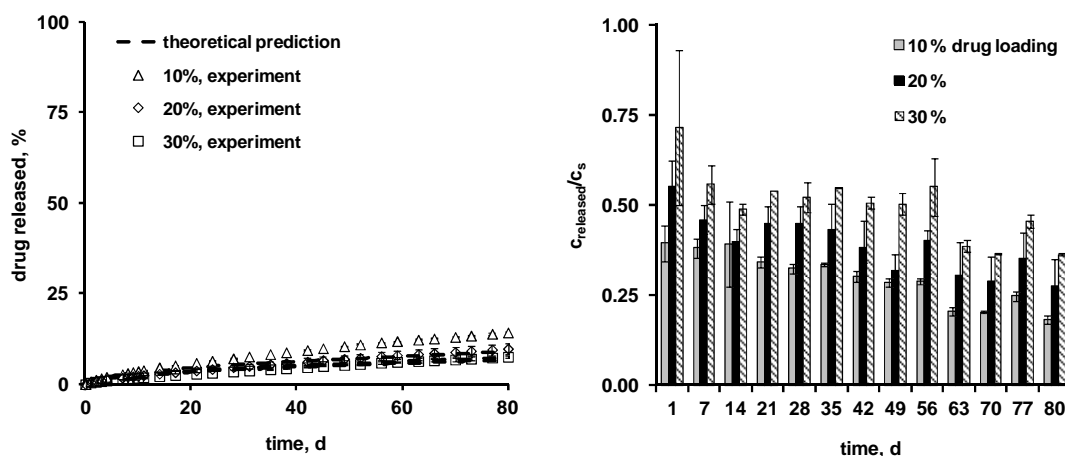
Figure 3.5.9: Dexamethasone release from silicone-based cochlear implants in 70 µL artificial perilymph (physiologically realistic "implant volume:perilymph volume" ratio) at 37 °C (no agitation): a) Theoretical predictions (dotted curves) and independent experiments (symbols), b) degree of drug saturation of the withdrawn samples (10, 20 and 30 % initial drug loading, as indicated).

higher relative drug release rates in the case of 500 mL release medium compared to 1 mL, because of the above described hindrance of further drug release by already released molecules. In order to evaluate the validity of these theoretical predictions, the respective extrudates were prepared in reality and drug release was measured experimentally in artificial perilymph at 37 °C. The symbols in Figure 3.5.8 show the independent experimental results. Importantly, good agreement was observed between the theoretical predictions and the independent experiments (curves and symbols). Thus, the proposed mathematical model can be used to reliably predict the impact of the geometry and dimensions of this type of advanced drug delivery systems on the resulting dexamethasone release kinetics. Since the targeted release periods are very long (often several months up to years), this can be highly beneficial to speed up implant optimization. Interestingly, the use of the presented *simplified* theory, neglecting limited drug solubility and potential non-sink conditions, is able to provide good estimations for the resulting drug release kinetics. Since it is not necessary to know the solubility of the drug in the polymeric matrix upon exposure to the release medium at 37 °C and since sink conditions are assumed, the model is much easier to be applied than more realistic theories. The reason for the observed good agreement between theoretical predictions and independent experiments despite the simplifications is likely to be the "lumped" nature of the determined diffusion coefficients, which "indirectly take into account" the impact of limited drug solubility and potential non sink conditions.

4 Summary

Matrix based controlled drug delivery systems represent an important alternative to reservoir systems, offering several advantages like the homogeneous character of the devices, simple manufacture in a single step process, and the absence of problems which could arise with coating techniques. Moreover, oral administration of matrix based drug delivery systems might prevent the risk of the all-or-nothing effect. The latter might occur due to premature release of the entire drug content from a reservoir system as a consequence of a deficit of the membrane functionality. Thus, severe side effects, especially for high potent drugs with a small therapeutic range can be minimized. Additionally, the simple manufacture is often related to shorter processing intervals and thus the stresses applied on the devices and the drugs are reduced. This offers the opportunity to process drugs exhibiting challenging formulation properties (e.g., protein drugs). Consequently, research on formulation strategies on the improvement of matrix performance has substantially grown in the past years.

The first aim of the present study was to investigate on the possibilities of preparing controlled release multiparticulate matrix dosage forms containing high loadings of 5-aminosalicylic acid, the most frequently used drug for the treatment of inflammatory bowel diseases (IBD). A major obstacle was to imply the elevated drug content and to achieve the suppression of premature drug release in the upper gastrointestinal tract. The latter was necessary since the drug easily undergoes degradation in this parts of the GIT and thus is less bioavailable. On the other hand, complete and controlled release had to be ensured once the dosage form entered the lower parts of the large bowel and the colon. Preliminary studies rapidly omitted the use of polymeric matrix materials, either due to undesired physicochemical properties of the dosage form, problems arising during manufacture or insufficient abilities to control the release profiles. Solely the use of triglyceride excipients of various fatty acid chain length and composition (fatty acid chain length: C12-20, mixed triglycerides) resulted in appropriate formulation and release characteristics. Two multiparticulate formulations were prepared, matrix pellets by extrusion/spheronization and mini tablets. Drug loadings of up to 60 % (w/w) 5-ASA were obtained for pellets. The most promising triglyceride, glyceryl palmitostearate effectively prevented premature drug release up to 8 h in simulated gastric and intestinal fluid containing GIT enzymes (25.4 % at 8 h of release). Additionally, storage stability was ensured under stress conditions for 6 months. The problematic of lipid modifications,

often encountered during process conditions at elevated temperatures were circumvented by appropriate curing of the dosage forms. Thermoanalytic measurements showed transformation of glyceryl palmitostearate into the stable β-modification after 7 d at 40 °C of curing. Mini tablet formulation exhibited similar release characteristics and were also considered suitable for colon targeted drug delivery purposes. Moreover, they offered an alternative preparation method.

A third excipient, responsible for the complete and controlled release in the lower parts of the GIT was Nutriose®, a branched soluble dextrin. The latter is known to be preferentially degraded by colon-specific bacteria. Consequently, by leaching out of the dextrin residues a porous network is formed in the devices promoting further imbibing of the surrounding bulk fluid into the lipid dosage form and thus enhanced dissolution of the incorporated drug. In order to achieve appropriate suppression of premature drug release a Nutriose® concentration of 15 % (w/w) proofed ideal when the 5-ASA concentration was kept constant at 60 % (w/w). In conclusion, the presented matrix pellets and mini tablets offer a promising alternative to coated dosage forms in the field of colon-targeted drug delivery.

Parenteral administration is necessary for drugs exhibiting poor oral bioavailability or instabilities in conditions present in the GIT, for example protein drugs, which gained increasing therapeutic importance in the last decades. In general, administration takes place by injection or infusion of a liquid formulation. Consequently, rapid plasma clearing rates and only short *in vivo* half lives of the proteins are achieved. Frequent application is necessary, which is undesired by the patient and results in reduced compliance. Hence, another study aimed at the feasibility of implantable lipid matrices for controlled protein delivery.

Manufacturing of protein containing therapeutics often consists of a freeze drying step harboring the risk of thermal protein denaturation and thus the loss of therapeutic activity. An important factor in optimization of protein formulations is to understand the mechanisms of denaturation. Raman microspectroscopic studies conducted on the model protein lysozyme using the chemical denaturants guanidine hydrochloride and urea demonstrated indirect interactions by alterations of the solvent properties induced by guanidine HCl and direct binding between urea and the protein. These observations are very important for the understanding of cold denaturation phenomena occurring during freeze drying. The latter led to changes in protein dynamics resulting in a "molten globule" state of the protein with intact secondary structure, which is also observed

during thermal denaturation. Low frequency Raman analysis in the presence of denaturants revealed the strong relationship between solvent and protein dynamics: a weakened hydrogen bond network is responsible for an increased molecular mobility of the protein and thus denaturation due to intermolecular interaction. In contrast, the addition of trehalose strengthened the hydrogen bond network and thus promoted preferential hydration, resulting in stabilization of the protein secondary structure. Raman microspectroscopic analysis was correlated to activity measurements of lysozyme. Both techniques can thus be considered as powerful tools in protein conformational analysis and helpful with the optimization of protein delivery devices.

The effect of cryo- and lyoprotectants on the freeze drying and storage stability of a second model protein, L-lactic dehydrogenase, was investigated. Saccharides (sucrose and trehalose), the sugar alcohol maltitol, PEG 6000 and polyvinylpyrrolidones were identified as effective stabilizers during freeze drying yielding virtually complete preservation of the protein activity. With the exception of PVP, which have predominantly lyostabilizing properties, all added stabilizers acted as cryo- and lyoprotectants. Results obtained by determination of the enzymatic activity of LDH were confirmed by Raman spectroscopic analysis of the samples. Trehalose and PVP, containing samples investigated in the characteristic amide I band region demonstrated no Raman shift, indicating intact secondary structures and also no peak broadening. In contrast, spectra of LDH samples containing low molecular weight PEG ($M_w = 400$ Da) showed a peak broadening due to the formation of protein aggregates. Blending of trehalose with glycerol, PEG 6000 or PVP K-90 in general improved the recovery of enzymatic activities demonstrating their superiority to single stabilizers partially due to additive effects.

Storage stability of LDH formulations at 4 °C was investigated and yielded 50 % recovery of enzymatic activity after 6 months when 0.5 M trehalose was added. Elevated storage temperatures led to a gradual loss of enzymatic activity (25 % recovery at 40 °C after 6 months). Stabilizer blends consisting of 1 % (w/V) PVP K-90 and 0.1 M trehalose were able to improve the LDH storage stability: up to 75 % of the initial activity was recovered at 4 °C. The blend ratios 1:9 to 9:1 proofed to be the most effective. At higher storage temperatures a dominant effect of trehalose was observed for but was not sufficient to prevent a significant loss. Activity results were confirmed by Raman microspectroscopy, with significant shifts of the amide I frequency after storage at 25 or

40 °C for 3 months. Again the benefit of using the two methods (Raman microspectroscopy and biochemical analysis) to investigate protein conformation was demonstrated.

In another part of this work lysozyme loaded lipid implants were analyzed for the enzymatic activity of (i) the released protein and (ii) the protein remaining in the implants. Lipid and protein could be investigated simultaneously by Raman spectroscopy because characteristic bands of the two components were detected at two distinct frequencies. It was shown that the manufacturing process had no detrimental effect on the lysozyme activity, whereas protein activity during release studies gradually decreased with progressing release (virtually complete inactive protein after 28 d of release). In order to improve the protein stability 0.05 M (w/w) of trehalose was added to the formulations. Enzymatic activities of up to 50 % of the initial values were measured demonstrating the stabilizing effect on lysozyme. According to the results of the Raman studies in *section 3.2.2 Effects of Denaturants in the Low Frequency Region*, trehalose acts as a "hydrogen bond maker" in aqueous solutions, thus stabilizing by preferential hydration of the protein. Consequently, the secondary structure is stabilized by hydrogen bonds between the protein and the hydration water. Moreover, Raman microspectroscopy conducted on the implants after 7 and 28 days of release also demonstrated intact lysozyme in the center of the implants confirming stabilization not only during manufacturing but also during release experiments.

The feasibility of incorporating dexamethasone, a hydrophobic anti-inflammatory drug, into the silicone elastomer part of a cochlear implant was investigated in another study. Homogenous distribution of the dispersed drug within the matrix was proven by SEM and thermal analysis. Mechanical properties analyzed for thin drug loaded films in dry state decreased with increasing drug load, due to a more porous silicone network and thus decreasing elasticity. However, analysis of films in the wet state resulted in constant mechanical properties of the films during the investigated interval. Release studies were conducted at sink conditions and, in order to obtain more detailed information on the properties of the systems *in vivo*, at conditions mimicking the "implant volume:perilymph volume ratio" *in vitro*. Release kinetics was exclusively governed by diffusion through the silicone matrix. Only 5 % of the incorporated dexamethasone was released after 60 d of analysis, demonstrating the suitability of the systems for long term therapy of insertion-induced inflammatory reactions of the cochlear tissue and hair cell

apoptosis. The experimental setup, namely sink conditions, has an important effect on the resulting drug release kinetics. Due to the low solubility of the drug in aqueous media, undissolved and dissolved drug co-exist in the matrix. Diffusion of dexamethasone from the silicone matrix is a function of the concentration gradient of the drug between the matrix and the surrounding bulk fluid. Thus, sink conditions resulted in faster drug release rates. Additionally, the initial concentration of the drug within the matrix was important: once the solubility of dexamethasone within the silicone matrix is reached, the release rate controlling parameter is the diffusion of the dissolved drug. Apparent drug mobilities in the silicone elastomer films were determined by applying solutions of Fick's second law of diffusion and subsequently used to develop a simplified model to quantitatively predict the release kinetics of dexamethasone from drug loaded extrudates and cochlear implants. The predicted kinetics were validated by independent drug release experiments with dexamethasone loaded extrudates and cochlear implants. Good correlation of the predicted release profiles and the experimental determined values was obtained proving the applicability of the proposed mathematical model. This allows for speeding up of device optimization of this type of advanced drug delivery systems by predicting the impact of key formulation parameters like system dimensions and composition on the resulting drug release kinetics.

5   Zusammenfassung

Matrixarzneiformen mit kontrollierter Wirkstofffreisetzung stellen eine bedeutende Alternative zu Reservoirsystemen dar, bieten sie doch etliche Vorteile wie z. B. eine homogene Wirkstoffverteilung und eine vereinfachte Herstellung (Einschrittverfahren). Ebenso können Probleme, die mit Befilmungsprozessen einhergehen, vermieden werden. Reservoirsysteme, die den Arzneistoff über eine semipermeable Membran kontrolliert freigeben, bergen zudem die Gefahr des Alles-oder-Nichts-Effekt, ein vorzeitiges komplettes Freisetzen des Arzneistoffs infolge von Membrandefekten. Die orale Darreichung von Matrixarzneiformen kann dies verhindern. Folglich können schwerwiegende unerwünschte Arzneistoffwirkungen, besonders bei der Verabreichung hochpotenter Arzneistoffe mit geringer therapeutischer Breite minimiert werden. Zusätzlich kann durch die einfache Herstellung die Prozesszeit verringert werden, wodurch der Arzneistoff geringerem Stress ausgesetzt wird. Dies verbessert die Möglichkeiten Arzneiformen für Arzneistoffe zu entwickeln, deren Eigenschaften bei der Formulierung eine Herausforderung darstellen (z. B Proteine). Folglich hat die Suche nach geeigneten Formulierungsstrategien zusammen mit der Verbesserung der Leistungsfähigkeit von Matrixarzneiformen in den letzten Jahren zunehmend an Bedeutung gewonnen.

Das erste Ziel der vorliegenden Arbeit war es Möglichkeiten zu untersuchen, multipartikuläre Matrixarzneiformen mit kontrollierter Wirkstofffreisetzung herzustellen, die zudem hohe Beladungen von 5-Aminosalicylsäure (5-ASA), dem Standardarzneistoff zur Behandlung chronisch entzündlicher Darmkrankheiten, enthalten. Die Hauptproblematik bestand dabei diese hohe Arzneistoffkonzentration zu gewährleisten und die vorzeitige Wirkstofffreisetzung im oberen Teil des Gastrointestinaltrakts (GIT) zu verhindern. 5-ASA wird im oberen Teil des GIT schnell degradiert und verliert somit seine Bioverfügbarkeit. Zudem sollte die vollständige und kontrollierte Wirkstofffreisetzung sichergestellt werden, sobald die Arzneiform den unteren Dickdarm und das Colon erreicht. Nach ersten Untersuchungen konnten Polymere als Matrixformer ausgeschlossen werden, da sie entweder in Arzneiformen mit ungenügenden physikalisch-chemischen Eigenschaften resultierten, Probleme bei der Herstellung auftraten oder die Wirkstofffreisetzung nicht dem gewünschten Profil entsprach. Dagegen zeigten Triglyceride, die aus Fettsäuren diverser Kettenlängen aufgebaut sind, sowie gemischte Triglyceride (C12-20) adäquate Formulierungs- und

Freisetzungscharakteristiken. Multipartikuläre Matrixarzneiformen wurden nach zwei Methoden hergestellt: Matrixpellets mit Hilfe von Extrusion/Spheronisation und Minitabletten. Pellets mit einer Wirkstoffbeladung von bis zu 60 % (m/m) 5-ASA konnten hergestellt werden. Glycerylpalmitostearat als Matrixbildner konnte die vorzeitige Wirkstofffreisetzung effektiv verhindern. Nur 25.4 % 5-ASA wurden nach 8 h in künstlichem Magen- und Darmsaft mit Zusatz von intestinalen Enzymen freigesetzt. Des Weiteren konnte die Stabilität der Wirkstofffreisetzung der hergestellten Matrixpellets unter Stressbedingungen nach 6 Monaten nachgewiesen werden. Die Problematik von Triglyceridmodifikationen, die häufig im Zusammenhang mit der Anwendung von erhöhten Verarbeitungstemperaturen bei der Herstellung entstehen, konnte durch adäquates Curing umgangen werden. Thermoanalytische Untersuchungen der Pellets zeigten eine reversible Umwandlung in die stabile β-Modifikation nach siebentägigem Curing bei 40 °C. Die zusätzlich hergestellten Minitabletten zeigten ähnliche Freisetzungskinetiken und sind somit ebenso geeignet, als kontrolliert freisetzende Arzneiformen im Colon zu agieren. Zudem bieten sie die Vorteile einer alternativen Herstellungsmethode.

Als Hilfsstoff, der die komplette und kontrollierte Wirkstofffreisetzung im unteren Dickdarm und im Colon sicherstellen sollte, wurde Nutriose®, ein verzweigtkettiges lösliches Dextrin, welches bevorzugt von colon-spezifischen Bakterien abgebaut wird, gewählt. Die nach dem Abbau des Dextrins freigesetzten Zuckerreste hinterlassen eine poröse Netzwerkstruktur innerhalb der Triglyceridarzneiform, was einen erhöhtem Einstrom von Bulkflüssigkeit und einer verstärkten Arzneistoffauflösung und -freisetzung zur Folge hat. Um die vorzeitige Wirkstofffreisetzung im oberen Teil des GIT möglichst niedrig zu halten, wurde eine Nutriose®-Konzentration von 15 % (m/m) bei gleichzeitiger Beibehaltung eines 60 % (m/m) 5-ASA-Anteils als optimal ermittelt. Die hergestellten Matrixpellets und Minitabletten stellen somit eine vielversprechende Alternative zu konventionellen überzogenen Arzneiformen bei der Behandlung chronisch entzündlicher Darmkrankheiten dar.

Arzneistoffe, die eine schlechte orale Bioverfügbarkeit verfügen oder Instabilitäten im GIT aufweisen müssen oft parenteral verabreicht werden. Dies gilt besonders für Proteinarzneistoffe, die in den letzten Jahrzehnten eine große therapeutische Bedeutung erlangt haben. Im Allgemeinen erfolgt die Applikation per Injektion oder Infusion von flüssigen Zubereitungen. Dies hat häufig eine rasche Eliminierung des verabreichten

Proteinarzneistoffs aus dem Blut und somit kurze Plasmahalbwertszeiten zur Folge. Aus diesem Grund sind häufige Arzneistoffgaben notwendig, was vom Patienten unerwünscht ist und meist mit sinkender Compliance einhergeht. Ein weiterer Teil dieser Arbeit umfasst daher die Herstellung und Optimierung von implantierbaren Lipidmatrizen zur kontrollierten Freisetzung von Proteinarzneistoffen.

Die Herstellung von Proteinarzneistoffen beinhaltet oft einen Gefriertrocknungsprozess, verbunden mit dem Risiko thermischer Deaktivierung der Proteinarzneistoffe und somit verringerter therapeutischer Aktivität. Ein wichtiger Faktor bei der Optimierung von Proteinarzneiformen ist das Verständnis der Mechanismen, die der Proteindenaturierung zugrunde liegen. Raman spektroskopische Untersuchungen am Modellprotein Lysozym in Anwesenheit chemischer Denaturantien wie Guanidinhydrochlorid und Harnstoff zeigten indirekte Interaktionen mit dem Protein durch Veränderung der Lösungsmitteleigenschaften bei Zusatz von Guanidinhydrochlorid und eine direkte Bindung zwischen Harnstoff und Protein über Wasserstoffbrückenbindungen. Letztere führten zu Änderungen der Proteindynamik und zur Ausbildung einer „molten globule"-Struktur mit intakter Sekundärstruktur, wie sie auch bei der thermischen Denaturierung von Proteinen auftritt. Diese Erkenntnisse sind wichtig, um die Mechanismen der Denaturierung während des Gefriertrocknungsprozesses zu verstehen. Ramanuntersuchungen im Niederfrequenzbereich in Anwesenheit von Denaturantien zeigten eindeutig den Zusammenhang zwischen Lösungsmittel- und Proteindynamik. Die Schwächung des Netzwerks von Wasserstoffbrückenbindungen bedingt eine verstärkte Mobilität des Proteinmoleküls und somit verstärkte intermolekulare Wechselwirkungen. Im Gegensatz dazu führt der Zusatz von Trehalose zu einer Stärkung des Netzwerks aus Wasserstoffbrückenbindungen, was eine bevorzugte Hydratation der Sekundärstruktur des Proteinmoleküls und somit dessen Stabilisierung zur Folge hat. Die Ergebnisse der Raman spektroskopischen Untersuchungen wurden zudem mit Messungen der Lysozymaktivitäten korreliert und es konnte gezeigt werden, dass die angewendeten Methoden vielversprechende Instrumente zur Strukturanalyse von Proteinen darstellen und sehr hilfreich bei der Optimierung von kontrolliert freisetzenden Proteinarzneiformen sind.

Des Weiteren wurde der Effekt von Cryo- und Lyoprotektoren auf die Stabilität von L-Lactatdehydrogenase (LDH) während der Gefriertrocknung und Lagerung untersucht. Saccharide (Sukrose und Trehalose), der Zuckeralkohol Maltitol, Polyethylenglykol 6000 (PEG 6000) und Polyvinylpyrrollidon waren die effizientesten Stabilisatoren und

ermöglichten den praktisch vollständigen Erhalt der Proteinaktivität. Mit Ausnahme von PVP, welches vorwiegend als Lyoprotektor agiert, besitzen alle genannten Stabilisatoren cryo- und lyoprotektive Eigenschaften. Ergebnisse aus der Bestimmung der enzymatischen Aktivität konnten auch hier mit Hilfe der Raman Spektroskopie bestätigt werden. Proben, die Trehalose und PVP enthielten und in dem für Proteine charakteristischen Bereich der Amid I Bande vermessen wurden, zeigten keine Raman-Verschiebung oder Peakverbreiterung, was auf eine intakte Sekundärstruktur der LDH hindeutete. Im Gegensatz dazu wurde bei Formulierungen, die PEG mit niedrigem Molekulargewicht enthielten ($M_{G=}$ 400 Da) eine Peakverbreiterung als Folge von Proteinaggregation beobachtet. Interessanterweise, konnten Kombinationen von Trehalose mit Glycerol, PEG 6000 oder PVP K-90 wesentlich effektiver zur Erhaltung der LDH-Aktivität beitragen. Dies lässt sich auf additive Effekte der Stabilisatoren zurückführen und zeigt deren Überlegenheit zu einzelnen Stabilisatoren.

Bei Aktivitätsmessungen von LDH Formulierungen mit Zusatz von 0.05 M Trehalose konnten nach 6 Monaten Lagerung bei 4 °C noch 50 % der initialen Aktivität nachgewiesen werden. Höhere Lagerungstemperaturen führten zu einem sukzessiven Verlust der verbleibenden enzymatischen Aktivität (25 % nach 6 Monaten bei 40 °C). Die Kombination von 1 % (m/V) PVP K-90 und 0.1 M Trehalose verbesserte die Lagerungsstabilität der entsprechenden LDH Formulierungen bei 4 °C. Bis zu 75 % der ursprünglichen Aktivität konnte hier erhalten werden. Die Mischungsverhältnisse 1:9 bis 9:1 zeigten dabei die höchste Effektivität. Bei erhöhten Lagerungstemperaturen zeigte es sich, dass Trehalose in der Kombination der Stabilisatoren die vorherrschende Komponente bei der Stabilisierung der Enzymaktivität war. Trotzdem konnte auch hier ein signifikanter Verlust der enzymatischen Aktivität nicht verhindert werden. Ramanspektroskopische Untersuchungen nach 3 monatiger Lagerung bei 25 bzw. 40 °C zeigten eine Verschiebung der Amid I Bande zu höheren Frequenzen. Erneut wurde die Zweckmäßigkeit beider Methoden (Aktivitätsmessungen und Ramanspektroskopie) durch die Korrelation der vorliegenden Ergebnisse bei der Analyse der Proteinstruktur gezeigt.

In einem weiteren Teil der vorliegenden Arbeit wurden das Freisetzungsverhalten und die Stabilität von Lysozym, welches als Modellarzneistoff in implantierbare Triglyceridmatrizen eingearbeitet wurde analysiert. An festgelegten Zeitpunkten der Freisetzungsversuche wurden sowohl die enzymatische Aktivität von freigesetztem Lysozym als auch das im Implantat verbliebene Protein untersucht. Da die charakteristischen Banden für alle Komponenten der Implantate an unterschiedlichen Frequenzen im Ramanspektrum vorlagen, war es möglich,

Lysozym gleichzeitig neben anderen Implantatkomponenten wie Triglyceride oder Trehalose zu untersuchen. Die enzymatische Aktivität des Lysozym wurde während des Herstellungsprozesses nicht negativ beeinflusst. Andererseits wurde eine sukzessive Abnahme der Stabilität des freigesetzten Lysozyms mit fortschreitender Freisetzungszeit gemessen (nahezu vollständig inaktiviertes Lysozym nach 28 tägiger Freisetzung). Um die Stabilität des eingearbeiteten Lysozyms zu erhöhen, wurde den Implantaten Trehalose in einer Konzentration von 0.05 M zugefügt. Bei nachfolgenden Messungen der enzymatischen Aktivität wurden Werte von 50 % der ursprünglichen Aktivität erreicht und belegten somit den stabilisierenden Effekt von Sacchariden, speziell Trehalose auf die Proteinstruktur. In Anlehnung an die Ergebnisse der Ramanspektroskopischen Analyse in *Abschnitt 3.2 „Effects of Denaturants in the Low-Frequency Region"* hat Trehalose einen stabilisierenden Effekt auf die Wasserstoffbrücken zwischen Hydratwasser und Protein und verhindert somit den Verlust der Sekundärstruktur. Zusätzlich durchgeführte Raman Messungen an Implantaten nach 7 beziehungsweise 28 Tagen Freisetzung ergaben aktives Lysozym sowohl an der Implantatoberfläche als auch im Zentrum des Implantats, was die stabilisierende Wirkung von Trehalose nicht nur während der Herstellung sondern auch bei der Freisetzung beweist.

Die Möglichkeit Dexamethason, einen antientzündlichen wirkenden Arzneistoff, in den Silikonelastomerteil von Cochleaimplantaten einzuarbeiten, war Thema des letzten Abschnitts dieser Arbeit. Rasterelektronenmikroskopie und Thermoanalyse von arzneistoffbeladenen Silikonfilmen und Extrudaten zeigten eine homogene Dispersion des Arzneistoffs in der Matrix. Die mechanischen Eigenschaften von dünnen arzneistoffhaltigen Filmen, die in trockenem Zustand untersucht wurden, nahmen mit steigender Arzneistoffbeladung ab. Dies ist auf die Ausbildung eines weniger kohärenten Silikonnetzwerkes mit zunehmendem Arzneistoffanteil zurückzuführen, was sich in abnehmender Elastizität der Filme widerspiegelte. Die Untersuchung der Filme in feuchtem Zustand ergab keine Änderung der mechanischen Eigenschaften der Filme. *In vitro* Freisetzungsstudien wurden unter Sinkbedingungen, sowie unter physiologisch realistischen Bedingungen durchgeführt. Das Ziel war dabei, detailliertere Informationen zu den Eigenschaften der untersuchten Systeme *in vivo*. Daher wurde das Verhältnis Implantatvolumen zu Volumen der Perilymphe (die wichtigste Flüssigeit in der Scala tympani der Cochlea) in vergrößertem Maßstab *in vitro* nachgebildet. Diffusion durch flüssigkeitsgefüllte Poren in der Silikonmatrix wurde als der dominante Transportmechanismus des Arzneistoffs aus den untersuchten Systemen identifiziert. Eine langsame Freisetzungskinetik (5 % freigesetztes Dexamethason nach

60 Tagen) empfehlen den Einsatz der hergestellten Systeme für eine Langzeittherapie bei implantationsbedingten Entzündungsreaktionen des Cochleagewebes bzw. zur Verhinderung der Apoptose von Haarzellen. Der experimentelle Aufbau, d.h. Sinkbedingungen, hat einen wichtigen Einfluss auf die resultierenden Freisetzungsprofile. Da Dexamethason eine niedrige Löslichkeit in wässrigen Medien aufweist, liegen gelöster und ungelöster Arzneistoff nebeneinander in der Silikonmatrix vor. Die treibende Kraft bei Diffusionsprozessen ist der Gradient zwischen gelöstem Arzneistoff innerhalb des Systems und der umgebenden Bulkflüssigkeit. Zur Diffusion ist nur gelöster Arzneistoff befähigt, daher war die Geschwindigkeit der Freisetzung bei Sinkbedingungen höher. Ebenso spielte die Ausgangskonzentration von Dexamethason eine Rolle, die bei Erreichen der Sättigungslöslichkeit innerhalb der Matrix den geschwindigkeitsbestimmenden Schritt für den Abtransport des gelösten Arzneistoffs darstellte.

Die Mobilität von gelöstem Dexamethason innerhalb der Silikonelastomerfilme wurde mit Hilfe von Fick's zweitem Gesetz der Diffusion berechnet. Fiktive Diffusionskoeffizienten wurden aus den gewonnenen Freisetzungsdaten der Filme ermittelt und ein vereinfachtes mathematisches Modell zur quantitativen Voraussage der Freisetzungskinetiken aus Silikonelastomerextrudaten und Cochleaimplantaten entwickelt. Die Vorhersagen wurden in unabhängigen Experimenten überprüft. Vorhersagen und experimentelle Überprüfung ergaben gute Übereinstimmung, was die Anwendbarkeit des entwickelten mathematischen Modells bestätigte. Die vorliegenden Ergebnisse können helfen, die Optimierung dieser Art kontrolliert freisetzender Arzneistoffsysteme zu verkürzen, da die Einflüsse von Schlüsselfaktoren, wie Maße und Zusammensetzung, auf die resultierenden Systeme vorhergesagt werden können.

6.   References

Abrahamsson, B., Alpsten, M., Jonsson, U.E., Lundberg, P., Sandberg, A., Sundgren, M., Svenheden, A., Tölli, J. (1996) Gastro-intestinal transit of a multiple-unit formulation (metoprolol CR/ZOK) and a non-disintegrating tablet with the emphasis on colon. International Journal of Pharmaceutics, 140, 229-235.

Adkin, D.A., Kenyon, C.J., Lerner, E.I., Landau, I., Strauss, E., Caron, D., Penhasi, A., Rubinstein, A., Wilding, I.R. (1997) The use of scintigraphy to provide "proof of concept" for novel polysaccharide preparations designed for colonic drug delivery. Pharmaceutical Research, 14, 103-107.

Ahrabi, S.F., Madsen, G., Dyrstad, K., Sande, S.A., Graffner, C. (2000) Development of pectin matrix tablets for colonic delivery of model drug ropivacaine. European Journal of Pharmaceutical Sciences, 10, 43-52.

Aiedeh, K., Taha, M.O. (1999) Synthesis of chitosan succinate and chitosan phthalate and their evaluation as suggested matrices in orally administered, colon-specific drug delivery systems. Archiv Der Pharmazie, 332, 103-107.

Allison, S.D., Dong, A., Carpenter, J.F. (1996) Counteracting effects of thiocyanate and sucrose on chymotrypsinogen secondary structure and aggregation during freezing, drying, and rehydration. Biophysical Journal, 71, 2022-2032.

Allison, S.D., Randolph, T.W., Manning, M.C., Middleton, K., Davis, A., Carpenter, J.F. (1998) Effects of drying methods and additives on structure and function of actin: Mechanisms of dehydration-induced damage and its inhibition. Archives of Biochemistry and Biophysics, 358, 171-181.

Allison, S.D., Chang, B., Randolph, T.W., Carpenter, J.F. (1999) Hydrogen bonding between sugar and protein is responsible for inhibition of dehydration-induced protein unfolding. Archives of Biochemistry and Biophysics, 365, 289-298.

Amrutkar, J., Gattani, S. (2009) Chitosan–chondroitin sulfate based matrix tablets for colon specific delivery of indomethacin. AAPS PharmSciTech, 10, 670-677.

Anchordoquy, T.J., Carpenter, J.F. (1996) Polymers protect lactate dehydrogenase during freeze-drying by inhibiting dissociation in the frozen state. Archives of Biochemistry and Biophysics, 332, 231-238.

Anchordoquy, T.J., Izutsu, K., Randolph, T.W., Carpenter, J.F. (2001) Maintenance of quaternary structure in the frozen state stabilizes lactate dehydrogenase during freeze-drying. Archives of Biochemistry and Biophysics, 390, 35-41.

Andrews, G.P., Laverty, T.P., Jones, D.S. (2009) Mucoadhesive polymeric platforms for controlled drug delivery. European Journal of Pharmaceutics and Biopharmaceutics, 71, 505-518.

Appel, B., Maschke, A., Weiser, B., Sarhan, H., Englert, C., Angele, P., Blunk, T., Göpferich, A. (2006) Lipidic implants for controlled release of bioactive insulin: Effects on cartilage engineered *in vitro*. International Journal of Pharmaceutics, 314, 170-178.

Arakawa, T., Timasheff, S.N. (1984) Protein stabilization and destabilization by guanidinium salts. Biochemistry, 23, 5924-5929.

Arakawa, T., Kita, Y., Carpenter, J. (1991) Protein–solvent interactions in pharmaceutical formulations. Pharmaceutical Research, 8, 285-291.

Arakawa, T., Prestrelski, S.J., Kenney, W.C., Carpenter, J.F. (2001) Factors affecting short-term and long-term stabilities of proteins. Advanced Drug Delivery Reviews, 46, 307-326.

Aranguren, M.I. (1998) Crystallization of polydimethylsiloxane: Effect of silica filler and curing. Polymer, 39, 4897-4903.

Ashford, M., Fell, J. T., Attwood, D., Woodhead, P. J. (1993a) An *in vitro* investigation into the suitability of pH-dependent polymers for colonic targeting. International Journal of Pharmaceutics, 91, 241-245.

Ashford, M., Fell, J. T., Attwood, D., Sharma, H., Woodhead, P. J. (1993b) An *in vivo* investigation into the suitability of pH dependent polymers for colonic targeting. International Journal of Pharmaceutics, 95, 193-199.

Ashford, M., Fell, J., Attwood, D., Sharma, H., Woodhead, P. (1993c) An evaluation of pectin as a carrier for drug targeting to the colon. Journal of Controlled Release, 26, 213-220.

Ashford, M., Fell, J., Attwood, D., Sharma, H., Woodhead, P. (1994) Studies on pectin formulations for colonic drug delivery. Journal of Controlled Release, 30, 225-232.

Banker, G.S., Rhodes, C.T. (2002) Modern Pharmaceutics, 4th edition, Marcel Dekker, New York, NY.

Bhat, R., Timasheff, S.N. (1992) Steric exclusion is the principal source of the preferential hydration of proteins in presence of polyethylene glycols. Protein Science : A Publication of the Protein Society, 1, 1133-1143.

Bhatnagar, B.S., Pikal, M.J., Bogner, R.H. (2008) Study of the individual contributions of ice formation and freeze-concentration on isothermal stability of lactate dehydrogenase during freezing. Journal of Pharmaceutical Sciences, 97, 798-814.

Bennion, B.J., Daggett, V. (2003) The molecular basis for the chemical denaturation of proteins by urea. Proceedings of the National Academy of Sciences of the United States of America, 100, 5142-5147.

Bernkop-Schnürch, A. (2005) Mucoadhesive systems in oral drug delivery. Drug Discovery Today: Technologies, 2, 83-87.

Bindschaedler, C. (2007) Lyophilization Process Validation. Freeze-Drying/Lyophilization of Pharmaceutical and Biological Products. 2nd edition, pp. 535-575, Informa Healthcare, New York, NY.

Biondi, M., Ungaro, F., Quaglia, F., Netti, P.A. (2008) Controlled drug delivery in tissue engineering. Advanced Drug Delivery Reviews, 60, 229-242.

Bodmeier, R., Xiaodi, G., Paeratakul, O. (1997) Process formulation factors affecting the drug release from pellets coated with ethylcellulose-pseudolatex Aquacoat. Aqueous polymeric coatings for pharmaceutical dosage forms. 2nd Edition. Marcel Dekker, New York, NY.

Borkholder, D.A. (2008) State-of-the-art mechanisms of intracochlear drug delivery. Current Opinion in Otolaryngology & Head and Neck Surgery, 16, 472-477.

Branca, C., Magazù, S., Maisano, G., Migliardo, P. (1999) Anomalous cryoprotective effectiveness of trehalose: Raman scattering evidences. The Journal of Chemical Physics, 111, 281-288.

Branca, C., Maccarrone, S., Magazù, S., Maisano, G., Bennington, S.M., Taylor, J. (2005) Tetrahedral order in homologous disaccharide-water mixtures. The Journal of Chemical Physics, 122, 174513-174519.

Brook, M.A., Holloway, A.C., Ng, K.K., Hrynyk, M., Moore, C., Lall, R. (2008) Using a drug to structure its release matrix and release profile. International Journal of Pharmaceutics, 358, 121–127.

Brøndsted, H., Andersen, C., Hovgaard, L. (1998) Crosslinked dextran - a new capsule material for colon targeting of drugs. Journal of Controlled Release, 53, 7-13.

Brøndsted, H., Hovgaard, L., Simonsen, L. (1995) Dextran hydrogels for colon-specific drug delivery. III: *In vitro* and *in vivo* degradation. STP Pharma Science, 5, 60-64.

Brown, J.N., Miller, J.M., Altschuler, R.A, Nuttall, A.L. (1993) Osmotic pump implant for chronic infusion of drugs into the inner ear. Hearing Research, 70, 167–172.

Caflisch, A., Karplus, M. (1999) Structural details of urea binding to barnase: A molecular dynamics analysis. Structure (London, England: 1993), 7, 477-488.

6 References

Calamai, M., Taddei, N., Stefani, M., Ramponi, G., Chiti, F. (2003) Relative influence of hydrophobicity and net charge in the aggregation of two homologous proteins. Biochemistry 42, 15078-15083.

Caliskan, G., Kisliuk, A., Tsai, A.M., Soles, C.L., Sokolov, A.P. (2003) Protein dynamics in viscous solvents. The Journal of Chemical Physics, 118, 4230-4237.

Caraballo, I., Millán, M., Rabasco, A.M., Leuenberger, H. (1996) Zero-order release periods in inert matrices. Influence of the distance to the percolation threshold. Pharmaceutica Acta Helvetiae, 71, 335-339.

Carpenter, J.F., Crowe, L.M., Crowe, J.H. (1987) Stabilization of phosphofructokinase with sugars during freeze-drying: characterization of enhanced protection in the presence of divalent cations. Biochimica et Biophysica Acta (BBA) - General Subjects, 923, 109-115.

Carpenter, J.F., Martin, B., Loomis, S.H., Crowe, J.H. (1988) Long-term preservation of dried phosphofructokinase by sugars and sugar/zinc mixtures. Cryobiology, 25, 372-376.

Carpenter, J.F., Crowe, J.H. (1989) An infrared spectroscopic study of the interactions of carbohydrates with dried proteins. Biochemistry, 28, 3916-3922.

Carpenter, J.F., Crowe, J.H., Arakawa, T. (1990) Comparison of solute-induced protein stabilization in aqueous solution and in the frozen and dried states. Journal of Dairy Science, 73, 3627-3636.

Carpenter, J.F., Prestrelski, S.J., Arakawa, T. (1993) Separation of freezing- and drying-induced denaturation of lyophilized proteins using stress-specific stabilization : I. enzyme activity and calorimetric studies. Archives of Biochemistry and Biophysics, 303, 456-464.

Carpenter, J.F., Izutsu, K., Randolph, T.W. (2007) Freezing- and drying-induced perturbations of protein structure and mechanisms of protein protection by stabilizing additives. Freeze-Drying/Lyophilization of Pharmaceutical and Biological Products. pp. 456-464, Informa Healthcare, New York, NY.

Carslaw, H.S. Jaeger, J.C. (1959) Conduction of Heat in Solids, Clarendon Press, Oxford,UK.

Castellanos, I.J., Cruz, G., Crespo, R., Griebenow, K. (2002) Encapsulation-induced aggregation and loss in activity of [gamma]-chymotrypsin and their prevention. Journal of Controlled Release, 81, 307–319.

Chang, B.S., Randall, C.S. (1992) Use of subambient thermal analysis to optimize protein lyophilization. Cryobiology, 29, 632-656.

Chang, B.S., Kendrick, B.S., Carpenter, J.F. (1996) Surface-induced denaturation of proteins during freezing and its inhibition by surfactants. Journal of Pharmaceutical Sciences, 85, 1325-1330.

Charman, W.N., Porter, C.J.H., Mithani, S., Dressman, J.B. (1997) Physicochemical and physiological mechanisms for the effects of food on drug absorption: The role of lipids and pH. Journal of Pharmaceutical Sciences, 86, 269-282.

Chen, Z., Kujawa, S.G., McKenna, M.J., Fiering, J.O., Mescher, M.J., Borenstein, J.T., Swan, E.E.L., Sewell, W.F. (2005) Inner ear drug delivery via a reciprocating perfusion system in the guinea pig. Journal of Controlled Release, 110, 1-19.

Chiu, H.C., Hsiue, G.H., Lee, Y.P., Huang, L.W. (1999) Synthesis and characterization of pH-sensitive dextran hydrogels as a potential colon-specific drug delivery system. Journal of Biomaterials Science. Polymer Edition, 10, 591-608.

Cochran, T., Nail, S.L. (2009) Ice nucleation temperature influences recovery of activity of a model protein after freeze drying. Journal of Pharmaceutical Sciences, 98, 3495-3498.

Colombo, P., Bettini, R., Santi, P., Peppas, N.A. (2000) Swellable matrices for controlled drug delivery: gel-ayer behaviour, mechanisms and optimal performance. Pharmaceutical Science & Technology Today, 3, 198-204.

Costantino, H.R., Carrasquillo, K.G., Cordero, R.A., Mumenthaler, M., Hsu, C.C., Griebenow, K. (1998) Effect of excipients on the stability and structure of lyophilized recombinant human growth hormone. Journal of Pharmaceutical Sciences, 87, 1412-1420.

Coupe, A., Davis, S., Wilding, I. (1991) Variation in gastrointestinal transit of pharmaceutical dosage forms in healthy subjects. Pharmaceutical Research, 8, 360-364.

Coupe, A.J., Davis, S.S., Evans, D.F., Wilding, I.R. (1992a) The effect of sleep on the gastrointestinal transit of pharmaceutical dosage forms. International Journal of Pharmaceutics, 78, 69-76.

Coupe, A.J., Davis, S.S., Evans, D.F., Wilding, I.R. (1992b) Nocturnal scintigraphic imaging to investigate the gastrointestinal transit of dosage forms. Journal of Controlled Release, 20, 155-162.

Courtenay, E.S., Capp, M.W., Record, M.T., Jr. (2001) Thermodynamics of interactions of urea and guanidinium salts with protein surface: Relationship between solute effects on protein processes and changes in water-accessible surface area. Protein Science: A Publication of the Protein Society, 10, 2485-2497.

6 References

Crank, J. (1975) The Mathematics of Diffusion. 2nd edition., pp. 1-7, Clarendon Press, Oxford, UK.

Crowe, J.H., Croze, L.M., Carpenter, J.F. (1993a) Preserving dry biomaterials: the water replacement hypothesis. Biopharmaceutics, 6, 28-37.

Crowe, J.H., Croze, L.M., Carpenter, J.F. (1993b) Preserving dry biomaterials: the water replacement hypothesis. Biopharmaceutics, 6, 40-43.

Cui, Z., Mumper, R.J. (2002) Genetic immunization using nanoparticles engineered from microemulsion precursors. Pharmaceutical Research, 19, 939-946.

Cummings, J.H., Milojevic, S., Harding, M., Coward, W.A., Gibson, G.R., Louise Botham, R., Ring, S.G., Wraight, E.P., Stockham, M.A., Allwood, M.C., Newton, J.M. (1996) *In vivo* studies of amylose- and ethylcellulose-coated [^{13}C]glucose microspheres as a model for drug delivery to the colon. Journal of Controlled Release, 40, 123-131.

Davies, P. (2009) Oral Solid Dosage Forms. Pharmaceutical Preformulation and Formulation. 2nd Edition. Informa Healthcare, New York, NY.

Davis, S.S., Hardy, J.G., Taylor, M.J., Whalley, D.R., Wilson, C.G. (1984a) A comparative study of the gastrointestinal transit of a pellet and tablet formulation. International Journal of Pharmaceutics, 21, 167-177.

Davis, S.S., Hardy, J.G., Taylor, M.J., Whalley, D.R., Wilson, C.G. (1984b) The effect of food on the gastrointestinal transit of pellets and an osmotic device (Osmet). International Journal of Pharmaceutics, 21, 331-340.

Davis, S.S. (1985) The design and evaluation of controlled release systems for the gastrointestinal tract. Journal of Controlled Release, 2, 27-38.

Davis, S.S., Hardy, J.G., Fara, J.W. (1986) Transit of pharmaceutical dosage forms through the small intestine. Gut, 27, 886 -892.

Davis, S.S. (2005) Formulation strategies for absorption windows. Drug Discovery Today, 10, 249-257.

De Brabander, C., Vervaet, C., Fiermans, L., Remon, J.P. (2000) Matrix mini-tablets based on starch/microcrystalline wax mixtures. International Journal of Pharmaceutics, 199, 195-203.

De Ceulaer, G., Johnson, S., Yperman, M., Daemers, K., Offeciers, F.E., O'Donoghue, G.M., Govaerts, P.J. (2003) Long-term evaluation of the effect of intracochlear steroid deposition on electrode impedance in cochlear implant patients. Otology & Neurotology, 24, 769-774.

Del Curto, M.D., Chicco, D., D'Antonio, M., Ciolli, V., Dannan, H., D'Urso, S., Neuteboom, B., Pompili, S., Schiesaro, S., Esposito, P. (2003) Lipid microparticles as sustained release system for a GnRH antagonist (Antide). Journal of Controlled Release 89, 297-310.

Dew, M.J., Hughes, P.J., Lee, M.G., Evans, B.K., Rhodes, J. (1982) An oral preparation to release drugs in the human colon. British Journal of Clinical Pharmacology, 14, 405-408.

Digenis, G.A., Sandefer, E.P., Parr, A.F., Beihn, R., McClain, C., Scheinthal, B.M., Ghebre-Sellassie, I., Iyer, U., Nesbitt, R.U., Randinitis, E. (1990) Gastrointestinal behavior of orally administered radiolabeled erythromycin pellets in man as determined by gamma scintigraphy. Journal of Clinical Pharmacology, 30, 621-631.

Dinh, C., Hoang, K., Haake, S. Chen, S. Angeli, S., Nong, E., Eshraghi, A.A., Balkany, T.J., Van De Water, T.R. (2008) Biopolymer-released dexamethasone prevents tumor necrosis factor [alpha]-induced loss of auditory hair cells in vitro: Implications toward the development of a drug-eluting cochlear implant electrode array, Otology Neurotology, 29, 1012-1019.

Dong, W., Bodmeier, R. (2006) Encapsulation of lipophilic drugs within enteric microparticles by a novel coacervation method. International Journal of Pharmaceutics, 326, 128-138.

Dong, A., Prestrelski, S.J., Allison, S.D., Carpenter, J.F. (1995) Infrared spectroscopic studies of lyophilization- and temperature-induced protein aggregation. Journal of Pharmaceutical Sciences, 84, 415-424.

Doyle, K.J., Bauch, C., Battista, R., Beatty, C., Hughes, G.B., Mason, J., Maw, J., Musiek, F.L. (2004) Intratympanic steroid treatment: A review. Otology & Neurotology 25, 1034-1039.

Duddu, S.P., Dal Monte, P.R. (1997) Effect of glass transition temperature on the stability of lyophilized formulations containing a chimeric therapeutic monoclonal antibody. Pharmaceutical Research, 14, 591-595.

Dunne, M., Corrigan, O.I., Ramtoola, Z. (2000) Influence of particle size and dissolution conditions on the degradation properties of polylactide-co-glycolide particles. Biomaterials 21, 1659-1668.

6 References

Dyer, A.M., Khan, K.A., Aulton, M.E. (1995) Effect of polymer loading on drug release from film-coated ibuprofen pellets prepared by extrusion-spheronization. Drug Development and Industrial Pharmacy, 21, 1841-1858.

Eastwood, H., Chang, A., Kel, G., Sly, D., Richardson, R., O'Leary, S.J. (2010) Round window delivery of dexamethasone ameliorates local and remote hearing loss produced by cochlear implantation into the second turn of the guinea pig cochlea. Hearing Research, 265, 25-29.

Eckburg, P.B., Bik, E.M., Bernstein, C.N., Purdom, E., Dethlefsen, L., Sargent, M., Gill, S.R., Nelson, K.E., Relman, D.A. (2005) Diversity of the human intestinal microbial flora. Science (New York, N.Y.), 308, 1635-1638.

Elkharraz, K., Ahmed, A.R., Dashevsky, A., Bodmeier, R. (2011) Encapsulation of water-soluble drugs by an o/o/o-solvent extraction microencapsulation method. International Journal of Pharmaceutics, 409, 89-95.

Elkordy, A.A., Forbes, R.T., Barry, B.W. (2008) Study of protein conformational stability and integrity using calorimetry and FT-Raman spectroscopy correlated with enzymatic activity. European Journal of Pharmaceutical Sciences, 33, 177-190.

Eriksen, S. (1979) The theory and Practice of Industrial Pharmacy. Lea and Fiebiger, Philadelphia, PA.

Eshraghi, A.A., Adil, E., He, J., Graves, R., Balkany, T.J., Van De Water, T.R. (2007) Local dexamethasone therapy conserves hearing in an animal model of electrode insertion trauma-induced hearing loss, Otology & Neurotology, 28, 842-849.

Espinosa, L., Schebor, C., Buera, P., Moreno, S., Chirife, J. (2006) Inhibition of trehalose crystallization by cytoplasmic yeast components. Cryobiology, 52, 157-160.

Estey, T., Kang, J., Schwendeman, S.P., Carpenter, J.F. (2006) BSA degradation under acidic conditions: A model for protein instability during release from PLGA delivery systems. Journal of Pharmaceutical Sciences, 95, 1626-1639.

Evans, D.F., Pye, G., Bramley, R., Clark, A.G., Dyson, T.J., Hardcastle, J.D. (1988) Measurement of gastrointestinal pH profiles in normal ambulant human subjects. Gut, 29, 1035-1041.

Ewe, K., Schwartz, S., Petersen, S., Press, A.G. (1999) Inflammation does not decrease intraluminal pH in chronic inflammatory bowel disease. Digestive Diseases and Sciences, 44, 1434-1439.

Fadda, H.M., McConnell, E.L., Short, M.D., Basit, A.W. (2008) Meal-induced acceleration of tablet transit through the human small intestine. Pharmaceutical Research, 26, 356-360.

Fallingborg, J., Christensen, L.A., Ingeman-Nielsen, M., Jacobsen, B.A., Abildgaard, K., Rasmussen, H.H. (1989) pH-profile and regional transit times of the normal gut measured by a radiotelemetry device. Alimentary Pharmacology & Therapeutics, 3, 605-613.

Fallingborg, J., Christensen, L.A., Jacobsen, B.A., Rasmussen, S.N. (1993) Very low intraluminal colonic pH in patients with active ulcerative colitis. Digestive Diseases and Sciences, 38, 1989-1993.

Fallingborg, J., Pedersen, P., Jacobsen, B.A. (1998) Small intestinal transit time and intraluminal pH in ileocecal resected patients with Crohn's disease. Digestive Diseases and Sciences, 43, 702-705.

Fan, L.T., Singh, S.K. (1989) Controlled release: A quantitative treatment. Springer Verlag, Berlin.

Farahmand Ghavi, F., Mirzadeh, H., Imani, M., Jolly, C., Farhadi, M. (2010) Corticosteroid-releasing cochlear implant: A novel hybrid of biomaterial and drug delivery system. Journal of Biomedical Materials Research Part B: Applied Biomaterials, 94B, 388-98.

Fernandez-Hervas, M.J., Fell, J.T. (1998) Pectin/chitosan mixtures as coatings for colon-specific drug delivery: An *in vitro* evaluation. International Journal of Pharmaceutics, 169, 115-119.

Fersht, A.R. (2001) Denaturation (Proteins). Encyclopedia of Genetics, p. 529, Academic Press, New York, NY.

Fields, G.B., Alonso, D.O.V., Stigter, D., Dill, K.A. (1992). Theory for the aggregation of proteins and copolymers. The Journal of Physical Chemistry 96, 3974-3981.

Firestone, D.E., Lauder, A.J. (2010). Chemistry and mechanics of commonly used sutures and needles. The Journal of Hand Surgery 35, 486-488.

Folkman, J. and Long, D.M. (1964) The use of silicone rubber as a carrier for prolonged drug therapy. Journal of Surgical Research, 4, 139-142.

Follonier, N. and Doelker, E. (1992) Biopharmaceutical comparison of oral multiple-unit and single-unit sustained-release dosage forms. S. T. P. Pharma Sciences 2, 141-158.

Franks, F. (1994) Long-term stabilization of biologicals. Bio/Technology (Nature Publishing Company), 12, 253-256.

Franks, F., Hatley, R.H., Friedman, H.L. (1988) The thermodynamics of protein stability. Cold destabilization as a general phenomenon. Biophysical Chemistry, 31, 307-315.

Frenning, G. Modelling drug release from inert matrix systems: From moving-boundary to continuous-field descriptions. International Journal of Pharmaceutics, 418, 88-99.

Friend, D.R. (2005) New oral delivery systems for treatment of inflammatory bowel disease. Advanced Drug Delivery Reviews, 57, 247–265.

Frieri, G., Pimpo, M., Galletti, B., Palumbo, G., Corrao, G., Latella, G., Chiaramonte, M., Caprilli, R. (2005). Long-term oral plus topical mesalazine in frequently relapsing ulcerative colitis. Digestive and Liver disease 37, 92–96.

Frohoff-Hülsmann, M.A., Lippold, B.C., McGinity, J.W. (1999) Aqueous ethyl cellulose dispersion containing plasticizers of different water solubility and hydroxypropyl methylcellulose as coating material for diffusion pellets II: Properties of sprayed films. European Journal of Pharmaceutics and Biopharmaceutics, 48, 67-75.

Fukui, E., Miyamura, N., Uemura, K., Kobayashi, M. (2000) Preparation of enteric coated timed-release press-coated tablets and evaluation of their function by *in vitro* and *in vivo* tests for colon targeting. International Journal of Pharmaceutics, 204, 7-15.

Gazzaniga, A., Iamartino, P., Maffione, G., Sangalli, M. (1994) Oral delayed-release system for colonic specific delivery. International Journal of Pharmaceutics, 108, 77-83.

Gentzkow, G.D., Iwasaki, S.D., Hershon, K.S., Mengel, M., Prendergast, J.J., Ricotta, J.J., Steed, D.P., Lipkin, S. (1996) Use of dermagraft, a cultured human dermis, to treat diabetic foot ulcers. Diabetes Care 19, 350-354.

Gibson, T.D. (1996) Protein stabilisation using additives based on multiple electrostatic interactions. Developments in Biological Standardization, 87, 207-217.

Ginebra, M., Traykova, T., Planell, J., (2006) Calcium phosphate cements as bone drug delivery systems: A review. Journal of Controlled Release 113, 102-110.

Giteau, A., Venier-Julienne, M., Aubert-Pouëssel, A., Benoit, J. (2008) How to achieve sustained and complete protein release from PLGA-based microparticles? International Journal of Pharmaceutics 350, 14-26.

Gliko-Kabir, I., Yagen, B., Baluom, M., Rubinstein, A. (2000) Phosphated crosslinked guar for colon-specific drug delivery. II. *In vitro* and *in vivo* evaluation in the rat. Journal of Controlled Release, 63, 129-134.

Golomb, G. Fisher, P. Rahamim, E. (1990) The relationship between drug release rate, particle size and swelling of silicone matrices, Journal of Controlled Release, 12, 121-132.

Goycoolea, M.V., Lundman, L. (1997) Round window membrane. Structure function and permeability: A review. Microscopy Research and Technique, 36, 201-211.

Greiff, D., Doumas, B.T., Malinin, T.I., Perry, B.W. (1976) Freeze-drying of solutions of serum albumin containing dimethylsulfoxide. Cryobiology, 13, 201-205.

Guarner, F., Malagelada, J.-R. (2003) Role of bacteria in experimental colitis. Best Practice & Research Clinical Gastroenterology, 17, 793-804.

Guse, C., Koennings, S., Kreye, F., Siepmann, F., Goepferich, A., Siepmann, J. (2006a) Drug release from lipid-based implants: Elucidation of the underlying mass transport mechanisms. International Journal of Pharmaceutics, 314, 137-144.

Guse, C., Koennings, S., Maschke, A., Hacker, M., Becker, C., Schreiner, S., Blunk, T., Spruss, T., Goepferich, A. (2006b) Biocompatibility and erosion behavior of implants made of triglycerides and blends with cholesterol and phospholipids. International Journal of Pharmaceutics, 314, 153-160.

Habraken, W., Wolke, J., Jansen, J., (2007) Ceramic composites as matrices and scaffolds for drug delivery in tissue engineering. Advanced Drug Delivery Reviews, 59, 234-248.

Hamdani, J., Moès, A.J., Amighi, K. (2002) Development and evaluation of prolonged release pellets obtained by the melt pelletization process. International Journal of Pharmaceutics, 245, 167–177.

Hamdani, J., Moës, A.J., Amighi, K. (2003) Physical and thermal characterisation of Precirol® and Compritol® as lipophilic glycerides used for the preparation of controlled-release matrix pellets. International Journal of Pharmaceutics, 260, 47-57.

Hans, M.L., Lowman, A.M. (2002) Biodegradable nanoparticles for drug delivery and targeting. Current Opinion in Solid State and Materials Science, 6, 319-327.

Hatefi, A., Amsden, B., (2002) Biodegradable injectable *in situ* forming drug delivery systems. Journal of Controlled Release, 80, 9-28.

Hatley, R.H., Franks, F. (1989) The effect of aqueous methanol cryosolvents on the heat- and cold-induced denaturation of lactate dehydrogenase. European Journal of Biochemistry / FEBS, 184, 237-240.

Hebden, J.M., Blackshaw, P.E., Perkins, A.C., Wilson, C.G., Spiller, R.C. (2000) Limited exposure of the healthy distal colon to orally-dosed formulation is further exaggerated

in active left-sided ulcerative colitis. Alimentary Pharmacology & Therapeutics, 14, 155-161.

Hédoux, A., Derollez, P., Guinet, Y., Dianoux, A.J., Descamps, M. (2001) Low-frequency vibrational excitations in the amorphous and crystalline states of triphenyl phosphite: A neutron and Raman scattering investigation. Physical Review B, 63, 144202.

Hédoux, A., Ionov, R., Willart, J.-F., Lerbret, A., Affouard, F., Guinet, Y., Descamps, M., Prévost, D., Paccou, L., Danéde, F. (2006a) Evidence of a two-stage thermal denaturation process in lysozyme: A Raman scattering and differential scanning calorimetry investigation. The Journal of Chemical Physics, 124, 14703.

Hédoux, A., Willart, J.-F., Ionov, R., Affouard, F., Guinet, Y., Paccou, L., Lerbret, A., Descamps, M. (2006b) Analysis of sugar bioprotective mechanisms on the thermal denaturation of lysozyme from Raman scattering and differential scanning calorimetry investigations. The Journal of Physical Chemistry. B, 110, 22886-22893.

Hédoux, A., Willart, J.-F., Paccou, L., Guinet, Y., Affouard, F., Lerbret, A., Descamps, M. (2009) Thermostabilization mechanism of bovine serum albumin by trehalose. The Journal of Physical Chemistry. B, 113, 6119-6126.

Heller, J., Robinson, J.R, Lee, V.H.L. (1987) Use of polymers in controlled release of active agents. Controlled Drug Delivery: Fundamentals and Applications, 2nd edition, pp. 179-212, Marcel Dekker, New York, NY.

Heller, M.C., Carpenter, J.F., Randolph, T.W. (1997) Manipulation of lyophilization-induced phase separation: Implications for pharmaceutical proteins. Biotechnology Progress, 13, 590-596.

Herrmann, S., Winter, G., Mohl, S., Siepmann, F., Siepmann, J. (2007a) Mechanisms controlling protein release from lipidic implants: Effects of PEG addition. Journal of Controlled Release, 118, 161-168.

Herrmann, S., Mohl, S., Siepmann, F., Siepmann, J., Winter, G. (2007b) New insight into the role of polyethylene glycol acting as protein release modifier in lipidic implants. Pharmaceutical Research, 24, 1527-1537.

Hill, M.J. (1995) Bacterial fermentation of complex carbohydrate in the human colon. European Journal of Cancer Prevention, 4, 353-358.

Hochmair, I., Nopp, P., Jolly, C., Schmidt, M., Schößer, H., Garnham, C., Anderson, I. (2006) MED-EL cochlear implants: State of the art and a glimpse into the future. Trends in amplification, 10, 201-219.

Hoffman, A.S. (2008) The origins and evolution of „controlled" drug delivery systems. Journal of Controlled Release, 132, 153-163.

Hui, H.-W., Robinson, J.R; Lee, V.H.L. (1987) Design and fabrication of oral controlled release drug delivery systems. Controlled Drug Delivery: Fundamentals and Applications, 2nd edition, pp 373-432, Marcel Dekker, New York, NY.

Ibekwe, V. C., Fadda, H. M., Parsons, G. E., Basit, A. W. (2006a) A comparative *in vitro* assessment of the drug release performance of pH-responsive polymers for ileo-colonic delivery. International Journal of Pharmaceutics, 308, 52-60.

Ibekwe, V., Fadda, H., McConnell, E., Khela, M., Evans, D., Basit, A. (2008) Interplay between intestinal pH, transit time and feed status on the i*n vivo* performance of pH-responsive ileo-colonic release systems. Pharmaceutical Research, 25, 1828-1835.

Igarashi, M., Ohashi, K., Ishii, M. (1986) Morphometric comparison of endolymphatic and perilymphatic spaces in human temporal bones. Acta Oto-Laryngologica, 101, 161-164.

Istrail, S., Schwartz, R., King, J. (1999) Lattice simulations of aggregation funnels for protein folding. Journal of Computational Biology: A Journal of Computational Molecular Cell Biology, 6, 143-162.

Izutsu, K., Yoshioka, S., Terao, T. (1993a) Stabilization of [beta]-galactosidase by amphiphilic additives during freeze-drying. International Journal of Pharmaceutics, 90, 187-194.

Izutsu, K., Yoshioka, S., Terao, T. (1993b) Decreased protein-stabilizing effects of cryoprotectants due to crystallization. Pharmaceutical Research, 10, 1232-1237.

Izutsu, K., Yoshioka, S., Kojima, S. (1995) Increased stabilizing effects of amphiphilic excipients on freeze-drying of lactate dehydrogenase (LDH) by dispersion into sugar matrices. Pharmaceutical Research, 12, 838-843.

Izutsu, K., Kojima, S. (2000) Freeze-concentration separates proteins and polymer excipients into different amorphous phases. Pharmaceutical Research, 17, 1316-1322.

Izutsu, K., Ocheda, S.O., Aoyagi, N., Kojima, S. (2004) Effects of sodium tetraborate and boric acid on nonisothermal mannitol crystallization in frozen solutions and freeze-dried solids. International Journal of Pharmaceutics, 273, 85-93.

Izutsu, K., Aoyagi, N., Kojima, S. (2005) Effect of polymer size and cosolutes on phase separation of poly(vinylpyrrolidone) (PVP) and dextran in frozen solutions. Journal of Pharmaceutical Sciences, 94, 709-717.

Izutsu, K., Kadoya, S., Yomota, C., Kawanishi, T., Yonemochi, E., Terada, K. (2009) Stabilization of protein structure in freeze-dried amorphous organic acid buffer salts. Chemical and Pharmaceutical Bulletin, 57, 1231-1236.

Jaenicke, R. (1990) Protein structure and function at low temperatures. Philosophical Transactions of the Royal Society of London. Series B, Biological Sciences, 326, 535-551; discussion 551-553.

Jereczek-Fossa, B.A., Zarowski, A., Milani, F., Orecchia, R. (2003) Radiotherapy-induced ear toxicity. Cancer Treatment Reviews, 29, 417-430.

Juhn, S. (1988) Barrier systems in the inner ear, Acta Otolaryngologica Supplement, 458, 79-83.

Juhn, S., Rybak, L. (1981) Labyrinthine barriers and cochlear homeostasis, Acta Otolaryngologica, 91, 529–534.

Jung, Y.J., Lee, J.S., Kim, Y.M. (2000) Synthesis and *in vitro*/*in vivo* evaluation of 5-aminosalicyl-glycine as a colon-specific prodrug of 5-aminosalicylic acid. Journal of Pharmaceutical Sciences, 89, 594-602.

Kadoya, S., Fujii, K., Izutsu, K., Yonemochi, E., Terada, K., Yomota, C., Kawanishi, T. (2010) Freeze-drying of proteins with glass-forming oligosaccharide-derived sugar alcohols. International Journal of Pharmaceutics, 389, 107-113.

Kaewvichit, S., Tucker, I.G. (1994) The release of macromolecules from fatty acid matrices: complete factorial study of factors affecting release. The Journal of Pharmacy and Pharmacology, 46, 708-713.

Kang, J., Schwendeman, S.P. (2002) Comparison of the effects of $Mg(OH)_2$ and sucrose on the stability of bovine serum albumin encapsulated in injectable poly(D,L-lactide-co-glycolide) implants. Biomaterials, 23, 239-245.

Kang, J., Lambert, O., Ausborn, M., Schwendeman, S.P. (2008) Stability of proteins encapsulated in injectable and biodegradable poly(lactide-co-glycolide)-glucose millicylinders. International Journal of Pharmaceutics, 357, 235-243.

Karrout, Y., Neut, C., Wils, D., Siepmann, F., Deremaux, L., Desreumaux, P., Siepmann, J. (2009a) Novel polymeric film coatings for colon targeting: How to adjust desired membrane properties. International Journal of Pharmaceutics, 371, 64-70.

Karrout, Y., Neut, C., Wils, D., Siepmann, F., Deremaux, L., Flament, M., Dubreuil, L., Desreumaux, P., Siepmann, J., (2009b) Novel polymeric film coatings for colon

targeting: Drug release from coated pellets. European Journal of Pharmaceutical Sciences, 37, 427-433.

Karrout, Y., Neut, C., Wils, D., Siepmann, F., Deremaux, L., Dubreuil, L., Desreumaux, P., Siepmann, J., (2009c) Colon targeting with bacteria-sensitive films adapted to the disease state. European Journal of Pharmaceutics and Biopharmaceutics, 73, 74-81.

Kasper, J.C., Friess, W. (2011) The freezing step in lyophilization: Physico-chemical fundamentals, freezing methods and consequences on process performance and quality attributes of biopharmaceuticals. European Journal of Pharmaceutics and Biopharmaceutics, 78, 248-263.

Kellens, M., Meeussen, W., Gehrke, R., Reynaers, H. (1991) Synchrotron radiation investigations of the polymorphic transitions of saturated monoacid triglycerides. Part 1: Tripalmitin and tristearin. Chemistry and Physics of Lipids, 58, 131-144.

Kellow, J. E., Borody, T. J., Phillips, S. F., Tucker, R L., Haddad, A. C. (1986) Human interdigestive motility: Variations in patterns from esophagus to colon. Gastroenterology 91, 386-395.

Kenyon, C.J., Nardi, R.V., Wong, D., Hooper, G., Wilding, I.R., Friend, D.R. (1997) Colonic delivery of dexamethasone: A pharmacoscintigraphic evaluation. Alimentary Pharmacology & Therapeutics, 11, 205-213.

Kerlin, P., Phillips, S. (1982) Variability of motility of the ileum and jejunum in healthy humans. Gastroenterology, 82, 694-700.

Khan, M. Z. I., Prebeg, Z., Kurjakovic, N. (1999) A pH-dependent colon targeted oral drug delivery system using methacrylic acid copolymers: I. Manipulation of drug release using Eudragit® L100-55 and Eudragit® S100 combinations. Journal of Controlled Release, 58, 215-222.

Killen, B.U., Corrigan, O.I. (2006) Effect of soluble filler on drug release from stearic acid based compacts. International Journal of Pharmaceutics, 316, 47-51.

Kim, H., Kim, D., Choi, D., Jeon, H., Han, J., Jung, Y., Kong, H., Kim, Y.M. (2008) Synthesis and properties of N,N′-bis(5-aminosalicyl)-L-cystine as a colon-specific deliverer of 5-aminosalicylic acid and cystine. Drug Delivery, 15, 37-42.

Klose, D., Laprais, M., Leroux, V., Siepmann, F., Deprez, B., Bordet, R., Siepmann, J. (2009) Fenofibrate-loaded PLGA microparticles: Effects on ischemic stroke. European Journal of Pharmaceutical Sciences, 37, 43-52.

Klose, D., Siepmann, F., Elkharraz, K., Krenzlin, S., Siepmann, J. (2006) How porosity and size affect the drug release mechanisms from PLGA-based microparticles. International Journal of Pharmaceutics 314, 198-206.

König, D. (2004) Natrium-Carboxymethylstärke und Konjac-Glucomannan als abbaubare Hilfsstoffe für das Colon-Targeting. Inaugeral Dissertation, Albert-Ludwigs-Universität Freiburg, Germany.

Koennings, S., Garcion, E., Faisant, N., Menei, P., Benoit, J.P., Goepferich, A. (2006) *In vitro* investigation of lipid implants as a controlled release system for interleukin-18. International Journal of Pharmaceutics, 314, 145-152.

Koennings, S., Sapin, A., Blunk, T., Menei, P., Goepferich, A. (2007a) Towards controlled release of BDNF -- Manufacturing strategies for protein-loaded lipid implants and biocompatibility evaluation in the brain. Journal of Controlled Release, 119, 163-172.

Koennings, S., Tessmar, J., Blunk, T., Göpferich, A. (2007b) Confocal microscopy for the elucidation of mass transport mechanisms involved in protein release from lipid-based matrices. Pharmaceutical Research, 24, 1325-1335.

Koppenol, S. (2007) Physical considerations in protein and peptide stability. Freeze-Drying/Lyophilization of Pharmaceutical and Biological Products. pp. 43-72. Informa Healthcare, New York, NY.

Kreilgaard, L., Frokjaer, S., Flink, J.M., Randolph, T.W., Carpenter, J.F. (1998) Effects of additives on the stability of recombinant human factor XIII during freeze-drying and storage in the dried solid, Archives of Biochemistry and Biophysics, 360, 121-134.

Kretlow, J.D., Klouda, L., Mikos, A.G., (2007) Injectable matrices and scaffolds for drug delivery in tissue engineering. Advanced Drug Delivery Reviews, 59, 263-273.

Kreye, F., Siepmann, F., Siepmann, J. (2008) Lipid implants as drug delivery systems. Expert Opinion on Drug Delivery, 5, 291-307.

Kreye, F., Siepmann, F., Siepmann, J. (2011a). Drug release mechanisms of compressed lipid implants. International Journal of Pharmaceutics, 404, 27-35.

Kreye, F., Siepmann, F., Willart, J.F., Descamps, M., Siepmann, J. (2011b) Drug release mechanisms of cast lipid implants. European Journal of Pharmaceutics and Biopharmaceutics, 78, 394-400.

Krishnaiah, Y.S., Satyanarayana, S., Rama Prasad, Y.V., Narasimha Rao, S. (1998) Gamma scintigraphic studies on guar gum matrix tablets for colonic drug delivery in healthy human volunteers. Journal of Controlled Release, 55, 245-252.

Krishnaiah, Y.S., Satyanarayana, S., Prasad, Y.V. (1999) Studies of guar gum compression-coated 5-aminosalicylic acid tablets for colon-specific drug delivery. Drug Development and Industrial Pharmacy, 25, 651-657.

Krishnaiah, Y.S.R., Veer Raju, P., Dinesh Kumar, B., Bhaskar, P., Satyanarayana, V. (2001) Development of colon targeted drug delivery systems for mebendazole. Journal of Controlled Release, 77, 87–95.

Krishnaiah, Y.S.R., Satyanarayana, V., Dinesh Kumar, B., Karthikeyan, R.S. (2002) *In vitro* drug release studies on guar gum-based colon targeted oral drug delivery systems of 5-fluorouracil. European Journal of Pharmaceutical Sciences, 16, 185-192.

Krishnaiah, Y.S.R., Veer Raju, P., Dinesh Kumar, B., Satyanarayana, V., Karthikeyan, R.S., Bhaskar, P. (2003a) Pharmacokinetic evaluation of guar gum-based colon-targeted drug delivery systems of mebendazole in healthy volunteers. Journal of Controlled Release, 88, 95-103.

Krishnaiah, Y.S.R., Satyanarayana, V., Dinesh Kumar, B., Karthikeyan, R.S., Bhaskar, P. (2003b) *In vivo* pharmacokinetics in human volunteers: Oral administered guar gum-based colon-targeted 5-fluorouracil tablets. European Journal of Pharmaceutical Sciences, 19, 355-362.

Lagarce, F., Faisant, N., Desfontis, J., Marescaux, L., Gautier, F., Richard, J., Menei, P., Benoit, J. (2005) Baclofen-loaded microspheres in gel suspensions for intrathecal drug delivery: *In vitro* and *in vivo* evaluation. European Journal of Pharmaceutics and Biopharmaceutics, 61, 171-180.

Lecomte, F., Siepmann, J., Walther, M., MacRae, R.J., Bodmeier, R. (2003) Blends of enteric and GIT-insoluble polymers used for film coating: physicochemical characterization and drug release patterns. Journal of Controlled Release, 89, 457-471.

Lecomte, F., Siepmann, J., Walther, M., MacRae, R.J., Bodmeier, R. (2004) Polymer blends used for the aqueous coating of solid dosage forms: importance of the type of plasticizer. Journal of Controlled Release, 99, 1-13.

Lee, C.-H., Bhatt, P.P., Chien, Y.W. (1997) Effect of excipient on drug release and permeation from silicone-based barrier devices. Journal of Controlled Release, 43, 283-290.

Lee, C.L., Johannson, O.K. (1969) Selective polymerization of reactive cyclosiloxanes to give non-equilibrium molecular weight distributions. Monodisperse siloxane polymers. Polymer Preprints, 10, 1361-1367.

Lee, H.Y., Kim, S.K., Kim, J.S., Jung, Y.H., Kim, J.I., Seo, Y.M., Lee, J.S., Seol, E.Y., Chang, S.G., Choi, H.I. (2005) Protein-containing lipid implant for sustained delivery and its preparation method. WO2005102284.

Lee, S.-H., Shin, H. (2007) Matrices and scaffolds for delivery of bioactive molecules in bone and cartilage tissue engineering. Advanced Drug Delivery Reviews, 59, 339-359.

Leong, K.W., Langer, R. (1988) Polymeric controlled drug delivery. Advanced Drug Delivery Reviews, 1, 199-233.

Lerbret, A., Bordat, P., Affouard, F., Guinet, Y., Hédoux, A., Paccou, L., Prévost, D., Descamps, M. (2005a) Influence of homologous disaccharides on the hydrogen-bond network of water: Complementary Raman scattering experiments and molecular dynamics simulations. Carbohydrate Research, 340, 881-887.

Lerbret, A., Bordat, P., Affouard, F., Descamps, M., Migliardo, F. (2005b) How homogeneous are the trehalose, maltose, and sucrose water solutions? An insight from molecular dynamics simulations. The Journal of Physical Chemistry. B, 109, 11046-11057.

Lerbret, A., Bordat, P., Affouard, F., Hédoux, A., Guinet, Y., Descamps, M. (2007) How do trehalose, maltose, and sucrose influence some structural and dynamical properties of lysozyme? Insight from molecular dynamics simulations. The Journal of Physical Chemistry. B, 111, 9410-9420.

Li, C., Cheng, L., Zhang, Y., Guo, S., Wu, W. (2010) Effects of implant diameter, drug loading and end-capping on praziquantel release from PCL implants. International Journal of Pharmaceutics, 386, 23-29.

Lin, S.Y. and Ayres, J.W. (1992) Calcium alginate beads as core carriers of 5-aminosalicylic acid. Pharmaceutical Research, 9, 1128-1131.

Lin, T., Timasheff, S.N. (1996) On the role of surface tension in the stabilization of globular proteins. Protein Science, 5, 372-381.

Linskens, R.K., Huijsdens, X.W., Savelkoul, P.H., Vandenbroucke-Grauls, C.M., Meuwissen, S.G. (2001) The bacterial flora in inflammatory bowel disease: current insights in pathogenesis and the influence of antibiotics and probiotics. Scandinavian Journal of Gastroenterology. Supplement, 234, 29-40.

Liu, W., Wang, D.Q., Nail, S.L. (2005) Freeze-drying of proteins from a sucrose-glycine excipient system: effect of formulation composition on the initial recovery of protein activity. AAPS PharmSciTech, 6, E150-157.

Lloyd, A.W. (2002) Interfacial bioengineering to enhance surface biocompatibility. Medical Device Technology, 13, 18-21.

Lorenzo-Lamosa, M.L., Remunan-Lopez, C., Vila-Jato, J.L., Alonso, M.J. (1998) Design of microencapsulated chitosan microspheres for colonic drug delivery. Journal of Controlled Release, 52, 109-118.

Lu, Y., Kim, S., Park, K. *In vitro-in vivo* correlation: Perspectives on model development. International Journal of Pharmaceutics, 418, 142-148.

Luginbuehl, V., Meinel, L., Merkle, H.P., Gander, B., (2004) Localized delivery of growth factors for bone repair. European Journal of Pharmaceutics and Biopharmaceutics, 58, 197-208.

Luthra, S., Obert, J.-P., Kalonia, D.S., Pikal, M.J. (2007a) Investigation of drying stresses on proteins during lyophilization: Differentiation between primary and secondary-drying stresses on lactate dehydrogenase using a humidity controlled mini freeze-dryer. Journal of Pharmaceutical Sciences, 96, 61-70.

Luthra, S., Obert, J.-P., Kalonia, D.S., Pikal, M.J. (2007b) Impact of critical process and formulation parameters affecting in-process stability of lactate dehydrogenase during the secondary drying stage of lyophilization: A mini freeze dryer study. Journal of Pharmaceutical Sciences, 96, 2242-2250.

Macleod, G.S., Fell, J.T., Collett, J.H. (1999) An *in vitro* investigation into the potential for bimodal drug release from pectin/chitosan/HPMC-coated tablets. International Journal of Pharmaceutics, 188, 11-18.

Macleod, G.S., Fell, J.T., Collett, J.H., Sharma, H.L., Smith, A. (1999) Selective drug delivery to the colon using pectin:chitosan:hydroxypropyl methylcellulose film coated tablets. International Journal of Pharmaceutics, 187, 251-257.

Magazù, S., Migliardo, F., Mondelli, C., Vadalà, M. (2005a) Correlation between bioprotective effectiveness and dynamic properties of trehalose-water, maltose-water and sucrose-water mixtures. Carbohydrate Research, 340, 2796-2801.

Magazù, S., Migliardo, F., Ramirez-Cuesta, A.J. (2005b) Inelastic neutron scattering study on bioprotectant systems. Journal of The Royal Society Interface, 2, 527-532.

Magazù, S., Migliardo, F., Telling, M.T.F. (2006) Alpha,alpha-trehalose-water solutions. VIII. Study of the diffusive dynamics of water by high-resolution quasi elastic neutron scattering. The Journal of Physical Chemistry. B, 110, 1020-1025.

Makhatadze, G.I., Privalov, P.L. (1992) Protein interactions with urea and guanidinium chloride. A calorimetric study. Journal of Molecular Biology, 226, 491-505.

Malaterre, V., Ogorka, J., Loggia, N., Gurny, R. (2009) Oral osmotically driven systems: 30 years of development and clinical use. European Journal of Pharmaceutics and Biopharmaceutics, 73, 311-323.

Malcolm, R.K., McCullagh, S., David Woolfson, A., Catney, M., Tallon, P. (2002) A dynamic mechanical method for determining the silicone elastomer solubility of drugs and pharmaceutical excipients in silicone intravaginal drug delivery rings. Biomaterials, 23, 3589-3594.

Malcolm, K., Woolfson, D., Russell, J., Tallon, P., McAuley, L., Craig, D. (2003) Influence of silicone elastomer solubility and diffusivity on the *in vitro* release of drugs from intravaginal rings. Journal of Controlled Release, 90, 217-225.

Maschke, A., Becker, C., Eyrich, D., Kiermaier, J., Blunk, T., Göpferich, A. (2007) Development of a spray congealing process for the preparation of insulin-loaded lipid microparticles and characterization thereof. European Journal of Pharmaceutics and Biopharmaceutics, 65, 175-187.

Mason, P.E., Neilson, G.W., Enderby, J.E., Saboungi, M.-L., Dempsey, C.E., MacKerell, A.D., Jr, Brady, J.W. (2004) The structure of aqueous guanidinium chloride solutions. Journal of the American Chemical Society, 126, 11462-11470.

Mason, P.E., Brady, J.W., Neilson, G.W., Dempsey, C.E. (2007) The interaction of guanidinium ions with a model peptide. Biophysical Journal, 93, L04-06.

Mathes, J., Friess, W. (2011) Influence of pH and ionic strength on IgG adsorption to vials. European Journal of Pharmaceutics and Biopharmaceutics, 78, 239-247.

Matthews, B.W. (1993) Structural and genetic analysis of protein stability. Annual Review of Biochemistry, 62, 139-160.

McConnell, E.L., Short, M.D., Basit, A.W. (2008a) An *in vivo* comparison of intestinal pH and bacteria as physiological trigger mechanisms for colonic targeting in man. Journal of Controlled Release, 130, 154-160.

McConnell, E.L., Fadda, H.M., Basit, A.W. (2008b) Gut instincts: explorations in intestinal physiology and drug delivery. International journal of pharmaceutics, 364, 213–226.

Mehta, A.M. (1997) Processing and equipment considerations for aqueous coatings. Aqueous polymeric coatings for pharmaceutical dosage forms. 2nd Edition, pp. 287-326, Marcel Dekker, New York, NY.

Mikulec, A.A., Hartsock, J.J., Salt, A.N. (2008) Permeability of the Round Window Membrane is Influenced by the Composition of Applied Drug Solutions and by Common Surgical Procedures. Otology & Neurotology, 29, 1020-1026.

Mills, D.J.S., Tuohy, K.M., Booth, J., Buck, M., Crabbe, M.J.C., Gibson, G.R, Ames, J.M. (2008) Dietary glycated protein modulates the colonic microbiota towards a more detrimental composition in ulcerative colitis patients and non-ulcerative colitis subjects. Journal of Applied Microbiology, 105, 706-714.

Milojevic, S., Newton, J.M., Cummings, J.H., Gibson, G.R., Louise Botham, R., Ring, S.G., Stockham, M., Allwood, M.C. (1996a) Amylose as a coating for drug delivery to the colon: Preparation and *in vitro* evaluation using 5-aminosalicylic acid pellets. Journal of Controlled Release, 38, 75-84.

Milojevic, S., Newton, J.M., Cummings, J.H., Gibson, G.R., Louise Botham, R., Ring, S.G., Stockham, M., Allwood, M.C. (1996b) Amylose as a coating for drug delivery to the colon: Preparation and *in vitro* evaluation using glucose pellets. Journal of Controlled Release, 38, 85-94.

Moebus, K., Siepmann, J., Bodmeier, R. (2009) Alginate-poloxamer microparticles for controlled drug delivery to mucosal tissue. European Journal of Pharmaceutics and Biopharmaceutics, 72, 42-53.

Mohl, S., Winter, G. (2004) Continuous release of rh-interferon [alpha]-2a from triglyceride matrices. Journal of Controlled Release, 97, 67-78.

Mohl, S., Winter, G. (2006) Continuous release of rh-interferon α-2a from triglyceride implants: Storage stability of the dosage forms. Pharmaceutical Development and Technology, 11, 103-110.

Moreira, T., Pendas, J., Gutierrez, A., Pomes, R., Duque, J., Franks, F. (1998) Effect of sucrose and raffinose on physical state and on lactate dehydrogenase activity of freeze-dried formulations. CryoLetters, 19, 115-122.

Müller, R.H., Lucks, S.J. (1993). Arzneistoffträger aus festen Lipidteilchen, Feste Lipidnanosphären (SLN), Medication vehicles made of solid lipid particles (solid lipid nanospheres – SLN). European Patent 0605497.

Mundargi, R.C., Patil, S.A., Agnihotri, S.A., Aminabhavi, T.M. (2007) Development of polysaccharide-based colon targeted drug delivery systems for the treatment of amoebiasis. Drug Development and Industrial Pharmacy, 33, 255-264.

Munjeri, O., Collett, J., Fell, J. (1997) Hydrogel beads based on amidated pectins for colon-specific drug delivery: The role of chitosan in modifying drug release. Journal of Controlled Release, 46, 273-278.

Munkholm, P., Langholz, E., Davidsen, M., Binder, V. (1993) Intestinal cancer risk and mortality in patients with Crohn's disease. Gastroenterology, 105, 1716-1723.

Muraoka, M., Hu, Z., Shimokawa, T., Sekino, S., Kurogoshi, R., Kuboi, Y., Yoshikawa, Y., Takada, K. (1998) Evaluation of intestinal pressure-controlled colon delivery capsule containing caffeine as a model drug in human volunteers. Journal of Controlled Release, 52, 119-129.

Muschert, S., Siepmann, F., Leclercq, B., Carlin, B., Siepmann, J. (2009) Drug release mechanisms from ethylcellulose: PVA-PEG graft copolymer-coated pellets. European Journal of Pharmaceutics and Biopharmaceutics, 72, 130-137.

Nail, S.L., Jiang, S., Chongprasert, S., Knopp, S.A. (2002) Fundamentals of freeze-drying. Pharmaceutical Biotechnology, 14, 281-360.

Nair, L.S., Laurencin, C.T. (August) Biodegradable polymers as biomaterials. Progress in Polymer Science, 32, 762-798.

Nakayama, T. (1998) Low-energy excitations in water: A simple-model analysis. Physical Review Letters, 80, 1244-1247.

Nema, S., Avis, K.E. (1993) Freeze-thaw studies of a model protein, lactate dehydrogenase, in the presence of cryoprotectants. Journal of Parenteral Science and Technology, 47, 76-83.

Newton, J.M. (2010) Gastric emptying of multi-particulate dosage forms. International Journal of Pharmaceutics, 395, 2-8.

Nolen, H., Fedorak, R.N., Friend, D.R. (1995) Budesonide-beta-D-glucuronide: A potential prodrug for treatment of ulcerative colitis. Journal of Pharmaceutical Sciences, 84, 677-681.

Nordang, L., Linder, B., Anniko, M. (2003) Morphologic changes in round window membrane after topical hydrocortisone and dexamethasone treatment. Otology & Neurotology, 24, 339.

Novikov, V.N., Duval, E., Kisliuk, A., Sokolov, A.P. (1995) A model of low-frequency Raman scattering in glasses: Comparison of Brillouin and Raman data. The Journal of Chemical Physics, 102, 4691-4699.

Nugent, S., Kumar, D., Rampton, D., Evans, D. (2001) Intestinal luminal pH in inflammatory bowel disease: Possible determinants and implications for therapy with aminosalicylates and other drugs. Gut, 48, 571-577.

Nykänen, P. (2003) Development of multiple-unit oral formulations for colon-specific drug delivery using enteric polymers and organic acids as excipients. Academic Dissertation, Yliopistopaino, Helsinki, Finland.

Ohyama, K., Salt, A.N., Thalmann, R. (1988) Volume flow rate of perilymph in the guinea-pig cochlea. Hearing Research, 35, 119-129.

Okarter, T.U., Singla, K. (2000) The effects of plasticizers on the release of metoprolol tartrate from granules coated with a polymethacrylate film. Drug Development and Industrial Pharmacy, 26, 323-329.

Olsson, C., Holmgren, S. (2001) The control of gut motility. Comparative Biochemistry and Physiology - Part A: Molecular & Integrative Physiology, 128, 479-501.

Ormiston, J.A., Serruys, P.W. (2009). Bioabsorbable Coronary Stents. Circulation: Cardiovascular Interventions 2, 255-260.

Paasche, G., Gibson, P., Averbeck, T., Becker, H., Lenarz, T., Stöver, T. (2003) Technical report: Modification of a cochlear implant electrode for drug delivery to the inner ear. Otology & Neurotology, 24, 222-227.

Paasche, G., Tasche, C., Stöver, T., Lesinski-Schiedat, A., Lenarz, T. (2009) The long-term effects of modified electrode surfaces and intracochlear corticosteroids on postoperative impedances in cochlear implant patients. Otology & Neurotology, 30, 592-598.

Packhaeuser, C.B., Schnieders, J., Oster, C.G., Kissel, T. (2004) *In situ* forming parenteral drug delivery systems: An overview. European Journal of Pharmaceutics and Biopharmaceutics, 58, 445-455.

Padilla, A.M., Ivanisevic, I., Yang, Y., Engers, D., Bogner, R.H., Pikal, M.J. (2011) The study of phase separation in amorphous freeze-dried systems. Part I: Raman mapping and computational analysis of XRPD data in model polymer systems. Journal of Pharmaceutical Sciences, 100, 206-222.

Pasman, W., Wils, D., Saniez, M.H., Kardinaal, A. (2006) Long-term gastrointestinal tolerance of Nutriose® FB in healthy men. European Journal of Clinical Nutrition, 60, 1024-34.

Padró, J.A., Martí, J. (2003) An interpretation of the low-frequency spectrum of liquid water. The Journal of Chemical Physics, 118, 452-454.

6 References

Patro, S.Y., Przybycien, T.M. (1994) Simulations of kinetically irreversible protein aggregate structure. Biophysical Journal, 66, 1274-1289.

Patro, S.Y., Przybycien, T.M. (1996) Simulations of reversible protein aggregate and crystal structure. Biophysical Journal, 70, 2888-2902.

Pawar, V.K., Kansal, S., Garg, G., Awasthi, R., Singodia, D., Kulkarni, G.T. (2011) Gastroretentive dosage forms: A review with special emphasis on floating drug delivery systems. Drug Delivery, 18, 97-110.

Pikal, M.J. (2007) Mechanisms of protein stabilization during freeze-drying and storage: The relative importance of thermodynamic stabilization and glassy state realxation dynamics. Freeze-Drying/Lyophilization of Pharmaceutical and Biological Products, pp. 63-107. Informa Healthcare, New York, NY.

Pikal, M.J., Shah, S. (1997) Intravial distribution of moisture during the secondary drying stage of freeze drying. Journal of Pharmaceutical Science and Technology / PDA, 51, 17-24.

Pikal-Cleland, K.A., Carpenter, J.F. (2001) Lyophilization-induced protein denaturation in phosphate buffer systems: monomeric and tetrameric beta-galactosidase. Journal of Pharmaceutical Sciences, 90, 1255-1268.

Pikal-Cleland, K.A., Cleland, J.L., Anchordoquy, T.J., Carpenter, J.F. (2002) Effect of glycine on pH changes and protein stability during freeze–thawing in phosphate buffer systems. Journal of Pharmaceutical Sciences, 91, 1969-1979.

Pike, A.C., Acharya, K.R. (1994) A structural basis for the interaction of urea with lysozyme. Protein Science: A Publication of the Protein Society, 3, 706-710.

Pillai, O., Dhanikula, A.B., Panchagnula, R. (2001) Drug delivery: an odyssey of 100 years. Current Opinion in Chemical Biology, 5, 439-446.

Plontke, S.K., Salt, A.N. (2003) Quantitative interpretation of corticosteroid pharmacokinetics in inner fluids using computer simulations. Hearing Research, 182, 34–42.

Plontke, S.K., Biegner, T., Kammerer, B., Delabar, U., Salt, A.N. (2008) Dexamethasone concentration gradients along scala tympani after application to the round window membrane. Otology and Neurotology, 29, 401-406.

Plontke, S.K., Mynatt, R., Gill, R.M., Borgmann, S., Salt, A.N. (2007) Concentration Gradient Along the Scala Tympani After Local Application of Gentamicin to the Round Window Membrane. The Laryngoscope, 117, 1191-1198.

Plontke, S.K., Siedow, N., Wegener, R., Zenner, H.-P., Salt, A.N. (2007) Cochlear pharmacokinetics with local inner ear drug delivery using a three-dimensional finite-element computer model. Audiology & Neurotology, 12, 37-48.

Plontke, S.K., Siedow, N., Hahn, H., Wegener. R., Zenner, H.P, Salt, A.N. (2004) 1D and 3D computer simulation for planning and interpretation of pharmacokinetic studies in the inner ear after round window drug delivery, ALTEX 21 Suppl. 3, 77-85.

Pongjanyakul, T., Medlicott, N.J., Tucker, I.G. (2004) Melted glyceryl palmitostearate (GPS) pellets for protein delivery. International Journal of Pharmaceutics, 271, 53-62.

Pozzi, F., Furlani, P., Gazzaniga, A., Davis, S., Wilding, I. (1994) The time clock system: A new oral dosage form for fast and complete release of drug after a predetermined lag time. Journal of Controlled Release, 31, 99-108.

Press, A.G., Hauptmann, I.A., Hauptmann, L., Fuchs, B., Fuchs, M., Ewe, K., Ramadori, G. (1998) Gastrointestinal pH profiles in patients with inflammatory bowel disease. Alimentary Pharmacology & Therapeutics, 12, 673-678.

Prestrelski, S.J., Arakawa, T., Carpenter, J.F. (1993a) Separation of freezing- and drying-induced denaturation of lyophilized proteins using stress-specific stabilization : II. Structural studies using infrared spectroscopy. Archives of Biochemistry and Biophysics, 303, 465-473.

Prestrelski, S.J., Tedeschi, N., Arakawa, T., Carpenter, J.F. (1993b) Dehydration-induced conformational transitions in proteins and their inhibition by stabilizers. Biophysical Journal, 65, 661-671.

Privalov, P.L. (1990) Cold denaturation of proteins. Critical Reviews in Biochemistry and Molecular Biology, 25, 281-305.

Qasim, A., Seery, J., O'Morain, C.A. (2001) 5-Aminosalicylates in inflammatory bowel disease: Choosing the right dose. Digestive and Liver Disease, 33, 393-398.

Querol, E., Perez-Pons, J.A., Mozo-Villarias, A. (1996) Analysis of protein conformational characteristics related to thermostability. Protein Engineering, 9, 265-271.

Rama Prasad, Y.V.R., Krishnaiah, Y.S.R., Satyanarayana, S. (1998) *In vitro* evaluation of guar gum as a carrier for colon-specific drug delivery. Journal of Controlled Release, 51, 281-287.

Ramos, A., Raven, N., Sharp, R., Bartolucci, S., Rossi, M., Cannio, R., Lebbink, J., Van Der Oost, J., De Vos, W., Santos, H. (1997) Stabilization of enzymes against thermal stress

and freeze-drying by mannosylglycerate. Applied Environmental Microbiology, 63, 4020-4025.

Rao, S.S., Sadeghi, P., Beaty, J., Kavlock, R., Ackerson, K. (2001) Ambulatory 24-h colonic manometry in healthy humans. American Journal of Physiology. Gastrointestinal and Liver Physiology, 280, G629-639.

Rao, K.A., Yazaki, E., Evans, D.F., Carbon, R. (2004) Objective evaluation of small bowel and colonic transit time using pH telemetry in athletes with gastrointestinal symptoms. British Journal of Sports Medicine, 38, 482-487.

Reithmeier, H., Herrmann, J., Göpferich, A. (2001) Lipid microparticles as a parenteral controlled release device for peptides. Journal of Controlled Release, 73, 339-350.

Rey, L. (2007) Glimpses into the realm of freeze-drying: Fundamental issues. Freeze-Drying/Lyophilization of Pharmaceutical and Biological Products, pp. 1-32. Informa Healthcare, New York, NY.

Ribeiro Dos Santos, I., Richard, J., Pech, B., Thies, C., Benoit, J.P. (2002) Microencapsulation of protein particles within lipids using a novel supercritical fluid process. International Journal of Pharmaceutics, 242, 69-78.

Richardson, R.T., Wise, A.K., Thompson, B.C., Flynn, B.O., Atkinson, P.J., Fretwell, N.J., Fallon, J.B., Wallace, G.G., Shepherd, R.K., Clark, G.M., O'Leary, S.J. (2009) Polypyrrole-coated electrodes for the delivery of charge and neurotrophins to cochlear neurons. Biomaterials, 30, 2614-2624.

Rowe, R.C. (1997) Defects in aqueous film-coated tablets. Aqueous polymeric coatings for pharmaceutical dosage forms. 2nd Edition, pp. 419-440, Marcel Dekker, New York, NY.

Rubinstein, A., Gliko-Kabir, I. (1995) Synthesis and swelling-dependent enzymatic degradation of borax-modified guar gum for colonic delivery purposes. STP Pharma Science, 5, 41-46.

Rubinstein, A., Radai, R. (1995) In vitro and in vivo analysis of colon specificity of calcium pectinate formulations. European Journal of Pharmaceutics and Biopharmaceutics, 41, 291-295.

Rubinstein, A., Nakar, D., Sintov, A. (1992a) Colonic drug delivery: Enhanced release of indomethacin from cross-linked chondroitin matrix in rat cecal content. Pharmaceutical Research, 9, 276-278.

Rubinstein, A., Nakar, D., Sintov, A. (1992b) Chondroitin sulfate: A potential biodegradable carrier for colon-specific drug delivery. International Journal of Pharmaceutics, 84, 141-150.

Rubinstein, A., Radai, R., Ezra, M., Pathak, S., Rokem, J.S. (1993) *In vitro* evaluation of calcium pectinate: A potential colon-specific drug delivery carrier. Pharmaceutical Research, 10, 258-263.

Ruddon, R.W., Bedows, E. (1997) Assisted protein folding. The Journal of Biological Chemistry, 272, 3125-3128.

Rupley, J.A., Careri, G. (1991) Protein hydration and function. Advances in Protein Chemistry, 41, 37-172.

Salt, A.N., Plontke, S.K. (2009) Principles of Local Drug Delivery to the Inner Ear. , Audiology & Neurootology14, 350-360.

Salt, A.N., Plontke, S.K. (2005) Local inner-ear drug delivery and pharmacokinetics. Drug Discovery Today 10, 1299–1306.

Salt, A.N., Sirjani, D.B., Hartsock, J.J., Gill, R.M., Plontke, S.K. (2007) Marker retention in the cochlea following injections through the round window membrane. Hearing Research, 232, 78-86.

Salyers, A.A., Vercellotti, J.R., West, S.E., Wilkins, T.D. (1977) Fermentation of mucin and plant polysaccharides by strains of Bacteroides from the human colon. Applied and Environmental Microbiology, 33, 319-322.

Sane, S.U., Wong, R., Hsu, C.C. (2004) Raman spectroscopic characterization of drying-induced structural changes in a therapeutic antibody: Correlating structural changes with long-term stability. Journal of Pharmaceutical Sciences, 93, 1005-1018.

Sarciaux, J., Mansour, S., Hageman, M.J., Nail, S.L. (1999) Effects of buffer composition and processing conditions on aggregation of bovine IgG during freeze-drying. Journal of Pharmaceutical Sciences, 88, 1354-1361.

Saviot, L., Duval, E., Surovtsev, N., Jal, J.F., Dianoux, A.J. (1999) Propagating to nonpropagating vibrational modes in amorphous polycarbonate. Physical Review B, 60, 18-21.

Scharnagl, C., Reif, M., Friedrich, J. (2005) Stability of proteins: Temperature, pressure and the role of the solvent. Biochimica et Biophysica Acta (BBA) - Proteins & Proteomics, 1749, 187-213.

Schebor, C., Burin, L., Buera, M.P., Aguilera, J.M., Chirife, J. (1997) Glassy state and thermal inactivation of invertase and lactase in dried amorphous matrices. Biotechnology Progress, 13, 857-863.

Schulze, S., Winter, G. (2009) Lipid extrudates as novel sustained release systems for pharmaceutical proteins. Journal of Controlled Release, 134, 177-185.

Schwartz, H.E., May, T.C., Fromm, S., Enzerink, R., Hubbard, E., Margetts, J., Denlinger, K., Cox, D. (1999). Meniscal Repair Device. United States Patent 6306159

Schwendeman, S.P. (2002) Recent advances in the stabilization of proteins encapsulated in injectable PLGA delivery systems. Critical Reviews in Therapeutic Drug Carrier Systems, 19, 73-98.

Semdé, R., Amighi, K., Pierre, D., Devleeschouwer, M.J., Moës, A.J. (1998) Leaching of pectin from mixed pectin/insoluble polymer films intended for colonic drug delivery. International Journal of Pharmaceutics, 174, 233-241.

Semdé, R., Amighi, K., Devleeschouwer, M.J., Moës, A.J. (2000a) Effect of pectinolytic enzymes on the theophylline release from pellets coated with water insoluble polymers containing pectin HM or calcium pectinate. International Journal of Pharmaceutics, 197, 169-179.

Semdé, R., Amighi, K., Devleeschouwer, M.J., Moës, A.J. (2000b) Studies of pectin HM/Eudragit RL/Eudragit NE film-coating formulations intended for colonic drug delivery. International Journal of Pharmaceutics, 197, 181-192.

Seo, J.-A., Hédoux, A., Guinet, Y., Paccou, L., Affouard, F., Lerbret, A., Descamps, M. (2010) Thermal denaturation of beta-lactoglobulin and stabilization mechanism by trehalose analyzed from Raman spectroscopy investigations. The Journal of Physical Chemistry. B, 114, 6675-6684.

Siepmann, F., Siepmann, J., Walther, M., MacRae, R., Bodmeier, R. (2008a) Polymer blends for controlled release coatings. Journal of Controlled Release, 125, 1-15.

Siepmann, F., Herrmann, S., Winter, G., Siepmann, J. (2008b) A novel mathematical model quantifying drug release from lipid implants. Journal of Controlled Release, 128, 233-240.

Siepmann, F. Siepmann, J. (2011a) Mathematical modeling of drug release from lipid dosage forms. International Journal of Pharmaceutics, 418, 42-53.

Siepmann, J., Göpferich, A. (2001) Mathematical modeling of bioerodible, polymeric drug delivery systems. Advanced Drug Delivery Reviews, 48, 229-247.

Siepmann, J., Siepmann, F. (2008) Mathematical modeling of drug delivery. International Journal of Pharmaceutics, 364, 328-343.

Siepmann J., Siepmann, F. (2011b) Modeling of diffusion controlled drug delivery. Journal of Controlled Release, in press.

Siew, L.F., Basit, A.W., Newton, J.M. (2000a) The potential of organic-based amylase-ethylcellulose film coatings as oral colon-specific drug delivery systems. AAPS PharmSciTech, 1, 53–61.

Siew, L.F., Basit, A.W., Newton, J.M. (2000b) The properties of amylose-ethylcellulose films cast from organic-based solvents as potential coatings for colonic drug delivery. European Journal of Pharmaceutical Sciences, 11, 133-139.

Sill, T.J., von Recum, H.A. (2008) Electrospinning: Applications in drug delivery and tissue engineering. Biomaterials, 29, 1989-2006.

Simchi, A., Tamjid, E., Pishbin, F., Boccaccini, A.R. (2011) Recent progress in inorganic and composite coatings with bactericidal capability for orthopaedic applications. Nanomedicine: Nanotechnology, Biology, and Medicine, 7, 22-39.

Simon, G.L., Gorbach, S.L. (1984) Intestinal flora in health and disease. Gastroenterology, 86, 174-193.

Simonsen, L., Hovgaard, L., Mortensen, P.B., Brøndsted, H. (1995) Dextran hydrogels for colon-specific drug delivery. V. Degradation in human intestinal incubation models. European Journal of Pharmaceutical Sciences, 3, 329-337.

Singh, R., Lillard Jr., J.W. (2009) Nanoparticle-based targeted drug delivery. Experimental and Molecular Pathology, 86, 215-223.

Sinha, V.R., Kumria, R. (2003) Microbially triggered drug delivery to the colon. European Speed, M.A., King, J., Wang, D.I.C. (1997) Polymerization mechanism of polypeptide chain aggregation. Biotechnology and Bioengineering, 54, 333-343.

Speed, M.A., King, J., Wang, D.I.C. (1997) Polymerization mechanism of polypeptide chain aggregation. Biotechnology and Bioengineering, 54, 333-343.

Staecker, H., Jolly, C., Garnham, C. (2010). Cochlear implantation: An opportunity for drug development. Drug Discovery Today 15, 314–321.

Strickley, R.G., Anderson, B.D. (1997) Solid-state stability of human insulin. II. Effect of water on reactive intermediate partitioning in lyophiles from pH 2-5 solutions: Stabilization against covalent dimer formation. Journal of Pharmaceutical Sciences, 86, 645-653.

6 References

Surewicz, W.K., Mantsch, H.H., Chapman, D. (1993) Determination of protein secondary structure by Fourier transform infrared spectroscopy: A critical assessment. Biochemistry, 32, 389-394.

Suzuki, T., Imamura, K., Fujimoto, H., Okazaki, M. (1998) Relation between Thermal Stabilizing Effect of Sucrose on LDH and Sucrose-LDH Hydrogen Bond. Journal of Chemical Engineering of Japan, 31, 565-570.

Swan, E.E., Mescher, M.J., Sewell, W.F., Tao, S.L., Borenstein, J.T. (2008) Inner ear drug delivery for auditory applications. Advanced Drug Delivery Reviews, 60, 1583–1599.

Szabó, Z., Klement, E., Jost, K., Zarándi, M., Soós, K., Penke, B. (1999) An FT-IR study of the beta-amyloid conformation: Standardization of aggregation grade. Biochemical and Biophysical Research Communications, 265, 297-300.

Takaya, T., Ikeda, C., Imagawa, N., Niwa, K., Takada, K. (1995) Development of a colon delivery capsule and the pharmacological activity of recombinant human granulocyte colony-stimulating factor (rhG-CSF) in beagle dogs. The Journal of Pharmacy and Pharmacology, 47, 474-478.

Takaya, T., Sawada, K., Suzuki, H., Funaoka, A., Matsuda, K., Takada, K. (1997) Application of a colon delivery capsule to 5-aminosalicylic acid and evaluation of the pharmacokinetic profile after oral administration to beagle dogs. Journal of Drug Targeting, 4, 271-276.

Tanaka, K., Takeda, T., Miyajima, K. (1991) Cryoprotective effect of saccharides on denaturation of catalase by freezedrying. Chemical & Pharmaceutical Bulletin, 39, 1091-1094.

Tanford, C. (1970) Protein denaturation. C. Theoretical models for the mechanism of denaturation. Advances in Protein Chemistry, 24, 1-95.

Tanford, C., Aune, K.C. (1970) Thermodynamics of the denaturation of lysozyme by guanidine hydrochloride. 3. Dependence on temperature. Biochemistry, 9, 206-211.

Tang, X.C., Pikal, M.J. (2005a) The effect of stabilizers and denaturants on the cold denaturation temperatures of proteins and implications for freeze-drying. Pharmaceutical Research, 22, 1167-1175.

Tang, X.C., Pikal, M.J. (2005b) Measurement of the kinetics of protein unfolding in viscous systems and implications for protein stability in freeze-drying. Pharmaceutical Research, 22, 1176-1185.

Timasheff, S.N. (1993) The control of protein stability and association by weak interactions with water: how do solvents affect these processes? Annual Review of Biophysics and Biomolecular Structure, 22, 67-97.

Timasheff, S.N. (2002) Thermodynamic binding and site occupancy in the light of the Schellman exchange concept. Biophysical Chemistry, 101-102, 99-111.

Tozaki, H., Komoike, J., Tada, C., Maruyama, T., Terabe, A., Suzuki, T., Yamamoto, A., Muranishi, S. (1997) Chitosan capsules for colon-specific drug delivery: Improvement of insulin absorption from the rat colon. Journal of Pharmaceutical Sciences, 86, 1016-1021.

Tozaki, H., Fujita, T., Odoriba, T., Terabe, A., Suzuki, T., Tanaka, C., Okabe, S., Muranishi, S., Yamamoto, A. (1999) Colon-specific delivery of R68070, a new thromboxane synthase inhibitor, using chitosan capsules: therapeutic effects against 2,4,6-trinitrobenzene sulfonic acid-induced ulcerative colitis in rats. Life Sciences, 64, 1155-1162.

Tozaki, H., Odoriba, T., Okada, N., Fujita, T., Terabe, A., Suzuki, T., Okabe, S., Muranishi, S., Yamamoto, A. (2002) Chitosan capsules for colon-specific drug delivery: enhanced localization of 5-aminosalicylic acid in the large intestine accelerates healing of TNBS-induced colitis in rats. Journal of Controlled Release, 82, 51-61.

Tran, V., Benoît, J., Venier-Julienne, M. (2011) Why and how to prepare biodegradable, monodispersed, polymeric microparticles in the field of pharmacy? International Journal of Pharmaceutics, 407, 1-11.

Travis, S.P.L., Stange, E.F., Lémann, M., Øresland, T., Bemelman, W.A., Chowers, Y., Colombel, J.F, D'Haens, G., Ghosh, S., Marteau, P., Kruis, W., Mortensen, N.J., Penninckx, F., Gassull, M. (2008) European evidence-based Consensus on the management of ulcerative colitis: Current management. Journal of Crohn's and Colitis, 2, 24-62.

Ueda, S., Hata, T., Asakura, S., Yamaguchi, H., Kotani, M., Ueda, Y. (1994) Development of a novel drug release system, time-controlled explosion system (TES). I. Concept and design. Journal of Drug Targeting, 2, 35-44.

Ueda, S., Yamaguchi, H., Kotani, M., Kimura, S., Tokunaga, Y., Kagayama, A., Hata, T. (1994) Development of a novel drug release system, time-controlled explosion system (TES). II: Design of multiparticulate TES and *in vitro* drug release properties. Chemical and Pharmaceutical Bulletin, 42, 359-363.

van den Heuvel, E.G.H.M., Wils, D., Pasman, W.J., Bakker, M., Saniez, M.H., Kardinaal, A.F.M. (2004) Short-term digestive tolerance of different doses of Nutriose® FB, a food dextrin, in adult men. European Journal of Clinical Nutrition, 58, 1046-1055.

van den Heuvel, E.G.H.M., Wils, D., Pasman, W.J., Saniez, M.-H., Kardinaal, A.F.M. (2005) Dietary supplementation of different doses of Nutriose® FB, a fermentable dextrin, alters the activity of faecal enzymes in healthy men. European Journal of Nutrition, 44, 445-451.

Varum, F.J., Merchant, H.A., Basit, A.W. (2010) Oral modified-release formulations in motion: The relationship between gastrointestinal transit and drug absorption. International Journal of Pharmaceutics, 395, 26-36.

Vassallo, M., Camilleri, M., Phillips, S.F., Brown, M.L., Chapman, N.J., Thomforde, G.M. (1992) Transit through the proximal colon influences stool weight in the irritable bowel syndrome. Gastroenterology, 102, 102-108.

Vergnaud, J.M. (1993) Controlled Drug Release of Oral Dosage Forms, Ellis Horwood, Chichester, UK.

Vervoort, L., Kinget, R. (1996) In vitro degradation by colonic bacteria of inulin HP incorporated in Eudragit RS films. International Journal of Pharmaceutics, 129, 185-190.

Vervoort, L., Rombaut, P., Van den Mooter, G., Augustijns, P., Kinget, R. (1998) Inulin hydrogels. II. *In vitro* degradation study. International Journal of Pharmaceutics, 172, 137-145.

Vilivalam, V.D., Illum, L., Iqbal, K. (2000) Starch capsules: An alternative system for oral drug delivery. Pharmaceutical Science & Technology Today, 3, 64-69.

Vogelhuber, W., Magni, E., Gazzaniga, A., Göpferich, A. (2003) Monolithic glyceryl trimyristate matrices for parenteral drug release applications. European Journal of Pharmaceutics and Biopharmaceutics, 55, 133-138.

Vorhies, J.S., Nemunaitis, J.J. (2009) Synthetic vs. natural/biodegradable polymers for delivery of shRNA-based cancer therapies. Methods in Molecular Biology (Clifton, N.J.), 480, 11-29.

Wakerly, Z., Fell, J., Attwood, D., Parkins, D. (1997) Studies on amidated pectins as potential carriers in colonic drug delivery. The Journal of Pharmacy and Pharmacology, 49, 622-625.

Wakerly, Z., Fell, J.T., Attwood, D., Parkins, D. (1996) Pectin/ethylcellulose film coating formulations for colonic drug delivery. Pharmaceutical Research, 13, 1210-1212.

Walrafen, G.E., Chu, Y.C., Piermarini, G.J. (1996) Low-Frequency Raman Scattering from Water at High Pressures and High Temperatures. The Journal of Physical Chemistry, 100, 10363-10372.

Wang, W. (2000) Lyophilization and development of solid protein pharmaceuticals. International Journal of Pharmaceutics, 203, 1-60.

Wang, W. (2005) Protein aggregation and its inhibition in biopharmaceutics. International Journal of Pharmaceutics, 289, 1-30.

Wang, W., Nema, S., Teagarden, D. (2010) Protein aggregation-Pathways and influencing factors. International Journal of Pharmaceutics, 390, 89-99.

Waterman, K.C. (2007) A critical review of gastric retentive controlled drug delivery. Pharmaceutical Development and Technology, 12, 1-10.

Watts, P.J., Lllum, L. (1997) Colonic drug delivery. Drug Development and Industrial Pharmacy, 23, 893-913.

Wen, H., Park, K. (2010). Oral Controlled Release Formulation Design and Drug Delivery: Theory to Practice. John Wiley and Sons, Hoboken, NJ.

Wheatley, T.A., Steuernagel, C.R. (1997) Latex emulsions for controlled drug delivery. Aqueous polymeric coatings for pharmaceutical dosage forms. 2nd edition, pp. 1-54, Marcel Dekker, New York, NY.

Wilding, I.R., Davis, S.S., Bakhshaee, M., Stevens, H.N.E., Sparrow, R.A., Brennan, J. (1992) Gastrointestinal transit and systemic absorption of captopril from a pulsed-release formulation. Pharmaceutical Research, 9, 654-657.

Willemer, H. (1992) Measurements of temperatures, ice evaporation rates and residual moisture contents in freeze-drying. Developments in Biological Standardization, 74, 123-134; discussion 135-136.

Williams, R.W., Dunker, A.K. (1981) Determination of the secondary structure of proteins from the amide I band of the laser Raman spectrum. Journal of Molecular Biology, 152, 783-813.

Williams, R.W., Dunker, A.K., Peticolas, W.L. (1980) A new method for determining protein secondary structure by laser raman spectroscopy applied to FD phage. Biophysical Journal, 32, 232-234.

6 References

Wilson, C.G. (2010) The transit of dosage forms through the colon. International Journal of Pharmaceutics, 395, 17-25.

Windbergs, M., Strachan, C.J., Kleinebudde, P. (2009) Tailor-made dissolution profiles by extruded matrices based on lipid polyethylene glycol mixtures. Journal of Controlled Release, 137, 211-216.

Winterhalter, M., Bürner, H., Marzinka, S., Benz, R., Kasianowicz, J.J. (1995) Interaction of poly(ethylene-glycols) with air-water interfaces and lipid monolayers: Investigations on surface pressure and surface potential. Biophysical Journal, 69, 1372-1381.

Wiwattanapatapee, R., Lomlim, L., Saramunee, K. (2003) Dendrimers conjugates for colonic delivery of 5-aminosalicylic acid. Journal of Controlled Release, 88, 1-9.

Wong, D., Larrabee, S., Clifford, K., Tremblay, J., Friend, D.R. (1997) USP Dissolution Apparatus III (reciprocating cylinder) for screening of guar-based colonic delivery formulations. Journal of Controlled Release, 47, 173-179.

Wu, P., Grainger, D.W. (2006) Drug/device combinations for local drug therapies and infection prophylaxis. Biomaterials, 27, 2450-2467.

Xie, G., Timasheff, S.N. (1997) The thermodynamic mechanism of protein stabilization by trehalose. Biophysical Chemistry, 64, 25-43.

Yang, L., Chu, J.S., Fix, J.A. (2002) Colon-specific drug delivery: New approaches and *in vitro/in vivo* evaluation. International Journal of Pharmaceutics, 235, 1-15.

Yong, Z., Yingjie, D., Xueli, W., Jinghua, X., Zhengqiang, L. (2009) Conformational and bioactivity analysis of insulin: Freeze-drying TBA/water co-solvent system in the presence of surfactant and sugar. International Journal of Pharmaceutics, 371, 71-81.

Yoshioka, S., Aso, Y., Izutsu, K., Terao, T. (1993) The effect of salts on the stability of β-galactosidase in aqueous solution, as related to the water mobility. Pharmaceutical Research, 10, 1484-1487.

Yuen, K.-H. (2010) The transit of dosage forms through the small intestine. International Journal of Pharmaceutics, 395, 9-16.

Zaffaroni, A. (1971) Bandage for administering drugs, Unitet States Patent 3598122.

Zaky, A., Elbakry, A., Ehmer, A., Breunig, M., Goepferich, A. (2010) The mechanism of protein release from triglyceride microspheres. Journal of Controlled Release, 147, 202-210.

Zambito, Y., Baggiani, A., Carelli, V., Serafini, M.F., Di Colo, G. (2005) Matrices for site-specific controlled-delivery of 5-fluorouracil to descending colon. Journal of Controlled Release, 102, 669-677.

Zou, M., Cheng, G., Okamoto, H., Hao, X., An, F., Cui, F., Danjo, K. (2005) Colon-specific drug delivery systems based on cyclodextrin prodrugs: *in vivo* evaluation of 5-aminosalicylic acid from its cyclodextrin conjugates. World Journal of Gastroenterology: WJG, 11, 7457-7460.

7   List of Publications

Research Articles

Klose, D., Siepmann, F., Elkharraz, K., Krenzlin, S., Siepmann, J. (2006) How porosity and size affect the drug release mechanisms from PLGA-based microparticles. International Journal of Pharmaceutics 314, 198-206.

Hedoux, A., Krenzlin, S., Paccou, L., Guinet, Y., Flament, M.-P., Siepmann, J. (2010) Influence of urea and guanidine hydrochloride on lysozyme stability and thermal denaturation; a correlation between activity, protein dynamics and conformational changes. Physical Chemistry Chemical Physics 12, 13189-13196.

Krenzlin, S., Siepmann, F., Wils, D., Guerin-Deremaux, L., Flament, M.-P., Siepmann, J. (2011) Non-coated multiparticulate matrix systems for colon targeting. Drug Development and Industrial Pharmacy 37, 1150-1159.

Krenzlin, S., Vincent, C., Munzke, L., Gnansia, D., Siepmann, J., Siepmann, F. Predictibility of drug release from miniaturized implants. *submitted*

Oral Communications

Krenzlin, S., Neut, C., Wils, D., Deremaux, L., Flament, M.-P., Siepmann, F., Dubreuil, L., Desreumaux, P., Siepmann, J. (2009) Novel multiple unit matrix systems for colon targeting. Young Pharmaceutical Scientists Meet in Nice: Pre-Satellite Meeting of the 2nd Pharmaceutical Sciences Fair & Exhibition (PharmSciFair). Nice, France. # SUN-DDT-11

Krenzlin, S., Neut, C., Wils, D., Deremaux, L., Flament, M.-P., Siepmann, F., Dubreuil, L., Desreumaux, P., Siepmann, J. (2009) Novel multiple unit matrix systems for colon targeting. 2nd Pharmaceutical Sciences Fair & Exhibition (PharmSciFair). Nice, France. # SC-36

Poster Presentations

Krenzlin, S., Hedoux, A., Paccou, L., Siepmann, F., Flament, M.-P., Siepmann, J. (2010) Conformational stability of L-lactic dehydrogenase during freeze drying and storage. 7th World Meeting on Pharmaceutics, Biopharmaceutics and Pharmaceutical Technology. Malta. # 222

Krenzlin, S., Hedoux, A., Guinet, Y., Paccou, L., Flament, M.-P., Siepmann, F., Siepmann, J. (2010) PVP:Trehalose blends for L-lactic dehydrogenase stabilization during freeze drying and long term storage. 2nd Conference Innovation in Drug Delivery: From Preformulation to Development through Innovative Evaluation Process. Aix-en-Provence, France. # 117

Krenzlin, S., Dutet, J., Hedoux, A., Guinet, Y., Paccou, L., Flament, M.-P., Siepmann, F., Siepmann, J. (2010) Lysozyme loaded lipid implants: How trehalose effectively preserves protein activity. 2nd Conference Innovation in Drug Delivery: From Preformulation to Development through Innovative Evaluation Process. Aix-en-Provence, France. # 118

Krenzlin, S., Siepmann, F., Vincent, C., Gnansia, D., Siepmann, J. (2011) Cochlear implant electrodes with time controlled dexamethasone release. 10th European Symposium on Paediatric Cochlear Implantation. Athens,Greece. # A038

Krenzlin, S., Siepmann, F., Vincent, C., Gnansia, D., Siepmann, J. (2011) Drug release from dexamethasone loaded cochlear implants: Experiment and theory. AAPS Annual Meeting and Exposition, Washington DC, USA. # T2201